N° d'ordre : 3068

THESE

présentée à

L'UNIVERSITE BORDEAUX 1

ECOLE DOCTORALE DES SCIENCES CHIMIQUES

par Denise MERY

POUR OBTENIR LE GRADE DE

DOCTEUR

SPECIALITE : Chimie Organométallique

****

DENDRIMERES INORGANIQUES ET ORGANOMETALLIQUES DESIGN ET CATALYSE

****

Soutenue le : 09 décembre 2005

Après avis de :

M. LAVIGNE Guy, Directeur de Recherche CNRS (Toulouse) Rapporteur
M. SAILLARD Jean-Yves, Professeur (Université de Rennes 1) Rapporteur

Devant la commission d'examen formée de :

M. ASTRUC Didier, Professeur (Université de Bordeaux 1)
M. BLAIS Jean-Claude, Directeur de Recherche CNRS (Paris VI)
Mme HEUZE Karine, Chargée de Recherche CNRS (Bordeaux)
M. LAVIGNE Guy, Directeur de Recherche CNRS (Toulouse)
Mme PERRIN Christiane, Directeur de Recherche CNRS (Rennes)
M. SAILLARD Jean-Yves, Professeur (Université de Rennes 1)
M. VERLHAC Jean-Baptiste, Professeur (Université de Bordeaux 1)

Remerciements

Les travaux présentés dans ce manuscrit ont été réalisés au **Laboratoire de Chimie Organique et Organométallique** (LCOO), unité mixte de recherche CNRS n°5802 de l'Université Bordeaux 1.

Tout d'abord, je tiens à exprimer ma plus profonde gratitude à **M. Didier Astruc**, Professeur à l'Université Bordeaux 1, pour m'avoir encadrée durant toutes ces années. Avec son enthousiasme et son dynamisme, j'ai appris que la recherche est faite de plaisir, d'envie et de curiosité. De plus, je le remercie pour son investissement quotidien dans ce travail.

Ensuite, je tiens à remercier mes deux rapporteurs, **M. Guy Lavigne**, Directeur de Recherche au CNRS, et **M. Jean-Yves Saillard**, Professeur à l'Université Rennes 1, pour avoir accepté d'examiner et de juger ce travail. Je désire aussi remercier **M. Jean-Baptiste Verlhac**, Professeur à l'Université Bordeaux 1, pour avoir accepté la présidence de mon jury de thèse, ainsi que tous les autres membres de mon jury : **M. Jean-Claude Blais**, Directeur de Recherche au CNRS, et **Mme Christiane Perrin**, Directrice de Recherche au CNRS.

J'ai eu une chance incroyable de rencontrer et de travailler avec des personnes formidables. Par exemple, **Mme Karine Heuzé** m'a encadrée sur toute la partie des métallodendrimères de palladium en me donnant une méthode de travail. Elle m'a aussi acceptée très gentiment dans son laboratoire en me prêtant une hotte pendant toute la période de ma thèse. Merci, Karine. Je remercie également **M. Jaime Ruiz** avec qui j'ai beaucoup travaillé notamment sur la partie fonctionnalisation des dendrimères et les clusters mais pas seulement. Jaime est une personne très enthousiaste et généreuse qui a fait l'électrochimie de mes complexes. J'aimerais aussi remercier **M. Sylvain Nlate** pour les dendrons pyridines et

les polymères en étoile mais aussi pour les nombreuses discussions sur la chimie, la vie et l'enseignement. Il m'a aidé à préparer mes enseignements à de nombreuses reprises.

Je tiens à remercier **Melle Lauriane Plault** pour les dendrons pyridines, **Melle Catia Ornelas** pour nos nombreuses collaborations sur la fonctionnalisation des dendrimères et les clusters, **Melle Julietta Lemo** pour avoir été une voisine de paillasse très agréable. Toutes les trois sont devenues bien plus que de simples collègues de travail. Je les remercie du fond du cœur.

Merci à deux anciens étudiants du laboratoire, **M. Sylvain Gatard**, qui m'a appris à me servir de la boîte à gants et lancer une manipulation organométallique ainsi que **M. Victor Martinez** qui m'a appris la technique de Schlenk, l'utilisation d'une rampe à vide et à faire un spectre RMN au CESAMO. Ils ont été tous deux d'une grande patience, tout en étant très enthousiastes.

Je tiens à remercier **M. Kaplan Kirakci**, **M. Stéphane Cordier** et **Mme Christiane Perrin** de l'Université Rennes 1, pour notre riche collaboration sur les clusters. Ils m'ont fait découvrir une chimie passionnante, la chimie du solide. De même, je remercie **M. Jean-Claude Blais** pour tous les spectres de masse de mes différents complexes.

Je ne terminerai pas mes remerciements sans avoir une pensée sympathique pour toutes les personnes du LCOO qui savent si bien rendre agréable le cadre de travail, et tout particulièrement : **M. Jean-Pierre Desvergne**, **Marie-Christine**, **Andréas**, **Feng**, **Henry**, **Yoann**, **Raymond**, **Nathan**, **Raph**, **Lolo**, **Anne**, **Magalie**, **Mélanie**, **Mervyn**, **M. Picard** ainsi que tous les membres du laboratoire passés et présents.

Merci

A mes adorables parents, Brigitte et Denis,
A mon aimé, Eric.

Sommaire

Partie II : Métathèse

Partie III : Fonctionnalisation de clusters inorganiques à l’aide de pyridines: dendrimères et métallodendrimères à cœur cluster

Introduction générale

L'architecture dendritique est une topologie très répandue dans la nature. Elle est observée, non seulement dans des systèmes non biologiques (cristaux de neige, érosion fractale), mais également au sein du monde biologique (neurones, systèmes vasculaires, arbres) où les dimensions varient du mètre (arbres), au millimètre (champignons), jusqu'au micromètre (neurones).

Un dendrimère, ou arbre moléculaire (du grec : *dendri* = arbre, et de *mère* pour polymère), est une macromolécule constituée de monomères qui s'associent selon un processus arborescent autour d'un cœur central. La construction arborescente s'effectue par la répétition d'une séquence de réactions jusqu'à l'obtention à la fin de chaque cycle réactionnel d'une nouvelle génération et d'un nombre croissant de branches identiques. Après quelques générations, le dendrimère prend une forme globulaire, hautement ramifiée et plurifonctionnalisée grâce aux nombreuses fonctions terminales (Schéma 1).[1-2]

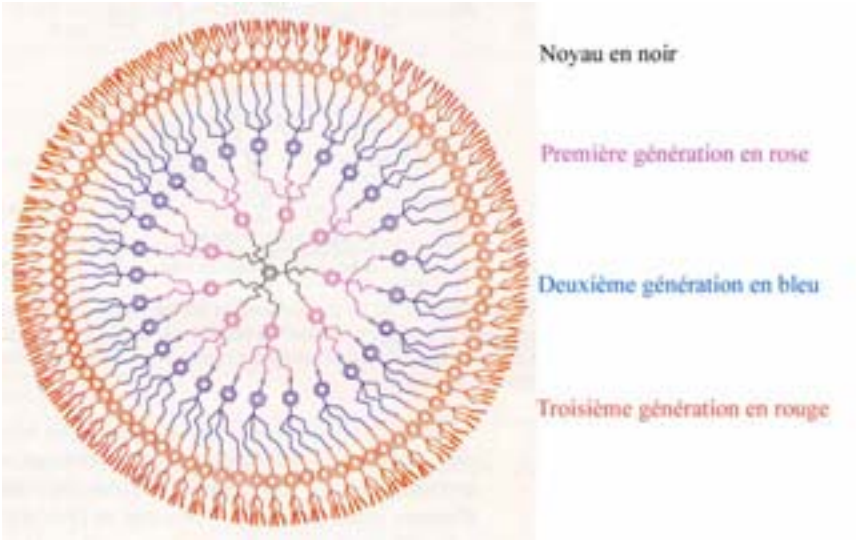

Schéma 1 : Structure d'un dendrimère

L'origine des structures moléculaires branchées remonte à 1941 avec les travaux de Flory qui a construit les premiers polymères hyperbranchés.[3] Cependant, les premiers travaux pour la synthèse de molécules par réactions itératives remontent à 1978 avec ceux de Vögtle et *coll.*.[4] Au même moment, le groupe d'Astruc a effectué les premières itérations de

peralkylations conduisant à des molécules en étoile contenant six branches.[5] Puis, en 1983, le groupe de Denkewalter propose une synthèse des dendrimères polylysines basée sur les stratégies employées en synthèse peptidique.[6] Par la suite, les groupes de Newkome et de Tomalia réussissent les premières synthèses de dendrimères symétriques en 1985.[7,8]

Deux types de méthodes de synthèse peuvent être employés pour obtenir des dendrimères covalents : la synthèse divergente et convergente. La première s'effectue du cœur vers la périphérie, en greffant un nombre de plus en plus grand de petites molécules sur la surface multifonctionnalisée du dendrimère. La synthèse convergente consiste à construire le dendrimère de la périphérie vers le cœur à l'aide de fragments dendritiques appelés dendrons qui sont rattachés lors d'une étape finale à un cœur plurifonctionnel.[1] Au laboratoire, plusieurs types d'assemblages ont été réalisés pour synthétiser des dendrimères : assemblage par liaison covalente, par liaison ionique, par liaison hydrogène ou encore par liaison de coordination sur une nanoparticule centrale ou sur un cœur inorganique (Schéma 2).

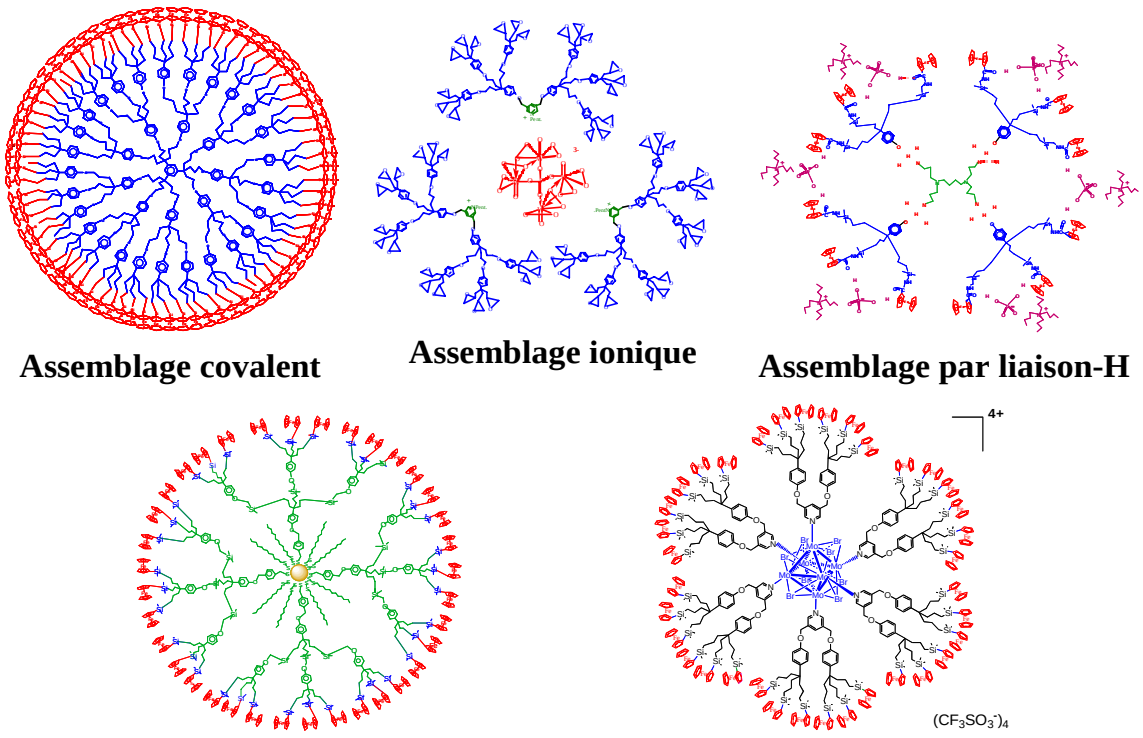

Schéma 2 : Différents types d'assemblage

Les propriétés particulières des dendrimères telles que la solubilité, la viscosité et la stabilité thermique offrent une large palette d'applications allant de la reconnaissance moléculaire aux matériaux en passant par les batteries moléculaires, la catalyse, l'encapsulation moléculaire (médicaments), etc… (Schéma 3). Ces applications découlent des propriétés intrinsèques des dendrimères : fonctions aisément accessibles en surface, porosité de ces macromolécules, flexibilité des branches internes, présence de cavités fonctionnalisables, accessibilité au cœur, etc... La plupart des grands secteurs industriels sont concernés par l'émergence de cette nouvelle classe de polymères.

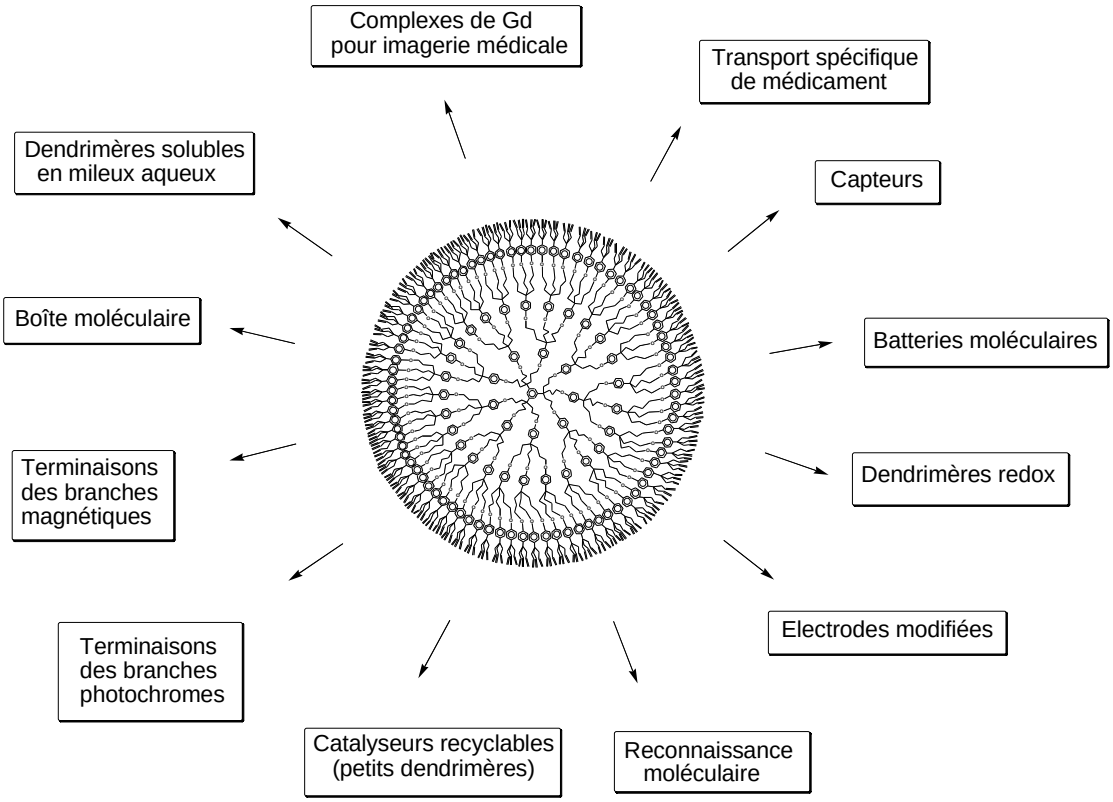

Schéma 3 : Quelques applications des dendrimères

La catalyse métallodendritique et les nouveaux matériaux passionnent particulièrement notre laboratoire.

Nous nous sommes intéressés à la synthèse et l'étude de catalyseurs métallodendritiques car ils combinent les avantages de la catalyse homogène et hétérogène. Effectivement, ces composés sont solubles dans les solvants réactionnels, ils sont facilement séparables du milieu par ultrafiltration, ultracentrifugation ou précipitation et peuvent donc

être recyclés. On voit très nettement l'intérêt de tels objets dans le concept de la *Chimie Verte*. En effet, la protection de l'environnement constitue un des enjeux majeurs de notre société. Les réglementations françaises, européennes et internationales vont imposer des contraintes de plus en plus sévères concernant les concentrations de métaux lourds et l'utilisation des produits chimiques en général. Les pionniers des métallodendrimères en catalyse sont les groupes van Leeuven dans l'industrie et de Reetz dans le domaine académique.[1]

De plus, notre laboratoire est le premier dans l'étude des effets dendritiques et dans l'élaboration des polymères en étoile. En effet, nous avons synthétisé de nouveaux métallodendrimères de ruthénium pour la catalyse de métathèse polymérisante par ouverture de cycle du norbornène, conduisant à ces polymères en étoile. Ces nouveaux matériaux pourraient trouver des applications dans le domaine de la microélectronique, par exemple.

Ensuite, nous avons travaillé sur des aspects plus fondamentaux telle que la fonctionnalisation de grands dendrimères par la métathèse croisée qui est actuellement une réaction clé.[9] Richard R. Schrock, Robert H. Grubbs et Yves Chauvin ont reçu le prix Nobel de chimie 2005 pour l'étude et le développement de cette méthode de synthèse organique originale.

Enfin, nous avons aussi synthétisé une famille de métallodendrimères à cœur cluster inorganique en collaboration avec le groupe de C. Perrin et S. Cordier de Rennes. Cette étude a essentiellement impliqué des fonctionnalisations par échanges de ligands halogénures apicaux par des pyridines, y comprit des pyridines dendroniques. Avant nous, Zheng et *coll.* ont aussi synthétisés des architectures complexes dont certaines dendritiques mais non fonctionnalisées.[10] Même si leur utilisation en catalyse n'est pas appropriée, nos dendrimères à cœur cluster ont cependant permis d'élaborer des capteurs de fragments d'ADN. D'autres stratégies pourront être éventuellement abordées par la suite pour l'utilisation des clusters de type Perrin en catalyse.

Après un rappel sur la catalyse métallodendritique, nous détaillerons donc dans la première partie les résultats obtenus avec les métallodendrimères de palladium pour la catalyse de la réaction de couplage carbone-carbone de type Sonogashira. Puis, une seconde partie sera consacrée à la synthèse de nouveaux polymères en étoile ainsi qu'à la fonctionnalisation de grands dendrimères par la catalyse de métathèse. Enfin, dans la dernière partie, nous présenterons l'élaboration de dendrimères et de métallodendrimères à cœur cluster inorganique. En annexe de ce manuscrit figurent deux articles qui approfondissent les sujets abordés.

Références :

1- D. Astruc, F. Chardac, *Chem. Rev.*, **2001**, *101*, 2991.

2- F. Zeng, S. C. Zimmermann, *Chem. Rev.*, **1997**, *97*, 1681.

3- a) P.J. Flory, *J. Am. Chem. Soc*., **1941**, *63*, 3083; b) P.J. Flory, *J. Am. Chem. Soc*., **1941**, *63*, 3091; c) P.J. Flory, *J. Am. Chem. Soc*., **1941**, *63*, 3096.

4- a) E. Buhleier, W. Wehner, F. Vögtle, *Synthesis*, **1978**, 155; b) F. Vögtle, E. Weber, *Angew. Chem. Int. Ed.*, **1979**, *18*, 753.

5- D. Astruc, J.-R. Hamon, G. Altholf, E. Roman, P. Batail, P. Michaud, J.-P. Mariot, F. Varret, D. Cozak, *J. Am. Chem. Soc.*, **1979**, *101*, 5445.

6- R. G. Denkewalter, J. F. Kolc, W. J. Lukesavage, *US Pat. 4410 688*, **1983**.

7- G. R. Newkome, G. R. Baker, V. K. Gupta, *J. Org. Chem.*, **1985**, *50*, 2003.

8- D. A. Tomalia, H. Baker, J. Dewald, M. Hall, G. Kallos, S. Martin, J. Roeck, J. Ryder, P. Smith, *Macromolecules*, **1986**, *19*, 2466.

9- D. Astruc, *New J. Chem.*, **2005**, *29*, 42.

10- a) H. D. Selby, B. K. Roland, Z. Zheng, *Acc. Chem. Res.*, **2003**, *36*, 933; b) R. Wang, Z. Zhang, *J. Am. Chem. Soc.*, **1999**, *121*, 3549.

Bibliographie

Dendritic Catalysis :

Major Concepts and Recent Progress

I . Introduction

Metallodendrimers are now a mature area of nanosciences with multiple potential applications [1-3]. Among them, catalysis stands as a major objective given the need to design environmentally safe processes [4] with regenerable catalysts. Indeed, dendritic catalysts are nanosized, and as such they are, as biomolecules, easily isolable from homogeneous reaction media by precipitation, filtration, ultrafiltration or ultracentrifugation [3,5-8]. The idea of using metallodendritic was first raised by van Leeuwen in 1992 [9], and the first example of recycling dendritic catalysts was reported by Reetz in 1997 [10]. Since the first reviews on the subject that appeared in 2001, several other more or less related reviews were reported [12-21] and dendritic catalysis was the subject of a multi-chapter section of the special triple issue of C. R. Chimie in 2003 [11]. The purpose of the present review is to summarize the major concepts and recent advances in the field. For extensive references older than 2001, the reader is referred to our comprehensive Chem. Rev. article [5]

II . Major Concepts

Several approaches to dendritic catalysis and dendrimers in catalysis have been reported, and a general picture of this diversity is shown on Scheme 1 [5].

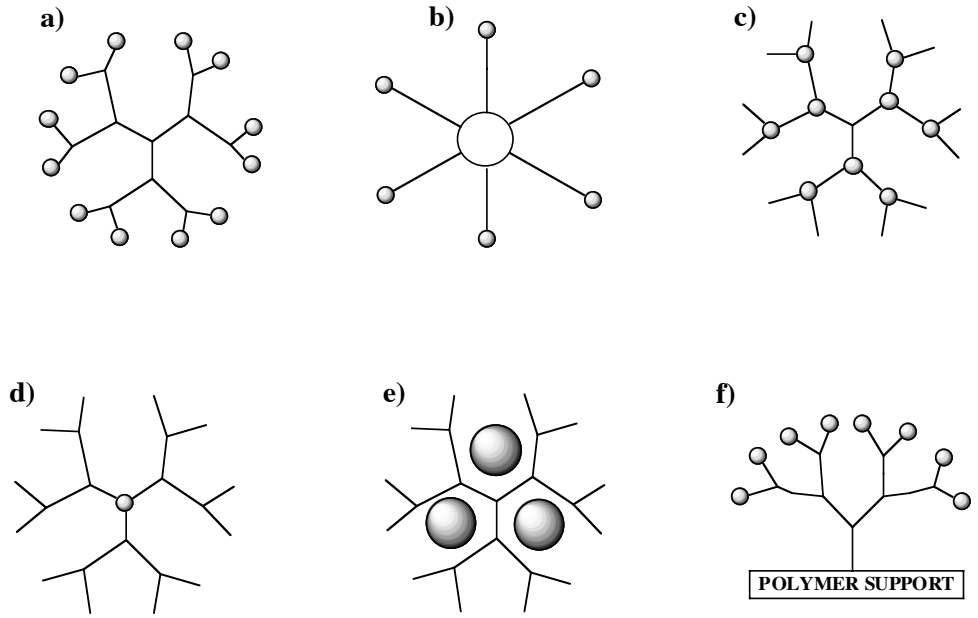

Scheme 1 : The various dendrimer topologies and metal locations in catalytically active metallodendrimers [5]

Indeed, the catalytically active metal centers can be located at the termini of the dendritic branches. In this case (a) in Scheme 1, bulk at the periphery increases as the dendrimer generation increases, and these branch termini have all the less tendency to back fold toward the dendrimer center as the terminal group is larger. This means that, for a given generation that depends on the length of the tethers, the dendrimer topology and the size of the termini, bulk will inhibit further dendritic construction. This may be related to the de Gennes dense packing limit whereby the limit generation is provided by the dendrimer surface area [22]. Recall that with small termini, dendrimer construction far beyond the dense packing limit in the Astruc group has demonstrated that this theory is not generally applicable [23], as suggested by other theoretical papers on dendrimers [24-27]. It applies, however, with large terminal groups [23] ; therefore, the Astruc group has suggested that stars (case b) in Scheme 1) represent a better topology than dendrimers for catalysis purpose, especially because substrate approach to the metal center is often a rate-limiting step is catalytic reactions [28]. The first experimental observation of kinetics that does not drop in star-shaped catalysts compared to monometallic catalysts whereas sterically bulky metal centers undergo dramatic kinetic limitation was reported by the Astruc group for the redox catalysis of nitrate cathodic reduction in aqueous solution (Scheme 2, [29,30]).

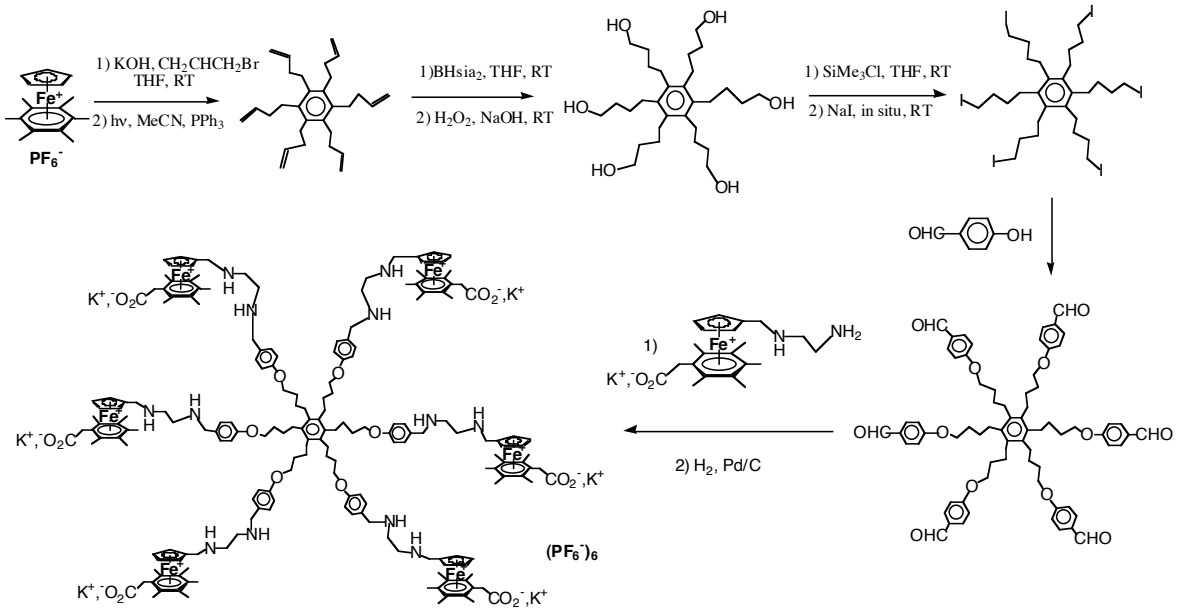

Scheme 2 : Design and synthesis of a water-soluble star-shaped catalyst for cathodic reduction of nitrates and nitrites to ammonia showing no kinetic drop from the monometallic to the star-shape catalyst.

On the other hand, it has been demonstrated in several occasions with various types of catalytic reactions using DAB-derived phosphine-metal catalysts (Ru in C=C metathesis [31,32], Pd in cross C-C coupling [33-35]) that a negative dendritic effect of the catalytic reaction kinetics encourages the use of low-generation dendrimers. This dichotomy further encourages the use of star-shaped recyclable catalysts in the future as their size is well sufficient for recovery and re-use. Another example of such classic dendrimer catalyst in which the nickel groups are located at the dendrimer periphery is that published in 1984 by van Koten and represented in Scheme 2. Its efficiency in Kharash reaction (addition of polyhanogenoalkanes onto double C=C bonds) slightly decreases from the monometallic catalyst to the corresponding metallodendritic one of Scheme 3 [8, 36].

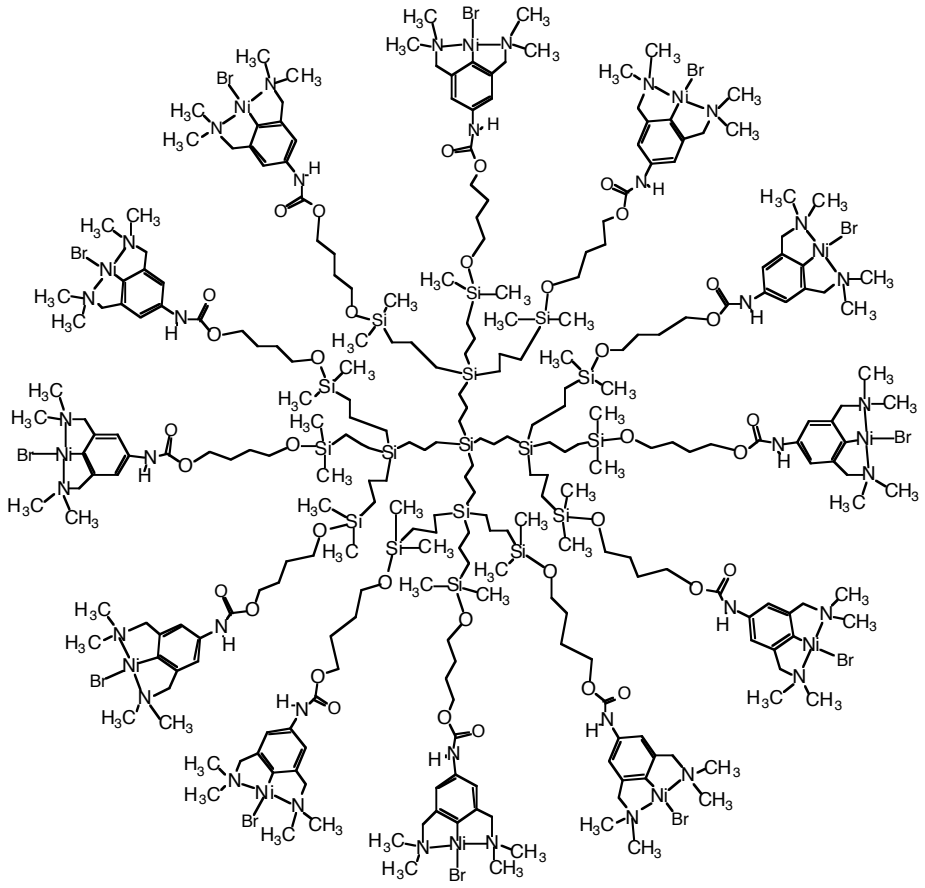

Scheme 3 : van Koten's pioneering dendritic nickel complex that catalyses the Kharash reaction with slightly negative dendritic effect on the reaction kinetics [8,36].

Another distinct approach is that using ionic bonds in connections with hydrogen bonds to attach the catalyst to the dendrimer pioneered by the van Leeuwen and Meijer groups. In this method, the phosphine-metal catalyst bearing a carboxylate chain is bonded to a tertiary ammonium ending of the polypropyleneimine dendrimer branches [11,37]. The reactivity does not decrease in the metallodendrimers compared to the monomers, although recycling attempts show a decrease of activity due to leaching. The topology c) of Scheme 1 whereby the phosphine ligands of the catalyst are located are the branching points all along the dendritic construction is rarely found but has been reported by Kakkar [13]. The challenging approach consisting in locating the catalyst at the center of the dendrimer has been reported *inter alia* with porphyrin-centered dendrimers for selective olefin epoxidation [38] and ferrocenylphosphine-centered dendrimers [39] shown in Scheme 4. In the later case, the kinetics decreases as expected as the dendrimer generation increases due to the increased steric bulk inhibiting approach to the catalytic metal center.

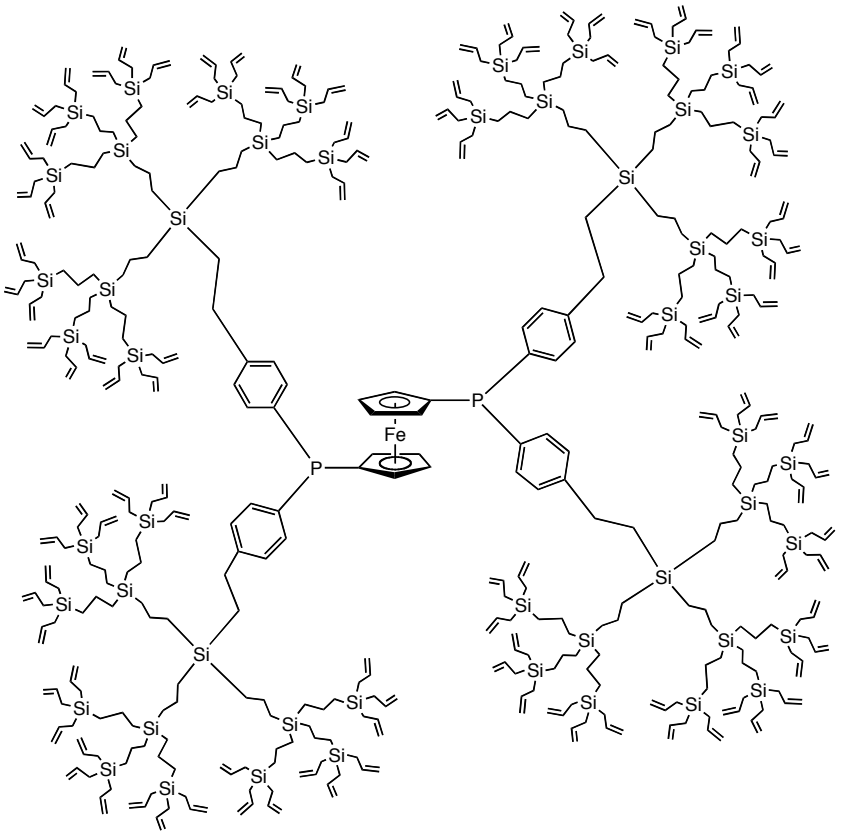

Scheme 4 : van Leeuwen's dendritic ferrocenyldiphosphine for Pd catalysis of allylic alkylation.

An elegant approach largely developed by Crooks involved the formation of catalytically active metal nanoparticles formed by reduction of metal cations coordinated to dendrimers containing amines such as the commercial polyamidoamines (PAMAM) synthesized by Tomalia. This strategy is shown in Figure e) of Scheme 1 and has been applied to various catalytic reactions in green media such as supercritical CO_2 or water and has involved nanoparticles prepared in this way from dendrimers and further fixed on heterogeneous supports [11,40-63].

Asymmetric catalysis has been pioneered by Brunner with dendrizymes [64], developed by Seebach [65,66] and an example by Togni [67] is shown in Scheme 5 in which a dendritic optically active ferrocenyl phosphine is used for the following enantioselective hydrogenation reaction :

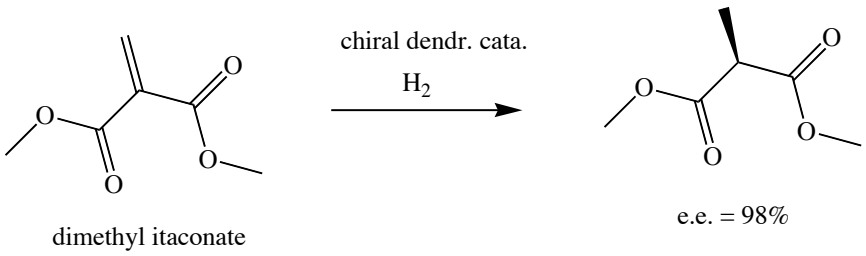

dimethyl itaconate

e.e. = 98%

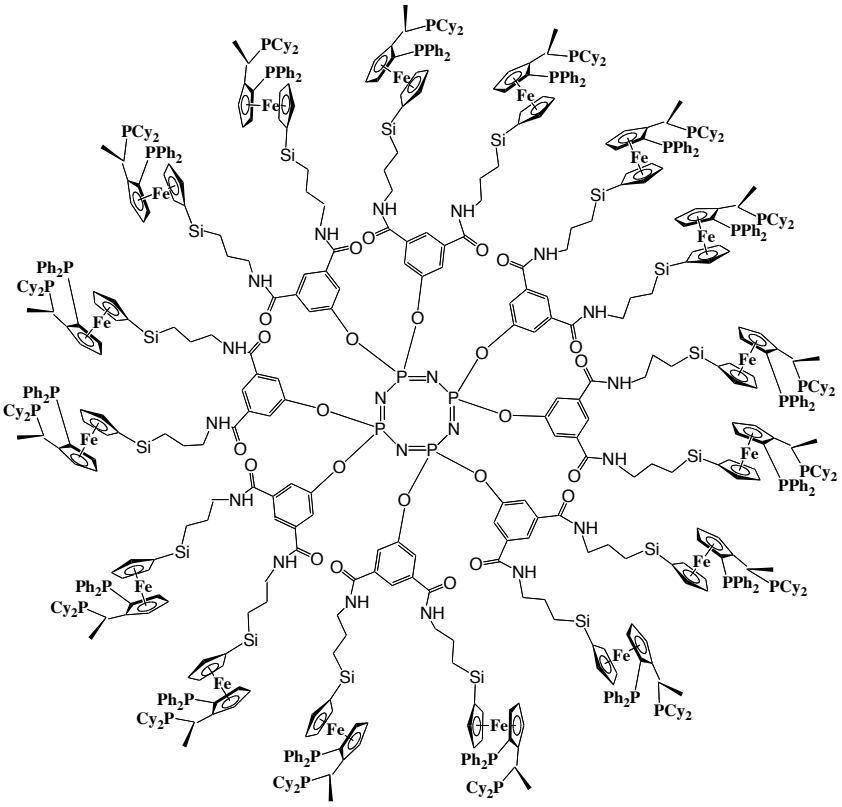

Scheme 5 : Togni's chiral ferrocenyl dendrimer for enantioselective hydrogenation [67]

Another approach pioneered by Alper [68,69] is that using polymer-supported metallodendrons shown in Schemes 1, Figure f and Scheme 6, that have been used *inter alia* for hydroformylation and Heck reactions. This strategy has been reviewed [70] and applied by Portnoy with dendritic effects [70-72].

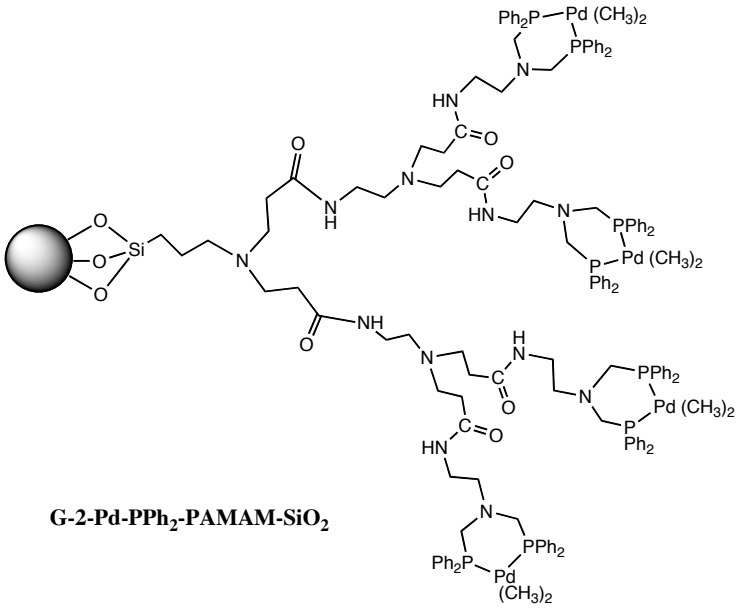

Scheme 6 : Alper's polymer-attached metallodendron for Heck catalysis

In our research group, we have also pioneered the dendritic protection of a catalyst by a dendronic periphery using ionic bonding between polyoxometallate core and dendrons that are cationic at the focal point that is an ammonium or pyridinium group. Indeed, polyoxometallates are excellent catalysts for various oxidation reactions (epoxidation of alkenes, oxidation of alcohols and sulfides). With linear ammonium counter cations, however, the catalyst is not recyclable and is decomposed as witnessed by the change of ^{31}P NMR of the phosphotungstate moiety. With dendritic encapsulation by tridentate ammonium cations of controlled size, it is possible to recycle and re-use the catalyst several times without decomposition as confirmed by ^{31}P NMR (Scheme 7) [73-75].

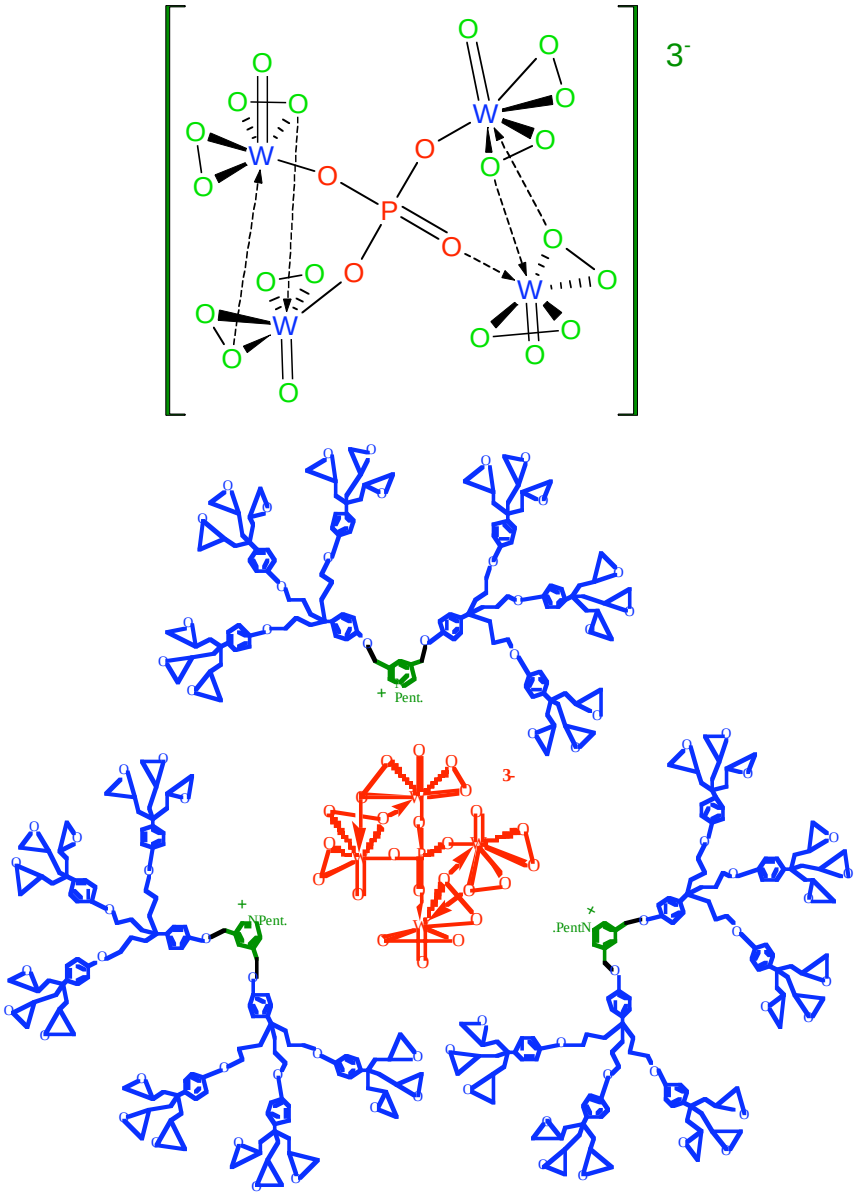

Scheme 7 : Phosphotungtate trianionic catalyst for olefin epoxidation and alcohol and sulfide oxidation (top) that is not recyclable with long-chain linear ammonium counter cation but becomes fully recyclable with ammonium or pyridinium dendronic counter cations of the type shown (bottom) [73-75].

III. Recent Advances

A. The Classic Approach Using Homogeneous Catalysts

1. Hydrogenation

The Reek-van Leeuwen group has examined the activity of Rh complexes of the dppf-type dendritic ligands in the hydrogenation of dimethyl itaconate in a continuous-flow membrane reactor showing a reasonable constant of formation of the product compared to the non-dendritic catalyst [76] Gade has used tripodal-terminated Rh-phosphine dendrimers to catalyze the hydrogenation of styrene and 1-hexene, and shown that the catalytic hydrogenation properties were not altered compared to the monomer with low-generation dendrimers [77]. Kakkar designed dendrimer containing phosphorus ligands at the branching points and looked at the catalysis of olefin hydrogenation upon variation of the dendritic structure [78].

2. Hydroformylation

Cole-Hamilton showed that Rh-phophine-terminated dendrimers based on polyhedral silsesquioxanes cores with 16 PPh_2 arms give much higher linear selectivities (14 : 1) than their small analogues (3.4 : 1) in the hydroformylation of cyclooct-1-ene [79,80]. The Reek-van Leeuwen Rh-dendritic phosphine catalysts used as indicated above in hydrogenation are also efficient for hydroformylation, and the activities obtained are as good as for monomers except in the case of the bulky substrate 4,4,4-triphenylbut-1-ene which gave a significant decrease of activity [76].

3. Hetero-C-C coupling : Heck, Sonogashira, Suzuki, Stille

Scretas reported that Pd complexes of DAB-dendr-(NH_2) modified with P,N ligands catalyze the Heck reaction of aryl bromides and noted a marked dependence of the conversion on the dendritic ligand / Pd ratio taken into account in terms of inhibiting steric bulk. Jayaraman compared three generations of Pd-alkylphosphine dendrimers in the Heck reactions with various olefins and reported that the second and third generations were found to exhibit better catalytic activity than the monomer and first-generation metallodendrimer [81], a trend also noted by Mapolie with poly(propyleneime)-iminopropyl-palladium [82]. On the other hand, three generations of bidentate DAB phosphinated Pd dendrimers that were found to be active in Sonogashira coupling of iodo-

and bromobenzene with phenylacetylene showed a negative dendritic effect attributed to increasing steric effect as the generation increases. These metallodendrimers can be recovered and recycled with little decrease of efficiency up to seven cycles. The nature of the alkyl substituents (cyclohexyl *vs*. *tert*-butyl) on the P ligand of the Pd catalyst also plays a role in efficiency, solubility and thus recycling ability. [33-35]

4. Oligomerization and polymerization

Several authors have studied the use of metallodendrimers in which the metal centers are initiators of olefin polymerization to catalyze the polymerization of ethylene. This strategy allows site isolation due to well-defined hyperbranched structure. As a consequence, the metallodendritic initiators can avoid side reactions encountered with monomeric initiators and thus provide a better result with a positive dendritic effect [83-88]

5. Other homogeneous catalytic reactions

Cobalt porphyrins are used as coenzyme B12 mimics [89] and in AIBN-mediated reactions with alkynes [90]. Rhodium terminated dendrimers significantly enhance the catalytic activity of $[\{Rh(CO)_2Cl\}_2]$ for the carbonylation of methanol [91]. New reports by the van Koten groups detail the good catalytic activity of nickel-pincer-terminated dendrimers [92] and platinum-pincer-terminated dendrimers [93]. PAMAM dendrimers terminated by Co(II) Schiff base groups disclose ligand effect on the phosphoesterase activity [94]. Al-Binol complexes show slightly improved activity and enantioselectivity than monometallic analogues for Diels-Alder reactions between cyclopentadiene and oxazolidinone derivatives [95]. Pd-terminated carbosilane dendrimers were tested as catalysts in the hydrovinylation of styrene and compared to monometallic models [96]. The Thayumanavan group showed that conformationally constrained dendrimers provide better access to dendritic cores compared to the more flexible counterparts, which should have implications in using dendrimers as scaffolds in catalysis [97]. Finally, metallodendritic complexes in electron-transfer processes and catalysis has been reviewed [98]. Palladium- and rhodium-phosphine catalysts containing benzoate substituents were linked to ammonium groups of PPI-type dendrimers by ionic bonds to achieve the Heck reaction of acrylate with iodobenzene at 100°C in toluene [99] and one-pot hydroformylation, Knovenagel reaction and hydrogenation of styrene [100].

Using dendrimers terminated with ruthenium benzylidene complexes containing the *cis*-chelating diphosphine chains of the dendrimers, the Astruc group has achieved ring-opening-metathesis

polymerization of norbornene at room temperature [31,32,101-103]. The metathesis reaction proceeds more slowly than with the Grubbs catalysts that have phosphines in *trans* position, but the *cis*-diphosphine is then firmly held in the dendrimer providing excellent stability. The metallodendrimers catalyzed the ROMP of norbornene more rapidly than the monometallic model, which was taken into account by the easier decoordination of a phosphorous ligand in the dendrimers than in the monometallic catalyst in the rate-limiting step [101]. Indeed, theoretical calculations by Khamal and Saillard showed that the interaction of the olefin onto the rurthenium center is non-bonding before phosphine decoordination showing that phosphine decoordination is necessary before catalysis [102]. As expected a negative dendritic effect is observed upon increasing the dendrimer generation from one to three because of concomitant increasing steric inhibition. This reaction leads to metallodendritic polymers, a rather new class of polymers [101-103].

Xi's group has synthesized star-shaped polymers with relatively low polydispersity using the ATRP method in the presence of CuBr / pentamethyldiethylene triamine [104] and star-block copolymers from dendrimers initiators by combining ROMP with ATRP [105]. Hedrick's group has synthesized dendritic-linear A_xB_x block copolymers by living ring-opening polymerization (ROP) of lactones. The A blocks are composed of the first-to third generation dendrons from 2,2-bis(hydroxymethyl)-propionic acid, and it is the B blocks that is poly(ε-caprolactone) prepared by ROP [106].

The interest in asymmetric catalytic, reviewed previously [5], is ongoing [107-114] with reports on asymmetric alkylation of aldehydes with diethyl zinc [108], allylic alkylation [113] and amination [111], aldol reactions [114], epoxidation, and hetero Diels-Alder reactions [109,110]. Most reports, however, are dealing with asymmetric hydrogenation [115-122].

B. Supported metallodendritic catalysts

Alper'strategy has been pursued with rhodium-supported resins for carbonylative ring expansion of aziridines to β-lactams [123]. Other reactions reported by the Alper group involve other carbonylation reactions including hydroformylation [124-129]. Chiral auxiliaries on silica have also been used for enantioselective addition of diethylzinc to benzaldehyde [130]. Van Koten's group has equipped dendronized polymers with NCN-palladium-pincer moieties compounds at their peripheries that catalyze the aldol condensation of benzaldehyde with methylisocyanate [131]. Portnoy has noted increase in catalytic activity and selectivity in intramolecular Pauson-Khand reaction for Co complexes, immobilized on second and third-generation dendron-functionalized polystyrene compared to analogues on non-dendronized support [71].

C. Dendritic Organic Catalysts

Hawker and Fréchet had pioneered the area of organic dendritic catalysts behaving as reverse micelles with a high density of inner aromatic rings and hydroxy groups stabilizing positively charged transition states as in enzymes [17]. Since cationic polymers and aggregates of quaternary ammonium ions are known to catalyze reactions of anionic compounds particularly in aqueous solution, polycationic dendrimers derived from PPI have been used for this purpose and behave as micellar catalysts in water [132-134]. Reymond has used peptide dendrimers for selective catalysis, including with a combinatorial approach ; for instance esterolysis activity is enhanced [135-138]. Other uses have been found as Lewis-acid dendritic catalysts [139, 140]. Organic catalysis is a growing area, and multiple uses of dendrimers are awaited shortly. Reports have appeared on the nitroaldol (Henry) reaction [141-143], mimic of glutathione peroxidase [144], esterification [145], acylation [146], aminolysis [147,148], enantioselective alkylation [149,150], activation of hydrogen peroxide [151,152].

IV. Conclusion

The field of dendritic catalysis is expanding with a variety of branches. To the classic concepts of catalysts attached to the termini of dendritic tethers that has been steadily applied to asymmetric catalysis, one now deals with new areas such as nanoparticle-encapsulated dendrimers and organic catalysis that were only in their infancy at the turn of the century. Catalysis inside dendrimers is a great idea that is difficult to apply as shown by attempts to use the metal-cored protected dendritic catalyst. The idea of dendron-protected catalytically active core works when ionic bonding between the cored catalyst and dendron is involved, but covalent dendrimers give poorer results. Emphasis is now placed on the recovery of the catalysts, and it is true that leaching is often a problem as in supported catalysis when a large number of catalytic recycling operation are desired. Progress have been made in the applied field of membrane filtration, and the recovery of catalytic material is possible with dendrimers or stars of moderate size. The concept of the reduction of the steric effect at the dendrimer periphery by using star-shaped catalysts instead of dendritic catalysts works rather well. Indeed, careful investigation of dendritic effects on the kinetics upon increase of the dendrimer generation most of the time leads to the finding of a negative dendritic effect due to increasing bulk that inhibits the approach of the catalytic metal center. Sophisticated nanomaterials combining molecular and materials aspects will undoubtedly lead to further improvement and bring this exciting area at the forefront of applicable catalysis.

V. References

[1] G.R. Newkome, C.N. Moorefield, F. Vögtle, Dendrons and Dendrimers. Concepts, Synthesis and Applications, Wiley-VCH, Weinheim, 2001.

[2] Dendrimers and other Dendritic Polymers (Eds.: D. Tomalia, J. M. J. Fréchet), Wiley-VCH, New York, 2002.

[3] Dendrimers and Nanosciences (Guest Ed.: D. Astruc), C. R. Chimie, 6 (2003) 709.

[4] "Green Chemistry" P.T. Anastas, T.C. Williamson Eds., ACS Symp. Ser. 626, ACS, Washington DC, 1996.

[5] D. Astruc, F. Chardac. Dendritic Catalysts and Dendrimers in Catalysis. Chem. Rev., 101 (2001) 2991.

[6] G.E. Oosterom, J.N.H. Reek, P.C.J. Kamer, P.W.N.M. van Leeuwen. Transition Metal Catalysis Using Functionalized Dendrimers. Angew. Chem. Int. Ed. Engl., 40 (2001) 1828.

[7] R. van Heerbeeck, P.C.J. Kamer, P.W.N.M. van Leuwen, J.N.H. Reek. Dendrimers as Support for Recoverable Catalysts and Reagents. Chem. Rev., 102 (2002) 3717.

[8] R. Kreiter, A.W. Kleij, R.J.M. Klein Gebbink, G. van Koten In F. Vögtle, C. Schalley, Eds., Dendrimers IV: Metal Coordination, Self-assembly, Catalysis, Vol. 217, Springer Verlag, Berlin, 2001, p. 163.

[9] R.A. Kleij, P.W.N.M. van Leeuwen, A.W. van der Made; EP0456317, 1991 [Chem. Abstr., 116 (1992) 129870].

[10] M.T. Reetz, G. Lohmer, R. Schwickardi. Synthesis and Catalytic activity of dendric diphosphane metal complexes. Angew. Chem. Int. Ed. Engl., 36 (1997) 1526.

[11] Y. Niu, R. M. Crooks, J. N. H. Reek, D. de Groot, G. E. Oosterom, P. J. Kamer, P. W. N. M. van Leeuwen, G. P. M. van Klink, H. P. Dijktra, G. van Koten, C.-M. Che, J.-S. Huang, J.-L. Zhang, D. Astruc, J.-C. Blais, M.-C. Daniel, S. Gatard, S. Nlate, J. Ruiz, In Dendrimers and Nanosciences, C. R. Chimie (Guest Ed.: D. Astruc) Vol. 6-8, 2003, p.1049.

[12] J.N.H. Reek, D. de Groot, G.E. Oosterom, P.C.J. Kamer, P.W.N.M. van Leeuwen. Core and periphery functionalized dendrimers for transition metal catalysis; a covalent and a non-covalent approach. Reviews in Molecular Biotechnology, 90 (2002) 159.

[13] M. Dasgupta, M.B. Peori, A.K. Kakkar. Designing dendritic polymers containing phosphorus donor ligands and their corresponding transition metal complexes. Coord. Chem. Rev., 233-234 (2002) 223.

[14] S. Hecht, J.M.J. Fréchet. Dendritic Encapsulation of Function: Applying Nature's Site Isolation Principle from Biomimetics to Materials Science. Angew. Chem. Int. Ed., 40 (2001) 74.

[15] J.M.J. Fréchet. Dendrimers and Other Dendritic Macromolecules: From Building Blocks to Functional Assemblies in Nanoscience and Nanotechnology. J. Polymer Science: Part A: Polymer Chemistry, 41 (2003) 3713.

[16] P.A. Chase, R.J.M. Klein Gebbink, G. van Koten. Where organometallics and dendrimers merge: the incorporation of organometallic species into dendritic molecules. J. Organometal. Chem., 689 (2004) 4016.

[17] C. Liang, J.M.J. Fréchet. Applying key concepts from nature: transition state stabilization, pre-concentration and cooperativity effects in dendritic biomimetics. Prog. Polym. Sci., 30 (2005) 385.

[18] R. van de Coevering, R.J.M. Klein Gebbink, G. van Koten. Soluble organic supports for the non-covalent immobilization of homogeneous catalyts: modular approaches towards sustainable catalysts. Prog. Polym. Sci., 30 (2005) 474.

[19] A. Dahan, M. Portnoy. Dendrons and Dendritic Catalysts Immobilized on Solid Support: Synthesis and Dendritic Effects in Catalysis. J. Polymer Science: Part A: Polymer Chemistry, 43 (2005) 235.

[20] D. Astruc, K. Heuzé, S. Gatard, D. Méry, S. Nlate, L. Plault. Metallodendritic Catalysis Redox and Carbon-Carbon Bond Formation Reactions: A Step towards Green Chemistry. Adv. Synth. Catal., 347 (2005) 2005.

[21] D. Astruc. La catalyse métallodendritique : une contribution efficace à la chimie verte. C. R. Chimie, 8 (2005) 1101.

[22] P.-G. de Gennes, H. Hervet. Statistic of « Starburst » polymers. J. Phys. Lett., 44 (1983) 351.

[23] J. Ruiz, G. Lafuente, S. Marcen, C. Ornelas, S. Lazarare, E. Cloutet, J.-C. Blais, D. Astruc. Construction of Giant Dendrimers Using a Tripodal Building Block. J. Am. Chem. Soc., 125 (2003) 7250.

[24] R.L. Lescanec, M. Muthukumar. Configurational characteristics and scaling behavior of starburst molecules: a computational study. Macromolecules, 23 (1990) 2280.

[25] M.L. Mansfield, L. Klushin. Monte Carlo studies of dendrimer macromolecules. Macromolecules, 26 (1993) 4262.

[26] D. Boris, M. Rubinstein. A Self-Consistent Mean Field Model of a Starburst Dendrimer: Dense Core vs Dense Shell. Macromolecules, 29 (1996) 7251.

[27] K. Naidoo, S.J. Hugues, J.R. Moss. Computational Investigations into the Potential Use of Poly(benzyl phenyl ether) Dendrimers as Supports for Organometallic Catalysts. Macromolecules, 32 (1999) 331.

[28] C. Valério, S. Rigaut, J. Ruiz, J.-L. Fillaut, M.-H. Delville, D. Astruc. Engineering Nanoscopic Macromolecules for Applications: Stars versus Dendrimers for Catalysis and Sensoring. Bull. Pol. Acad. Sc., 46 (1998) 309.

[29] S. Rigaut, M.-H. Delville, D. Astruc. Triple C-H/N-H Activation by O_2 for Molecular Engineering : Heterobifunctionalization of the 19-Electron Redox Catalysts FeICp(arene). J. Am. Chem. Soc., 119 (1997) 11132.

[30] S. Rigaut, M.-H. Delville, J. Losada, D. Astruc. Water-soluble Mono- and Star-shaped Hexanuclear Functional Organometallic Catalysts for Nitrate and Nitrite Reduction in Water : Syntheses and Electroanalytical Study. Inorg. Chim. Acta, 334 (2002) 225.

[31] S. Gatard, S. Nlate, E. Cloutet, G. Bravic, J.-C. Blais, D. Astruc. Dendritic Stars by Ring-Opening-Metathesis Polymerization From Ruthenium-Carbene Dendrimers. Angew. Chem. Int. Ed., 42 (2003) 452.

[32] S. Gatard, S. Kahlal, D. Méry, S. Nlate, E. Cloutet, J.-Y. Saillard, D. Astruc. Synthesis, Chemistry, DFT Calculations and ROMP Activity of Monomeric Benzylidene Complexes Containing a Chelating Diphosphine and of Four Generations of Metallodendritic Analogues. Positive and Negative Dendritic Effects and Formation of Dendritic Ruthenium-Polynorbornene Stars. Organometallics, 23 (2004) 1313.

[33] K. Heuzé, D. Méry, D. Gauss, D. Astruc. Copper-free Recoverable Dendritic Catalysts for the Sonogashira Reaction. Chem. Commun., (2003) 2274.

[34] K. Heuzé, D. Méry, D. Gauss, J.-C. Blais, D. Astruc. Copper-Free Monomeric and Dendritic Palladium Catalysts for the Sonogashira Reaction: Substituent Effects, Synthetic Applications, and the Recovery and Re-Use of the Catalysts. Chem. Eur. J., 10 (2004) 3936.

[35] J. Lemo, K. Heuzé, D. Astruc. Efficient Dendritic Diphosphino Pd(II) Catalysts for the Suzuki Reaction of Chloroarenes. Org. Lett., 7 (2005) 2253.

[36] J.W.J. Knapen, A.W. van der Made, J.C. de Wilde, P.W.N.M. van Leeuwen, P. Wijkens, D.M. Grove, G. van Koten. Homogeneous catalysts based on silane dendrimers functionalized with arylnickel(II) complexes. Nature, 372 (1994) 659.

[37] D. de Groot, B.F.M. de Waal, J.N.H. Reek, A.P.H.J. Shenning, P.C.J. Kamer, E.W. Meijer, P.W.N.M. van Leeuwen. Noncovalently Functionalized Dendrimers as Recyclable Catalysts. J. Am. Chem. Soc., 123 (2001) 8453.

[38] P. Byrappa, J.K. Young, J.S. Moore, K.S. Suslick. Dendrimer-Metalloporphyrins: Synthesis and Catalysis. J. Am. Chem. Soc., 118 (1996) 5708.

[39] G.E. Oosterom, R.J. van Haaren, J.N.H. Reek, P.C.J. Kamer, P.W.N.M. van Leeuwen. Catalysis in the core of a carbosilane dendrimer. Chem. Commun., 5 (1999) 1119.

[40] R.M. Crooks, M. Zhao, L. Sun, V. Chechik, L.K. Yeung. Dendrimer-Encapsulated Metal Nanoparticles: Synthesis, Characterization, and Applications to Catalysis. Acc. Chem. Research, 34 (2001) 181.

[41] R.W.J. Scott, O.M. Wilson, R.M. Crooks. Synthesis, Characterization, and Applications of Dendrimer-Encapsulated Nanoparticles. J. Phys. Chem. B, 109 (2005) 692.

[42] R.W.J. Scott, O.M. Wilson, S-K. Oh, E.A. Kenik, R.M. Crooks. Bimetallic Palladium-Gold Dendrimer-Encapsulated Catalysts. J. Am. Chem. Soc., 126 (2004) 15583.

[43] R.W.J. Scott, A.K. Datye, R.M. Crooks. Bimetallic Palladium-Platinum Dendrimer-Encapsulated Catalysts. J. Am. Chem. Soc., 125 (2003) 3708.

[44] Y. Niu, L.K. Yeung, R.M. Crooks. Size-Selective Hydrogenation of Olefins by Dendrimer-Encapsulated Palladium Nanoparticles. J. Am. Chem. Soc., 123 (2001) 6840.

[45] L. Sun, R.M. Crooks. Dendrimer-Mediated Immobilization of Catalytic Nanoparticles on Flat, Solid Supports. Langmuir, 18 (2002) 8231.

[45] R.M. Crooks, M. Zhao, L. Sun, V. Chechik, L.K. Yeung. Dendrimer-Encapsulated Metal Nanoparticles: Synthesis, Characterization, and Applications to Catalysis. Acc. Chem. Research, 34 (2001) 181.

[47] K. Esumi, H. Houdatsu, T. Yoshimura. Antioxidant Action by Gold-PAMAM Dendrimer Nanocomposites. Langmuir, 20 (2004) 2536.

[48] K.R. Gopidas, J.K. Whitesell, M.A. Fox. Synthesis, Characterization, and Catalytic Applications of a Palladium-Nanoparticle-Cored Dendrimer. Nano Letters, 3 (2003) 1757.

[49] L.K. Yeung, R.M. Crooks. Heck Heterocoupling within a Dendritic Nanoreactor. Nano Letters, 1 (2001) 14.

[50] L.K. Yeung, C.T. Lee Jr., K.P. Johnston, R.M. Crooks. Catalysis in supercritical CO2 using dendrimer-encapsulated palladium nanoparticles. Chem. Commun., (2001) 2290.

[51] E.H. Rahim, F.S. Kamounah, J. Frederiksen, J.B. Christensen. Heck Reactions Catalyzed by PAMAM-Dendrimer Encapsulated Pd(0) Nanoparticles. Nano Letters, 1 (2001) 499.

[52] J.C. Garcia-Martinez, R. Lezutekong, R.M. Crooks. Dendrimer-Encapsulated Pd Nanoparticles as Aqueous, Room-Temperature Catalysts for the Stille Reaction. J. Am. Chem. Soc. 127 (2005) 5097.

[53] W.J. Scott, C. Sivadinarayana, O.M. Wilson, Z. Yan, D.W. Goodman, R.M. Crooks. Titania-Supported PdAu Bimetallic Catalysts Preparated from Dendrimer-Encapsulated Nanoparticle Precursors. J. Am. Chem. Soc., 127 (2005) 1380.

[54] M. Pittelkow, K. Moth-Poulsen, U. Boas, J.B. Christensen. Poly(amidoamine)-Dendrimer-Stalilized Pd(0) Nanoparticles as a Catalyst for the Susuki Reaction. Langmuir, 19 (2003) 7682.

[55] G. Larsen, S. Noriega. Dendrimer-mediated formation of Cu-CuOx nanoparticles on silica and their physical and catalytic characterization. Appl. Catal., 278 (2004) 73.

[56] H. Lang, R.A. May, B.L. Iversen, B.D. Chandler. Dendrimer-Encapsulated Nanoparticle Presurcors to Supported Platinum Catalysts. J. Am. Chem. Soc., 125 (203) 14832.

[57] H. Lang, S. Maldonado, K.L. Stevenson, B.D. Chandler. Synthesis and Characterization of Dendrimer Templated Supported Bimetallic Pt-Au Nanoparticles. J. Am. Chem. 126 (2004) 12949.

[58] K. Hayakawa, T. Yoshimura, K. Esumi. Preparation of Gold-Dendrimer Nanocomposites by Laser Irradiation and Their Catalytic Reduction of 4-Nitrophenol. Langmuir, 19 (2003) 5517.

[59] K. Esumi, R. Isono, T. Yoshimura. Preparation of PAMAM- and PPI-Metal (Silver, Platinum, and Palladium) Nanocomposites and Their Catalytic Activities for Reduction of 4-Nitrophenol. Langmuir, 20 (2004) 237.

[60] T. Endo, T. Yoshimura, K. Esumi. Synthesis and catalytic activity of gold-silver binary nanoparticles stabilized by PAMAM dendrimer. J. Colloid Interface Sci., 286 (2005) 602.

[61] K. Esumi, K. Miyamoto, T. Yoshimura. Comparison of PAMAM-Au and PPI-Au Nanocomposites and Their Catalytic Activity for Reduction of 4-Nitrophenol. J. Colloid Interface Sci., 254 (2002) 402.

[62] Y.-M. Chung, H.-K. Rhee. Dendritic chiral auxiliaries on silica: a new heterogeneous catalyst for enantioselective addition of diethylzinc to benzaldehyde. Chem. Commun., (2002) 238.

[63] L. Balogh, D.A. Tomalia. Poly(amidoamine) dendrimer-templated nanocomposites. 1. Synthesis of zerovalent copper nanoclusters [5]. J. Am. Chem. Soc., 120 (1998) 7355.

[64] H. Brunner. Dendrizymes: Expanded ligands for enantioselective catalysis. J. Organomet. Chem., 500 (1995) 39.

[65] D. Seebach, H. Sellner. Dendritically Cross-Linking Chiral Ligands: High Stability of a Polystyrene-Bound Ti-TADDOLate Catalyst with Diffusion Control. Angew. Chem. Int. Ed., 38 (1999) 1918

[66] D. Seebach, A.K. Beck, A. Heckel. TADDOLs, Their Derivatives, and TADDOL Analogues: Versatile Chiral Auxiliaries. Angew. Chem. Int. Ed., Engl., 40 (2001) 92.

[67] C. Köllner, B. Pugin, A. Togni. Dendrimers Containing Chiral Ferrocenyl Diphosphine Ligands for Asymmetric Catalysis. J. Am. Chem. Soc., 120 (1998) 10274.

[68] P. Arya, N.V. Rao, J. Singkhonrat, H. Alper, S.C. Bourque, L.E. Manzer. A divergent, solid-phase approach to dendritic ligands on beads. Heterogeneous catalysis for hydroformylation reactions . J. Org. Chem., 65 (2000) 1881.

[69] P. Arya, G. Panda, N.V. Rao, H. Alper, S.C. Bourque, L.E. Manzer. Solid-phase catalysis: A biomimetic approach toward ligands on dendritic arms to explore recyclable hydroformylation reactions. J. Am. Chem. Soc., 123 (2001) 2889.

[70] A. Dahan, M. Portnoy. Dendrons and Dendritic Catalysts Immobilized on Solid Support: Synthesis and Dendritic Effects in Catalysis. J. Polymer Science: Part A: Polymer Chemistry, 43 (2005) 235.

[71] A. Dahan, M. Portnoy. Dendritic effect in polymer-supported catalysis of the intramolecular Pauson-Khand reaction. Chem. Comm., 22 (2002) 2700.

[72] A. Dahan, M. Portnoy. Remarkable Dendritic Effect in the Polymer-Supported Catalysis of the Heck Arylation of Olefins. Organic Letters, 5 (2003) 1197.

[73] L. Plault, A. Hauseler, S. Nlate, D. Astruc, J. Ruiz, S. Gatard, R. Neumann. Synthesis of Dendritic Polyoxometalate Complexes Assembled by Ionic Bonding and Their Function as Recoverable and Reusable Oxidation Catalysts. Angew. Chem. Int. Ed., 43 (2004) 2924.

[74] S. Nlate, D. Astruc, R. Neumann. Synthesis, Catalytic Activity in Oxidation Reactions, and Recyclability of Stable Polyoxometalate-Centred Dendrimers. Adv. Synth. Catal., 346 (2004) 1445.

[75] M.V. Vasylyev, D. Astruc, R. Neumann. Dendritic Phosphonates and the in situ Assembly of Polyperoxophosphotungstates: Synthesis and Catalytic Epoxidation of Alkenes with Hydrogen Peroxide. Adv. Synth. Catal., 347 (2005) 39.

[76] G.E. Oosterom, S. Steffens, J.N.H. Reek, P.C.J. Kamer, P.W.N.M. van Leeuwen. Core-functionalized dendrimeric mono- and diphosphine rhodium complexes; application in hydroformylation and hydrogenation. Top. Catal., 19 (2002) 1.

[77] R.A. Findeis, L.H. Gade. Tripodal Phosphane Ligands with Novel Linker Units and Their Rhodium Complexes as Building Blocks for Dendrimer Catalysts. Eur. J. Inorg. Chem., (2003) 99.

[78] A.K. Kakkar. Dendritic Polymers: From Efficient Catalysis to Drug Delivery. Macromol. Symp., 196 (2003) 145.

[79] L. Ropartz, R.E. Morris, D.F. Foster, D.J. Cole-Hamilton. Increased selectivity in hydroformylation reactions using dendrimer based catalysts; a positive dendrimer effect. Chem. Commun., (2001), 361.

[80] L. Ropartz, R. E. Morris, D. F. Foster, D. Cole-Hamilton. Phosphine-containing carbosilane dendrimers based on polyhedral silsesquioxane cores as ligands for hydroformylation reaction of oct-1-ene. J. Mol. Cat. A: Chem., 182-183 (2002) 99.

[81] T.R. Krishna and N. Jayaraman. Synthesis and catalytic activities of PdII-phosphine complexes modified poly(ether imine) dendrimers. Tetrahedron, 60 (2004) 10325.

[82] G.S. Smith, S.F. Mapolie. Iminopyridyl-palladium dendritic catalyst precursors: evaluation in Heck reactions. J. Mol. Cat. A: Chem., 213 (2004) 187.

[83] C. Müller, L.J. Ackerman, J.N.H. Reek, P.C.J. Kamer and P.W.N.M. van Leeuwen. Site-Isolation in a Dendritic Nickel Catalyst for the Oligomerization of Ethylene. J. Am. Chem. Soc., 126 (2004) 14960.

[84] G. Smith, R. Chen, S. Mapolie. The synthesis and catalytic activity of a first-generation poly(propylene imine) pyridylimine palladium metallodendrimer. J. Organometal. Chem., 673 (2003) 111.

[85] R. Andrés, E. de Jésus, F. Javier de la Mata, J.C. Flores and R. Gómez. Titanocene and Zirconocene Complexes containing Dendrimer-Substituted Cyclopentadienyl Ligands – Synthesis and Ethylene Polymerization. Eur. J. Inorg. Chem., (2002) 2281.

[86] M. Mager, S. Becke, H. Windisch and U. Denninger. Noncoordinating Dendrimer Polyanions: Cocatalysts for the Metallocene-Catalyzed Olefin Polymerization. Angew. Chem. Int. Ed., 40 (2001) 1898.

[87] R. Andrés, E. de Jesus, F.J. de la Mata, J.C. Flores, R. Gomez. Dendritic β-diketiminato titanium and zirconium complexes: synthesis and ethylene polymerisation. J. Organometal. Chem., 690 (2005) 939.

[88] Z.-J. Zheng, J. Chen, Y.-S. Li. The synthesis and catalytic of poly(bis(imino)pyridyl) iron(II) metallodendrimer. J. Organometal. Chem., 689 (2004) 3040.

[89] M. Uyemura, T. Aida. Steric Control of Organic Transformation by a Dendrimer Cage: Organocobalt Dendrimer Porphyrins as Novel Coenzyme B12 Mimics. J. Am. Chem. Soc., 124 (2002) 11392.

[90] M. Uyemura, T. Aida. Characteristics of Organic Transformations in a Confined Dendritic Core: Studies on the AINBN-Initiated Reaction of Dendrimer Cobalt(II) Porphyrins with Alkynes. Chem. Eur. J., 9 (2003) 3492.

[91] F. Chérioux, C.M. Thomas, B. Therrien, G. Süss-Fink. Dendritic Systems Based on Dinuclear Ruthenium or Rhodium Units Generating Peripheral Catalytic Sites. Chem. Eur. J., 8 (2002) 4377.

[92] M. Albrecht, N.J. Hovestad, J. Boersma, G. van Koten. Multiple Use of Soluble Metallodendritic Materials as Catalysts and Dyes. Chem. Eur. J., 7 (2001) 1289.

[93] M.Q. Slagt, J.T.B.H. Jastrzebski, R.J.M. Klein Gebbink, H.J. van Ramesdonk, J.W.Verhoeven, D.D. Ellis, A.L. Spek, G. van Koten. Pyrenoxy-Based NCN-Pincer Palladium(II) Molecular Tweezers: Synthesis, Properties in Solution and Catalysis. Eur. J. Org. Chem., (2003) 1692.

[94] Z. Zhang, X. Yu, L.K. Fong, L.D. Margerum. Ligand effects on the phosphoesterase activity of Co(II) Schiff base complexes built on PAMAM dendrimers. Inorg. Chim. Acta, 317 (2001).

[95] H.-F. Chow, C.-W. Wan. Multicenter Homogeneous Dendritic Catalysts: The Higher the Generation, the Better the Reactivity and Selectivity? – A comparative Study of the Catalytic Efficiency of Dendrimeric [1,1'-Binaphtalene]-2,2'-diol-Derived Catalysts. Helvetica Chimica Acta, 85 (2002).

[96] M. Benito, O. Rossell, M. Seco, G. Muller, J.I. Ordinas, M. Font-Bardia, X. Solans. Palladium and Platinium Units Grafted on the Periphery of Carbosilane Dendrimers. Eur. J. Inorg. Chem., (2002) 2477.

[97] S.V. Aathimanikandan, B.S. Sandanaraj, C.G. Arges, C.J. Bardeen, S. Thayumanavan. Effect of Guest Molecule Flexibility in Access to Denditic Interiors. Organic Letters,7 (2005) 2809.

[98] D. Astruc, J.-C. Blais, M.-C. Daniel, V. Martinez, S. Nlate, J. Ruiz. Nano-Scale Metallodendritic Complexes in Electron-Transfer Processes and Catalysis. Macromol. Symp., 196 (2003) 1.

[99] M. Ooe, M. Murata, T. Mizugaki, K. Ebitani, K. Kaneda. Supramolecular Catalysts by Encapsulating Palladium Complexes within Dendrimers. J. Am. Chem. Soc., 126 (2004) 1604.

[100] T. Mizugaki, Y. Miyauchi, M. Murata, K. Ebitani, K. Kaneda. Dendritic Nanoreactor Encapsulating Rh Complex Catalyst for Hydroformylation. Chemistry Letters, 34 (2005).

[101] D. Méry, D. Astruc. Synthesis of monomeric and dendritic ruthenium benzylidene cis-bis-tertiobutyl phosphine complexes that catalyze the ROMP of norbornene under ambient conditions. J. Molecular Catal., 227 (2005) 1.

[102] S. Gatard, S. Kahlal, D. Méry, S. Nlate, E. Cloutet, J.-Y. Saillard, D. Astruc. Synthesis, Chemistry, DFT Calculations, and ROMP Activity of Monomeric Benzylidene Complexes Containing a Chelating Diphosphine and of Four Generations of Metallodendritic Analogues. Positive and Negative Dendritic Effects and Formation of Dendritic Ruthenium – Polynorbornene Stars. Organometallics, 23, (2004) 1313.

[103] D. Astruc, J.-C. Blais, M.-C. Daniel, S. Gatard, S. Nlate, J. Ruiz. Metallodendrimers and dendronized gold colloids as nanocatalysts, nanosensors and nanomaterials for molecular electronics. C. R. Chimie, 6-8 (2003)1049.

[104] Y. Zhao, Y. Chen, C. Chen, F. Xi. Synthesis of well-defined star polymers and star block copolymers from dendrimer initiators by atom-transfer-radical polymerization. Polymer, 46 (2005) 5808.

[105] Y. Zhao, X. Shuai, C. Chen, F. Xi. Synthesis of Star Block Copolymers from Dendrimer Initiators by Combining Ring-Opening Polymerization and Atom Transfer Radical Polymerization. Macromolecules, 37 (2004) 8854.

[106] A. Würsch, M. Möller, T. Glauser, L.S. Lim, S.B. Voytek, J.L. Hedrick. Dendritic – Linear AxBx Block Copolymers Prepared via Controlled Ring-Opening Polymerization of Lactones from Orthogonally Protected Multifunctional Initiators. Macromolecules, 34 (2001) 6601.

[107] T. Arai, T. Sekiguti, Y. Iizuka, S. Takizawa, S. Sakamoto, K. Yamaguchi, H. Sasai. A dendrimer-supported heterobimetallic asymmetric catalyst. Tetrahedron: Asymmetry, 13 (2002) 2083.

[108] Q.-H. Fan, G.-H. Liu, X.-M. Chen, G.-J. Deng, A.S.C. Chan. The synthesis of dendritic BINOL ligands and their applications in the enantioselective Lewis acid catalysed addition of diethylzinc to aldehyde. Tetrahedron: Asymmetry, 13 (2001) 1559.

[109] H. Sellner, J.K. Karjalainen, D. Seebach. Preparation of Dendritic and Non-Dendritic Styryl-Substituted Salens for Cross-Linking Suspension Copolymerization with Styrene and Multiple Use of the Corresponding Mn and Cr Complexes in Enantioselective Epoxidations and Hetero-Diels – Alder Reactions. Chem. Eur. J., 7 (2001) 2873.

[110] B. Ji, Y. Yuan, J. Meng. Assembled Dendritic Titanium Catalysts for Enantioselective Hetero-Diels – Alder Reaction of Aldehydes with Danishefsky's Diene. Chem. Eur. J., 9 (2003) 5989.

[111] Y. Ribourdouille, G.D. Engel, M. Richard-Plouet, L.H. Gade. A strongly positive dendrimer effect in asymmetric catalysis: allylic aminations with Pyrphos-palladium functionalised PPI and PAMAM dendrimers. Chem. Commun., (2003) 1228.

[112] G. Guillena, R. Kreiter, R. van de Coevering, R.J.M. Klein Gebbing, G. van Koten, P. Mazon, R. Chinchilla, C. Najera. Chiroptical properties and applications in PTC of new dendritic cinchonidine-derived ammonium salts. Tetrahedron Asymmetry, 14 (2003) 3705.

[113] M. Malkoch, K. Hallman, S. Lutsenko, A. Hult, E. Malmström, C. Moberg. Dendritic Oxazoline Ligands in Enantioselective Palladium-Catalyzed Allylic Alkylations. J. Org. Chem., 67 (2002) 8197.

[114] B.-Y. Yang, X.-M. Chen, G.-J. Deng, Y.-L. Zhang, Q.-H. Fan. Chiral dendritic bis(oxazoline) copper(II) complexes as Lewis acid catalysts for enantioselective aldol reactions in aqueous media. Tetrahedron Letters, 44 (2003) 3535.

[115] P.N.M. Botman, A. Amore, R. van Heerbeek, J.W. Back, H. Hiemstra, J.N.H. Reek, J.H. van Maarseveen. Dendritic phosphoramidite ligands in Rh-catalysed asymmetric hydrogenations. Tetrahedron Letters, 45 (2004) 5999.

[116] G.-J. Deng, B. Yi, Y.-Y. Huang, W.-J. Tang, Y.-M. He, Q.-H. Fan. Dendronized Poly(Ru-BINAP) Complexes: Highly Effective and Easily Recyclable Catalysts for Asymmetric Hydrogenation. Adv. Synth. Catal. 346 (2004) 1440.

[117] P.N. Liu, Y.C. Chen, X.Q. Li, Y.Q. Tu and J.G. Deng. Dendritic catalysts for asymmetric transfer hydrogenation based (1S,2R)-norephedrine derived ligandsTetrahedron: Asymmetry, 14 (2003) 2481.

[118] Y-C. Chen, T-F. Wu, L. Jiang, J-G. Deng, H. Liu, J. Zhu. Y-Z. Jiang. Synthesis of Dendritic Catalysts and Application in Asymmetric Transfer Hydrogenation. J. Org. Chem., 70 (2005) 1006.

[119] G.D. Engel and L.H. Gade. Construction and Probing of Multisite Chiral Catalysts: Dendrimer Fixation of C2-Symmetrical Diphosphinerhodium Complexes. Chem. Eur. J., 8 (2002) 4319.

[120] G-J. Deng, Q-H. Fan, X-M. Chen, D-S. Liu, A.S.C. Chan. A novel system consisting of easily recyclable dendritic Ru-BINAP catalyst for asymmetric hydrogenation. Chem. Commun., (2002) 1570.

[121] Y-C. Chen, T-F. Wu, J-G. Deng, H. Liu, X. Cui, J. Zhu, Y-Z. Jiang, M.C.K. Choi, A.S.C. Chan. Multiple Dendritic Catalysts for Asymmetric Transfer Hydrogenation J. Org. Chem. 67 (2002) 5301.

[122] C. Köllner, A. Tigni. Synthesis, characterization, and application in asymmetric catalysis of dendrimers containing chiral ferrocenyl diphosphines. Can. J. Chem., 79 (2001) 1762.

[123] S-M. Lu, H. Alper. Carbonylative Ring Expansion of Aziridines to β-Lactams with Rhodium-Complexed Dendrimers on a Resin. J. Org. Chem., 69 (2004) 3558.

[124] P. Arya, G. Panda, N.V. Rao, H. Alper, S.C. Bourque and L.E. Manzer. Solid-Phase Catalysis: A Biomimetic Approach toward Ligands on Dendritic Arms to Explore Recyclable Hydroformylation Reactions. J. Am. Chem. Soc., 123 (2001) 2889.

[125] S-M. Lu and H. Alper. Hydroformylation Reactions with Recyclable Rhodium-Complexed Dendrimers on a Resin. J. Am. Chem. Soc., 125 (2003) 13126.

[126] J.P.K. Reynhardt, Y. Yang, A. Sayari, H. Alper. Periodic Mesoporous Silica-Supported Recyclable Rhodium-Complexed Dendrimer Catalysts. Chem. Mater., 16 (2004) 4095.

[127] R. Touzani, H. Alper. PAMAM dendrimer-palladium complex catalysed synthesis of five-, six- or seven membered ring lactones and lactams by cyclocarbonylation methodology. J. Mol. Catal., 227 (2005) 197.

[128] S. Antebi, P. Arya, L.E. Manzer, H. Alper. Carbonylation Reactions of Iodoarenes with PAMAM Dendrimer-Palladium Catalysts Immobilized on Silica. J. Org. Chem., 67 (2002) 6623.

[129] R. Chanthateyanonth, H. Alper. Recyclable Tridentate Stable Palladium(II) PCP-Type Catalysts Supported on Silica for the Selective Synthesis of Lactones. Adv. Synth. Catal., 346 (2004) 1375.

[130] Y-M. Chung, H-K. Rhee. Dendritic chiral auxiliaries on silica: a new heterogeneous catalyst for enantioselective addition of diethylzinc to benzaldehyde. Chem. Commun., (2002) 238.

[131] B.M.L.M. Suijkerbuijk, L. Shu, R.J.M. Klein Gebbink, A. Dieter Schlüter, G. van Koten. Single-Site Catalysts on a Cylindrical Support beyond Nanosize Organometallics, 22 (2003) 4175.

[132] T. Mizugaki, C.E. Hetrick, M. Murata, K. Ebitani, M. D. Amiridis, K. Kaneda. Quaternary Ammonium Dendrimers as Lewis Base Catalysts for Mukaiyama-Aldol Reaction. Chemistry Letters, 34 (2005) 420.

[133] J.L. Kreider, W.T. Ford. Quaternary Ammonium Ion Dendrimers from Methylation of Poly(propylene imine)s. J. Polym. Sciences, 39 (2001) 821.

[134] E. Murugan, R.L. Sherman, Jr., H.O. Spivey, W.T. Ford. Catalysis by Hydophobically Modified Poly(propylenimine) Dendrimers Having Quaternary Ammonium and Tertiary Amine Functionality. Langmuir, 20 (2004) 8307.

[135] A. Clouet, T. Darbre, J.-L. Reymond. A combinatorial Approach to Catalytic Peptide Dendrimers. Angew. Chem. Int. Ed., 43 (2004) 4612.

[136] A. Esposito, E. Delort, D. Lagnoux, F. Djojo, J.-L. Reymond. Catalytic Peptide Dendrimers. Angew. Chem. Int. Ed., 42 (2003) 1381.

[137] D. Lagnoux, E. Delort, C. Douat-Casassus, A. Esposito, J.-L. Reymond. Synthesis and Esterolytic Activity of Catalytic Peptide Dendrimers. Chem. Eur. J., 10 (2004) 1215.

[138] C. Douat-Casassus, T. Darbre, J.-L. Reymond. Selective Catalysis with Peptide Dendrimers. J. Am. Chem. Soc., 126 (2004) 7817.

[139] R. Roesler, B.J.N. Har, W.E. Piers. Synthesis and Characterization of (Perfluoroaryl)borane-Functionalized Carbosilane Dendrimers and Their Use as Lewis Acid Catalysts for the Hydrosilation of Acetophenone. Organometallics, 21 (2002) 4300.

[140] H. Sellner, P.B. Rheiner, D. Seebach. Preparation of Polystyrene Beads with Dendritically Embedded TADDOL and Use in Enantioselective Lewis Acid Catalysis. Helvitica Chimica Acta, 85 (2002) 352.

[141] A.V. Davis, M. Driffield, D.K. Smith. A Dendritic Active Site: Catalysis of the Henry Reaction. Organic Letters, 3 (2001) 3075.

[142] A. Zubia, F.P. Cossio, I. Morao, M. Rieumont, X. Lopez. Quantitative Evaluation of the Catalytic Activity of Dendrimers with Only One Active Center at the Core: Application to the Nitroaldol (Henry) Reaction. J. Am. Chem. Soc., 126 (2004) 5243.

[143] A. Sarkar, P. Ilankumaran, P. Kisanga, J.G. Verkade. First Synthesis of a Highly Basic Dendrimer and its Catalytic Application in Organic Methodology. Adv. Synth. Catal., 346 (2004) 1093.

[144] X. Zhang, H. Xu, Z. Dong, Y. Wang, J. Liu, J. Shen. Highly Efficient Dendrimer-Based Mimic of Glutathione Peroxidase. J. Am. Chem. Soc., 126 (2004) 10556.

[145] C.O. Liang. B. Helms. C.J. Hawker, J.M.J. Fréchet. Dendronized cyclocopolymers with a radial gradient of polarity and their use to catalyze a difficult esterification. Chem. Commun., (2003) 2524.

[146] B. Helms, C.O. Liang, C.J. Hawker, J.M.J. Fréchet. Effects of Polymer Architecture and Nanoenvironment in Acylation Reactions Employing Dendritic (Dialkylamino)pyridine Catalysts. Macomolecules, 38 (2005) 5411.

[147] I.K. Martin, L.J. Twyman. Acceleration of an aminolysis reaction using a PAMAM dendrimer with 64 terminal amine groups. Tetrahedron Letters, 42 (2001) 1123.

[148] L. J. Twyman, A. S. H. King, I. K. Martin. Catalysis inside dendrimers. Chem. Soc. Rev., 31 (2002) 69.

[149] I. Sato, K. Hosoi, R. Kodaka, K. Soai. Asymmetric Synthesis of N-(Diphenylphosphinyl)amines Promoted by Chiral Carbosilane Dendritic Ligands in the Enanthioselective Addition of Dialkylzinc Compounds to N-(Diphenylphosphinyl)imines. Eur. J. Org. Chem., (2002) 3115.

[150] I. Sato, R. Kodaka, K. Hosoi, K. Soai. Highly enantioselective addition of dialkylzincs to aldehydes using dendritic chiral catalysts with flexible carbosilane backbones. Tetrahedron: Asymmetry, 13 (2002) 805.

[151] C. Francvilla, M.D. Drake, F.V. Bright, M.R. Detty. Dendrimeric Organochalcogen Catalysts for the Activation of Hydrogen Peroxide: Improved Catalytic through Statistical Effects and Cooperativity in Successive Generations. J. Am. Chem. Soc., 123 (2001) 57.

[152] M.D. Drake, F.V. Bright, M.R. Detty. Dendrimeric Organochalcogen Catalysts for the Activation of Hydrogen Peroxide: Origins of the “Dendrimer Effect” with Catalysts Terminating in Phenylseleno Groups. J. Am. Chem. Soc., 125 (2003) 12558.

Partie I

Métallodendrimères de Palladium pour la catalyse de la réaction de Sonogashira

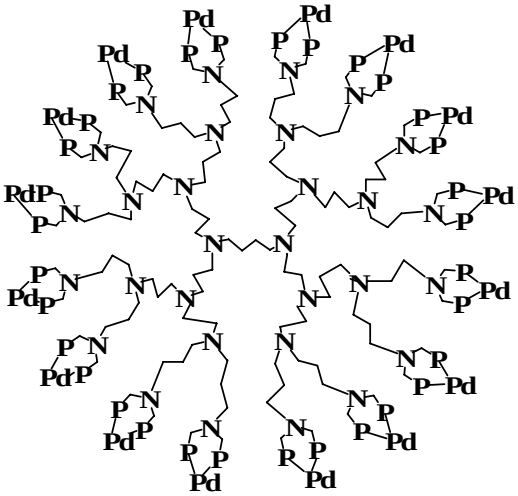

La protection de l'environnement constitue un des enjeux majeurs de notre société. Les réglementations françaises, européennes et internationales sont en train d'imposer des contraintes de plus en plus sévères concernant la concentration de métaux lourds et l'utilisation des produits chimiques en général. Des recherches doivent donc être mises en œuvre pour trouver des solutions alternatives, des procédés propres et des voies viables en accord avec les normes de la *Chimie Verte*.

C'est dans cet objectif que nous avons élaboré de nouveaux métallodendrimères de palladium afin de catalyser la réaction de Sonogashira (Schéma 1). En effet, les catalyseurs métallodendritiques combinent les avantages de la catalyse homogène et hétérogène. Ces complexes sont solubles dans les solvants réactionnels, ils sont facilement séparables du milieu par ultrafiltration, ultracentrifugation ou précipitation et peuvent donc être recyclés.

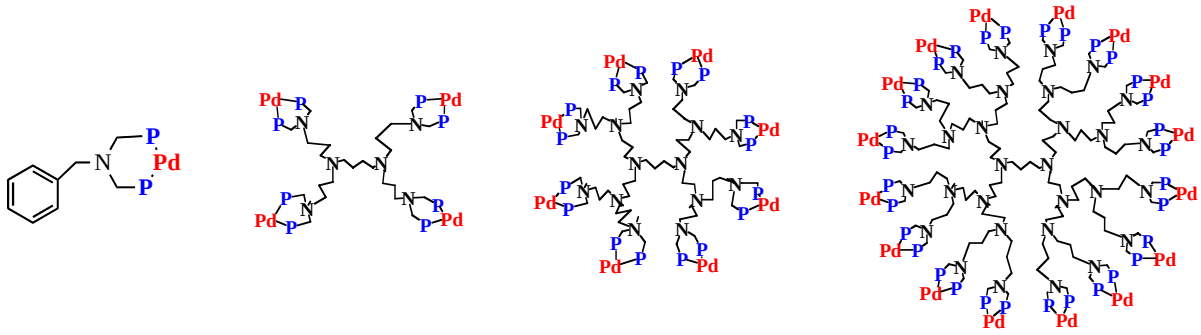

Schéma 1 : Complexes modèle et dendritiques de Palladium (P = Pt-Bu$_2$ et Pd = Pd(OAc)$_2$)

Nous avons utilisé ces complexes pour la catalyse de la réaction de Sonogashira, qui est une réaction de couplage carbone-carbone (Équation 1). La réaction met en jeu un halogénure de vinyle ou d'aryle et un acétylénique. Elle est sans doute, avec la réaction de Heck, la plus spectaculaire des méthodes de couplage car ces deux méthodes ne nécessitent pas la préparation d'un organométallique.

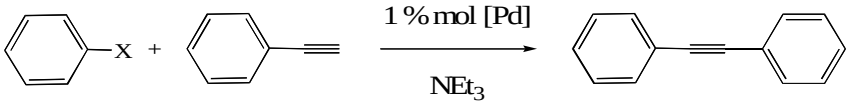

X = I, Br, Cl

Équation 1 : Réaction de Sonogashira

Dans une étude préliminaire, nos travaux se sont inscrits dans l'élaboration d'un nouveau complexe modèle de palladium dérivé de l'acétate de palladium (Schéma 1). Ses propriétés catalytiques ont été étudiées pour la réaction de Sonogashira avec des dérivés iodés, bromés et chlorés. Ces travaux sur le complexe modèle de palladium (II) ont fait l'objet d'une note publiée à *Chemical Communications* et intitulée "**A very efficient, copper-free palladium catalyst for the Sonogashira reaction with aryl halides**".

Ensuite, trois générations de métallodendrimères di*tert*butylphosphines de palladium (II) ont été synthétisées (Schéma 1), et leurs activités catalytiques ont été étudiées. L'effet dendritique entre les différentes générations est discuté, de même que leurs recyclabilités. Parallèlement à cette série, des complexes dicyclohexylphosphines de palladium (II) ont aussi été élaborés par K. Heuzé et D. Gauss. L'effet du groupement alkyle de la phosphine a ainsi pu être discuté. Ces travaux sur les complexes dendritiques de palladium (II) ont fait l'objet d'une note publiée à *Chemical Communications* et intitulée "**Copper-free, recoverable dendritic Pd catalysts for the Sonogashira reaction**".

Pour finir, les activités catalytiques de nos métallodendrimères de différentes générations et des complexes modèles ont été comparées. Nous avons aussi effectué la réaction de Sonogashira sur des substrats hexafonctionnels en étoile. L'ensemble de ces travaux, rassemblant également les deux notes précédentes, a fait l'objet d'un mémoire publié à *Chemistry - A European Journal* et intitulé "**Copper-Free Monomeric and Dendritic Palladium Catalysts for the Sonogashira Reaction: Substituent Effects, Synthetic Applications, and the Recovery and Re-Use of the Catalysts**". Dans cet article, notre laboratoire a collaboré avec Jean-Claude Blais, du LCSOB à Paris VI, qui a réalisé les spectres de masse.

COMMUNICATION

ChemComm
www.rsc.org/chemcomm

A very efficient, copper-free palladium catalyst for the Sonogashira reaction with aryl halides

Denise Méry, Karine Heuzé and Didier Astruc
Groupe Nanosciences Moléculaires et Catalyse, LCOO, UMR N° 5802, Université Bordeaux 1, 351 Cours de la Libération, 33405 Talence Cedex, France

Received (in Cambridge, UK) 13th May 2003, Accepted 16th June 2003
First published as an Advance Article on the web 1st July 2003

The new complex [Pd{*t*-Bu$_2$PCH$_2$N(CH$_2$Ph)CH$_2$P*t*-Bu$_2$}(OAc)$_2$] is a very efficient catalyst for the Sonogashira cross-coupling reaction of aryl halides with acetylenes at room temperature, without co-catalyst.

The Sonogashira cross-coupling reaction is a useful straightforward synthetic strategy for the synthesis of aryl or vinyl acetylenes from aryl or vinyl halides and terminal alkynes (eqn. 1). The most usual procedure for this reaction uses Pd(0)/Cu(I)-catalysts and a base (often an amine as solvent).[1,2] Actually, Pd(II) catalysts generally exhibit greater long-term stability than Pd(0) species and can be stored under normal laboratory conditions for several months. In the Pd(II)/Cu(I)-catalytic system, the active 14-electron Pd(0) catalyst is formed by Cu(I)-catalyzed bis-alkynylation of the Pd complex followed by reductive elimination of diphenyldiacetylene.

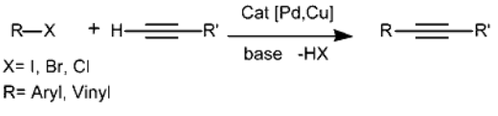

(1)

Many applications of the Sonogashira coupling of aryl halides with terminal alkynes have been reported in the literature since 1975. For instance, Ryu recently described such a coupling in ionic liquids with the purpose of recycling the catalyst,[3] and Mori used TBAF/Ag$_2$O system as co-catalyst reagents.[4] The use of aryl bromide or chloride, however, has only been recently explored owing to their poor reactivity.[5] Nevertheless, it is of great interest to extend the scope of this reaction to these aryl halides because of their low cost, especially for synthetic laboratory and industrial chemistry.

On the other hand, very few examples of single "palladium-only" catalysts have been reported to be active in this cross-coupling reaction without the presence of a co-catalyst. Recently, Böhm and Hermann proposed a copper-free procedure using [Pd$_2$(dba)$_3$/P(*t*-Bu)$_3$] as a catalyst for the Sonogashira reaction of aryl bromides at room temperature.[6] Pal *et al.* used [PdCl$_2$(PPh$_3$)$_2$] at 80 °C in a copper-free procedure to synthesize 4-substituted-aryl-1-butanones from aryl bromides.[7] The Pd(OAc)$_2$/PPh$_3$ mixture has been used by Fu *et al.* in a copper-free catalyzed cross-coupling reaction of vinyl tosylates with terminal acetylenes, and Nájera *et al.* described an amine-free and copper-free Sonogashira coupling procedure of aryl iodides and bromides catalyzed by oxime palladacycles with high TON's.[8] These improved procedures in the absence of a co-catalyst avoid the oxidative homo-coupling reaction of the acetylenic reagent that is observed in the presence of a Cu(I) co-catalyst. Some Cu(I) acetylides are formed *in situ* and can undergo oxidative dimerization to diphenyldiacetylenes if they are exposed to air (a reaction known as the Glaser coupling).[9] These by-products are generally not easy to separate from the desired products.

We now report the synthesis and the remarkable catalytic activity in Sonogashira cross-coupling of complex **1** in which a bulky and electron-rich chelating bis-*tert*-butylphosphine ligand (Chart 1) is coordinated to Pd(II).

Bis{*tert*-butylaminomethylphosphine} has been synthesized by addition of benzylamine onto a bis-*tert*-butylhydroxymethylphosphonium salt prepared according to a known procedure.[10] The palladium complex was synthesized by treatment of bis{*tert*-butylaminomethylphosphine} with palladium acetate at room temperature for one hour. This Pd(II) complex **1** was purified by further precipitations from CH$_2$Cl$_2$/pentane, and was stored under nitrogen. It was isolated with 95% yield and was characterized by ^{1}H, ^{13}C and ^{31}P NMR.†

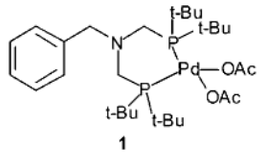

1

Chart 1

The ability of **1** to cross-couple acetylenes with aryl halides in a simple one-pot procedure without a co-catalyst and at low catalyst concentrations is summarized in Table 1 and eqn. 2. All reactions were carried out using triethylamine as both the base and solvent, and between −40 °C and 80 °C. The products were purified and analyzed by ^{1}H NMR. Isolated yields were determined after silica-gel column chromatography (Table 1). The cross-coupling reactions are quantitative, and very fast conversions are obtained at 1 mol% Pd loading for iodobenzene and bromobenzene (entries 1, 2, 10 and 11) even at room temperature. Note that the reaction also occur at low temperatures in good yields (entries 3 and 4). The Pd complex **1** shows excellent activity, and we even obtained turnover numbers as high as 10^5 for entry 9. Trimethylsilylacetylene was cross-coupled with both iodobenzene and bromobenzene at room temperature in good but not quantitative yields (entries 5 and 13). Indeed, Nolan reported Sonogashira cross-coupling of aryl halides with the TMS group of substituted trimethylsilyl-acetylenes, giving substituted phenylacetylenes in good yields.[11] In our case dealing with trimethylsilyacetylene itself, however, products resulting from its dimerization are formed as indicated by mass spectral evidence, which lowers the cross-coupling yields (entries 5 and 13).

Substantial reactivity of aryl chlorides with acetylenes is found in our system even at room temperature (entries 14–21). For instance, activated aryl chlorides give the cross-coupling products in 30% yield (entry 20). The yields are low due to the low rates of the cross-coupling reactions compared to the faster homo-coupling of the alkyne that provides the by-product.

In summary, we have disclosed a very efficient Pd(II) catalyst for the Sonogashira cross-coupling of aryl halides with acetylenes in a simple one-pot procedure free of co-catalyst at room temperature. The yields are good to excellent with arylbromide and iodide and, under these mild conditions, even aryl chlorides give significant results. Future work is directed towards further use of such a ligand, its late-transition-metal

DOI: 10.1039/b305391c

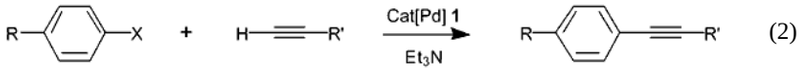

(2)

Table 1 Reactions conditions, conversions and turnover numbers (TON) for the Sonogashira coupling of aryl halides with alkynes using **1** as the sole catalyst[a]

Entry	X	R	R′	Temperature/°C	Catalyst **1** (mol%)	React. time	Conv. (%)[b]	TON
1	I	H	C_6H_5	80	1	15 min	100	100
2	I	H	C_6H_5	25	1	30 min	100	100
3	I	H	C_6H_5	−20	1	1 d	70	70
4	I	H	C_6H_5	−40	1	2 d	51	51
5	I	H	$Si(CH_3)_3$	25	1	8 h	76	76
6	I	H	C_6H_5	80	0.5	15 min	100	200
7	I	H	C_6H_5	80	0.1	2 h	100	1000
8	I	H	C_6H_5	80	0.01	1 d	87	8700
9	I	H	C_6H_5	80	0.001	7 d	71	71000
10	Br	H	C_6H_5	80	1	20 min	100	100
11	Br	H	C_6H_5	25	1	1 h	100	100
12	Br	Me	C_6H_5	80	1	3 h	96	96
13	Br	H	$Si(CH_3)_3$	25	1	15 h	54	54
14	Cl	H	C_6H_5	80	1	50 min	4	4
15	Cl	H	C_6H_5	25	1	3 h	9	9
16	Cl	H	$Si(CH_3)_3$	25	1	2 d	5	5
17	Cl	CN	C_6H_5	80	1	5 d	13	13
18	Cl	F	C_6H_5	80	1	5 d	14	14
19	Cl	$COOCH_3$	C_6H_5	25	1	3 d	15	15
20	Cl	$COOCH_3$	C_6H_5	80	2	3 d	30	30
21	Cl	$COOCH_3$	C_6H_5	40	1	3 d	22	22

[a] *Reaction conditions*: aryl halide (2 mmol), alkyne (3 mmol), Et_3N (6 mL). [b] Unoptimized isolated yield.

complexes and their derivatives including the synthesis of complex molecules.

Notes and references

† Selected data for **1**: ^{1}H NMR ($CDCl_3$, 400 MHz): δ (ppm) 7.25 (m, 5H, Ph), 3.58 (s, 2H, NCH_2), 2.66 (s, 4H, NCH_2P), 1.89 (s, 6H, CH_3), 1.39 (s, 18H, *t*-Bu), 1.32 (s,18H, *t*-Bu). ^{13}C{^{1}H} NMR ($CDCl_3$, 75 MHz): δ (ppm) 31.8 (s, *t*-Bu), 33.2 (s, *t*-Bu), 36.3 (s, Me), 44.1 (s, NCH_2P), 67.5 (s, CH_2N), 128.6–135.1 (s, CH and C arom.), 176 (s, CO). ^{31}P{^{1}H} NMR ($CDCl_3$): δ 27ppm.

1 (*a*) K. Sonogashira, Y. Tohda and N. Hagihara, *Tetrahedron Lett.*, 1975, **50**, 4467; (*b*) *Modern Arene Chemistry*, ed. D. Astruc, Wiley-VCH, Weinheim, 2002.

2 I. B. Campbell, in *Organocopper Reagents: A Practical Approach*, ed. R. J. K. Taylor, OUP, New York, 1994, ch. 10, p. 218; K. Sonogashira, *Comprehensive Organic Synthesis*, ed. B. M. Trost and I. Fleming, Pergamon Press, Oxford, 1991, **vol. 3**, p. 521; R. Rossi, A. Carpita and F. Bellina, *Org. Prep. Proc. Int.*, 1995, **27**, 129.

3 T. Fukuyama, M. Shinmen, S. Nishitani, M. Sato and I. Ryu, *Org. Lett.*, 2002, **4**, 1691.

4 A. Mori, J. Kawashima, T. Shimada, M. Suguro, K. Hirabayashi and Y. Nishihara, *Org. Lett.*, 2000, **2**, 2935.

5 For recent examples, see: B. M. Choudary, S. Madhi, N. S. Chowdari, M. L. Kantam and B. Sreedhar, *J. Am. Chem. Soc.*, 2002, **124**, 14127; M. R. Eberhard, Z. Wang and C. M. Jensen, *Chem. Commun.*, 2002, 818; T. Hundertmark, A. F. Littke, S. L. Buchwald and G. C. Fu, *Org. Lett.*, 2000, **2**, 1729; M. Alami, B. Crousse and F. Ferri, *J. Organomet. Chem.*, 2001, **624**, 114; M. Ansorge and T. J. J. Müller, *J. Organomet. Chem.*, 1999, **585**, 174; S. Thorand and N. Krause, *J. Org. Chem.*, 1998, **63**, 8551.

6 V. P. Böhm and W. A. Hermann, *Eur. J. Org. Chem.*, 2000, 3679.

7 M. Pal, K. Parasuraman, S. Gupta and K. R. Yeleswarapu, *Synlett*, 2002, **12**, 1976 and references therein.

8 X. Fu, S. Zhang, J. Yin and D. Schumacher, *Tetrahedron Lett.*, 2002, **43**, 6673; D. A. Alonso, C. Nájera and M. C. Pacheco, *Tetrahedron Lett.*, 2002, **43**, 9365 and references therein.

9 P. Siemsen, R. C. Livingston and F. Diederich, *Angew. Chem., Int. Ed.*, 2000, **39**, 2632.

10 J. Fawcett, P. A. T. Hoye, R. D. W. Kemmitt, D. J. Law and D. R. Russell, *J. Chem. Soc., Dalton Trans.*, 1993, 2563.

11 C. Yang and S. P. Nolan, *Organometallics*, 2002, **21**, 1020.

COMMUNICATION

ChemComm
www.rsc.org/chemcomm

Copper-free, recoverable dendritic Pd catalysts for the Sonogashira reaction

Karine Heuzé, Denise Méry, Dominik Gauss and Didier Astruc

Groupe Nanosciences Moléculaires et Catalyse, LCOO, UMR CNRS N°5802, Université de Bordeaux 1, 351 cours de la libération, 33405 Talence Cedex, France. E-mail: d.astruc@lcoo.u-bordeaux1.fr, k.heuze@lcoo.u-bordeaux1.fr; Fax: +33 (0)5 4000 6646; Tel: +33 (0)5 4000 6271

Received (in Cambridge, UK) 20th June 2003, Accepted 6th August 2003
First published as an Advance Article on the web 19th August 2003

Three generations of bidentate phosphinated Pd(II) dendrimers are efficient catalysts in the absence of copper co-catalyst for the Sonogashira reaction and are, with two cyclohexyl substituents on the phosphorus atoms, recovered by precipitation and re-used.

Metallodendrimers[1] have been known since the early 90's, and one of their most attractive applications is in catalysis.[2] They might be extremely useful in this area, because they are well-defined and appropriate for classic mechanistic studies typical of homogeneous catalysts. Yet, their nanoscopic size should allow their removal from the reaction medium using methods known for biomolecules. This key property will allow their re-use, an essential perspective in green chemistry involving both ecological and economical reasons. The first example of a recoverable metallodendritic catalyst was reported in 1997 by Reetz for the Heck reaction using Pd dendrimers derived from the dendritic phosphines DAB-dendr-$[N(CH_2PPh_2)_2]_x$ obtained by double phosphinomethylation of the commercial DSM polyamino dendrimers DAB-dendr-$(NH_2)_x$ (x = 4, 8 or 16 for generation 1, 2 or 3 respectively).[3] There has recently been a strong focus on specific techniques aiming at the recovery of metallodendritic catalysts which now need to be applied.[2,4]

Therefore, we report three generations of new palladodendritic complexes **2a–f** based on dendritic phosphine ligands **1a–f** closely related to Reetz's dendrimers that serve as copper-free recoverable catalysts for the Sonogashira coupling between aryl halides and alkynes. These two families of palladodendrimers (Scheme 1, R = Cy *vs.* *t*-Bu) show impressively distinct reactivities and recoverabilities, but a rather similar dendritic effect in the Sonogashira reaction.

The Sonogashira-type carbon–carbon coupling reaction is a very convenient and useful methodology for the preparation of arylalkynes or conjugated enynes, and it is of crucial importance in the synthesis of numerous biologically active compounds.[5] Generally, this coupling is achieved by a palladium–copper catalyzed reaction of aryl or vinyl halide and terminal alkyne.[6]

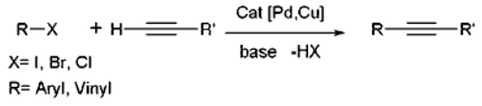

The presence of the copper co-catalyst is an obstacle, however, towards the metallodendritic approach of the catalytic system. In addition, it favors the oxidative homocoupling (Glaser coupling)[7] of the terminal alkyne to the corresponding diyne by-product which is also difficult to separate. Only very few examples of copper-free procedures have been recently reported,[8] involving for instance *in situ* Pd(0) complex formation with bulky phosphines.[9]

As the monomers,[10] the Pd(II) dendrimers **2a–f** were readily obtained by treatment of the aminophosphines **1a–f** with $Pd(OAc)_2$ (Scheme 1), and fully characterized by ^1H, ^{13}C, ^{31}P NMR and elemental analysis.† The ^{31}P NMR spectrum of **2** did not show any signal for the residual free phosphine at δ = −17.5 ppm, (**1a–c**) and δ = 12.9 ppm (**1a–f**) but only one singlet at δ = 26.5 ppm (**2a–c**) and δ = 35.9 ppm (**2d–f**).

Coupling between phenylacetylene and iodobenzene or bromobenzene in a copper-free Sonogashira procedure was investigated using these dendrimers. Et_3N was used as solvent, the catalyst amount was 1 mol% per catalytic group (*i.e.* 1/4, 1/8 and 1/16 mol% depending on the dendrimer generation, respectively; generation 1, 2 and 3), and the temperature range was 25–120 °C (Table 1). Good conversions were obtained with the 1st and 2nd generation dendrimers **2a,b** at 80 °C in the case of iodo coupling (entries 1 and 2). A negative dendritic effect (Fig. 1) is clearly observed for the metallodendrimer of 3rd generation **2c**, however, for which a substantially lower reactivity was obtained (entry 3). This effect is best taken into account by the increased steric effect as the generation number increases. Raising the reaction temperature upon replacing Et_3N by amines with higher boiling points (Bu_2NH, Bu_3N) did not improve the conversion rates, presumably due to the cleavage of

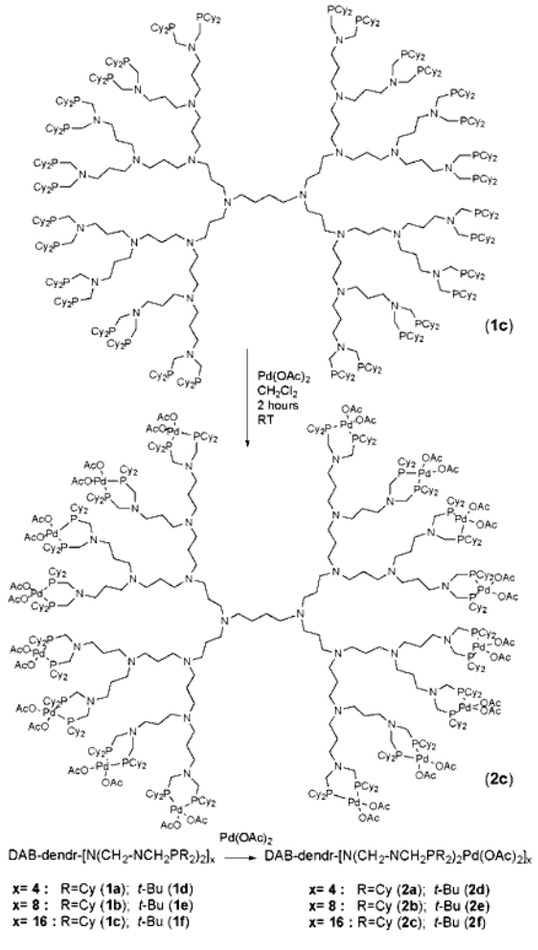

Scheme 1

DOI: 10.1039/b307116m

the P–C bonds of the catalyst at such high temperatures.[11] The same effect is observed with dendrimers **2d–f** containing the di-*tert*-butylphosphine ligand which were considerably more reactive than **2a–c**. Indeed, **2d** provided a quantitative conversion at RT within a few hours (entries 4 and 11) whereas complete conversion required 2 days with the dendrimers of 2nd and 3rd generation **2e,f** (entries 5, 6, 12 and 13).

The dendritic catalysts **2a–f** showed very weak reactivity with the aryl chloride substrates, only traces of expected product being observed (conversion below 5%), although monomeric parent compounds were responsible for higher reactivity in particular with aryl chloride substrates.[10]

A major purpose of this work was to investigate the possibilities of recovering the metallodendritic catalysts, which was indeed achieved by precipitation of **2b** and **2c** after the reaction using pentane. However, the catalysts **2d–f** are too soluble in pentane and other common solvents for recovery, because of the presence of the *t*-Bu substituents. In a typical procedure, the reaction was carried out under nitrogen at 80 °C with **2b** or **2c** (2 mol%). After decantation in pentane, **2b** was recovered at least six times with an average of 46% conversion and **2c** was recovered at least seven times with an average of 35% conversion, both without loss of activity along these cycles. The recovery of the dendritic catalyst was confirmed by ^{31}P NMR, the signal of **2c** or **2d**, initially at 27 ppm, remaining unchanged after each cycle. Nevertheless, a slight shift to 24 ppm of the ^{31}P NMR phosphine signal was observed during the catalytic reaction, which shows the intermediacy of a catalytically active species.

In summary, the synthesis and efficacy of three generations of new recoverable dendritic copper-free catalysts for the Sonogashira reaction has been shown for the first time. These studies have also demonstrated the dendritic effect and the strong influence of the nature of the diphosphine substituents on the reactivity and recoverability of the catalysts.

Table 1 Sonogashira coupling of aryl halide substrates with phenylacetylene[a]

Entry	Aryl halide	Solvent	Catalyst (1 mol%)	Temperature/°C	React. time/h[b]	Conversion (%)[c]
1	Iodobenzene	Et_3N	**2a**	80	24	79
2	Iodobenzene	Et_3N	**2b**	80	24	72
3	Iodobenzene	Et_3N	**2c**	80	24	46
4	Iodobenzene	Et_3N	**2d**	25	15	97
5	Iodobenzene	Et_3N	**2e**	25	40	100
6	Iodobenzene	Et_3N	**2f**	25	48	100
7	Bromobenzene	Et_3N	**2a**	80	48	17
8	Bromobenzene	Et_3N	**2b**	80	48	15
9	Bromobenzene	Bu_2NH	**2b**	120	20	20
10	Bromobenzene	Et_3N	**2c**	80	48	6
11	Bromobenzene	Et_3N	**2d**	25	17	100
12	Bromobenzene	Et_3N	**2e**	25	48	93
13	Bromobenzene	Et_3N	**2f**	25	48	96

[a] Reaction conditions: aryl halide (2 mmol), phenylacetylene (3 mmol), solvent (6 mL), catalyst (1 mol %), N_2. [b] The reaction was monitored by TLC. [c] The product was isolated by column chromatography after the reaction was completed.

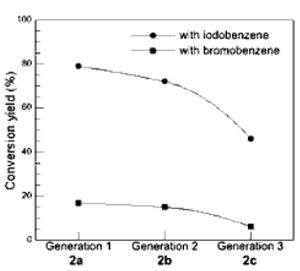

Fig. 1 Conversion of aryl halides with phenylacetylene catalyzed by **2a–c** at 80 °C.

Notes and references

† Selected data for **2a**: ^{1}H NMR ($CDCl_3$, 300 MHz) δ 1.16 (br, 68H, CH_2, CH_{2Cy}), 1.30 (br, 8H, CH_2), 1.59 (br, 32H, CH_{2Cy}), 1.71 (br, 64H, CH_{2Cy}), 1.89 (s, 24H, CH_3), 2.34 (s, 20H, CH_2N), 2.55 (s, 32H, NCH_2P, CHP_{Cy}); ^{13}C NMR ($CDCl_3$, 62.9 MHz) δ 23.5 (CH_2), 26.3 (CH_{2Cy}), 27.4 (CH_{2Cy}), 29.1 (CH_{2Cy}), 30.5 (CH_3), 33.4 (CH_{2Cy}), 48.9 (CH_2N), 52.0 (CH_2N), 61.0 (CHP), 175.9 (CO); ^{31}P NMR ($CDCl_3$, 121.5 MHz) δ 26.5; elemental anal. (calc.) C 56.39%, H 8.63%; (found) C 55.65%, H 8.71%.

1 G. R. Newkome, C. N. Moorefield, F. Vögtle, Dendrimers and A. Dendrons, *Concepts, Syntheses and Applications*, Wiley-VCH, Weinheim, 2002; A. W. Bosman, H. M. Janssen and E. W. Meijer, *Chem. Rev.*, 1999, **99**, 1665; G. R. Newkome, E. He and C. N. Moorefield, *Chem. Rev.*, 1999, **99**, 1689.

2 D. Astruc and F. Chardac, *Chem. Rev.*, 2001, **101**, 2991; G. E. Oosterom, J. N. H. Reek, P. C. J. Kamer and P. W. N. M. van Leeuwen, *Angew. Chem., Int. Ed.*, 2001, **40**, 1828; R. van Heerbeek, P. C. J. Kamer, P. W. N. M. van Leeuwen and J. N. H. Reek, *Chem. Rev.*, 2002, **10**, 3717; R. Kreiter, A. W. Kleij, R. J. M. Klein Gebbink and G. van Koten, *Top. Curr. Chem.*, 2001, **217**, 163.

3 M. T. Reetz, G. Lohmer and R. Schwickardi, *Angew. Chem., Int. Ed. Engl.*, 1997, **36**, 1526; S. Gatard, S. Nlate, E. Cloutet, G. Bravic, J.-C. Blais and D. Astruc, *Angew. Chem., Int. Ed.*., 2003, **42**, 452.

4 D. de Groot, J. N. H. Reek, P. C. J. Kamer and P. W. N. M. van Leeuwen, *Eur. J. Org. Chem.*, 2002, 1085; M. Albrecht, N. J. Hovestad, J. Boersman and G. van Koten, *Chem. Eur. J.*, 2001, **7**, 1289; N. Brinkmann, D. Giebel, G. Lohmer, M. T. Reetz and U. Kragl, *J.Catal.*, 1999, **183**, 163; T. Mizugaki, M. Murata, M. Ooe, K. Ebitani and K. Kaneda, *Chem. Commun.*, 2002, 52.

5 K. Sonogashira, in *Comprehensive Organic Synthesis*, ed. B. M. Trost and I. Fleming, Pergamon Press, Oxford, 1991, vol. 3, p. 521; *Modern Arene Chemistry*, ed. D. Astruc, Wiley-VCH, Weinheim, 2002.

6 K. Sonogashira, Y. Tohda and N. Hagihara, *Tetrahedron Lett.*, 1975, **50**, 4467; I. B. Campbell, *Organocopper reagents : A practical approach*, ed R. J. K. Taylor, 1994, 218; R. Rossi, A. Carpita and F. Bellina, *Org. Prep. Proc.*, 1995, **27**, 129.

7 C. Glaser, *Ber. Dtsch. Chem. Ges.*, 1869, **2**, 422.

8 Y. Uozumi and Y. Kobayashi, *Heterocycles*, 2003, **59**, 71; Pal, M, K. Parasuraman, S. Gupta and K. R. Yeleswarapu, *Synlett*, 2002, **12**, 1976; X. Fu, S. Zhang, J. Yin and D. P. Schumacher, *Tetrahedron Lett.*, 2002, **43**, 6673; D. A. Alonso, C. Nájera and M. C. Pacheco, *Tetrahedron Lett.*, 2002, 9365; V. Farina, S. Kapadia, B. Krishnan, C. Wang and S. L. Liebeskind, *J. Org. Chem.*, 1994, **59**, 5905.

9 V. Böhm and W. A. Herrmann, *Eur. J. Org. Chem.*, 2000, **22**, 3679.

10 D. Mery, K. Heuzé and D. Astruc, *Chem. Commun.*, 2003, 1934.

11 P. W. N. M. van Leeuwen, *Appl. Catal. A*, 2001, **212**, 61.

Copper-Free Monomeric and Dendritic Palladium Catalysts for the Sonogashira Reaction: Substituent Effects, Synthetic Applications, and the Recovery and Re-Use of the Catalysts

Karine Heuzé,*[a] Denise Méry,[a] Dominique Gauss,[a] Jean-Claude Blais,[b] and Didier Astruc*[a]

Abstract: A series of bis(*tert*-butylphosphine)- and bis(cyclohexylphosphine)-functionalized Pd^{II} monomers and polyamino (DAB) dendritic catalysts were synthesized and investigated for Sonogashira carbon–carbon coupling reactions in a copper-free procedure. The influence of phosphine substituents (*t*Bu versus Cy) on the reaction kinetics was investigated by a GPC technique to monitor the reactions. The dendritic catalysts containing the cyclohexylphosphine ligands could be recovered and reused without loss of efficiency until the fifth cycle. The dendritic Pd^{II} catalysts show a negative dendritic effect, that is, the catalyst efficiency decreases as the dendrimer generation increases.

Keywords: catalysis · C–C coupling · dendrimers · P ligands · palladium · star-shaped molecules

Introduction

One of the most promising applications of dendrimers[1] is their use as recoverable and reusable homogeneous catalysts.[2] Indeed, they combine the potential kinetic information available for monomeric homogeneous catalysts and the possibility of insolubilization as for heterogeneous catalysts. The considerable richness and perfection of their molecular definition makes them superior to supported catalysts. The use of metallodendrimers in catalysis has been known for a decade, and reusable dendritic catalysts have started to appear more recently.[3,4]

A large body of work along this line has been achieved by the van Leeuwen and van Koten groups with particular emphasis on membrane filtration for catalyst recovery. Recently, we published a preliminary report on a family of recoverable pallado-dendritic catalysts for the Sonogashira coupling in a copper-free procedure.[4] These catalysts exhibited tremendous differences in their reactivities and recoverabilities that were dependent on the phosphine substituents (*t*Bu versus Cy).

The Sonogashira cross-coupling reaction has become a standard method for the synthesis of functionalized acetylides (Scheme 1). Its popularity is based on its wide tolerance to functional groups, the availability of common aryl halides and access to pharmacologically important compounds.[5] The Sonogashira cross-coupling reaction usually proceeds with Pd^0/Cu^I catalysts and a base as the solvent,[6] if necessary starting from the more convenient Pd^{II}/Cu^I system. Active 14-electron Pd^0 species are generated in situ by a bis-alkynylation of the Pd complex followed by reductive elimination of diacetylene. Nevertheless, only a few examples of efficient copper-free procedures have been described with aryl bromides or aryl chlorides.[7] Recently, we reported a Pd^{II} complex based on a bulky, electron-rich chelating bis(*tert*-butylphosphine) ligand coordinated to a Pd^{II} center that allowed very high turnover numbers (TONs).[8] The absence of Cu^I in the reaction medium allowed avoidance of the oxidative Glaser homo-coupling of the acetylenic reagent.[9]

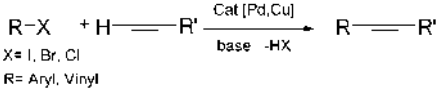

Scheme 1. Sonogashira coupling of aryl or vinyl halides with alkynes.

Herein, we report an advanced study of the reactivity, kinetics and recoverability of monomeric and dendritic bis-

[a] Dr. K. Heuzé, D. Méry, D. Gauss, Prof. Dr. D. Astruc
Nanosciences and Catalysis Group, LCOO, UMR CNRS No. 5802
University Bordeaux I
351 cours de la Libération, 33405 Talence Cedex (France)
Fax: (+33) 5-4000-6646.
E-mail: k.heuze@lcoo.u-bordeaux1.fr
d.astruc@lcoo.u-bordeaux1.fr

[b] Dr. J.-C. Blais
LCSOB, UMR CNRS No. 7613, University Paris VI
4 place Jussieu, 75252 Paris (France)

DOI: 10.1002/chem.200400150

(*tert*-butylphosphine) and bis(cyclohexylphosphine)palladium(II) complexes and an example of their application to the synthesis of star-shaped organoiron-centered and organic molecules.

Results and Discussion

Synthesis and characterization of monomeric and dendritic bis{alkylaminomethylphosphine}palladium(II) complexes: We have synthesized monomeric and dendritic Pd^{II}-based catalysts in which bulky and electron-rich chelating bisphosphine ligands (bis(*tert*-butylphosphines) and bis(cyclohexylphosphines)) are coordinated to a Pd^{II} center. The six dendritic complexes are derived from the commercial polyamino dendrimers DAB-dendr-$(NH_2)_x$ ($x = 4$, 8, or 16 for generation 1, 2, or 3, respectively).

The bis(*tert*-butyl)aminomethylphosphine (**1a**) and bis(cyclohexyl)aminomethylphosphine (**1b**) were obtained from the corresponding phosphines by addition of benzylamine to the bis(*tert*-butyl)- or bis(cyclohexyl)hydroxymethylphosphonium salts according to a known procedure (Scheme 2).[10] The Pd^{II} complexes **1c** and **1d** (Scheme 2) were then readily obtained by treatment of **1a** and **1b**, respectively, with $[Pd(OAc)_2]$.

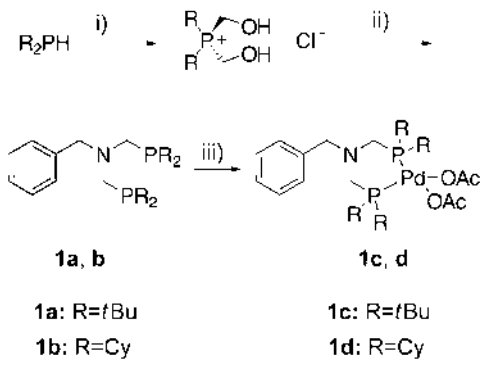

Scheme 2. Synthesis of **1a**–**d**. Reagents and conditions: i) HCHO, HCl; ii) Et_3N, $MeOH/H_2O$, $PhCH_2NH_2$; iii) $[Pd(OAc)_2]$, CH_2Cl_2.

The monomers, the Pd^{II} dendrimers of the first, second, and third generation, **2c**,**d**, **3c**,**d**, and **4c**,**d**, respectively, were readily prepared by treatment of the corresponding aminophosphines **2a**,**b**, **3a**,**b**, **4a**,**b** with $[Pd(OAc)_2]$ (Schemes 3 and 4). All the compounds were characterized by ^1H, ^{13}C, and ^{31}P NMR spectroscopy and by elemental analysis of the Pd^{II} complexes. Chemical shifts of the inner CH_2 of the dendrimers were determined in accordance with the literature.[11]

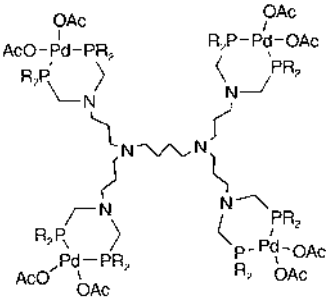

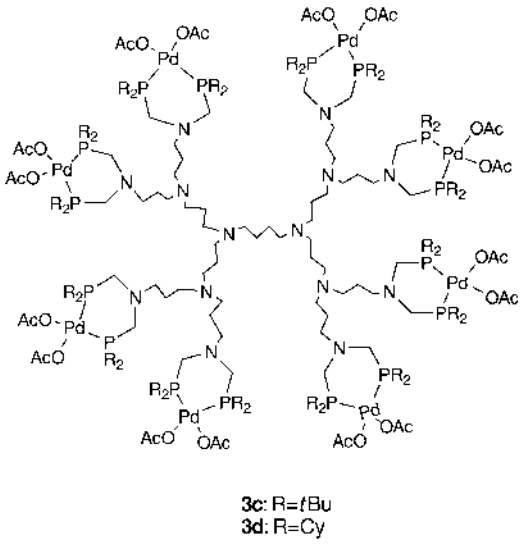

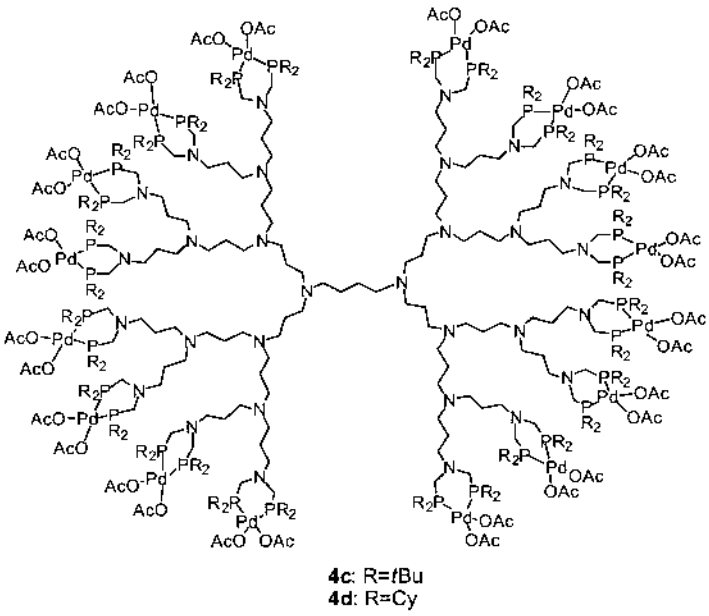

Complete metallation was established by ^{31}P NMR spectroscopy. Thus, the ^{31}P NMR spectra clearly demonstrate the absence of unreacted phosphine units after complete conversion, which occurs within a few hours at most. The corresponding Pd^{II} complexes **1c**–**4c** (with *tert*-butylphosphine substituents) were very soluble in various solvents (including even pentane) and were stable towards moisture. However, they were stored under nitrogen because since some degradation occurred after a few days in air. Conversely, the Pd^{II} complexes **1d**–**4d** (with cyclohexylphophine substituents) were stable towards air and moisture for at least one year.

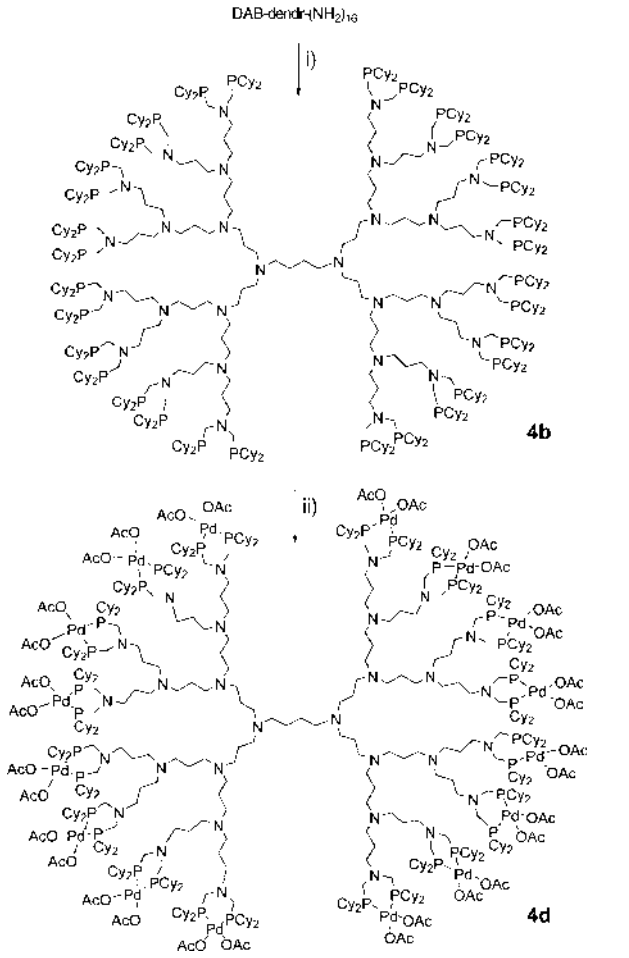

Scheme 3. Synthesis of **4b** and **4d**.Reagents and conditions: i) HCHO, HCl, $HPCy_2$; ii) $[Pd(OAc)_2]$, CH_2Cl_2.

DAB-dendr-$[N(CH_2PR_2)_2]_x$ ⟶ DAB-dendr-$[N(CH_2PR_2)_2Pd(OAc)_2]_x$

x= 4 : R=*t*Bu (**2a**); Cy (**2b**)	x= 4 : R=*t*Bu (**2c**); Cy (**2d**)
x= 8 : R=*t*Bu (**3a**); Cy (**3b**)	x= 8 : R=*t*Bu (**3c**); Cy (**3d**)
x= 16 : R=*t*Bu (**4a**); Cy (**4b**)	x= 16 : R=*t*Bu (**4c**); Cy (**4d**)

Scheme 4.

Catalytic C–C cross-coupling between acetylenes and aryl halides: In previous work,[8] the reactivity of **1c** towards aryl iodides, bromides and chlorides was investigated in a Sonogashira copper-free procedure (Table 1). Excellent activity was observed towards aryl iodides with TONs as high as 71000. Good activity was also obtained for aryl bromides and a substantial reactivity was found with aryl chlorides, thus demonstrating the efficiency of bis(*tert*-butylphosphine) ligands in such C–C cross-coupling. Nevertheless, **1d** showed a lower, albeit good, activity towards aryl iodides and bromides in copper-free Sonogashira procedures (Table 2). The conversion observed for aryl iodides and bromides with the dendritic series of catalysts **2c**,**d**, **3c**,**d**, **4c**,**d** revealed the same distinction in the reactivity between the phosphine substituents (*tert*-butyl versus cyclohexyl)(Table 3). Also, a negative dendritic effect was demonstrated for metallodendrimers of the third generation (**4c** and **4d**) for which a lower reactivity was observed (Figure 1).[4]

In all the experiments, triethylamine was chosen both as a base and as a solvent. The functional group tolerance inherent to the Sonogashira reaction, however, means that any co-solvent may be used when required to help solubilize the reagents or to improve the reactivity by increasing the reaction temperature. Thus, solvents other than triethylamine were tested (Table 4). No significant improvement in reactivity with these solvents was observed, however, because a degradation of the catalyst occurred rapidly at such high temperatures as a result of the P–C bond degradation in the phosphine ligands.[12]

Application to the construction of organoiron and organic stars: Recently, we were able to extend the $CpFe^+$-induced hexabenzylation of hexamethylbenzene[5d] to *p*-$BrCH_2$-C_6H_4Br in excellent yields under mild conditions.[13] The hexabenzylated stars bearing bromo substituents in the *para* position of the arene rings are excellent candidates for the Sonogashira reaction.

The cross-coupling of phenylacetylene with the iron complex $[FeCp\{C_6(CH_2CH_2C_6H_4Br)_6\}][PF_6]$[13] was investigated (Scheme 5). The good activity (one-step six C–C coupling) and the good tolerance toward functional groups of the Pd catalyst **1c** was demonstrated because the hoped-for iron complex product was obtained. In addition, cross-coupling of phenylacetylene with the iron-free star $C_6(CH_2CH_2C_6H_4Br)_6$ allowed the isolation of the product resulting from cross-coupling (Scheme 5). This original one-step multiple C–C cross-coupling reaction provides a valuable strategy for the synthesis of stars and dendrimers.

Kinetics of the reactions with *t*Bu and Cy ligand-based catalysts: We carried out kinetic investigations in order to obtain a better quantification of the differences in reactivity between the *tert*-butylphosphine- and cyclohexylphosphine-functionalized catalysts. Mechanistic and kinetic studies of Pd^{II} catalytic systems have often been reported in detail and have highlighted the intermediacy of catalytic species in the cross-coupling reactions.[14] Different techniques may be used, such as NMR spectroscopy,[15] analytical techniques (conductivity measurements)[16] or electrochemical techniques (cyclic voltammetry).[17] This study was based on the overall reaction, that is, only the final product was isolated. The *tert*-butyl– and cyclohexylpalladium(II) catalysts **1c** (1 mol%) and **1d** (1 mol%) were used in a typical Sonogashira reaction procedure involving iodobenzene (4 mmol) and phenylacetylene (6 mmol) in Et_3N (10 mL). A GPC technique was used to monitor the appearance of diphenylacetylene and the disappearance of iodobenzene from which the rate constants were determined. To study the kinetics with **1c**, the GPC samples were frozen in liquid nitrogen as soon as they were taken from the reaction because the kinetics were too fast compared to the retention times for each GPC experiment. The variation of $\ln x$ versus time ($x = c/c_0$) was linear for both plots (Figure 2a and b). This establishes an overall reaction order of +1. The observed apparent rate constants k_{obs} for the overall reactions were then

Table 1. Sonogashira coupling of aryl halide substrates with phenylacetylene and the monomeric catalyst **1c**.[a]

Entry	X	R	R′	T[°C]	Catalyst [mol %]	Reaction time	Conversion [%][b]	TON
1	I	C_6H_5	C_6H_5	80	1	15 min	100	100
2	I	C_6H_5	C_6H_5	25	1	30 min	100	100
3	I	C_6H_5	C_6H_5	−20	1	1 day	70	70
4	I	C_6H_5	C_6H_5	−40	1	2 days	51	51
5	I	C_6H_5	$Si(CH_3)_3$	25	1	8 h	76	76
6	I	C_6H_5	C_6H_5	80	0.5	15 min	100	200
7	I	C_6H_5	C_6H_5	80	0.1	2 h	100	1000
8	I	C_6H_5	C_6H_5	80	0.01	1 day	87	8700
9	I	C_6H_5	C_6H_5	80	0.001	7 days	71	71 000
10	Br	C_6H_5	C_6H_5	80	1	20 min	100	100
11	Br	C_6H_5	C_6H_5	25	1	1 h	100	100
12	Br	(*p*-Me)C_6H_5	C_6H_5	80	1	3 h	96	96
13	Br	C_6H_5	$Si(CH_3)_3$	25	1	15 h	54	54
14	Cl	C_6H_5	C_6H_5	80	1	50 min	4	4
15	Cl	C_6H_5	C_6H_5	25	1	3 h	9	9
16	Cl	C_6H_5	$Si(CH_3)_3$	25	1	2 days	5	5
17	Cl	(*p*-CN)C_6H_5	C_6H_5	80	1	5 days	13	13
18	Cl	(*p*-F)C_6H_5	C_6H_5	80	1	5 days	14	14
19	Cl	(*p*-$COOCH_3$)C_6H_5	C_6H_5	25	1	3 days	15	15
20	Cl	(*p*-$COOCH_3$)C_6H_5	C_6H_5	80	2	3 days	30	30
21	Cl	(*p*-$COOCH_3$)C_6H_5	C_6H_5	40	1	3 days	22	22

[a] Reaction conditions: aryl halide (2 mmol), acetylene (3 mmol), Et_3N (6 mL). [b] Yield of isolated product.

Table 2. Sonogashira coupling of aryl halide substrates with phenylacetylene and the monomeric catalyst **1d**.[a]

Entry	X	R	R′	T[°C]	Reaction time	Conversion [%][b]	TON
1	I	C_6H_5	C_6H_5	80	5 h	76	76
2	I	C_6H_5	C_6H_5	45	3 days	100	100
3	Br	C_6H_5	C_6H_5	80	4 h	71	71
4	Cl	C_6H_5	C_6H_5	80	5 h	traces	–

[a] Reaction conditions: aryl halide (2 mmol), phenylacetylene (3 mmol), catalyst **1d** (1 mol %), Et_3N (6 mL). [b] Yield of isolated product.

Table 3. Sonogashira coupling of aryl halide substrates with phenylacetylene and dendrimeric catalysts **2c**,**d**, **3c**,**d** and **4c**,**d**.[a]

Entry	Aryl halide	Solvent	Catalyst [1 mol %]	T[°C]	Reaction time [h][b]	Conversion [%][c]
1	iodobenzene	Et_3N	**2d**	80	24	79
2	iodobenzene	Et_3N	**3d**	80	24	72
3	iodobenzene	Et_3N	**4d**	80	24	46
4	iodobenzene	Et_3N	**2c**	25	15	97
5	iodobenzene	Et_3N	**3c**	25	40	100
6	iodobenzene	Et_3N	**4c**	25	48	100
7	bromobenzene	Et_3N	**2d**	80	48	17
8	bromobenzene	Et_3N	**3d**	80	48	15
9	bromobenzene	Bu_2NH	**3d**	120	20	20
10	bromobenzene	Et_3N	**4d**	80	48	6
11	bromobenzene	Et_3N	**2c**	25	17	100
12	bromobenzene	Et_3N	**3c**	25	48	93
13	bromobenzene	Et_3N	**4c**	25	48	96

[a] Reaction conditions: aryl halide (2 mmol), phenylacetylene (3 mmol), Et_3N (6 mL). [b] The reaction was monitored by TLC. [c] Yield of isolated product.

determined from the slopes of the regression for each plot. The calculated rate constants were 0.925 mol L^{-1} h^{-1} at 25 °C for **1c** and 0.028 mol L^{-1} h^{-1} 27 °C for **1d**. This gives a k(**1c**)/k(**1d**) ratio of ≈33.

Recovery of metallodendritic catalysts: Various techniques can be used to recycle the metallodendritic catalysts.[3a] The most recent one required CFMR devices based on nanofiltration through membranes. Very often, however, the catalyst was recovered by precipitation from the product solution once the reaction was complete.[3b,18]

We have processed a set of recycling experiments based on the precipitation of the metallodendritic catalyst. In a typical procedure, iodobenzene (2 mmol) in Et_3N (8 mL) with catalyst **2d**, **3d** or **4d** (2 mol % based on the catalytic sites) was treated with phenylacetylene (3 mmol) at 80 °C for 48 h. The reaction time was chosen in order to complete all the reactions, even with the dendritic catalyst of third generation whose reactivity is lower than that of the first and second ones (see above). Subsequently, pentane (30 mL) was added to the reaction mixture to precipitate the catalyst and extract the product. The pentane extraction was carried out five times to optimize product recovery. The reactants and solvents were then re-added to the dried catalyst under nitrogen to proceed to the next cycles. The results are summarized in Table 5 and Figure 3. The catalytic activity for all the generations of dendrimers remained the same up to the fifth cycle. However, a significant drop in the activity was observed from the fifth cycle for all the generations of dendrimers. This behavior mostly resulted from a decomposition of the dendritic ligand because no leaching was observed. The subsequent decomposition was confirmed

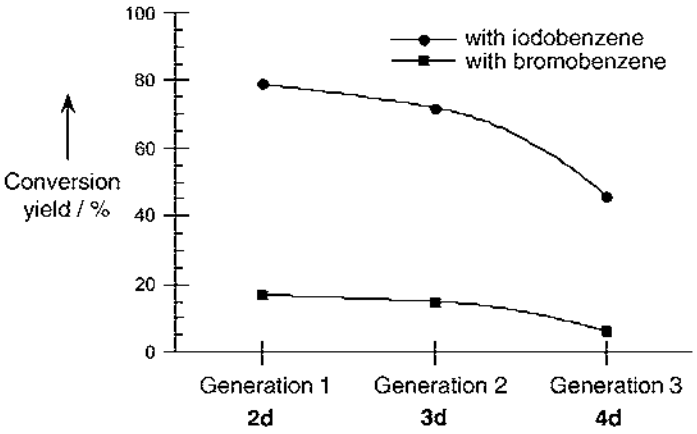

Figure 1. Conversion of aryl halides with phenylacetylene catalyzed by **2d**, **3d**, and **4d** at 80 °C.

Table 4. Solvent effect in the Sonogashira coupling between iodobenzene and phenylacetylene with the dendritic catalyst **3d**.[a]

Entry	Solvent	T [°C]	Reaction time [h]	Conversion [%][b]
1	Et_3N	80	5	72
2	Et_3N/DMF	140	3	34
3	Bu_3N	140	8	16
4	Bu_2NH	120	8	31

[a] Reaction conditions: iodobenzene (2 mmol), phenylacetylene (3 mmol), solvent (6 mL). [b] Yield of isolated product.

by ^{31}P NMR analysis of the catalyst after the cycles. Indeed, the appearance of several peaks at $\delta \approx 50$ ppm confirmed the presence of oxidation and decomposition species. However, the signal for the active catalytic species was still observed at $\delta = 25$ ppm (with a slight shift of 2 ppm in comparison with the initial signal of the Pd^{II} catalyst). This decomposition has also been reported with a variety of other dendritic systems that employ either precipitation or other recovery techniques. Interestingly, the fifth cycle often seems to be of crucial importance in the reactivity drop.[18a,19]

Conclusion

New copper-free Sonogashira Pd catalysts were synthesized. that exhibit very good reactivity under mild conditions with aryl iodides, bromides, and even some reactivity with activated aryl chlorides. The catalytic activity was much higher with *t*Bu substituents on the phosphines than with Cy substituents. The monomeric Pd catalyst bearing *t*Bu substituents on the phosphines was applied to the synthesis of organoiron and organic stars whereby six Sonogashira C–C coupling reactions occur. Dendritic versions of these copper-free catalysts were designed, synthesised and used with a reactivity that showed a negative dendritic effect, the largest dendritic catalysts being the less active ones. This negative dendritic effect is attributed to the increasing steric bulk around the active metal centres as the dendrimer generation increases, and this finding confirms similar observations made previously.[20] The kinetics of the reaction, monitored by GPC, are much faster with *t*Bu substituents on the phosphine ligands than with Cy substituents. The dendritic cata-

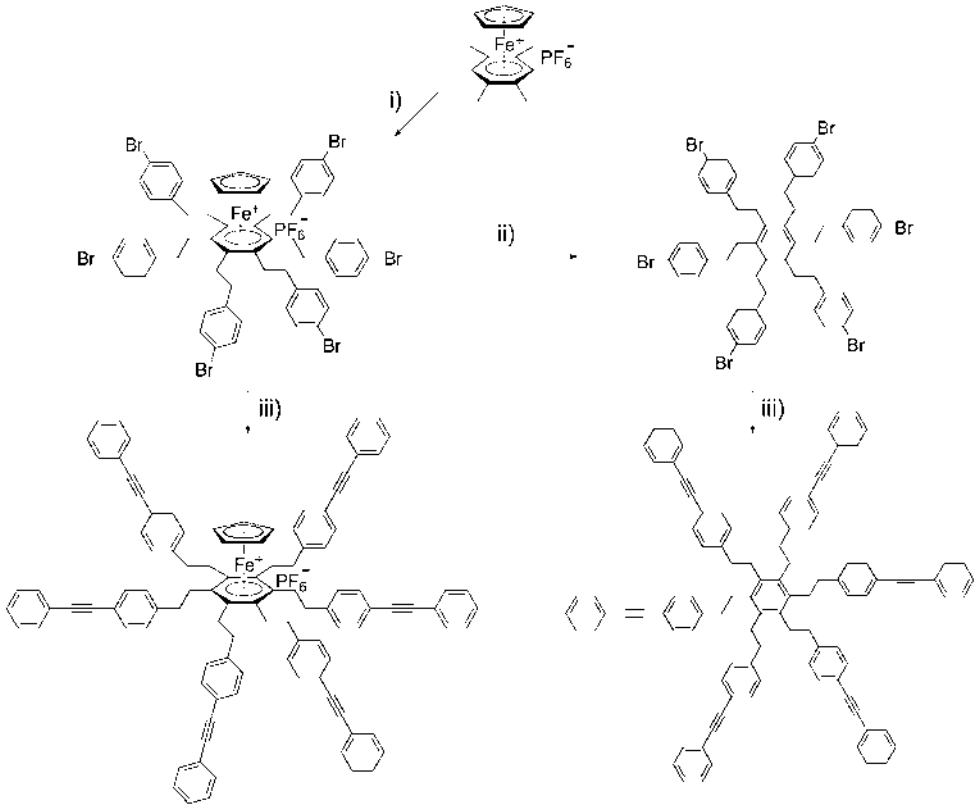

Scheme 5. Reagents and conditions: i) *p*-Br-$C_6H_5CH_2Br$, KOH, DME, 40 °C, 6 days; ii) PPh_3, MeCN, 24 h, (Xe lamp); iii) phenylacetylene, Et_3N, catalyst **1c**.

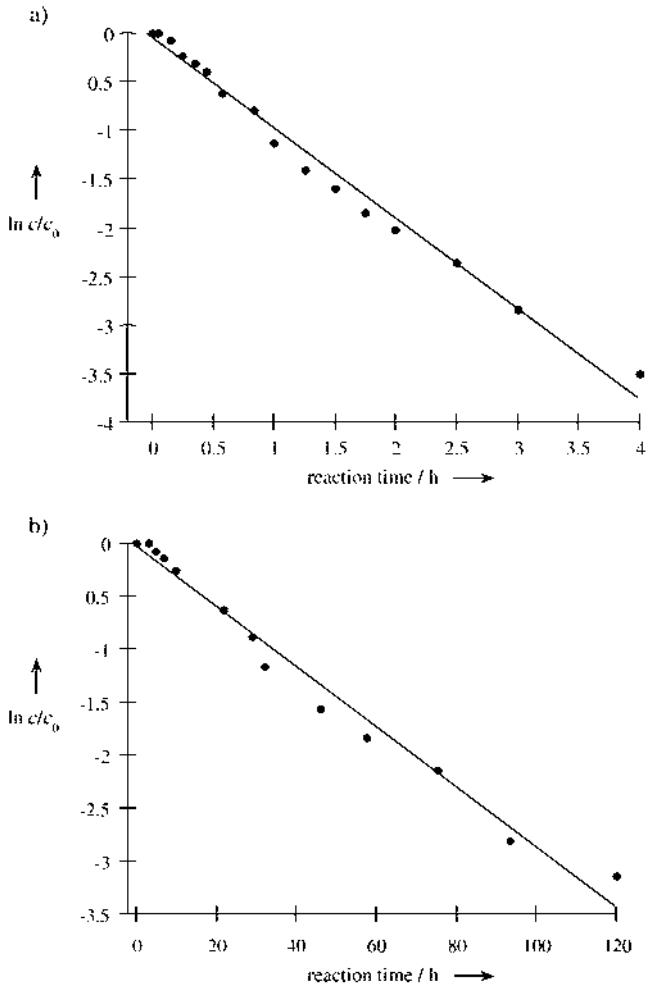

Figure 2. Kinetics of the disappearance of iodobenzene in a Sonogashira reaction with a) **1c** at 25 °C, and b) **1d** at 27 °C. Variation of $\ln(c/c_0)$ versus time (c: concentration of iodobenzene at t, c_0: initial concentration of iodobenzene).

Table 5. Coupling of iodobenzene with phenylacetylene and the dendritic catalysts **2d**, **3d** and **4d**.[a]

Catalyst	Cycle	Conversion [%][b]
2d	first	92
	second	74
	third	61
	fourth	56
	fifth	26
	sixth	26
3d	first	83
	second	66
	third	66
	fourth	71
	fifth	21
	sixth	26
	seventh	16
4d	first	78
	second	70
	third	78
	fourth	76
	fifth	51
	sixth	46
	seventh	39

[a] Reaction conditions: iodobenzene (2 mmol), phenylacetylene (3 mmol), Et_3N (8 mL), catalyst (2 mol %), N_2. [b] Yield of isolated product.

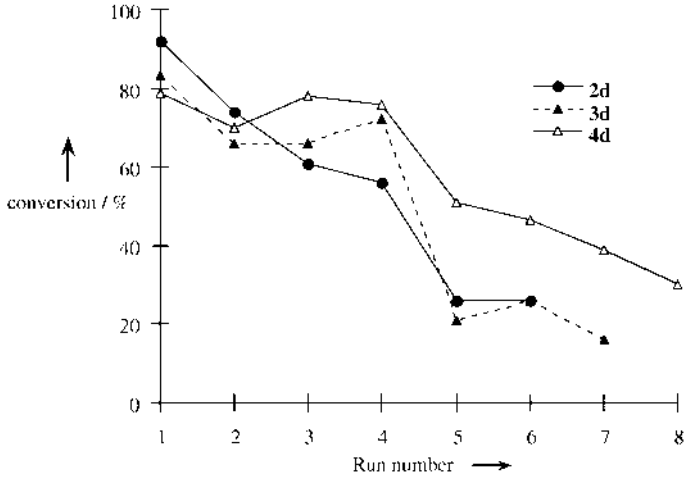

Figure 3. Reaction conditions: iodobenzene (4 mmol), phenylacetylene (6 mmol), catalyst (1 mol %), Et_3N (10 mL), 80 °C, 48 h. The product was extracted and purified by silica gel column chromatography.

lysts with R = Cy are recoverable by precipitation with pentane and can be reused up to five times with a good activity level. However, the dendritic catalysts with R = *t*Bu could not be easily recovered by this method on account of their high solubility in pentane. Ongoing studies are underway in our laboratory in order to investigate catalysts for Pd-catalyzed C–C coupling that are both extremely reactive and recoverable.

Experimental Section

All reactions were performed under a nitrogen atmosphere in standard (Schlenk) glassware. The solvents were dried according to standard procedures and saturated with nitrogen. The ^1H, ^{13}C and ^{31}P NMR spectra were recorded with the following spectrometers: Brucker DPX200 FT NMR spectrometer (^1H: 200.16, ^{13}C: 50.33, ^{31}P: 81.02 MHz), Brucker AC250 FT NMR spectrometer (^1H: 250.13, ^{13}C: 62.90 MHz) and Avance 300 FT NMR spectrometer (^1H: 300.13, ^{13}C: 75.46, ^{31}P: 121.49 MHz). Mass spectroscopic measurements (MALDI-TOF) were performed at the LCSOB, University of Paris 6. The elemental analyses were carried out in the analysis laboratory of the elemental analysis department at CNRS-Vernaison. The starting materials were obtained commercially and were used without further purification.

General procedure for the syntheses of aminophosphine 1a and 1b monomers:

Bis(*tert*-butylaminophosphine) (1a): Triethylamine (0.29 mL, 2.1 mmol) was added to a stirred solution of the phosphonium salt (0.5 g, 2.1 mmol) in water/methanol (2:1, 3 mL). On addition of benzylamine (0.11 mL, 1 mmol) the mixture became viscous, thus toluene (3 mL) was added. The solution was refluxed for 1 h. On cooling, two layers separated, and the organic layer was extracted and dried over sodium sulfate. Methanol was added to precipitate a white gummy solid. The solvents were removed, and the solid was dried under a high vacuum to yield the product as a white solid (385 mg, 91 %). ^1H NMR (200.16 MHz, $CDCl_3$, 300 K): δ = 7.24 (m, 5H, CH_{arom}), 3.79 (s, 2H, CH_2N), 2.73 (s, 4H, PCH_2N), 1.09 (s, 18H, *t*Bu), 1.04 ppm (s, 18H, *t*Bu); $\{^1H\}^{13}C$ NMR (62.90 MHz, $CDCl_3$, 300 K): δ = 130.14 (C_{arom}), 129.1 (C_{arom}), 128.2 (C_{arom}), 127.6 (C_{arom}), 61.0 (CH_2N), 60.7 (PCH_2N), 33.4 (*t*Bu), 27.3 (*t*Bu), 26.9 ppm (*t*Bu); $\{^1H\}^{31}P$ NMR (81.02 MHz, $CDCl_3$, 300 K): δ = 12.9 ppm.

Bis(cyclohexylaminophosphine) (1b): The same procedure as for **1a** was used. Phosphonium salt (1.466 g, 5 mmol), triethylamine (0.68 mL, 5 mmol), benzylamine (0.27 mL, 2.5 mmol). Yield: 1.07 g (82 %) of a

white solid. ^{1}H NMR (200.16 MHz, $CDCl_3$, 300 K): δ = 7.25 (m, 5H, CH_{arom}), 3.77 (s, 2H, CH_2N), 2.82 (s, 4H, PCH_2N), 2.45 (s, 4H, PCH_{Cy}), 2.37 (s, 4H, CH_{Cy}), 1.73–1.21 ppm (m, 40H, $CH_{2,Cy}$); $\{^1H\}^{13}$C NMR (62.90 MHz, $CDCl_3$, 300 K): δ = 129.7 (C_{arom}), 129.1 (C_{arom}), 128.2 (C_{arom}), 127.8 (C_{arom}), 61.4 (CH_2N), 60.7 (PCH_2N), 32.9 (Cy), 29.7 (Cy), 27.3 (Cy), 26.6 ppm (Cy); $\{^1H\}^{31}$P NMR (81.02 MHz, $CDCl_3$, 300 K): δ = −17.4 ppm; elemental analysis calcd (%) for $C_{33}H_{55}P_2N$ (527.75): C 75.10, H 10.50; found: C 73.87, H 10.37.

General procedure for the syntheses of aminophosphine dendrimers 2a, 3a, 4a and monomers 2b, 3b, 4b:

G1-DAB-*dendr*-[bis(*tert*-butylaminophosphine)]$_4$ (2a): Di-*tert*-butylphosphine (1.05 mL, 6 mmol) and paraformaldehyde (0.17 g, 6 mmol) in methanol (5 mL) were heated at 65 °C for 10 min. Upon cooling, DAB-*dendr*-$(NH_2)_4$ (0.2 g, 0.7 mmol) in methanol (3 mL) was added, and the mixture was stirred at room temperature for 30 min. Toluene (15 mL) was added, and the mixture was heated at 65 °C for 30 min. The reaction medium was stirred at room temperature for another 12 h. The solvent was removed under vacuum, and the solid was recrystallised (cold pentane) and dried to yield the aminophosphine dendrimer as a white solid (830 mg, 75 %). ^{1}H NMR (250.13 MHz, $CDCl_3$, 300 K): δ = 2.74 (m, 16H, NCH_2P), 2.39 (m, 20H, NCH_2), 1.24 (m, 12H, CH_2-CH_2), 1.16 (s, 72H, *t*Bu), 1.11 ppm (s, 72H, *t*Bu); $\{^1H\}^{13}$C NMR (62.90 MHz, $CDCl_3$, 300 K): δ = 54.8 (NCH_2), 53.2 (NCH_2), 52.4 (NCH_2), 29.6 (*t*Bu), 29.5 (*t*Bu), 24.7 ($CH_{2,dendr}$), 23.4 ppm ($CH_{2,dendr}$); $\{^1H\}^{31}$P NMR (81.03 MHz, $CDCl_3$, 300 K): δ = 12.2 ppm; elemental analysis calcd (%) for $C_{88}H_{192}P_8N_6$ (1579.792): C 66.80, H 12.23; found: C 66.76, H 12.17.

G2-DAB-*dendr*-[bis(*tert*-butylaminophosphine)]$_8$ (3a): The same procedure as for **2a** was used with di-*tert*-butylphosphine (0.86 mL, 4.6 mmol), paraformaldehyde (0.14 g, 4.6 mmol) and DAB-*dendr*-$(NH_2)_8$ (0.2 g, 0.26 mmol). Yield: 1.05 g (91 %) of a white solid. ^{1}H NMR (250.13 MHz, $CDCl_3$, 300 K): δ = 2.73 (m, 32H, NCH_2P), 2.39 (m, 52H, NCH_2), 1.24 (m, 28H, CH_2-CH_2), 1.16 (s, 144H, *t*Bu), 1.11 (s, 144H, *t*Bu); $\{^1H\}^{13}$C NMR (62.90 MHz, $CDCl_3$, 300 K): δ = 54.7(NCH_2), 53.6 (NCH_2), 52.4 (NCH_2), 29.7 (*t*Bu), 29.6 (*t*Bu), 24.9 ($CH_{2,dendr}$), 23.6 ($CH_{2,dendr}$); $\{^1H\}^{31}$P NMR (81.03 MHz, $CDCl_3$, 300 K): δ = 12.2; elemental analysis calcd (%) for $C_{184}H_{400}P_{16}N_{14}$ (4434.974): C 66.87, H 12.20; found: C 66.45, H 11.98.

G3-DAB-*dendr*-[bis(*tert*-butylaminophosphine)]$_{16}$ (4a): The same procedure as for **2a** was used with di-*tert*-butylphosphine (0.79 mL, 4.2 mmol), paraformaldehyde (126 mg, 4.2 mmol), and DAB-*dendr*-$(NH_2)_{16}$ (0.2 g, 0.12 mmol). Yield: 0.727 g (90 %) of a white solid. ^{1}H NMR (250.13 MHz, $CDCl_3$, 300 K): δ = 2.73 (m, 64H, NCH_2P), 2.39 (m, 116H, NCH_2), 1.28 (m, 60H, CH_2-CH_2), 1.16 (s, 288H, *t*Bu), 1.11 ppm (s, 288H, *t*Bu); $\{^1H\}^{13}$C NMR (62.90 MHz, $CDCl_3$, 300 K): δ = 54.7(NCH_2), 53.3 (NCH_2), 52.2 (NCH_2), 30.0 (*t*Bu), 29.7 (*t*Bu), 24.6 ($CH_{2,dendr}$), 23.5 ppm ($CH_{2,dendr}$); $\{^1H\}^{31}$P NMR (81.03 MHz, $CDCl_3$, 300 K): δ = 12.2 ppm; elemental analysis calcd (%) for $C_{376}H_{816}P_{32}N_{30}$ (6739.168): C 66.91, H 12.18; found: C 66.22, H 11.53.

G1-DAB-*dendr*-[bis(cyclohexylaminophosphine)]$_4$ (2b): The same procedure as for **2a** was used with dicyclohexylphosphine (2.82 mL, 13.98 mmol), paraformaldehyde (0.46 g, 13.98 mmol), and DAB-*dendr*-$(NH_2)_4$ (500 mg, 1.58 mmol). Yield: 2.29 g (73 %) of a white solid. ^{1}H NMR (200.16 MHz, $CDCl_3$, 300 K): δ = 2.72 (m, 16H, PCH_2N), 2.65 (m, 16H, PCH_{Cy}), 2.37 (m, 20H, CH_2N), 1.72 (m, 80H, $CH_{2,Cy}$), 1.53 (m, 12H, $CH_2CH_{2,dendr}$), 1.20 ppm (m, 80H, $CH_{2,Cy}$); $\{^1H\}^{13}$C NMR (50.33 MHz, $CDCl_3$, 300 K): δ = 55.35 ($CH_2N_{central}$), 52.48 (CH_2N + PCH_2N), 32.7 ($d_{,Cy}$), 29.7 ($t_{,Cy}$), 28.89 (CH_2-$CH_{2,dendr}$) 27.16 (d, Cy), 27.35 (s, Cy), 25.24 ppm ($CH_{2,dendr}$); $\{^1H\}^{31}$P NMR (81.02 MHz, $CDCl_3$, 300 K): δ = −17.8 ppm.

G2-DAB-*dendr*-[bis(cyclohexylaminophosphine)]$_8$ (3b): The same procedure as for **2a** was used with dicyclohexylphosphine (2.54 mL, 12.56 mmol), paraformaldehyde (342 mg, 11.44 mmol), and DAB-*dendr*-$(NH_2)_8$ (500 mg, 0.64 mmol). Yield: 1.64 g (64 %) of a white solid. ^{1}H NMR (200.16 MHz, $CDCl_3$, 300 K): δ = 2.73 (m, 32H, PCH_2N), 2.63 (m, 32H, PCH_{Cy}), 2.34 (m, 52H, CH_2N), 1.74 (m, 160H, $CH_{2,Cy}$), 1.54 (m, 28H, $CH_2CH_{2,dendr}$), 1.21 ppm (m, 160H, $CH_{2,Cy}$); $\{^1H\}^{31}$P NMR (81.02 MHz, $CDCl_3$, 300 K): δ = −17.8 ppm.

G3-DAB-*dendr*-[bis(cyclohexylaminophosphine)]$_{16}$ (4b): The same procedure as for **2a** was used with dicyclohexylphosphine (3.35 mL, 16.5 mmol), paraformaldehyde (454 mg, 15.1 mmol), and DAB-*dendr*-$(NH_2)_{16}$ (720 mg, 42.7 mmol). Yield: 2.5 g (70 %) of a white solid. ^{1}H NMR (200.16 MHz, $CDCl_3$, 300 K): δ = 2.69 (m, 64H, PCH_2N), 2.58 (m, 64H, PCH_{Cy}), 2.33 (m, 116H, CH_2N), 1.70 (m, 320H, $CH_{2,Cy}$), 1.50 (m, 60H, $CH_2CH_{2,dendr}$), 1.17 ppm (m, 320H, $CH_{2,Cy}$); $\{^1H\}^{13}$C NMR (75.47 MHz, $CDCl_3$, 300 K): δ = 53.86 ($CH_2N_{central}$), 51.72 (CH_2N + PCH_2N + PCH), 31.9 ($d_{,Cy}$), 29.05 (dd, Cy), 28.75 (CH_2-$CH_{2,dendr}$) 26.4 ($d_{,Cy}$), 25.7 (Cy), 22.66 ppm ($CH_{2,dendr}$); $\{^1H\}^{31}$P NMR (81.02 MHz, $CDCl_3$, 300 K): δ = −18.1 ppm.

General procedure for the syntheses of (*tert*-butylaminophosphine)palladium(II) monomer 1c and dendrimers 2c, 3c, 4c:

Bis(*tert*-butylaminophosphine)palladium(II) complex 1c: $[Pd(OAc)_2]$ (70 mg, 0.32 mmol) was added to a solution of aminophosphine **1a** (132 mg, 0.32 mmol) in CH_2Cl_2 (5 mL). The solution was stirred for 2 h at room temperature. The solvent was removed under vacuum to give a solid that was washed with cold pentane and dried under vacuum to yield complex **1c** as a yellowish solid (190 mg, 94 %). ^{1}H NMR (300.13 MHz, $CDCl_3$, 300 K): δ = 7.25 (m, 5H, CH_{arom}), 3.58 (s, 2H, CH_2N), 2.66 (s, 4H, PCH_2N), 1.89 (s, 6H, CH_3), 1.39 (s, 18H, *t*Bu), 1.32 ppm (s, 18H, *t*Bu); $\{^1H\}^{13}$C NMR (62.90 MHz, $CDCl_3$, 300 K): δ = 176.0 (CO), 135.1–128.6 (C_{arom}), 67.5 (CH_2N), 54.6 (PCH_2N), 36.3 (CH_3), 33.2 (Bu), 31.8 ppm (*t*Bu); $\{^1H\}^{31}$P NMR (81.02 MHz, $CDCl_3$, 300 K): δ = 35.9 ppm. elemental analysis calcd (%) for $C_{29}H_{53}P_2NO_4Pd$ (648.10): C 53.74, H 8.24, P 9.56; found: C 53.23, H 8.02, P 9.44.

G1-DAB-*dendr*-[bis(*tert*-butylaminophosphine)]$_4$pallaium(II) complex 2c: The same procedure as for **1c** was used with $[Pd(OAc)_2]$ (100 mg, 0.44 mmol) and aminophosphine **2a** (170 mg, 0.11 mmol). Yield: 204 mg (75 %) of a yellow solid; ^{1}H NMR (250.13 MHz, $CDCl_3$, 300 K): δ = 2.75 (m, 16H, NCH_2P), 2.40 (m, 20H, NCH_2), 1.89, (s, 24H, CH_3), 1.46 (s, 72H, *t*Bu), 1.39 (s, 72H, *t*Bu), 1.26 ppm (m, 12H, CH_2-CH_2); $\{^1H\}^{13}$C NMR (62.90 MHz, $CDCl_3$, 300 K): δ = 176.2 (CO), 54.4(NCH_2), 53.5 (NCH_2), 52.9 (NCH_2), 30.1 ($CH_{3,OAc}$), 29.7 (*t*Bu), 29.5 (*t*Bu), 24.9 ($CH_{2,dendr}$), 23.5 ppm ($CH_{2,dendr}$); $\{^1H\}^{31}$P NMR (81.03 MHz, $CDCl_3$, 300 K): δ = 35.20 ppm; elemental analysis calcd (%) for $C_{104}H_{216}P_8N_6O_{16}Pd_4$ (2480.360): C 50.36, H 8.78; found: C 50.11, H 8.53.

G2-DAB-*dendr*-[bis(*tert*-butylaminophosphine)]$_8$pallaium(II) complex 3c: The same procedure as for **1c** was used with $[Pd(OAc)_2]$ (100 mg, 0.44 mmol) and aminophosphine **3a** (184 mg, 0.056 mmol). Yield: 182 mg (64 %) of a yellow solid; ^{1}H NMR (200.16 MHz, $CDCl_3$, 300 K): δ = 2.71 (m, 32H, NCH_2P), 2.34 (m, 52H, NCH_2), 1.89, (s, 48H, CH_3), 1.47 (s, 144H, *t*Bu), 1.40 (s, 144H, *t*Bu), 1.28 ppm (m, 28H, CH_2-CH_2); $\{^1H\}^{13}$C NMR (62.90 MHz, $CDCl_3$, 300 K): δ = 177.0 (CO), 54.8(NCH_2), 53.6 (NCH_2), 52.5 (NCH_2), 30.5 ($CH_{3,OAc}$), 30.0 (*t*Bu), 29.9 (*t*Bu), 24.6 ($CH_{2,dendr}$), 23.3 ppm ($CH_{2,dendr}$); $\{^1H\}^{31}$P NMR (81.03 MHz, $CDCl_3$, 300 K): δ = 35.22 ppm; elemental analysis calcd (%) for $C_{216}H_{448}P_{16}N_{14}O_{32}Pd_8$ (5094.944): C 50.86, H 8.85; found: C 50.53, H 8.45.

G3-DAB-*dendr*-[bis(*tert*-butylaminophosphine)]$_{16}$palladium(II) complex 4c: The same procedure as for **1c** was used with $[Pd(OAc)_2]$ (100 mg, 0.44 mmol) and aminophosphine **4a** (188 mg, 0.028 mmol). Yield: 199 mg (69 %) of a yellow solid; ^{1}H NMR (200.16 MHz, $CDCl_3$, 300 K): δ = 2.73 (m, 64H, NCH_2P), 2.39 (m, 116H, NCH_2), 1.90, (s, 96H, CH_3), 1.47 (s, 288H, *t*Bu), 1.40 (s, 288H, *t*Bu), 1.26 ppm (m, 60H, CH_2-CH_2); $\{^1H\}^{13}$C NMR (62.9 MHz, $CDCl_3$, 300 K): δ = 176.9 (CO), 54.7(NCH_2), 53.7 (NCH_2), 52.6 (NCH_2), 30.8 ($CH_{3,OAc}$), 30.5 (*t*Bu), 30.2 (*t*Bu), 24.6 ($CH_{2,dendr}$), 23.6 ppm ($CH_{2,dendr}$); $\{^1H\}^{31}$P NMR (81.03 MHz, $CDCl_3$, 300 K): δ = 35.30 ppm; elemental analysis calcd (%) for $C_{440}H_{912}P_{32}N_{30}O_{64}Pd_{16}$ (10329.888): C 51.10, H 8.89; found: C 50.79, H 8.61.

General procedure for the syntheses of (cyclohexylaminophosphine)palladium(II) monomer 1d and dendrimers 2d, 3d, 4d:

Bis(cyclohexylaminophosphine)palladium(II) complex 1d: $[Pd(OAc)_2]$ (326 mg, 1.45 mmol) was added to a solution of aminophosphine **1b** (765 mg, 1.45 mmol) in CH_2Cl_2 (50 mL). The solution was stirred for 2 h at room temperature. The volume was reduced to 10 mL, and pentane was added to precipitate complex **1d** that was dried under vacuum to yield a yellow solid (803 mg, 87 %). ^{1}H NMR (200.16 MHz, $CDCl_3$, 300 K): δ = 7.37–7.25 (m, 5H, CH_{arom}), 3.58 (s, 2H, CH_2N), 2.58 (s, 4H, PCH_2N), 2.26 (s, 4H, PCH_{Cy}), 1.95 (s, 6H, CH_3), 1.65–1.19 ppm (m, 40H, $CH_{2,Cy}$); $\{^1H\}^{13}$C NMR (75.47 MHz, $CDCl_3$, 300 K): δ = 177.1 (CO), 135.74 (CH_{arom}),130.23 (CH_{arom}), 128.81 (CH_{arom}), 128.40 (CH_{arom}), 67.5 (PCH_{Cyclo}), 47.73 (CH_2N + PCH_2N), 35.3 (dt, $CH_{2,Cy}$), 28.7 ($CH_{2,Cy}$),

27.24 (dt, $CH_{2,Cy}$), 25.78 (CH_3), 24.19 ppm ($CH_{2,Cy}$); $\{^1H\}^{31}P$ NMR (81.02 MHz, $CDCl_3$, 300 K): δ = 26.5 ppm; elemental analysis calcd (%) for $C_{37}H_{61}P_2NO_4Pd$ (752.263): C 59.08, H 8.17, N 1.86; found: C 58.34, H 8.24 N 1.96.

G1-DAB-*dendr*-[bis(cyclohexylaminophosphine)]$_4$palladium(II) complex 2d: The same procedure as for **1d** was used with $[Pd(OAc)_2]$ (900 mg, 4 mmol) and aminophosphine **2b** (2 g, 1 mmol). Yield: 2.175 g (75%) of a yellow solid; ^1H NMR (300.13 MHz, $CDCl_3$, 300 K): δ = 2.55 (m, 32H, PCH_2N + PCH_{Cy}), 2.33 (m, 20H, CH_2N), 1.89 (s, 24H, CH_3), 1.70 (m, 80H, $CH_{2,Cy}$), 1.59 (m, 12H, $CH_2CH_{2,dendr}$), 1.16 ppm (m, 80H, $CH_{2,Cy}$); $\{^1H\}^{13}C$ NMR (62.90 MHz, $CDCl_3$, 300 K): δ = 175.9 (CO), 61.0 (CHP), 52.0 ($CH_2N_{central}$), 48.94 (CH_2N + PCH_2N), 30.5 (CH_3), 29.79–26.25 ($CH_{2,Cy}$), 23.52 ppm ($CH_{2,dendr}$); $\{^1H\}^{31}P$ NMR (121.49 MHz, $CDCl_3$, 300 K): δ = 27 ppm; elemental analysis calcd (%) for $C_{136}H_{248}P_8N_6O_{16}Pd_4$ (2896.966): C 56.39, H 8.63; found: C 55.65, H 8.71.

G2-DAB-*dendr*-[bis(cyclohexylaminophosphine)]$_8$palladium(II) complex 3d: The same procedure as for **1d** was used with $[Pd(OAc)_2]$ (736 mg, 3.3 mmol) and aminophosphine **3b** (1.64 g, 0.41 mmol). Yield: 2.3 g (96%) of a yellow solid; ^1H NMR (300.13 MHz, $CDCl_3$, 300 K): δ = 2.61 (m, 64H, PCH_2N + PCH_{Cy}), 2.42 (m, 52H, CH_2N), 1.96 (s, 48H, CH_3), 1.79 (m, 160H, $CH_{2,Cy}$), 1.66 (m, 12H, CH_2CH_2), 1.24 ppm (m, 160H, $CH_{2,Cy}$); $\{^1H\}^{31}P$ NMR (121.49 MHz, $CDCl_3$, 300 K): δ = 27.2 ppm; elemental analysis calcd (%) for $C_{280}H_{512}P_{16}N_{14}O_{32}Pd_8$ (5934.161): C 56.67, H 8.63; found: C 54.98, H 8.79.

G3-DAB-*dendr*-[bis(cyclohexylaminophosphine)]$_{16}$palladium(II) complex 4d: The same procedure as for **1d** was used with $[Pd(OAc)_2]$ (592 mg, 2.64 mmol) and aminophosphine **4b** (1.39 g, 0.17 mmol). Yield: 1.6 g (81%) of a yellow solid; ^1H NMR (300.13 MHz, $CDCl_3$, 300 K): δ = 2.57 (m, 128H, PCH_2N + PCH_{Cy}), 2.29 (m, 104H, CH_2N), 1.91 (s, 96H, CH_3), 1.77 (m, 320H, $CH_{2,Cy}$), 1.63 (m, 12H, $CH_2CH_{2,dendr}$) 1.23 ppm (m, 320H, $CH_{2,Cy}$); $\{^1H\}^{13}C$ NMR (75.47 MHz, $CDCl_3$, 300 K): δ = 175.1 (CO), 59.35 (CHP), 50.2 ($CH_2N_{central}$), 47.1 (CH_2N + PCH_2N), 32.4 (CH_3), 27.1–24.29 ($CH_{2,Cy}$), 22.32 ppm ($CH_{2,dendr}$); $\{^1H\}^{31}P$ NMR (121.49 MHz, $CDCl_3$, 300 K): δ = 27.3 ppm.

Synthesis of $[FeCp\{C_6(CH_2CH_2C_6H_4CCC_6H_5)_6\}][PF_6]$: To a solution of $[FeCp\{C_6(CH_2CH_2C_6H_4Br)_6\}][PF_6]$ (1 g, 0.7 mmol) and catalyst **1c** (27 mg, 6 mol%) in dry Et_3N (3 mL) was added dropwise a solution of phenylacetylene (0.7 mL, 6 mmol) in dry Et_3N (3 mL).The mixture was heated to 80°C for three days. Et_3N was then removed, and the product was extracted with ether (5×20 mL). The organic layer was dried over Na_2SO_4, and flash silica gel chromatography with petroleum ether yielded a light brown solid (291 mg, 27%); ^1H NMR (300.13 MHz, $CDCl_3$, 300 K): δ = 7.02–7.59 (m, 54H, H_{ar}), 5.35 (s, 5H, Cp), 2.78 and 2.88 ppm (m, 12H, CH_2); $\{^1H\}^{13}C$ NMR (62.90 MHz, $CDCl_3$, 300 K): δ = 120.82–140.93 (C_{ar}), 80.11 (Cp), 37.12 (CH_2), 33.05 ppm (CH_2); MS (MALDI-TOF, *m*/*z*): calcd: 1424.68; found: 1425.38 $[M-PF_6]^+$.

Synthesis of $C_6(CH_2CH_2C_6H_4CCC_6H_5)_6$: To a solution of $C_6(CH_2CH_2C_6H_4Br)_6$ (0.2 g, 0.17 mmol) and catalyst **1c** (7 mg, 6 mol%) in dry Et_3N (3 mL) was added dropwise a solution of phenylacetylene (0.16 mL, 1.5 mmol) in dry Et_3N (3 mL). The mixture was heated at 80°C for 8 h. Et_3N then was removed, and the product was extracted with ether (3×20 mL). The organic layer was dried over Na_2SO_4, and flash silica gel chromatography with petroleum ether yielded a light brown solid (141 mg, 59%). ^1H NMR (300.13 MHz, $CDCl_3$, 300 K): δ = 7.03–7.45 (m, 54H, H_{ar}), 2.79 and 2.89 ppm (m, 12H, CH_2); $\{^1H\}^{13}C$ NMR (62.90 MHz, $CDCl_3$, 300 K): δ = 122.24–139.59 (C_{ar}), 37.02 (CH_2), 33.15 ppm (CH_2); elemental analysis calcd (%) for $C_{102}H_{78}$ (1403.741): C 93.97, H 6.03; found: C 93.28, H 5.59; MS (MALDI-TOF): *m*/*z* (%):calcd: 1411.61; found: 1411.54 (100) $[M+Ag]^+$.

Acknowledgment

The Institut Universitaire de France (IUF, D.A.), the Centre National de la Recherche Scientifique (CNRS), the Universities Bordeaux I and Paris VI, and the Ministère de la Recherche et de la Technologie (MRT, PhD grant to D.M.) are acknowledged for financial support.

[1] a) *Dendrimers and Nanosciences* (Ed.: D. Astruc) C. R. Chimie, Elsevier, **2003**, *Vol. 8–10*; b) G. R. Newkome, C. N. Moorefield, F. Vögtle, *Dendrimers and Dendrons, Concepts, Syntheses and Applications*, Wiley-VCH, Weinheim, **2002**; c) *Dendrimers and other dendritic polymers* (Eds.: J. M. J. Fréchet, D. A. Tomalia), Wiley, Chichester, **2001**.

[2] D. Astruc, F. Chardac, *Chem. Rev.* **2001**, *101*, 2991; G. E. Oosterom, J. N. H. Reek, P. C. J. Kamer, P. W. N. M. van Leeuwen, *Angew. Chem.* **2001**, *113*, 1878; *Angew. Chem. Int. Ed.* **2001**, *40*, 1828; R. Kreiter, A. W. Kleij, R. J. M. Klein Gebbink, G. van Koten, *Top. Curr. Chem.* **2001**, 217, 163.

[3] a) R. van Heerbeek, P. C. J. Kamer, P. W. N. M. van Leeuwen, J. N. H. Reek, *Chem. Rev.* **2002**, *102*, 3717; b) M. T. Reetz, G. Lohmer, R. Schwickardi, *Angew. Chem.* **1998**, *110*, 492; *Angew. Chem. Int. Ed. Engl.* **1997**, *36*, 1526.

[4] K. Heuzé, D. Méry, D. Gauss, D. Astruc, *Chem. Commun.* **2003**, 2274.

[5] a) J. S. Moore, *Acc.Chem. Res.* **1997**, *30*, 402; b) T. Hiyama in *Metal-Catalyzed Cross-Coupling Reactions* (Eds.: F. Diederich, P. J. Stang), Wiley-VCH, Weinheim, **1998**, Chapt. 10; c) E.-J. Negishi, L. Anastasia, *Chem. Rev.* **2003**, *103*, 1979; d) *Modern Arene Chemistry* (Ed.: D. Astruc), Wiley-VCH, Weinheim, **2002**; e) L. Brandsma, S. F. Vasilevsky, H. D. Verkruijsse, *Application of Transition Metal Catalysts in Organic Synthesis*, Springer, Berlin, **1988**, Chapt. 10; f) K. C. Nicolaou, E. J. Sorensen, *Classics in Total Synthesis*, Wiley-VCH, Weinheim, **1966**, p. 582.

[6] a) K. Sonogashira, Y. Tohoda, N. Hagihara, *Tetrahedron Lett.* **1975**, *16*, 4467; b) I. B. Campbell in *Organocopper Reagents: A Practical Approach* (Ed.: R. J. K. Taylor), OUP, New York, **1994**, Chapt. 10, p. 218; c) K. Sonogashira, *Comprehensive Organic Synthesis* (Ed.: B. M. Trost, I. Fleming) Pergamon Press, Oxford, **1991**, *Vol. 3*, p. 521; d) R. Rossi, A. Carpita, F. Bellina, *Org. Prep. Proced.* **1995**, *27*, 129.

[7] J.-P. Genêt, E. Blart, M. Savignac, *Synlett* **1992**, 715; V. P. Böhm, W. A. Hermann, *Eur. J. Org. Chem.* **2000**, 3679; M. Alami, F. Ferri, G. Linstrumelle, *Tetrahedron Lett.* **1993**, *34*, 6403; D. A. Alonso, C. Nájera, M. C. Pacheco, *Tetrahedron Lett.* **2002**, *43*, 9365; X. Fu, S. Zhang, J. Yin, D. Schumacher, *Tetrahedron Lett.* **2002**, *43*, 6673; M. Pal, K. Parasuraman, S. Gupta, K. R. Yeleswarapu, *Synlett Synlett.* **2002**, *12*, 1976; T. Fukayama, M. Shinmen, S. Nishitani, M. Sato, I. Ryu, *Org. Lett.* **2002**, *4*, 1691; D. A. Alonso, C. Najera, M. C. Pachecco, *Adv. Synth. Catal.* **2003**, *345*, 1146; D. Gelman, S. L. Buchwald, *Angew. Chem.* **2003**, *115*, 6175; *Angew. Chem. Int. Ed.* **2003**, *42*, 5993; ; L. Djakovitch, P. Rollet, *Tetrahedron Lett.* **2004**, *45*, 1367.

[8] D. Méry, K. Heuzé, D. Astruc, *Chem. Commun.* **2003**, 1934.

[9] C. Glaser, *Ber. Dtsch. Chem. Ges.* **1869**, *2*, 422; P. Siemsen, R. C. Livingston, F. Diederich, Angew. Chem. **2000**, *112*, 2740; *Angew. Chem. Int. Ed.* **2000**, *39*, 2632.

[10] J. Fawcett, P. A. T. Hoye, R. D. W. Kemmit, D. J. Law, D. R. Russell, *J. Chem. Soc. Dalton Trans.* **1993**, 2563.

[11] M. Chai, Y. Niu, W. J. Youngs, P. L. Rinaldi, *J. Am. Chem. Soc.* **2001**, *123*, 4670.

[12] P. W. N. M. van Leeuwen, *Appl. Catal. A* **2001**, *212*, 61; P. E. Garrou, *Chem. Rev.* **1985**, *85*, 171.

[13] B. Alonso, J.-C. Blais, D. Astruc, *Organometallics* **2002**, *21*, 1001.

[14] C. Amatore, A. Jutand, *J. Organomet. Chem.* **1999**, *576*, 254.

[15] L. J. Ackerman, J. P. Sadighi, D. M. Kurtz, J. A. Labinger, J. B. Bercaw, *Organometallics* **2003**, *22*, 3884.

[16] A. Jutand, *Eur. J. Inorg. Chem.* **2003**, 2017; C. Amatore, A. A. Bahsoun, A. Jutand, G. Meyer, A. N. Ntepe, L. Ricard, *J. Am. Chem. Soc.* **2003**, *125*, 4212.

[17] C. Amatore, A. Bucaille, A. Fuxa, A. Jutand, G. Meyer, A. N. Ntepe, *Chem. Eur. J.* **2001**, *7*, 2134.

[18] a) Y.-C. Chen, T.-F. Wu, J.-G. Dend, H. Liu, Y.-Z. Jiang, M. C. K. Choi, A. S. C. Chan, *Chem. Commun.* **2001**, 1488; b) Q.-H. Fan, Y.-M. Chen, X.-M. Chen, D.-Z. Jiang, F. Xi, A. S. C. Chan, *Chem. Commun.* **2000**, 789; c) V. Maraval, R. Laurent, A.-M. Caminade, J.-P. Majoral, *Organometallics* **2000**, *19*, 4025; d) H. Zeng, G. R. Newkome, C. L. Hill, *Angew. Chem. Int. Ed.* **2000**, *39*, 1771; *Angew. Chem.* **2000**, *112*, 1841; e) Q.-S. Hu, V. Pugh, M. Sabat, L. Pu, *J. Org. Chem.* **1999**, *64*, 7528; f) M. Petrucci-Samija, V. Guillemette,

M. Dasgupta, A. K. Kakkar, *J. Am. Chem. Soc.* **1999**, *121*, 1968; g) S.-I. Murahashi, T. Naota, H. Taki, M. Mizuno, H. Takaya, S. Komiya, Y. Mizuho, N. Oyasato, M. Hiraoka, M. Hirano, A. Fukuoka, *J. Am. Chem. Soc.* **1995**, *117*, 12436.

[19] P. Arya, N. Vrnugopal Rao, J. Singkhonrat, *J. Org. Chem.* **2000**, *65*, 1881; P. Arya, G. Panda, N. Vrnugopal Rao, H. Alper, C. Bourque, L. Manzer, *J. Am. Chem. Soc.* **2001**, *123*, 2889.

[20] S. Gatard, S. Nlate, G. Bravic, J.-C. Blais, D. Astruc, *Angew. Chem.* **2003**, *115*, 468; *Angew. Chem. Int. Ed.* **2003**, *42*, 452; ; S. Gatard, S. Kahlal, D. Méry, S. Nlate, E. Cloutet, J.-Y. Saillard, *Organometallics* **2004**, *23*, ASAP.

Received: February 13, 2004
Published online: June 24, 2004

Partie II

Métathèse

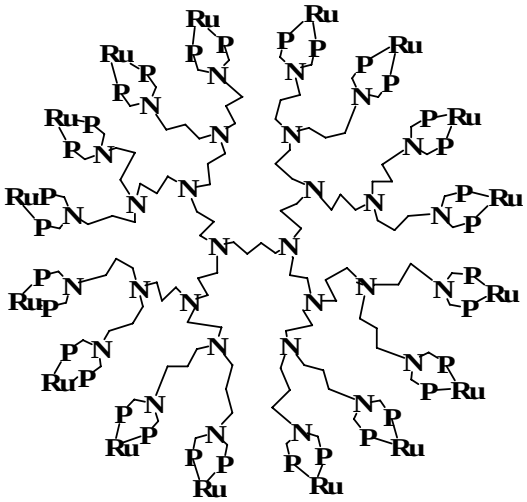

A. Introduction

De nos jours, la formation de liaisons C=C par métathèse des oléfines, constitue une thématique primordiale dans le monde de la chimie organique et de la chimie industrielle. Cette réaction a été récompensée par le prix Nobel de chimie 2005 attribué au directeur de recherche français Yves Chauvin ainsi qu'aux professeurs américains, Richard R. Schrock et Robert H. Grubbs, pour leurs travaux précurseurs sur l'étude et le développement de cette méthode de synthèse organique. L'étymologie du mot métathèse vient du grec « *meta* » (changer) et de « *tera* » (place), soit littéralement « changer de place ». Effectivement, il s'agit ici de la redistribution quasiment statistique, sous contrôle thermodynamique, des doubles liaisons oléfiniques. Il existe différents types de métathèse (Schéma 1) :

- la métathèse polymérisante par ouverture de cycle (**ROMP**)
- la fermeture de cycle par métathèse (**RCM**)
- la polymérisation d'un diène acyclique (**ADMEP**)
- la métathèse croisée (**CM**)

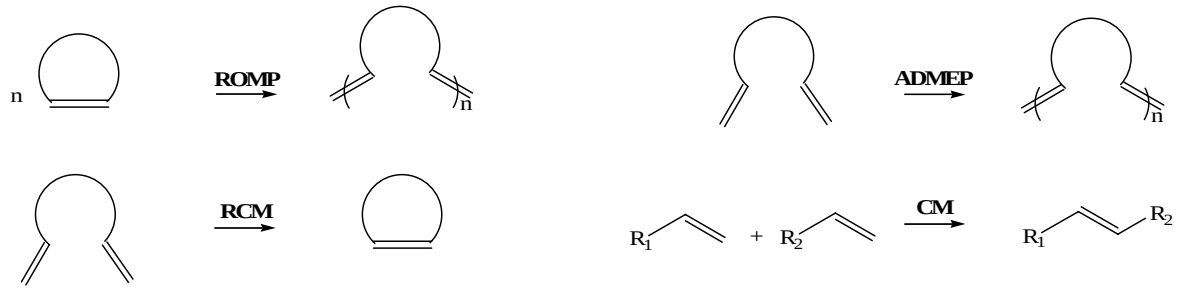

Schéma 1 : Les différents types de métathèse

La métathèse permet l'accès à des molécules insaturées difficilement accessibles par une autre voie, à des polymères fonctionnalisés, à des systèmes hétérocycliques et à des oléfines portant des groupes fonctionnels. La compréhension du mécanisme réactionnel par le groupe de Chauvin à l'Institut Français du Pétrole en 1971 (Schéma 2), a permis la synthèse de nouveaux catalyseurs très actifs et efficaces.

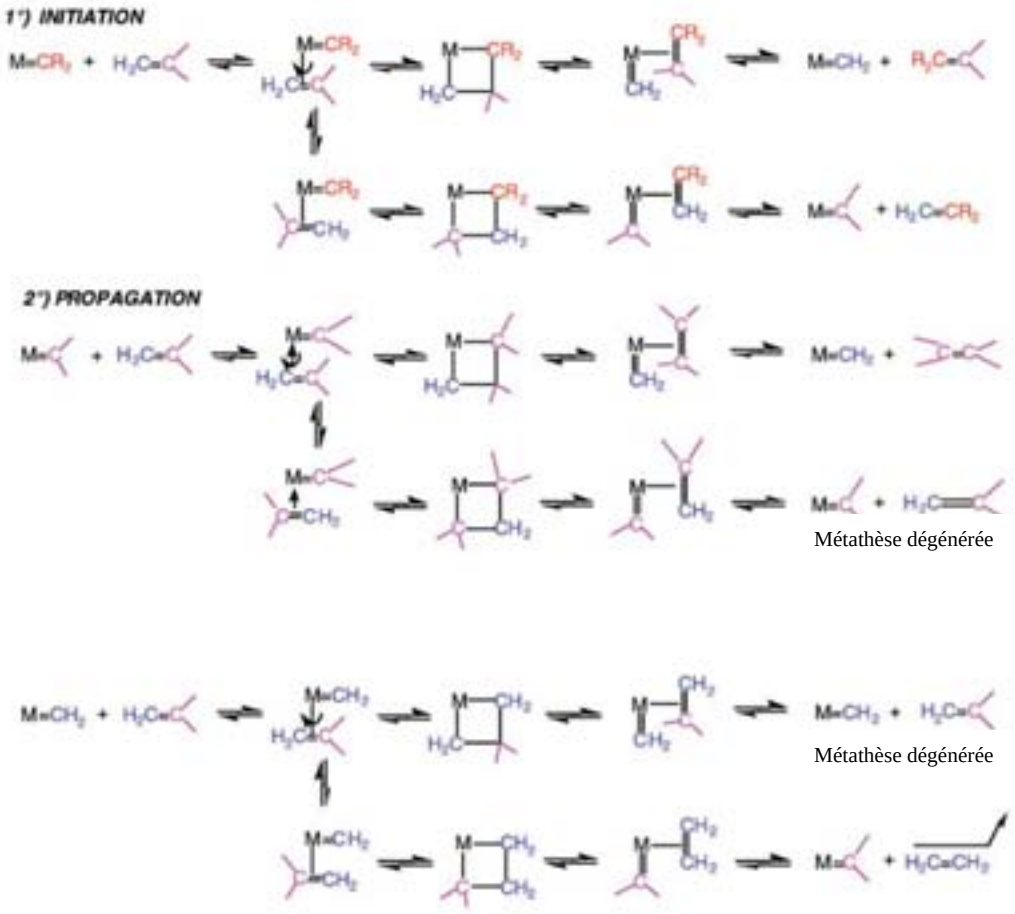

Schéma 2 : Mécanisme de Chauvin

En effet, le groupe de Schrock (1980) puis celui de Grubbs (1992) ont synthétisés différents catalyseurs de molybdène, de tungstène et de ruthénium (Schéma 3). Les catalyseurs de Grubbs sont à présent très largement utilisés par les chimistes organiciens, non seulement parce qu'ils sont commerciaux et peu coûteux mais aussi en raison de leur tolérance pour les fonctions organiques. Par la suite, le groupe d'Hoveyda a synthétisé un complexe dérivé du catalyseur de Grubbs première génération très actif en catalyse et très stable à l'air contrairement aux précédents complexes (Schéma 3).

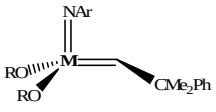

*Formule générale de la famille des catalyseurs de Schrock (**M** = **Mo** ou **W**; R et Ar substituants stériquement encombrés) 1990*

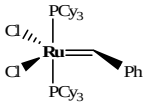

Catalyseur de Grubbs première génération 1995

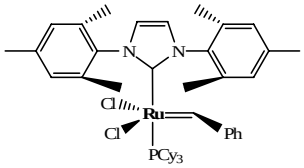

Catalyseur de Grubbs seconde génération 1999

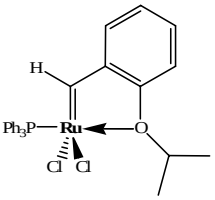

Catalyseur d'Hoveyda première génération 1999

Schéma 3 : Quelques catalyseurs de la réaction de métathèse

B. Synthèses des polymères en étoile

Dans un premier temps, nous avons réalisé la synthèse de nouveaux complexes modèles et dendritiques de ruthénium dérivés du catalyseur d'Hoveyda pour la métathèse polymérisante par ouverture de cycle (ROMP) du norbornène (Schéma 4), dans la continuité de la thèse de S. Gatard au laboratoire (voir mémoire en annexe 1).

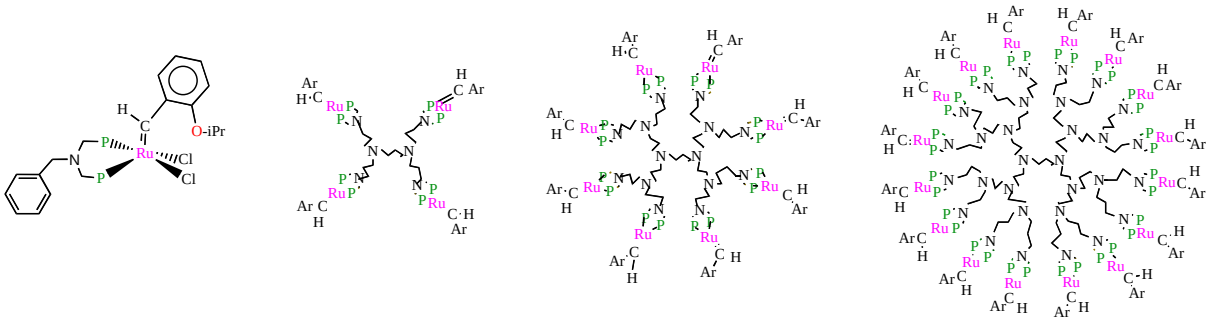

Schéma 4 : Complexes modèles et dendritiques de ruthénium (P = Pt-Bu$_2$ et Ru = RuCl$_2$)

L'activité des catalyseurs dendritiques a été comparée à celle du complexe modèle en tant qu'amorceur de la ROMP du norbornène. De plus, l'effet dendritique, en comparant les différentes générations entre elles, a été étudié. Il est à noter que dans cette étude nous formons de nouveaux matériaux : les polymères en étoile (Équation 1).

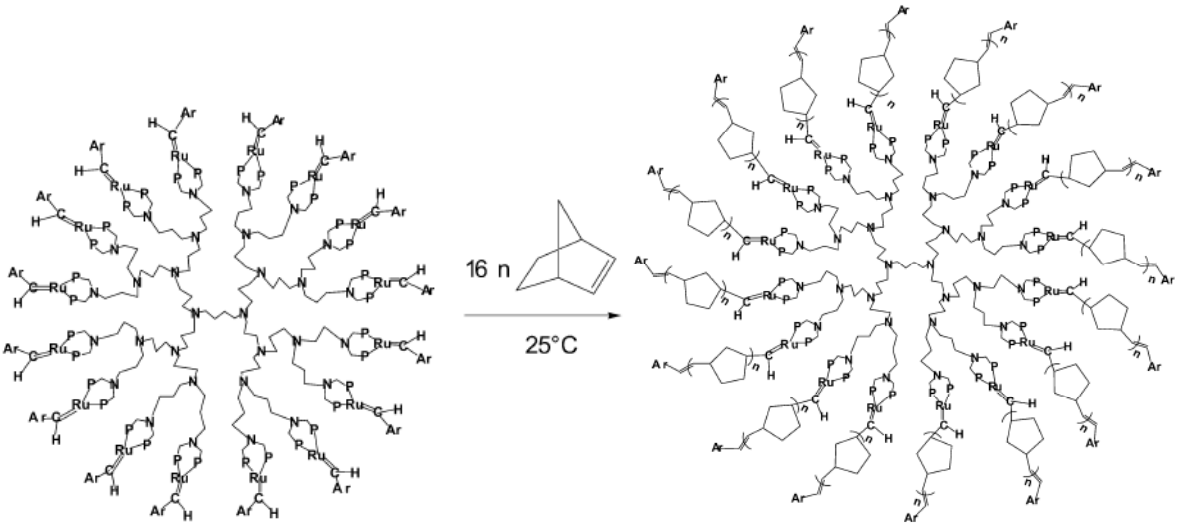

Équation 1 : Synthèse d'un polymère en étoile (P = Pt-Bu$_2$ et Ru = RuCl$_2$)

L'effet du groupement alkyle de la phosphine sur les métallodendrimères a été étudié par comparaison de nos travaux avec ceux de S. Gatard et *coll.* (voir Annexe 1).

Ces travaux sur les métallodendrimères de ruthénium ont fait l'objet d'un court mémoire publié au *Journal of Molecular Catalysis A: Chemical* et intitulé "**Synthesis of Monomeric and Dendritic Ruthenium Benzylidene cis-bis-*tertio*butyl phosphine Complexes that Catalyze the ROMP of Norbornene under Ambient Conditions**".

C. Fonctionnalisation des dendrimères

Dans un second temps, nous nous sommes intéressés à un aspect plus fondamental de la chimie des dendrimères. En effet, des dendrimères ont été bifonctionnalisés en une seule étape par les réactions de métathèse de fermeture de cycle et de métathèse croisée (Équation 2).

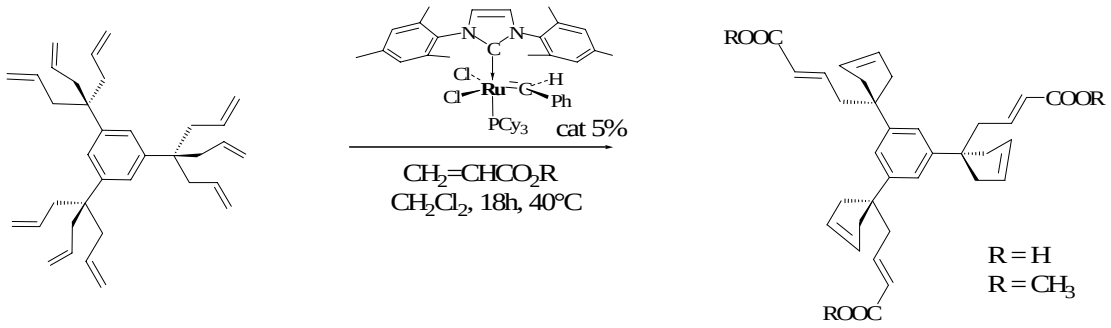

Équation 2 : Dendrimère bifonctionnalisé

Ce résultat est à comparer à l'homocouplage obtenu au laboratoire dans le cadre de la thèse de V. Martinez (Schéma 5).

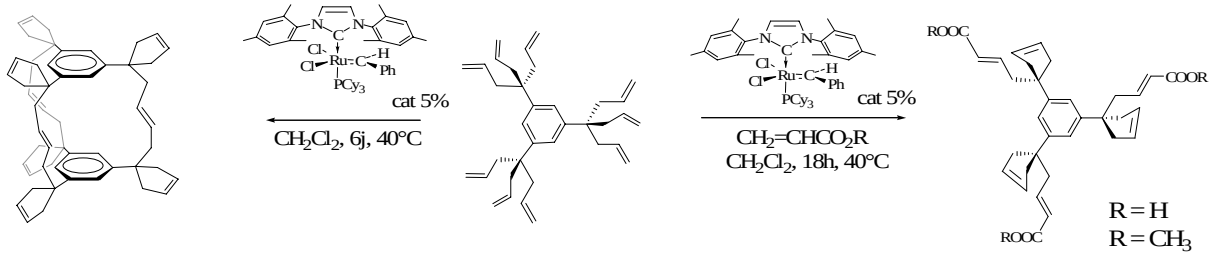

Schéma 5 : Compétition entre les différents types de métathèse

De plus, grâce à une stratégie de rallongement des branches, la métathèse de fermeture de cycle a été inhibée, ce qui a permis la monofonctionnalisation des dendrimères acides ou esters à partir des dendrimères oléfiniques à longues branches (Équation 3).

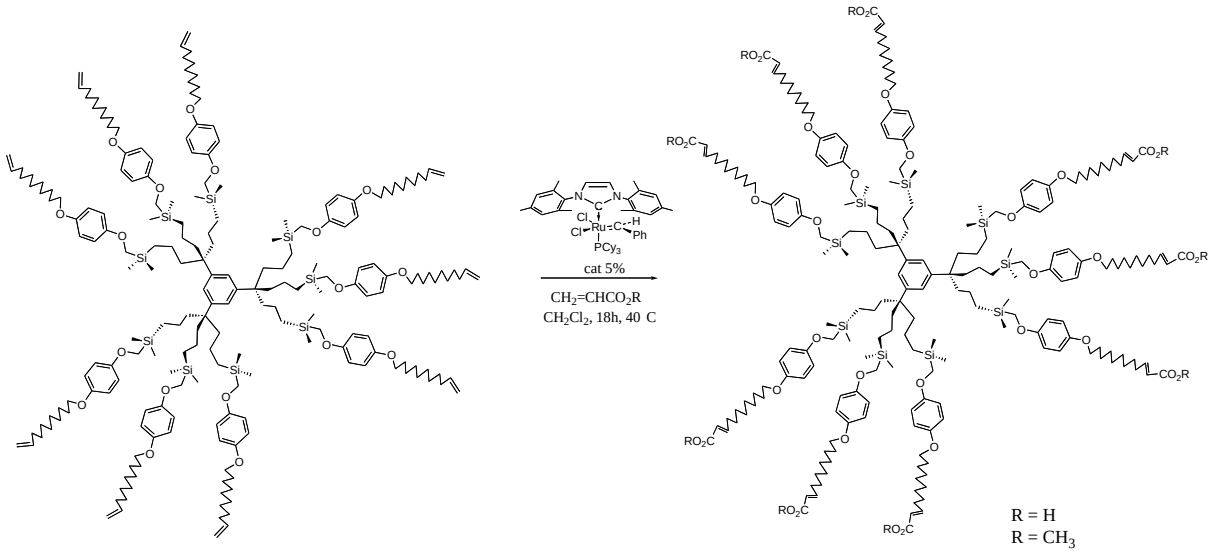

Équation 3 : Dendrimère à longues branches monofonctionnalisé

Ces travaux ont fait l'objet d'une note publiée à *Angewandte Chemie International Edition* et intitulée "**Efficient Mono- and Bifunctionnalization of Poly-olefin Dendrimers by Olefin Metathesis** ". Dans cette note, notre laboratoire a collaboré avec Jean-Claude Blais, du LCSOB à Paris VI, et Eric Cloutet, du LPCO à Bordeaux, qui ont réalisé les spectres de masse et les S.E.C., respectivement. D'autre part, l'ingénierie de rallongement des branches, les réactions de métathèse sur les dendrimères à 27 et 81 branches, et la fonctionnalisation du dendrimères à 81 branches acides par une amine triferrocénique ont été réalisés par C. Ornelas et J. Ruiz.

Available online at www.sciencedirect.com
SCIENCE DIRECT®
Journal of Molecular Catalysis A: Chemical 227 (2005) 1–5
JOURNAL OF MOLECULAR CATALYSIS A: CHEMICAL
www.elsevier.com/locate/molcata

Synthesis of monomeric and dendritic ruthenium benzylidene *cis*-bis-tertiobutyl phosphine complexes that catalyze the ROMP of norbornene under ambient conditions

Denise Méry, Didier Astruc*

Nanosciences and Catalysis Group, LCOO, UMR CNRS No. 5802, Université Bordeaux I, 33405 Talence Cedex, France

Received 5 August 2004; accepted 31 August 2004
Available online 11 November 2004

Abstract

The synthesis of monomeric and dendritic ruthenium benzylidene *cis*-bis-phosphine complexes that catalyze norbornene ROMP previously reported with dicyclohexyl bis-phosphines has now been extended to monomeric and dendritic bis-tertiobutyl phosphines. The reaction of Hoveyda's catalyst $[RuCl_2(=CH\text{-}o\text{-}O\text{-}iPrC_6H_4)PPh_3]$ (**1**) with the diphosphine $PhCH_2N(CH_2PtBu_2)_2$ (**2**) gives the new air-stable green ruthenium carbene complex (**3**) in which (**2**) models a dendritic branch of poly(diphosphine) dendrimers DAB-*dendr*-$[N(CH_2PtBu_2)_2]_n$ (G_1, $n = 4$; G_2, $n = 8$; G_3, $n = 16$). Metallodendrimers DAB-*dendr*-$[N(CH_2PtBu_2)_2Ru(=CHAr)(Cl)_2]_n$ (**4**)–(**6**) derived from the three first generations of DAB polyamines containing, respectively, 4, 8 and 16 ruthenium branches have been synthesized. These dendritic ruthenium–benzylidene complexes initiate the ROMP of norbornene at room temperature to form star-shaped metallodendritic polymers slightly more rapidly than the analogues with bis-cyclohexyl phosphines. Interestingly, the metallodendrimers G_1 (**4**) initiates the ROMP of norbornene much faster than the model ruthenium complex (**3**) the overall rate order being $G_1 > G_2 > G_3 >$ model, these positive and negative dendritic effects being comparable with those found for the dicyclohexyl bis-phosphine complexes.

Keywords: Dendrimers; Catalysis; Ruthenium; Metathesis; Diphosphines; Polymerization

1. Introduction

Metallodendritic catalysts have started to emerge as a promising alternative to classic homogeneous and heterogeneous catalysts, because of their perfect molecular definition, solubility allowing mechanistic investigations and ease of recovery and re-use [1]. Among the metathesis reactions, ROMP is a popular one, among other techniques [2], leading to well-defined polymers [3]. We recently reported, in both a communication and a full publication [4], three generations of dendritic ruthenium benzylidene *cis*-bis-phosphine complexes that did not catalyse RCM reactions but were efficient ROMP catalysts under ambient conditions. Dendrimer-cored polymer stars, an original form of polymers, could be synthesized in a living ROMP process by polymerization of norbornene. The chelating bis-phosphine used had the formula $RN(CH_2PR_2)_2$ in which R = Cy [5]. Since Hofmann reported very efficient metathesis catalysts with *cis*-bis-phosphines in which the phosphorus atoms had *tert*-Bu substituents [6,7], we decided to investigate the $RN(CH_2PR_2)_2$ bis-phosphine with the *tert*-Bu substituents for the R groups and the resulting effect on the ROMP of norbornene. The increase of bulk on the metal center and increased electron density are supposed to favor metathesis activity in Grubbs' type catalysts, and this effect was indeed also positive on *cis*-phosphine ruthenium metathesis catalysts. Thus, we are reporting here the synthesis of ruthenium benzylidene complexes analogous to those previously reported with the Cy substituents with *cis*-bis-phosphine ligands $RN\{CH_2P(tert\text{-}$

* Corresponding author. Tel.: +33 556 84 62 71; fax: +33 556 84 66 46.
E-mail address: d.astruc@lcoo.u-bordeaux1.fr (D. Astruc).

1381-1169/$ – see front matter © 2004 Elsevier B.V. All rights reserved.
doi:10.1016/j.molcata.2004.08.050

Bu)$_2$}$_2$ including a monomeric model (R = PhCH$_2$) and three dendrimer generations and the ROMP of norbornene with these new monomeric and metallodendritic ROMP catalysts.

2. Results

2.1. Synthesis of the new ruthenium–benzylidene complex (3)

The reaction of Hoveyda's metathesis catalyst (**1**) [8] with the chelating bis-phosphine (**2**) bearing *tert*-Bu substituents in CH_2Cl_2 at 25 °C gives the new ruthenium benzylidene [9] complex (**3**) (Eq. (1)) whose ^{1}H NMR spectrum shows the carbene proton at δ = 15.6 ppm as a triplet indicating the coupling with two equivalent phosphorus atoms. The later give rise to a singlet at 41 ppm in the ^{31}P NMR spectrum confirming their equivalence. The triphenylphosphine signal have disappeared, indicating the substitution of this ligand and the ether oxygen atom by the chelating bis-phosphine (**2**). The presence of a deshieded signal at δ = 9.65 ppm for an arene proton is characteristic of a non-coordinated oxygen atom. This complex was also characterized by a correct elemental analysis. It is thus analogous to the one previously obtained with the Cy substituent on the phosphorus atoms of the bis-phosphine, and serves as a model for the synthesis of the corresponding dendritic benzylidene complexes with dendritic bis-phosphines also bearing the *tert*-Bu substituents.

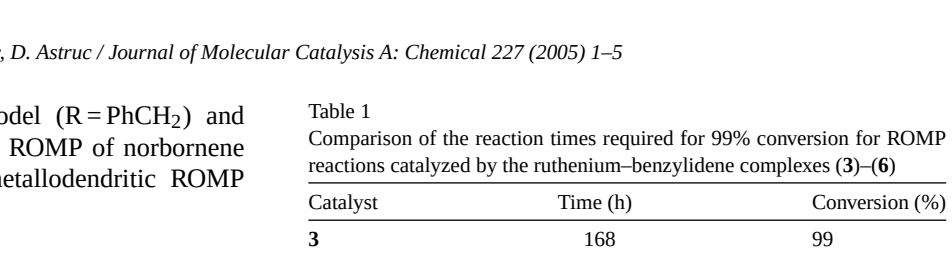

1

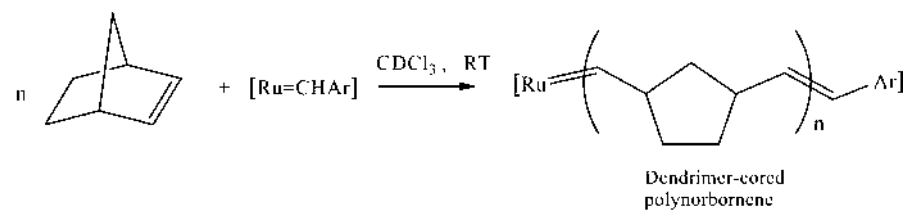

2

2.2. Synthesis of the new dendritic ruthenium–benzylidene complexes (4)–(6)

Given the result for the synthesis of the model complex (**3**), we have extended the synthetic procedure under ambient conditions to the three first generations of dendritic phosphines. These reactions yielded the corresponding dendritic ruthenium benzylidene complexes (**4**)–(**6**) that also showed the dowfield triplet for the carbene proton and the singlet in ^{31}P NMR. Besides satisfactory spectroscopic data for these three metallodendrimers (**4**)–(**6**), the first-generation metallodendrimer (G_1), namely (**4**) was also characterized by elemental analysis (Scheme 1).

Table 1
Comparison of the reaction times required for 99% conversion for ROMP reactions catalyzed by the ruthenium–benzylidene complexes (**3**)–(**6**)

Catalyst	Time (h)	Conversion (%)
3	168	99
4	15	99
5	22	99
6	24	99

These reaction times were obtained upon following the ROMP reactions by ^{1}H NMR *cis*/*trans* ratio: 30/70.

2.3. ROMP of norbornene to form metallodendritic stars

The ROMP reaction of norbornene catalyzed by the model complex (**3**) and by the dendritic ruthenium benzylidene complexes (**4**)–(**6**) was carried out at 25 °C under an inert atmosphere (Eq. (2)). The model complex yielded a linear polymer, and the metallodendritic complexes gave dendrimer-cored polynorbornene stars analogous to those previously obtained with Cy phosphine substituents. The kinetics of the ROMP reactions was followed by ^{1}H NMR, and the data are gathered in Table 1).

Table 1 clearly shows that the reaction time required for 99% conversion is considerably longer (of the order of 10 times) for the model complex (**3**) than for the dendrimers (**4**)–(**6**). It also shows a negative dendritic effect on the catalytic efficiency, i.e. the reaction times slightly increases as the dendrimer generation also increases.

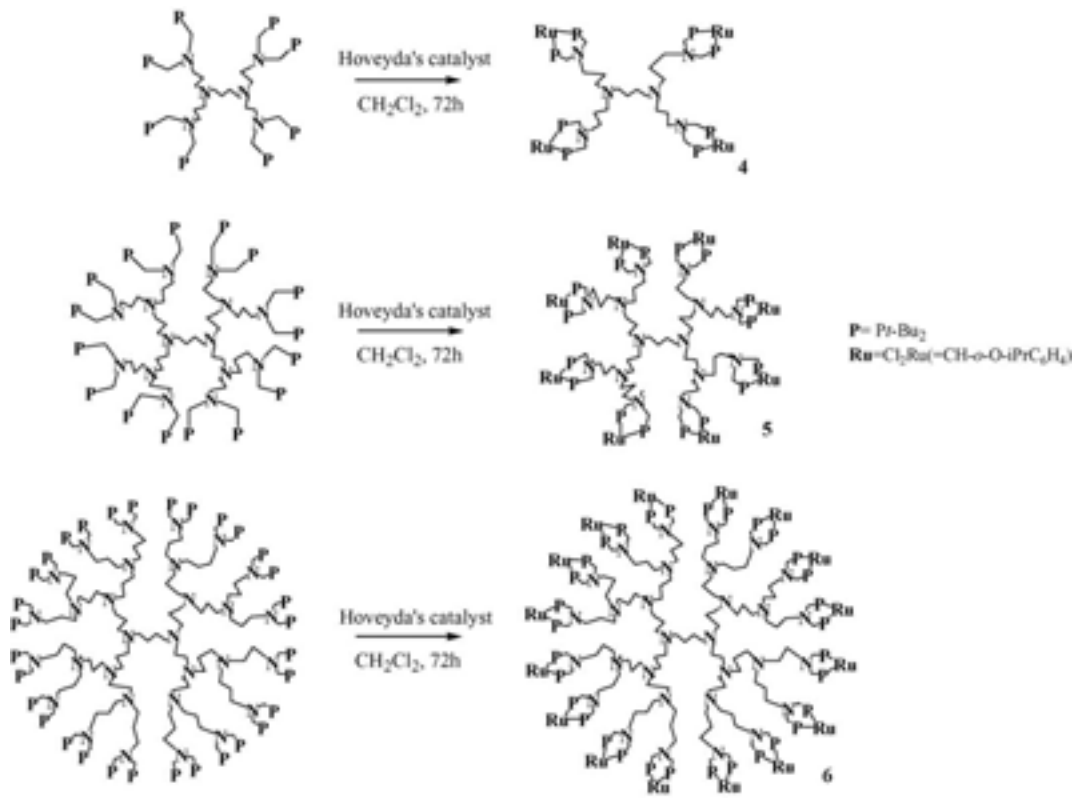

Scheme 1. Synthesis of the three first generations of dendritic ruthenium–benzylidene complexes (**4**)–(**6**) with P = P(*tert*-Bu)$_2$. The *tert*-Bu substituents on phosphorus atoms the chloride ligands and the benzylidene ligand on Ru atoms are omitted for clarity.

3. Discussion

The synthesis and chemistry of the new ruthenium benzylidene complex (**3**) and of the new dendritic benzylidene complexes (**4**)–(**6**) is analogous to that of the complexes in which the bis-phosphine bears Cy groups instead of *tert*-Bu groups. In synthesizing the *tert*-Bu series, we were hoping that these ruthenium benzylidene complexes would be more efficient as metathesis catalysts than the Cy analogues. In fact, the ROMP reaction of norbornene catalyzed by the *tert*-Bu series of complexes is only slightly faster than that using the Cy series. With the most efficient catalyst that is the first-generation dendrimer (**4**), the 99% conversion is reached after 15 h whereas the corresponding first-generation dendrimer with Cy substituents required 25 h to reach 99% conversion. Thus, it can be concluded that the *tert*-Bu group is slightly more favorable than the Cy group. No RCM metathesis was obtained with catalyst (**4**)–(**6**) which was already the case for the Cy series. We speculated, in the Cy series, that the initial step for metathesis was the decoordination of a phosphine ligand on the basis of the much slower catalytic activity compared to Grubbs catalysts. DTF calculation, increased reactivity of dendrimer compared to the monomer and air sensitivity of the metallodendrimers whereas the monomer was air stable, were in agreement with this proposal. The same trend is found here, confirming this hypothesis.

4. Concluding remarks

1. A new family of thermally stable monomeric and dendrimeric ruthenium benzylidene complexes (including three dendrimer generations) with bis-phosphines bearing *tert*-Bu substituents has been synthesized and characterized. The monomer is moderately air stable and the metallodendrimers are air sensitive as in the Cy series. These new compounds are analogous to those previously reported in the Cy series.
2. The new complexes are only slightly more active catalysts for the ROMP of norbornene than their analogues of the Cy series. The metallodendrimers catalyze the ROMP of norbornene much more rapidly than the monomer (positive dendritic effect probably due to the easier decoordination of a phosphine in the dendrimers than in the monomer), but the catalytic efficiency decreases upon increasing the dendrimer generation (negative dendritic effect probably due to increased steric inhibition upon increasing the generation). These effects are analogous to those already found in the Cy series.
3. Neither series is active for RCM metathesis. Other synthetic strategies are now clearly called for in order to reach dendritic ruthenium carbene complexes active in RCM and cross metathesis that is most useful in organic chemistry.

5. Experimental

5.1. General data

All manipulations were carried out using Schlenk techniques or in a nitrogen-filled Vacuum Atmosphere drylab. Solvents were freshly distilled under nitrogen. Reagent-grade CH_2Cl_2 and pentane were predried over Na foil and distilled from sodium-benzophenone anion under argon immediately prior to use. All other chemicals were used as received. ^{1}H NMR spectra were recorded at 25 °C with a Bruker AC 300 (300 MHz) spectrometer. ^{13}C NMR spectra were obtained in the pulsed FT mode at 75 MHz with a Brucker AC 300 spectrometer. All chemical shifts are reported in parts per million (δ, ppm) with reference to Me_4Si (TMS). Elemental analyses were carried out at the Vernaison CNRS Center.

5.2. Synthesis of ruthenium–benzylidene complexes (3)–(6)

The mixture of the diphosphine or dendritic phosphine DAB-*dendr*-$N(CH_2\text{-}PtBu_2)_2)_n$ and Hoveyda's catalyst, $[RuCl_2(=CH\text{-}o\text{-}O\text{-}iPrC_6H_4)PPh_3]$ (**1**) was stirred at room temperature in CH_2Cl_2 under nitrogen for 72 h. The reaction mixture was concentrated under reduced pressure to about 2 mL, and pentane (20 mL) was added. The product precipitated in the form of green powder.

Monomer (**3**). Yield: 90%. ^{1}H NMR ($CDCl_3$, 300 MHz), δ_{ppm}: 1.32 (s, *t*Bu), 1.36 (s, *t*Bu), 1.41 (d, $OCH(CH_3)_2$), 2.74 (m, NCH_2P), 3.60 (m, NCH_2Ph), 4.80 (m, $OCH(CH_3)_2$), 6.71–7.62 (m, H_{Ar}), 9.65 (m, H_{Ar}), 15.60 (t, Ru=CH). ^{31}P NMR ($CDCl_3$, 81.03 MHz), δ_{ppm}: 40.8 ($PtBu_2$). ^{13}C NMR (62.9 MHz, $CDCl_3$): δ 135.9–127.4 (C_{Ar}), 70.1 (OCH), 68.3 (CH_2N), 55.9 (PCH_2N), 33.2 (*t*Bu), 32.8 (*t*Bu), 31.8 ($OCH(CH_3)_2$). Anal. calcd for $C_{35}H_{59}Cl_2NOP_2Ru$: C, 56.52; H, 8.00. Found: C, 56.23; H, 7.89.

G_1-Ru_4P_8 (**4**). Yield: 63%. ^{1}H NMR ($CDCl_3$, 300 MHz), δ_{ppm}: 1.24 (m, CH_2CH_2), 1.29 (s, *t*Bu), 1.33 (s, *t*Bu), 1.40 (d, $OCH(CH_3)_2$), 2.70 (m, NCH_2), 3.54 (m, NCH_2Ph), 4.72 (m, $OCH(CH_3)_2$), 7.01–7.83 (m, Har), 9.55 (m, Har), 15.51 (t, Ru=CH). ^{31}P NMR ($CDCl_3$, 81.03 MHz), δ_{ppm}: 40.8 ($PtBu_2$). ^{13}C NMR (62.9 MHz, $CDCl_3$): δ 134.9–126.5 (Car), 70.1 (OCH), 59.4 (CH_2N), 55.9 (PCH_2N), 33.1 (*t*Bu), 32.7 (*t*Bu), 31.8 ($OCH(CH_3)_2$). Anal. calcd for $C_{128}H_{240}Cl_8N_6O_4P_8Ru_4$: C, 56.52; H, 8.00. Found: C, 56.23; H, 7.89.

G_2-Ru_8P_{16} (**5**). Yield: 65%. ^{1}H NMR ($CDCl_3$, 300 MHz), δ_{ppm}: 1.23 (m, CH_2CH_2), 1.30 (s, *t*Bu), 1.36 (s, *t*Bu), 1.39 (d, $OCH(CH_3)_2$), 2.72 (m, NCH_2), 3.57 (m, NCH_2Ph), 4.75 (m, $OCH(CH_3)_2$), 6.99–7.79 (m, H_{Ar}), 9.54 (m, H_{Ar}), 15.51 (t, Ru=CH). ^{31}P NMR ($CDCl_3$, 81.03 MHz), δ_{ppm}: 40.8 ($PtBu_2$). ^{13}C NMR (62.9 MHz, $CDCl_3$): δ 134.3–126.9 (C_{Ar}), 69.9 (OCH), 59.3 (CH_2N), 55.6 (PCH_2N), 33.1 (*t*Bu), 32.9 (*t*Bu), 31.8 ($OCH(CH_3)_2$).

G_3-$Ru_{16}P_{32}$ (**6**). Yield: 64%. ^{1}H NMR ($CDCl_3$, 300 MHz), δ_{ppm}: 1.20 (m, CH_2CH_2), 1.33 (s, *t*Bu), 1.39 (s, *t*Bu), 1.42 (d, $OCH(CH_3)_2$), 2.74 (m, NCH_2), 3.59 (m, NCH_2Ph), 4.72 (m, $OCH(CH_3)_2$), 6.87–7.42 (m, H_{Ar}), 9.49 (m, H_{Ar}), 15.49 (t, Ru=CH). ^{31}P NMR ($CDCl_3$, 81.03 MHz), δ_{ppm}: 40.8 ($PtBu_2$). ^{13}C NMR (62.9 MHz, $CDCl_3$): δ 135.1–127.0 (C_{Ar}), 70.1 (OCH), 59.5 (CH_2N), 55.8 (PCH_2N), 33.2 (*t*Bu), 32.8 (*t*Bu), 31.9 ($OCH(CH_3)_2$).

5.3. Polymerization of norbornene by monomeric and dendrimeric ruthenium complexes

Norbornene and the ruthenium–benzylidene catalyst (0.003 mmol) were introduced in a dry Schlenk tube under an inert atmosphere in 2 mL of $CDCl_3$, and the reaction was followed at 25 °C by ^{1}H NMR (see data in Table 1 and characterizations in Ref. [4]).

Acknowledgments

We are grateful to Drs. S. Gatard, K. Heuze, S. Nlate and J. Ruiz for helpful discussions. Financial support from the IUF, CNRS, MRT and the University Bordeaux I is gratefully acknowledged.

References

[1] (a) D. Astruc, F. Chardac, Chem. Rev. 101 (2001) 2991;
(b) G.E. Oosterom, J.N.H. Reek, P.C.J. Kamer, P.W.N.M. van Leeuwen, Angew. Chem. Int. Ed. Engl. 40 (2001) 1828;
(c) R. Kreiter, A.W. Kleij, R.J.M. Klein Gebbink, van Koten, G. In Dendrimers IV: Metal Coordination, Self Assembly, Catalysis, F. Vögtle, C.A. Schalley (Eds.), Top. Curr. Chem., Springer-Verlag, Berlin, 2001. vol. 217, p. 163;
(d) R. van Heerbeeck, P.C.J. Kamer, P.W.N.M. van Leuwen, J.N.H. Reek, Chem. Rev. 102 (2002) 3717.

[2] E. Cloutet, J.-L. Fillaut, Y. Gnanou, D. Astruc, J. Chem. Soc., Chem. Commun. (1994) 2433;
M.R. Leduc, C.J. Hawker, J. Dao, J.M.J. Fréchet, J. Am. Chem. Soc. 118 (1996) 11111.

[3] (a) T.M. Trnka, R.H. Grubbs, Acc. Chem. Res. 34 (2001) 18;
(b) R.H. Grubbs (Ed.), Handbook of Metathesis, Applications in Polymer Synthesis, vol. 3, Wiley–VCH, Weinheim, 2003.

[4] (a) S. Gatard, S. Nlate, E. Cloutet, G. Bravic, J.-C. Blais, D. Astruc, Angew. Chem. Int. Ed. 42 (2003) 452;
(b) S. Gatard, S. Kahlal, D. Méry, S. Nlate, E. Cloutet, J.-Y. Saillard, D. Astruc, Organometallics 23 (2004) 1313.

[5] M.T. Reetz, G. Lohmer, R. Schwickardi, Angew. Chem. Int. Ed. 36 (1997) 1526;
for the synthesis of the monomeric and dendritic bis-phosphines $RN\{CH_2P(tert\text{-}Bu)_2\}_2$ (R = $PhCH_2$ or DSM dendritic core) and their use in Pd catalysis, see;
(b) D. Méry, K. Heuze, D. Astruc, Chem. Commun. (2003) 1934;
K. Heuze, D. Méry, D. Gauss, D. Astruc, Chem. Commun. (2003) 2274.

[6] S.M. Hansen, M.A.O. Volland, F. Rominger, F. Eisenträger, P. Hofmann, Angew. Chem. Int. Ed. 38 (1999) 1273;
S. Hansen, F. Rominger, M. Metz, P. Hofmann, Chem. Eur. J. 5 (1999) 557;
C. Adlhart, M.A.O. Volland, P. Hofmann, P. Chen, Helv. Chim. Acta 83 (2000) 3306.

[7] For other metathesis catalysts with *cis*-bis-phosphine ruthenium complexes, see;
D. Amoroso, D.E. Fogg, Macromolecules 33 (2000) 2815;
C. Six, K. Beck, A. Wegner, W. Leitner, Organometallics 19 (2000) 4639.
[8] S.B. Garber, J.S. Kingsbury, B.L. Gray, A.H. Hoveyda, J. Am. Chem. Soc. 122 (2000) 8168.
[9] For previous reports of dendritic meta-carbene complexes and their metathesis activity, see Ref. [4,8] and;
P. Wijkens, J.T.B.H. Jastrzebski, P.A. van der Schaaf, R. Kolly, A. Hafner, G. van Koten, Org. Lett. 2 (2000) 1621;
H. Beerens, F. Verpoort, L. Verdonck, J. Mol. Cat. 151 (2000) 279;
H. Beerens, F. Verpoort, L. Verdonck, J. Mol. Cat. 159 (2000) 197.

Polyolefins

DOI: 10.1002/anie.200502848

Efficient Mono- and Bifunctionalization of Polyolefin Dendrimers by Olefin Metathesis**

*Cátia Ornelas, Denise Méry, Jean-Claude Blais, Eric Cloutet, Jaime Ruiz Aranzaes, and Didier Astruc**

Olefin metathesis has recently transformed the way molecular chemists think about synthetic strategies.[1] Remarkable examples can be found in transition-metal architectures, such as ring-closing metathesis (RCM) of olefin-terminated ligands.[2,3] van Koten and Newkome have used stars for the nanofabrication of giant ring structures by using RCM,[4] and Zimmerman and co-workers have shown that RCM successfully allows molecular imprinting inside dendrimers and can be applied to the fabrication of nanotubes.[5] Indeed, RCM and ring-opening-metathesis polymerization (ROMP) are probably the most popular facets of olefin metathesis because of their considerable impact on the synthesis of biologically important cyclic compounds and polymers, respectively.[1] At first sight, cross metathesis (CM) is marred by the thermodynamic equilibrium that produces a mixture of compounds, but Blechert and co-workers showed that the excess of one olefin together with the Schrock Mo catalyst[1b] favors the formation of the cross product, whereas steric factors favor *E* stereoselectivity.[6] Grubbs and co-workers have shown that when a terminal olefin is metathesized with the second-generation Ru catalyst **A** (Cy = cyclohexyl) in the presence of another olefin bearing a strongly electron-withdrawing substituent, the stereoselectivity leads to high yields of the *E*-functionalized cross olefin.[7]

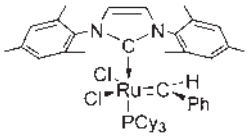

A

Despite the usefulness of this property in organic synthesis,[7] it has not been used in dendrimer chemistry.[8] Dendrimer functionalization is considerably more challenging than that of mono-olefin molecules, because it requires a clean and quantitative reaction to avoid the formation of mixtures among the branch termini.[8]

The $CpFe^+$-induced (Cp = cyclopentadienyl) activation of polymethylbenzenes under ambient or near-ambient conditions is known to efficiently produce polyolefin star and dendritic cores by reaction of such arene complexes with excess KOH and alkenyl halides in THF.[9] The reaction was extended to aryl ether complexes to yield to the phenol dendron p-$HOC_6H_4C(allyl)_3$ (**1**),[10a] which served as a brick for further dendrimer construction; for example, hydrosilylation of the polyolefin core with $HSiMe_2CH_2Cl$ followed by reaction of **1** yielded dendrimers with 3^n allyl branches ($n = 2$–10) starting from mesitylene.[10b] We now report that these star- and dendritic-shaped polyolefin dendrimers can be cleanly and stereospecifically mono- or bifunctionalized by CM or a combination of RCM + CM, respectively, using catalyst **A**. A quick, overall synthesis of water-soluble dendrimers from simple polymethylbenzenes, such as mesitylene and hexamethylbenzene, is therefore provided.

The reaction of $[CpFe(C_6Me_6)][PF_6]$ (**2**) with KOH + allyl bromide or 1-undecenyl iodide in THF, followed by visible-light irradiation in MeCN gives nearly quantitative yields of the known hexaolefin stars **4**[11a] and **5**,[11b] which give high yields of the new hexafunctionalized *trans* olefins **7** and **8** as the only reaction products upon reaction with $CH_2{=}CHCO_2R$ (R = H or Me) in the presence of 5 mol% of **A** (Scheme 1). The iron complex $[CpFe\{C_6(CH_2CH_2CH{=}CH_2)_6\}][PF_6]$ (**3**), the precursor of **4**, also gives hexafunctionalized iron complex **6a** upon metathesis with $CH_2{=}CHCO_2H$ using **A**, although partial decomplexation leads to reduced yields of the complexes.

In the case of mesitylene, complexation by the $CpFe^+$ species, reaction with KOH and allyl bromide in THF under ambient conditions, and decomplexation gives the known dendritic core $C_6H_3[C(CH_2CH{=}CH_2)_3]_3$ (**10**; generation 0 (G0)),[11c] whose metathetic reaction with $CH_2{=}CHCO_2R$ using **A** gives the new hetero-bifunctional compound **11**. This RCM + CM series of reactions inhibits the formation of the known capsule **12** formed from **10** in the absence of $CH_2{=}CHCO_2R$ with the same catalyst **A** (Scheme 2).[11d] As the tris-homofunctionalization of the triallylmethyl tripod is much less favored than RCM as an approach to form the cyclopentenyl group, we lengthened the dendritic tethers to prevent RCM. This lengthening of the tether was achieved by hydrosilylation of **10** with $HSiMe_2CH_2Cl$ followed by reaction with p-$OHC_6H_4O(CH_2)_9CH{=}CH_2$, thus giving the nonaolefin **13**. Contrary to **10**, the metathesis reaction of **13** with $CH_2{=}CHCO_2R$ only gives the CM product **14** (only *trans* isomers) which results from terminal-olefin functionalization (Scheme 2). Likewise, the tethers of the known 27- and 81-allyl dendrimers **15** and **18** (G1 and G2), which result from sequential hydrosilylation of **10** with $HSiMe_2CH_2Cl$,

[*] C. Ornelas, D. Méry, Dr. J. Ruiz Aranzaes, Prof. D. Astruc
Nanosciences and Catalysis Group
LCOO, UMR CNRS No. 5802
University Bordeaux I
33405 Talence Cedex (France)
Fax: (+33) 5-4000-6646
E-mail: d.astruc@lcoo.u-bordeaux1.fr
Dr. J.-C. Blais
LCSOB, UMR CNRS No. 7613
Université Paris 6
75252 Paris Cedex (France)
E. Cloutet
LCPO, UMR CNRS No. 5629
University Bordeaux I
33405 Talence Cedex (France)

[**] We are grateful to the Institut Universitaire de France (IUF; D.A.), Fundaçao para a Ciência e a Tecnologia (FCT), Portugal (PhD grant to C.O.), MRT (PhD grant to D.M.), CNRS, University Bordeaux I, and University Paris VI for financial support.

Supporting information for this article is available on the WWW under http://www.angewandte.org or from the author.

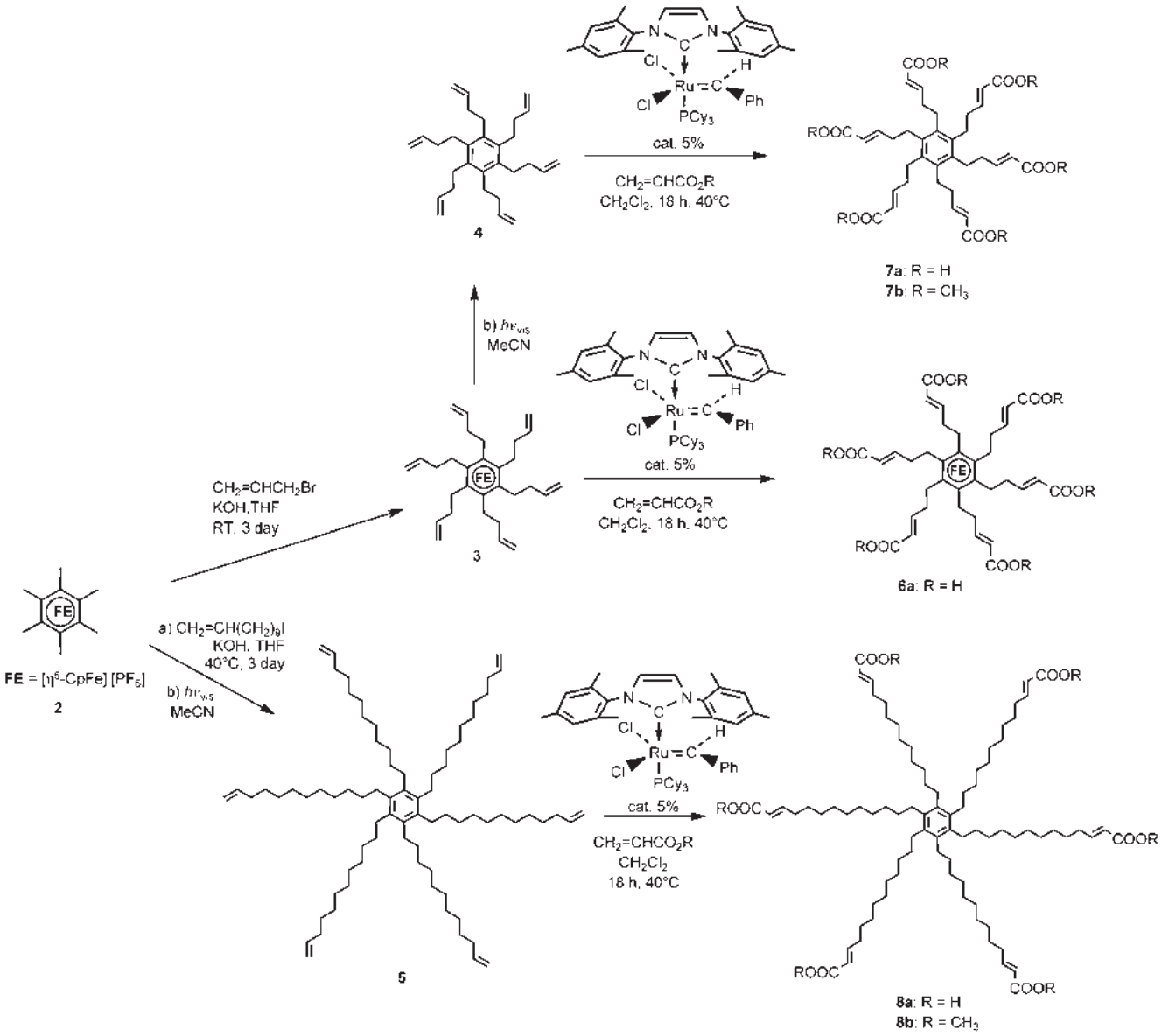

Scheme 1. Synthesis of hexafunctionalized *trans* olefins **7** and **8**.

reaction with NaI, and treatment with p-$HOC_6H_4C(allyl)_3$, were lengthened in the same way to give the new 27- and 81-olefin dendrimers **16** and **19**; their metathesis with CH_2=$CHCO_2R$ proceeded analogously with **A** to give the polyfunctional dendrimers **17** and **20** (Schemes 3 and 4). All the polyfunctionalized dendrimers were characterized by ^1H, ^{13}C, and ^{29}Si NMR spectroscopy and elemental analysis. In addition, the MALDI-TOF mass spectra of **8a**, **8b**, **14a**, and **14b** only show the molecular peaks (see the Supporting Information), and size-exclusion chromatography (SEC) showing Gaussian-type distributions (Figure 1) confirm the monodispersities of the three generations of polyallyl and polyester dendrimers.

The poly(carboxylic acid) dendrimers give water- or methanol-soluble sodium carboxylate salts upon contact with aqueous NaOH or NaOH in methanol. Water-soluble dendrimers are used for applications such as molecular micelles and cation binding and transport.[12] The poly(carboxylic acid) dendrimers are also very useful for their reactions with various amines, a further functionalization procedure. For example, reaction of the new amine dendron $N[(CH_2)_4Fc]_3$ (Fc = ferrocenyl; **21**) with **20a** quantitatively yields the 243-ferrocenyl dendrimer **22** (Scheme 4) that shows a single wave in cyclic-voltammetric studies (see the Supporting Information), which is a key feature for redox sensing—the large dendrimer size also being favorable for electrode modification.[13] The formation of the 81 ammonium carboxylate linkages is shown by the change in solubility, from **20a** that is insoluble in CH_2Cl_2 (but soluble in acetone) to **22** that becomes soluble in CH_2Cl_2. Moreover, the ^1H and ^{13}C NMR signals of the methylene groups attached to the carboxylate and amine groups, respectively, are strongly shifted as expected in **22** relative to the precursors **20a** and **21** (see the Supporting Information).

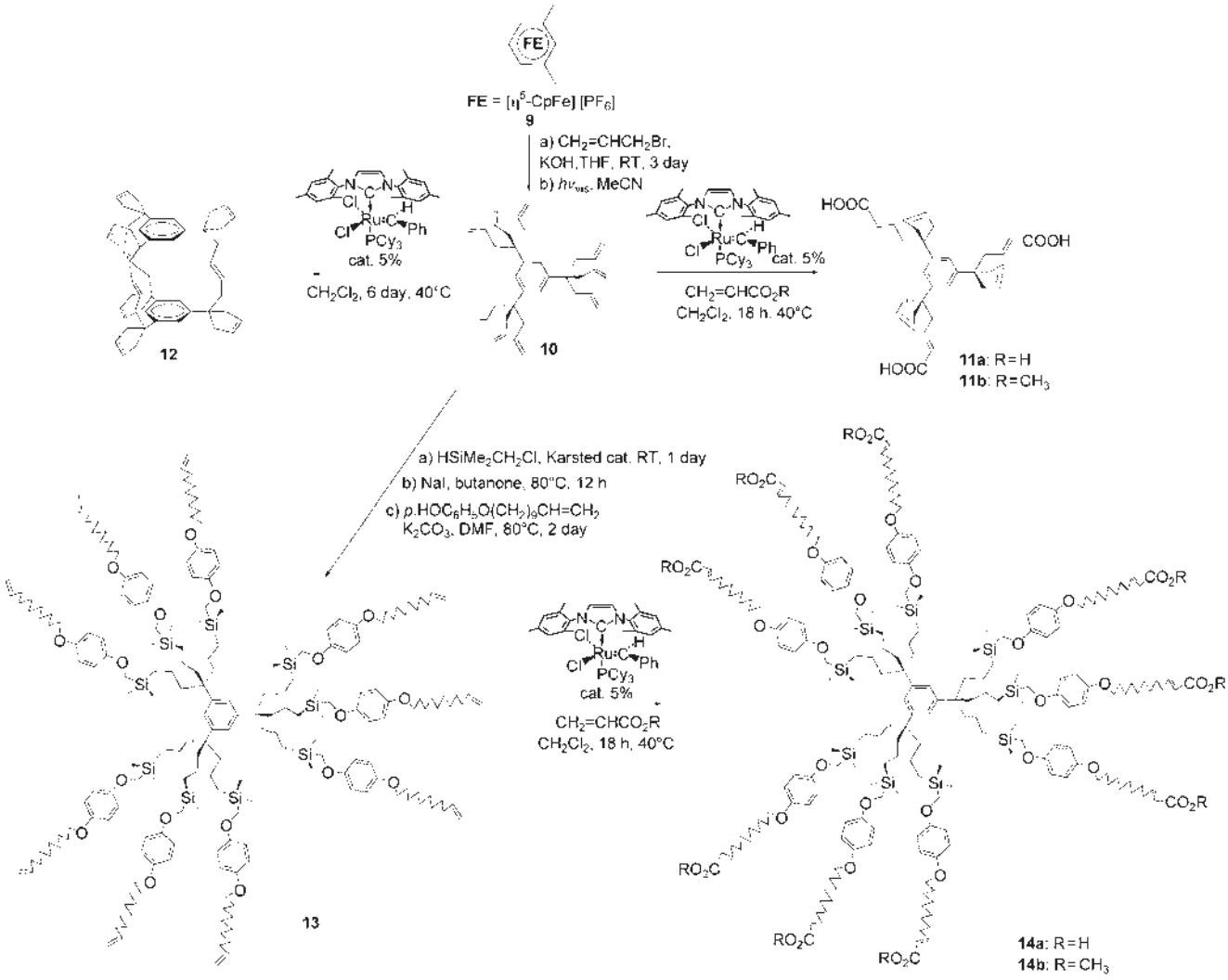

Scheme 2. Synthesis of the CM product **14**.

In conclusion, the finding of this remarkable quantitative chemio-, regio-, and stereoselective cross olefin metathesis with dendrimers using catalyst **A** provides a unique way to functionalize polyolefin-terminated dendrimers and to solubilize them in water and methanol. This reaction makes such useful dendrimers readily accessible on large scales from simple polymethylbenzenes in a few steps.[14]

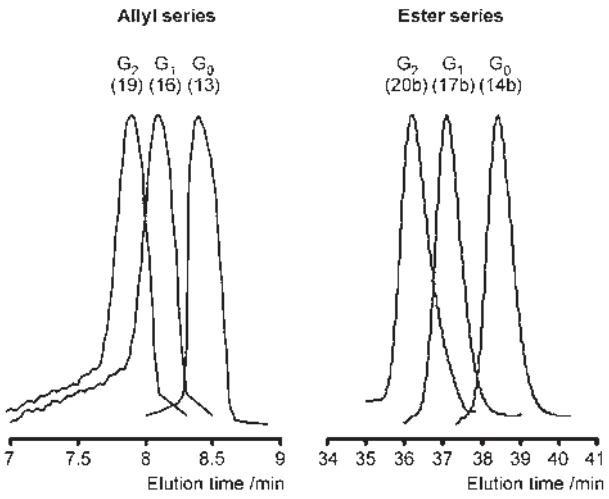

Figure 1. Size-exclusion chromatograms of the three generations of dendrimers (9, 27, and 81 tethers, respectively) before (left) and after (right) functionalization by cross metathesis with methylacrylate. The polydispersity indices obtained from these chromatograms have values between 1.00 and 1.02. Apparent molar masses of the dendrimers were determined by using two different size-exclusion chromatographic apparatus, both equipped with a refractive index (RI; Jasco) and UV/Vis (Varian 2550, $l = 254$ nm) detectors. The columns used were four TSK-gel columns (7.8×300 mm, G 2000, G 3000, G 4000, G 5000 with particle sizes of 5, 6, 6, and 9 mm, respectively) and one PL Poly Pore column (7.5×300 mm, particle size = 5 mm). The eluent was THF (0.7 mL min^{-1}) at 25 °C and calibration was carried out using linear polystyrene standards.

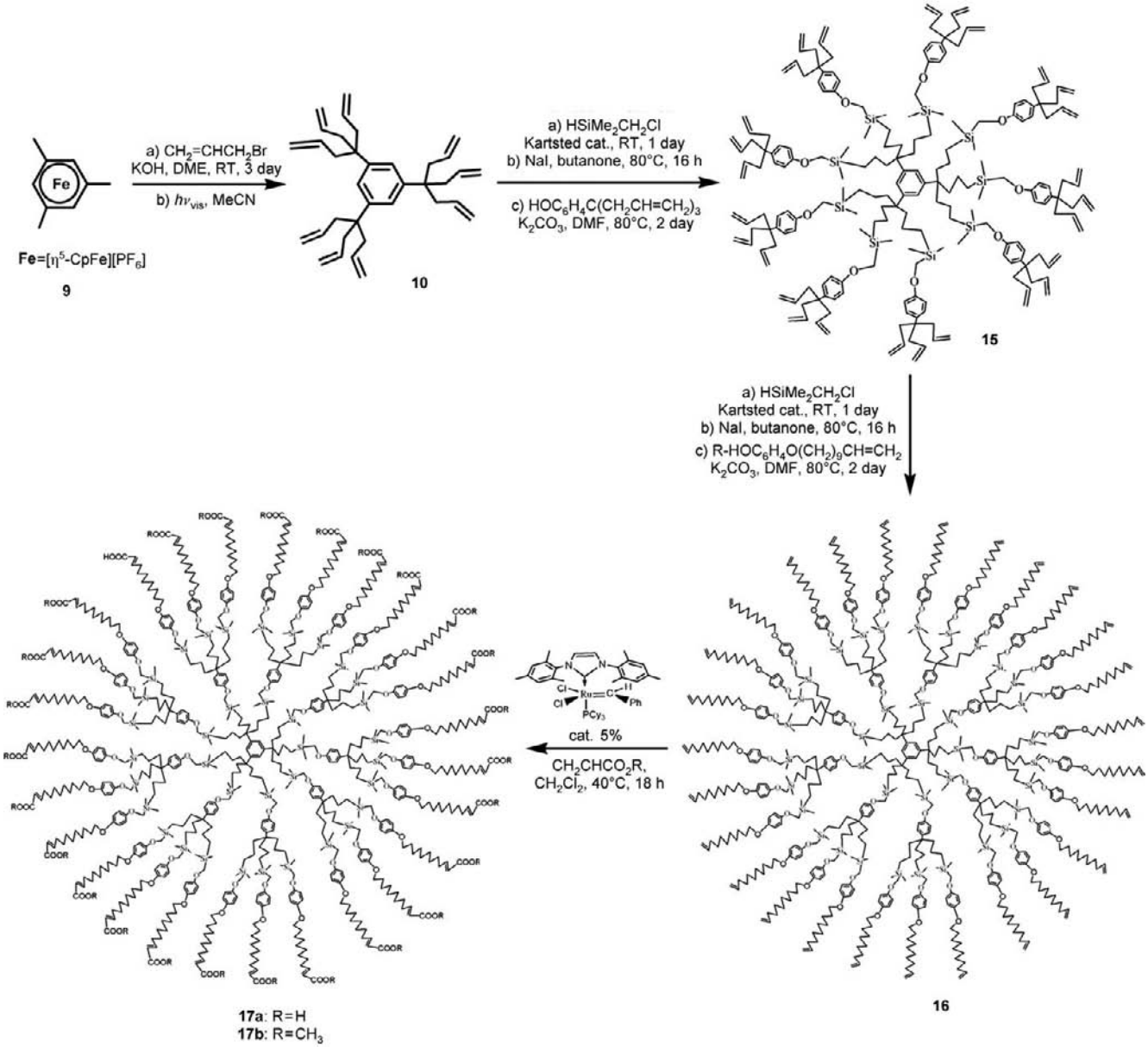

Scheme 3. Synthesis of the polyfunctional dendrimer **17**.

Experimental Section

General metathesis experiments: the polyolefin dendrimer (0.0418 mmol/n dendritic tethers), dry CH_2Cl_2 (10–50 mL), methyl acrylate or acrylic acid (0.221 mmol), and catalyst **A** (5 mol% equivalents per dendritic branch, 0.0114 g, 0.0134 mmol) were successively introduced into a Schlenk flask in an inert atmosphere. The reaction solution was warmed to 40 °C for 18 h. After removal of the solvent under vacuum, the product was washed with methanol and precipitated by addition of a tenfold excess of methanol to a solution of the polyester dendrimers in CH_2Cl_2 or to a solution of the polycarboxylic acid dendrimers in THF. The colorless waxy organic dendrimers were usually obtained in 95–99% yield and were characterized by ^1H, ^{13}C, and ^{29}Si NMR spectroscopy; MALDI-TOF-MS of **8a**, **8b**, **14a**, **14b**, **16**, **17a**, **17b**, and **21** (observation of the molecular peak and absence of other peaks); elemental analysis; and size-exclusion chromatography (SEC, Figure 1).

Received: August 10, 2005
Published online: October 25, 2005

Keywords: dendrimers · ferrocenes · iron · metathesis · organometallic reagents

[1] a) *Handbook of Metathesis, Vols. 1–3* (Ed.: R. H. Grubbs), Wiley-VCH, Weinheim, **2003**; b) R. R. Schrock, A. H. Hoveyda, *Angew. Chem.* **2003**, *115*, 4703; *Angew. Chem. Int. Ed.* **2003**, *42*, 4592; c) A. Fürstner, *Angew. Chem.* **2000**, *112*, 3140; *Angew. Chem. Int. Ed.* **2000**, *39*, 3012; d) for a recent historical perspective, see: D. Astruc, *New J. Chem.* **2005**, *29*, 42; see, also http://nobelprize.org/chemistry/laureates/2005/chemreading.html.

[2] A. M. Martin-Alvarez, F. Hampel, A. M. Arif, J. A. Gladysz, *Organometallics* **1999**, *18*, 955; E. B. Bauer, J. Ruwwe, F. A. Hampel, S. Szafert, J. A. Gladysz, *Chem. Commun.* **2000**, *22*, 2261; C. R. Horn, J. M. Martin-Alvarez, J. A. Gladysz, *Organometallics* **2002**, *21*, 5386; E. B. Bauer, F. Hampel, J. A. Gladysz, *Organometallics*, **2003**, *22*, 5567; T. Shima, E. B. Bauer, F. Hampel, J. A. Gladysz, *Dalton Trans.* **2004**, *7*, 1012; T. Shima,

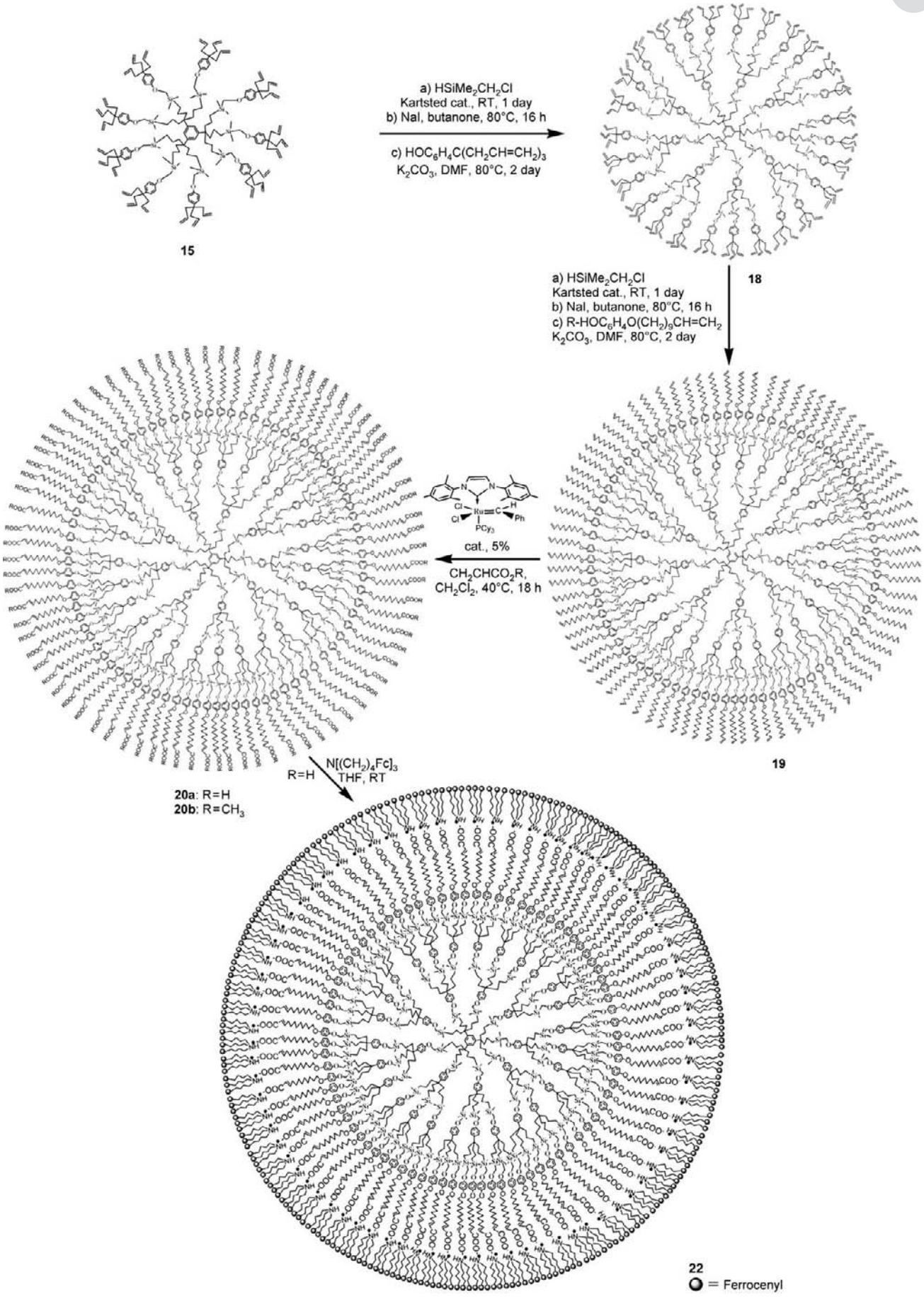

Scheme 4. Synthesis of the polyfunctional dendrimer **22**.

F. Hampel, J. A. Gladysz, *Angew. Chem.* **2004**, *116*, 5653; *Angew. Chem. Int. Ed.* **2004**, *43*, 5537.

[3] a) C. Dietrich-Bucherer, G. Rapenne, J.-P. Sauvage, *Chem. Commun.* **1997**, 2053; b) M. Weck, B. Mohr, J.-P. Sauvage, R.-H. Grubbs, *J. Org. Chem.* **1999**, *64*, 5463; c) G. Rapenne, C. Dietrich-Bucherer, J.-P. Sauvage, *J. Am. Chem. Soc.* **1999**, *121*, 994.

[4] a) A. V. Chuchryukin, H. P. Dijkstra, B. M. J. M. Suijkerbuijk, R. J. M. Klein Gebbink, G. P. M. van Klink, A. M. Mills, A. L. Spek, G. van Koten, *Angew. Chem.* **2003**, *115*, 238; *Angew. Chem. Int. Ed.* **2003**, *42*, 228; b) P. Wang, C. N. Moorefield, G. R. Newkome, *Angew. Chem.* **2005**, *117*, 1707; *Angew. Chem. Int. Ed.* **2005**, *44*, 1679.

[5] a) M. S. Wendland, S. C. Zimmerman, *J. Am. Chem. Soc.* **1999**, *121*, 1389; b) S. C. Zimmerman, I. Zharov, M. S. Wendland, N. A. Rakow, K. S. Suslick, *J. Am. Chem. Soc.* **2003**, *125*, 13504; c) Y. Kim, M. F. Mayer, S. C. Zimmerman, *Angew. Chem.* **2003**, *115*, 1153; *Angew. Chem. Int. Ed.* **2003**, *42*, 1121; d) N. G. Lemcoff, T. A. Spurlin, A. A. Gewirth, S. C. Zimmerman, J. B. Beil, S. L. Elmer, H. G. Vandeveer, *J. Am. Chem. Soc.* **2004**, *126*, 11420; e) J. Beil, N. G. Lemcoff, S. C. Zimmerman, *J. Am. Chem. Soc.* **2004**, *126*, 13576.

[6] O. Brümmer, A. Rückert, S. Blechert, *Chem. Eur. J.* **1997**, *3*, 441; M. Schuster, S. Blechert, *Angew. Chem.* **1997**, *109*, 2124; *Angew. Chem. Int. Ed. Engl.* **1997**, *36*, 2036; S. J. Connor, S. Blechert, *Angew. Chem.* **2003**, *115*, 1944; *Angew. Chem. Int. Ed.* **2003**, *42*, 1900.

[7] A. K. Chatterjee, J. P. Morgan, M. Scholl, R. H. Grubbs, *J. Am. Chem. Soc.* **2000**, *122*, 3783; A. K. Chatterjee, T.-L. Choi, D. P. Sanders, R. H. Grubbs, *J. Am. Chem. Soc.* **2003**, *125*, 11360; A. K. Chatterjee in reference [1a], *Vol. 2*, chap. 2.8, p. 246; for catalyst **A**, see also, for example: R. H. Grubbs, *Acc. Chem. Res.* **2001**, *34*, 18.

[8] a) G. R. Newkome, C. N. Moorefield, F. Vögtle, *Dendrons and Dendrimers. Concepts, Synthesis and Applications*, Wiley-VCH, Weinheim, **2001**; b) *Dendrimers and other Dendritic Polymers* (Eds.: D. Tomalia, J. M. J. Fréchet), Wiley-VCH, New York, **2002**; c) *Dendrimers and Nanosciences* (Ed.: D. Astruc), *C. R. Chimie*, **2003**, *6*, p. 709.

[9] D. Astruc, S. Nlate, J. Ruiz in *Modern Arene Chemistry* (Ed.: D. Astruc), Wiley-VCH, Weinheim, **2003**, p. 400.

[10] a) V. Sartor, J.-L. Fillaut, L. Djakovitch, F. Moulines, V. Marvaud, F. Neveu, J.-C. Blais, D. Astruc, *J. Am. Chem. Soc.* **1999**, *121*, 2929; b) J. Ruiz, G. Lafuente, S. Marcen, C. Ornelas, S. Lazarre, J.-C. Blais, E. Cloutet, D. Astruc, *J. Am. Chem. Soc.* **2003**, *125*, 7250.

[11] a) F. Moulines, D. Astruc, *Angew. Chem.* **1988**, *100*, 1394; *Angew. Chem. Int. Ed. Engl.* **1988**, *27*, 1347; b) F. Moulines, L. Djakovitch, R. Boese, B. Gloaguen, W. Thiel, J.-L. Fillaut, M.-H. Delville, D. Astruc, *Angew. Chem.* **1993**, *105*, 1132; *Angew. Chem. Int. Ed. Engl.* **1993**, *32*, 1075; c) J.-L. Fillaut, J. Linares, D. Astruc, *Angew. Chem.* **1994**, *106*, 2540; *Angew. Chem. Int. Ed. Engl.* **1994**, *33*, 2460; d) V. Martinez, J.-C. Blais, D. Astruc, *Angew. Chem.* **2003**, *115*, 4502; *Angew. Chem. Int. Ed.* **2003**, *42*, 4366; e) L. Plault, A. Hauseler, S. Nlate, D. Astruc, S. Gatard, R. Neumann, *Angew. Chem.* **2004**, *116*, 2984; *Angew. Chem. Int. Ed.* **2004**, *43*, 2924.

[12] a) G. R. Newkome, C. N. Moorefield, G. R. Baker, M. J. Saunders, S. H. Grossman, *Angew. Chem.* **1991**, *103*, 1207; *Angew. Chem. Int. Ed. Engl.* **1991**, *30*, 1178; b) G. R. Newkome, *Pure Appl. Chem.* **1988**, *60*, 2337; c) K. R. Gopidas, A. R. Leheny, G. Caminati, N. J. Turro, D. A. Tomalia, *J. Am. Chem. Soc.* **1991**, *113*, 7335; d) J. F. G. A. Jansen, E. M. M. de Brabander-van-den Berg, E. W. Meijers, *Science* **1994**, 1226; e) V. Balzani, P. Ceroni, S. Gestermann, M. Gorka, C. Kauffmann, F. Vögtle, *Tetrahedron* **2002**, *58*, 629.

[13] For a comprehensive review on ferrocene dendrimers and their electrochemistry, see for example: C. M. Casado, M. Moran, B. Alonso, B. Garcia, J. Gonzales, J. Losada, *Coord. Chem. Rev.* **1999**, *185/186*, 53.

[14] For other appealing hexafunctionalizations of arenes, see for example: a) R. Boese, J. R. Green, J. Ittendorf, D. L. Mohler, K. P. C. Volhardt, *Angew. Chem.* **1992**, *104*, 1643; *Angew. Chem. Int. Ed. Engl.* **1992**, *31*, 1643; b) P. Prinz, A. Lansky, B. Knieriem, A. de Meijere, T. Haumann, R. Boese, M. Noltemeyer, *Angew. Chem.* **1997**, *109*, 1343; *Angew. Chem. Int. Ed. Engl.* **1997**, *36*, 1289.

Partie III

Fonctionnalisation de clusters inorganiques à l'aide de pyridines: dendrimères et métallodendrimères à cœur cluster

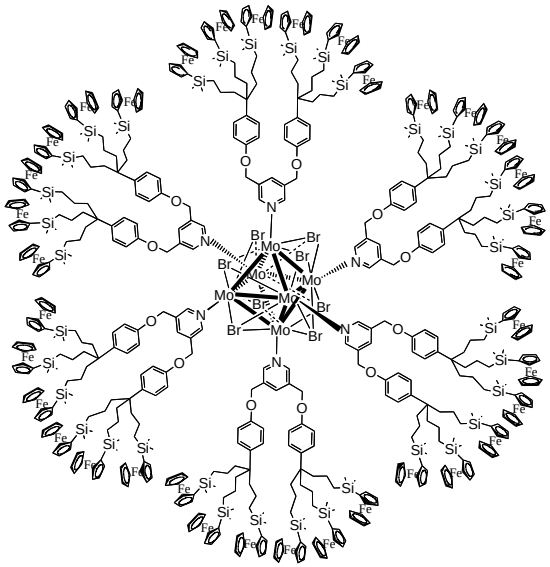

Les clusters, ou agrégats, constituent une classe majeure de la chimie du solide. Les unités $[(M_6L^i_8)L^a_6]$ (^{a} = apical, ^{i} = interne) sont les blocs les plus courants dans la chimie des clusters octaédriques du molybdène, du tungstène et du rhénium. Ces composés sont facilement obtenus par synthèse en voie solide avec des métaux de transition (M) et des halogènes ou des chalcogènes (L). Les propriétés intrinsèques de ce type de clusters - processus redox réversible, magnétisme et luminescence - dépendent de la nature des métaux et des ligands. Les clusters octaédriques de molybdène de type $M_xMo_6Y_8$ (Y = chalcogène) sont très répandus à cause de leurs propriétés de supraconductivité, connues comme phase de Chevel.

Au laboratoire, nous nous intéressons aussi à l'aspect fondamental des dendrimères, notamment à l'influence du cœur (organique, organométallique, colloïdal, cluster…) sur les propriétés de ces derniers. De ce fait, nous avons élaboré de nouveaux dendrimères à cœur inorganique à l'aide des clusters de molybdène synthétisés au LCSIM par K. Kirakci, S. Cordier et C. Perrin (Schéma 1, Annexe 2). Pour ces synthèses, nous avons utilisé des dendrons pyridines, synthétisés au laboratoire par L. Plault et S. Nlate, car ils sont de très bons ligands par liaison de coordination. Nous avons ainsi pu noter l'importance des liaisons qui lient le cœur du dendrimère aux dendrons.

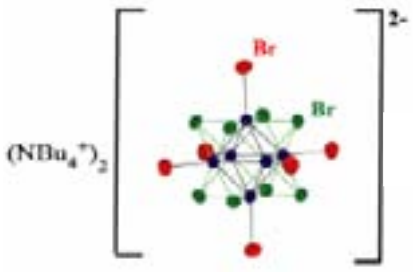

Schéma 1 : Cluster de molybdène synthétisés au LCSIM

Dans un premier temps, nos travaux se sont inscrits dans la synthèse de métallodendrimères à cœur cluster par échange de six ligands apicaux (Schéma 2). Effectivement, nous avons greffé une pyridine contenant un complexe organométallique de fer grâce à l'hexasubstitution des atomes de brome sur un cœur inorganique de molybdène. Le complexe ruthénium-alcynyl pyridine et le cluster correspondant ont été synthétisés par C. Ornelas et J. Ruiz, en collaboration avec J. Rodrigues de l'Université de Madère. Ces travaux

ont fait l'objet d'une note publiée aux *Comptes Rendus Chimiques* et intitulée "**Mo_6Br_8-Cluster-cored Organometallic Stars and Dendrimers**"**.** Dans cet article, notre laboratoire a collaboré avec Jean-Claude Blais, du LCSOB à Paris VI, qui a réalisé les spectres de masse des complexes de ruthénium et de fer.

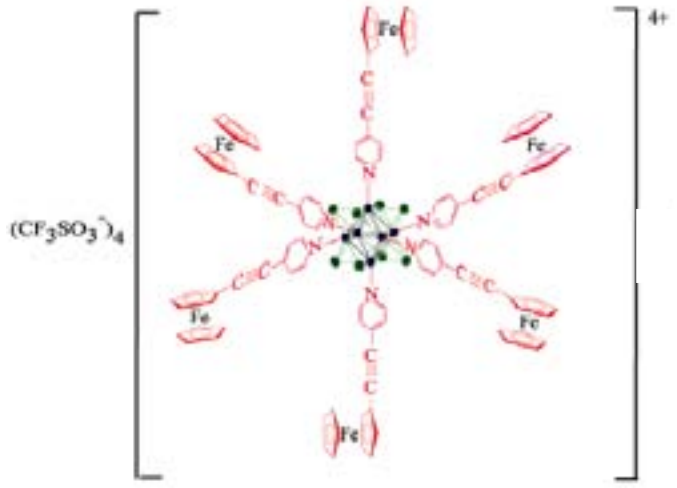

Schéma 2 : Métallodendrimère de fer à cœur inorganique

Ensuite, des dendrimères à cœur cluster ont été élaborés à partir de dendrons pyridines et des clusters de molybdène. Ainsi, une molécule contenant trente-six oléfines terminales a été synthétisée très aisément à partir d'un complexe inorganique (Schéma 3). Ces travaux ont fait l'objet d'une note publiée au *Zeitschrift für Anorganische und Allgemeine Chemie* et intitulée "**The Simple Hexapyridine Cluster $[Mo_6Br_8Py_6][OSO_2CF_3]_4$ and Substituted Hexapyridine Clusters Including a Cluster-cored Polyolefin Dendrimer**"**.**

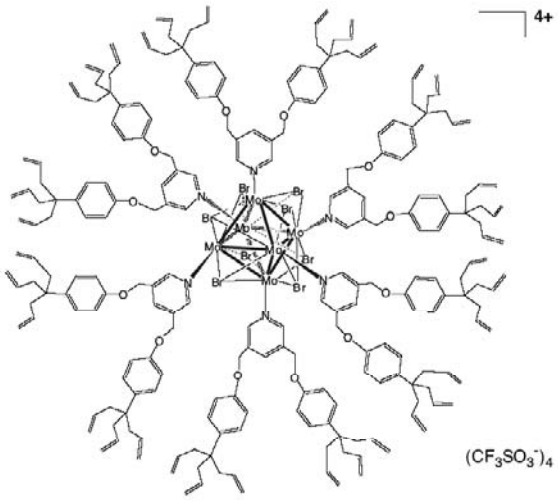

Schéma 3 : Dendrimère à cœur inorganique contenant 36 oléfines terminales

Pour finir, un métallodendrimère contenant trente-six ferrocènes à la périphérie a été synthétisé grâce à l'hexasubstitution des ligands apicaux du cluster par des dendrons pyridines. Par ailleurs, nous avons étudié la monosubtitution de pyridines simples et dendroniques. Un dendron à cœur cluster contenant douze complexes de fer a ainsi été assemblé grâce à la monosubstitution d'un ligand du cluster par une pyridine dendronique (Schéma 4). Un mémoire est terminé sur ce sujet et s'intitule "**From Simple Monopyridine Clusters $[Mo_6Br_{13}(Py\text{-}R)_6][n\text{-}Bu_4N]$ and Hexapyridine Clusters $[Mo_6X_8(Py\text{-}R)_6][OSO_2CF_3]_4$ (X = Br or I) to Cluster-cored Organometallic Stars, Dendrons and Dendrimers**".

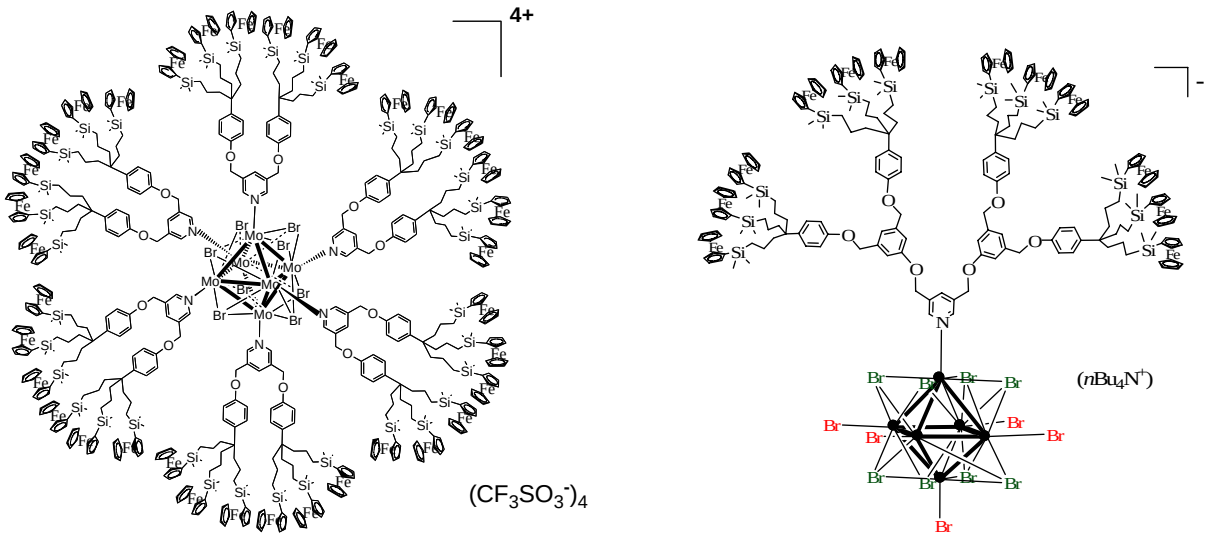

Métallodendrimère à cœur cluster **Dendron à cœur cluster**

Schéma 4 : Dendrimère et dendron à cœur cluster inorganique

Available online at www.sciencedirect.com
SCIENCE DIRECT®
C. R. Chimie ■■ (2005) ■■■-■■■
COMPTES RENDUS CHIMIE
http://france.elsevier.com/direct/CRAS2C/

Full paper / Mémoire

Mo_6Br_8-Cluster-cored organometallic stars and dendrimers

Denise Méry [a], Cátia Ornelas [a,b], Marie-Christine Daniel [a], Jaime Ruiz [a], João Rodrigues [b], Didier Astruc [a,*], Stéphane Cordier [c], Kaplan Kirakci [c], Christiane Perrin [c,*]

[a] *Nanosciences and Catalysis Group, LCOO, UMR CNRS N° 5802, université Bordeaux-1, 351, cours de la Libération, 33405 Talence cedex, France*

[b] *Centro de Química da Madeira, LOCMM, Departamento de Química, Universidade da Madeira, Campus da Penteada, 9000-390 Funchal, Portugal*

[c] *Laboratoire de chimie du solide et inorganique moléculaire, Institut de chimie de Rennes, UMR CNRS 6511, université Rennes-1, av. du Général-Leclerc, 35042 Rennes cedex, France*

Received 27 July 2004; accepted after revision 26 November 2004

Abstract

The octahedral molybdenum cluster $[n\text{-}Bu_4N]_2[Mo_6Br_8(CF_3SO_3)_6]$ undergoes substitution of all six terminal triflate ligands with the organometallic pyridine ligands $[RuCp(PPh_3)_2(\eta^1\text{-}C_2\text{-}4\text{-pyridinyl})]$, **1**, and 1-ferrocenyl-2-(4-pyridinyl) acetylene, **5**, to give the new light and air sensitive hexa-functionalized Mo_6 clusters **4** and **7** respectively, and with the dendronic phenolate ligand $p\text{-NaO–}C_6H_4C\{CH_2CH_2CH_2Si(Me)_2Fc\}_3$, **8**, to give the air-sensitive Mo_6-cluster-cored octadecylferrocenyl dendrimer **9** that discloses a single CV wave in CH_2Cl_2 and recognizes the biologically important adenosyl triphosphate di-anion (ATP^{2-}). The organometallic pyridines **1** and **5** were also coordinated to Ag^+ to give the new trinuclear $AgRu_2$ and $AgFc_2$ cationic complexes **2** and **6** respectively for comparison of the structures and electronic delocalization with those of the clusters. ***To cite this article: D. Méry et al., C. R. Chimie 8 (2005)***.

Résumé

L'agrégat octaédrique $[n\text{-}Bu_4N]_2[Mo_6Br_8(CF_3SO_3)_6]$ subit la substitution des six coordinats triflates terminaux avec les ligands pyridiniques organométalliques $[RuCp(PPh_3)_2(\eta^1\text{-}C_2\text{-}4\text{-pyridinyl})]$, **1**, et 1-ferrocenyl-2-(4-pyridinyl) acetylene, **5**, pour donner de nouveaux agrégats hexamolybdène hexafonctionnels **4** et **7**, respectivement. Avec le phénate dendronique $p\text{-NaO–}C_6H_4C\{CH_2CH_2CH_2Si(Me)_2Fc\}_3$, **8**, le dendrimère hexamolybdène octadécylferrocényle **9** est obtenu. Ce composé donne une seule vague en voltammétrie cyclique dans CH_2Cl_2 et reconnaît le dianion de l'ATP, dont l'importance est connue en biologie.

* Corresponding author.
E-mail addresses: d.astruc@lcoo.u-bordeaux1.fr (D. Astruc), christiane.perrin@univ-rennes1.fr (C. Perrin).

1631-0748/$ - see front matter © 2005 Académie des sciences. Published by Elsevier SAS. All rights reserved.
doi:10.1016/j.crci.2005.02.023 CRAS2C-2492

Les pyridines organométalliques **1** et **5** ont aussi été coordonées à Ag^+ pour donner les nouveaux complexes trinucléaires $AgRu_2$ et $AgFc_2$ **2** et **6** respectivement, afin de comparer leur structure électronique à celles des agrégats. ***Pour citer cet article : D. Méry et al., C. R. Chimie 8 (2005)***.

Keywords: Cluster; Star; Dendrimer; Organometallics; Assembly; Redox; Anion recognition; ATP

Mots-clés : Agrégats ; Étoile ; Organométallique ; Assemblée ; Redox ; Reconnaissance ; ATP ; Dendrimères

1. Introduction

There is now an increased effort to focus on the design and assembly of molecular devices that contain nano-clusters [1] given their potential application in catalysis [2], magnetic materials [3] electronics [2] and optics [4,5]. In this context, the bridge between solid-state and molecular materials is an appealing entry into these areas of nanosciences and a starting point towards a broad range of chemistry [6]. Branched molecular architectures [7] also offer another facet to these concepts and allow designing materials with cluster moieties at the core [8] and extremities [9] of dendritic nanostructures [10]. The inorganic clusters $[Mo_6X_{14}]^{2-}$ have been known for 60 years [11,12] and the related superconducting octahedral Mo_6 clusters $PbMo_6S_8$, known as Chevrel phases [13], as well as their redox and photo-physical properties [14] added further interest. The Mo(II) halide clusters consist of a substitution-resistant core $[Mo_6X_8]^{4+}$ with eight face-bridging inner ligands and semi-labile outer (non-bridging, i.e. terminal) ligands. The outer ligand substitution chemistry has been extensively investigated for almost half a century [15], the substitution of the two apical ligands being easier than that of the four equatorial ones [16]. The hexa-methoxy cluster prepared by Nannelli and Block [17] and the hexa-triflate reported by Shriver's group [18] are the most useful starting materials for further substitution [8b].

Our strategy has consisted in investigating the substitution, *via* the intermediacy of the hexa-triflate (Equation 1), of all six terminal bromide ligands in $[n\text{-}Bu_4N]_2[Mo_6Br^i{}_8Br^o{}_6]$ by phenolate and bipyridine ligands connected to redox-active rigid or dendronic organometallic groups. Iron- and ruthenium-centered sandwich and piano-stool structures have been chosen as organometallic connectors, since they have well-known redox properties that can be useful for redox recognition and molecular electronics [19], especially in the dendritic context [20].

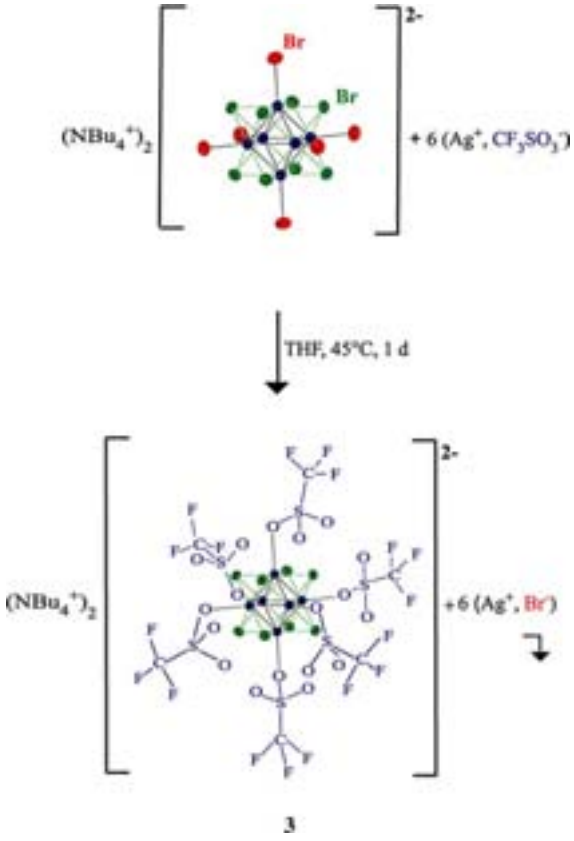

Equation 1.

2. Results

2.1. Coordination of a pyridinyl-alcynyl-organo-ruthenium rod

The rigid organo-ruthenium pyridine ligand **1** was known [21]. We best synthesized it by a different route,

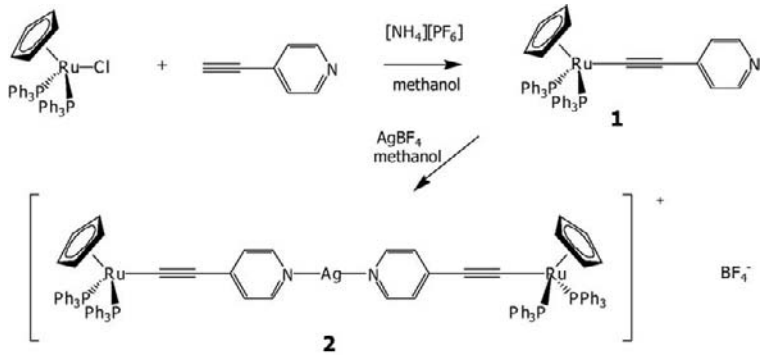

Scheme 1.

however, involving the reaction of 4-ethynylpyridine with $[RuCp(PPh_3)_2Cl]$ in the presence of triethylamine and $[NH_4][PF_6]$ in methanol (Scheme 1). This general procedure was reported [22] for the synthesis of the complexes $[RuCp(PPh_3)_2(\eta^1\text{-alcynyl})]$ with $(Cp = \eta^5\text{-}C_5H_5)$. The yellow complex **1** was characterized by standard spectroscopic techniques including ^{31}P NMR, infrared spectroscopy ($\nu_{CC} = 2070\ cm^{-1}$) and the MALDI TOF mass spectrum with the dominant molecular peak at 794 Dalton.

In order to compare the coordination of **1** to a single metal center with that in the Mo_6 cluster, the orange silver complex **2** was synthesized from the ligand **1** and $AgBF_4$ in methanol. In the infrared spectrum of the trimetallic complex **2**, the alkynyl CC band was found at 2016 cm^{-1}. Then, the reaction of **1** with the cluster $[Mo_6Br_8(CF_3SO_3)_6][n\text{-}Bu_4N]_2$, **3**, was carried out in refluxing THF for a week.

The new hexa-ruthenium hexa-molybdenum compound **4** was recovered by slow precipitation using pentane. A single peak was found in the ^{31}P NMR spectrum, a single Cp peak was observed in the ^1H NMR spectrum at $\delta = 4.42$ ppm, and a single infrared absorption was obtained at $\nu_{CC} = 2018\ cm^{-1}$. This behavior is in accord with the coordination of the cluster by the six organo-ruthenium pyridine ligands and the absence of free pyridine ligand in the sample (Equation 2).

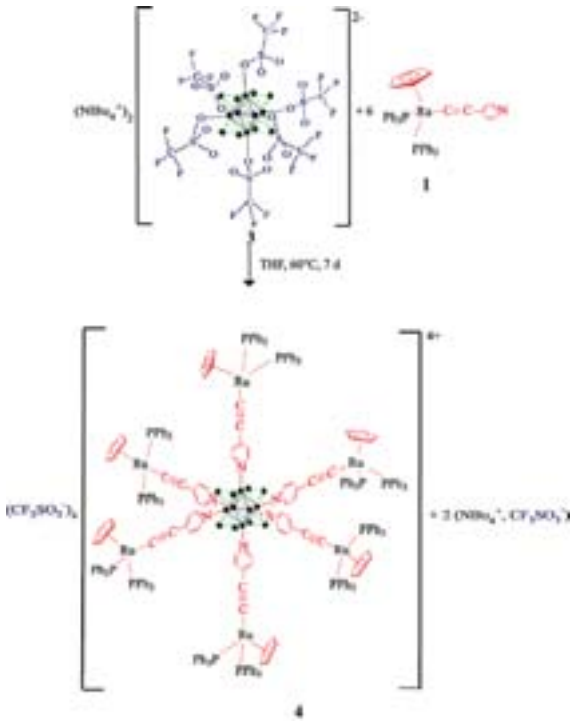

Equation 2.

2.2. Coordination of a ferrocenyl-alcynyl-pyridine rod

In a similar approach, the red complex 1-ferrocenyl-2-(4-pyridinyl)acetylene, **5**, was synthesized using the reaction of the Vargas' group (Scheme 2) [23]. The reaction of **5** with $AgSO_3CF_3$ or $AgBF_4$ at room temperature in $CDCl_3$ gives a red trimetallic complex **6** (shown with the triflate anion) resulting from the coordination of two equivalents of the pyridine nitrogen atom on the silver cation (Scheme 2). The compound **6** is light and air sensitive.

The reaction of the ferrocenyl-containing pyridinyl ligand **5** with the cluster **3** was carried out in refluxing THF for a week to give the new hexasubstituted hexaferrocenyl Mo_6 cluster **7**. The red compound **7** was isolated by precipitation from a THF solution by slow addition of pentane and characterized inter alia by an

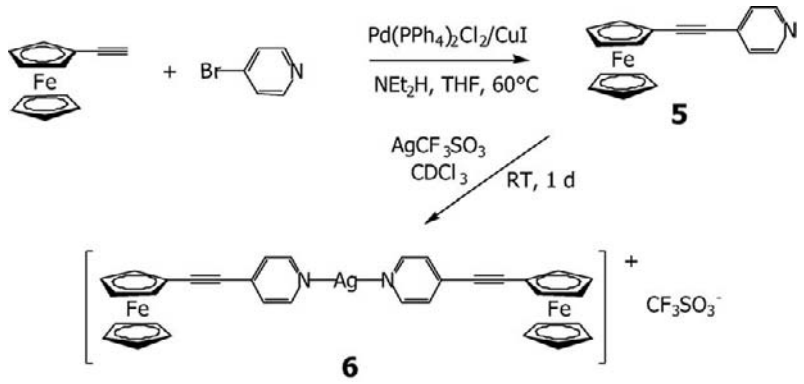

Scheme 2.

infrared alcynyl absorption at 2181 cm^{-1}, ferrocene signals including a single Cp signal for the free Cp rings in the ^{1}H and ^{13}C NMR spectra (Equation 3). This complex **7** is very light and air sensitive. Its CV in CH_2Cl_2 shows two close reversible ferrocenyl waves at $E_{1/2}$ = 0.800 V vs. [FeCp*$_2$] with a less intense shoulder at $E_{1/2}$ = 0.710 V vs. [FeCp*$_2$]; these values compare with the value obtained for the starting monomeric complex **5**, $E_{1/2}$ = 0.720 V vs. [FeCp*$_2$].

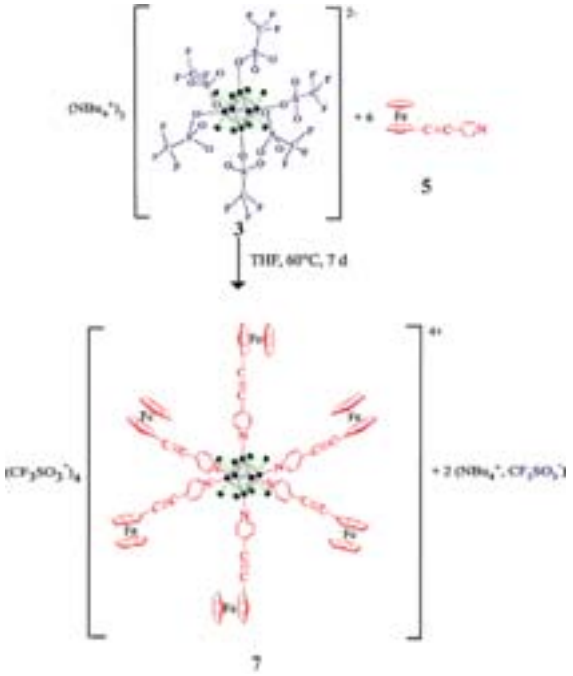

Equation 3.

2.3. Coordination of a tri-silylferrocenyl-phenolate dendron

The known tri-silylferrocenyl phenolate dendron *p*-HO-$C_6H_4C\{CH_2CH_2CH_2Si(Me)_2Fc\}_3$, **8**, has already been used as part of a dendritic gold-nanoparticle-cored device for the recognition of inorganic oxo-anions [24]. Its reaction with the Mo_6 cluster **3** was inspired by previous studies of substitution of the six outer (terminal) halide ligands including Gorman's work that involved dendronic phenolates [8b]. Thus, reaction of **8** with **3** was carried out overnight in THF at 60 °C, then in toluene at 80 °C for two days which eventually led to completion of the substitution reaction, giving the air-sensitive cluster-cored octadecylsilylferrocenyl dendrimer **9**. The end of the reaction was indicated by the correct ratio of the *n*-Bu_4N^+ cation/dendron signals in ^{1}H NMR of **9** that was obtained only then (Equation 4).

The CV of **9** showed a single oxidation wave for the 18 ferrocenyl redox centers indicating that these 18 ferrocenyl centers are seemingly equivalent as in other polyferrocenyl dendrimers [25]. Addition of [*n*-$Bu_4N]_2$[ATP] to the electrochemical cell leads to the appearance of a new ferrocenyl wave at less positive potential (ΔE = 90 mV) whose intensity is proportional to the proportion of [*n*-$Bu_4N]_2$[ATP] salt added. This is the indication of an interaction of strong type according to the Kaifer–Echegoyen model [26] as already observed previously with other polyamidoferrocenyl and polysilylferrocenyl dendrimers (Fig. 1). It is noteworthy that the shift of potential (Fig. 1) is much smaller than in gold-nanocluster-cored dendrimers.

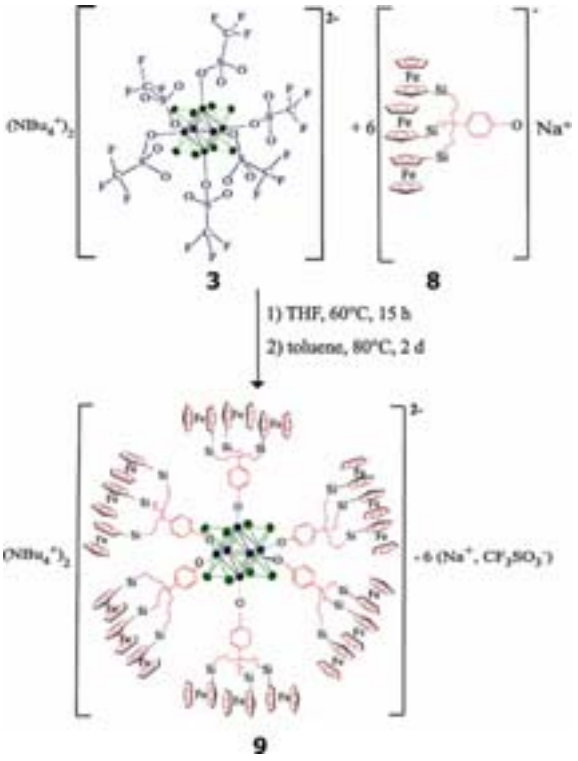

Equation 4.

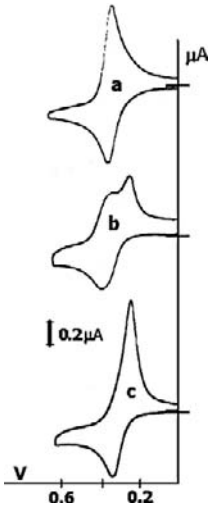

Fig. 1. Titration of $(Bu_4N)_2[MoBr_8(OC_6H_4C(C_3H_6SiC_2H_6Fc)_3)_6]$ in CH_2Cl_2 (Pt, $[Bu_4N][PF_6]$ 0.1 M, 20 °C, reference: $[FeCp_2^*]$, not shown) with $[Bu_4N]_2[ATP]$; a) Before the addition, $E_{1/2} = 0.40$ V; b) with 0.30 equiv. of anion; c) with an excess of anions, $E_{1/2} = 0.31$ V. The two methyl substituents on all Si atoms are ommited for clarity.

3. Discussion

Precedents showing hexa-substitution of the outer (terminal) halides in the octahedral inorganic clusters such as **3** [8b,18] provided the basis for the new hexa-substitution reactions described in this work. The rigidity and electronic delocalization in the hexa-pyridine-substituted clusters on one hand, and the bulk of the flexible phenolate dendron on the other hand, however, were factors rendering this chemistry challenging. Finally, the two new hexa-substituted pyridine clusters are light- and air-sensitive, and the cluster-cored 18-ferrocenyl dendrimer is air sensitive which made their work-up and use tedious. Thus, parallel reactions with the mononuclear silver salts, although also very light sensitive, were welcome to facilitate assignments and help understand the spectroscopic intricacies. The substitution reactions could indeed be followed by ^{1}H NMR using the relative intensity ratio of appropriate signals, and this technique allowed us to confirm the difficulty of hexa-substitution and the long heating time therefore required. We made the choice to follow Shriver's and Gorman's indications involving the hexa-triflates as intermediates for the substitution reactions.

It turned out that the hexa-substituted clusters (in particular the dendritic one) were very difficult to purify in order to obtain correct elemental analyses. These analytical data had to be submitted several times for each product to yield mediocre results, although the ^{1}H NMR monitoring clearly showed the end of the substitution reactions. Inorganic impurities were obviously difficult to separate given the low carbon contents systematically obtained. Although this may be partly due to the air and light sensitivity of the compounds, it appears that triflate salts formed in the reactions may be systematic impurities due to the difficulty of their complete separation and detection. The light and air sensitivity of the hexa-alkynyl-pyridine clusters was probably also responsible for our lack of success in obtaining suitable crystals for X-ray crystal structure determinations. Yet, Schriver's group reported the crystal structure of a hexa-ferrocenyl cluster, but with carboxylate ligands [27].

The location of the alkyne C–C band in the infrared spectrum is very sensitive to the coordination and nature of alkyne substituent. For instance, this band is shifted from 2070 cm^{-1} in the free organoruthenium-pyridine **1** to 2016 and 2018 cm^{-1} in the silver- and cluster com-

plexes **2** and **4** respectively. Likewise, in the ferrocenylalkynyl pyridine, the band is shifted from 2210 cm^{-1} in the free ligand to 2176 and 2181 cm^{-1} in the silver and cluster complexes respectively. These shifts show the decrease of electronic density on the triple bond due to charge transfer from the pyridine ligands to the metals. Likewise, the Cp peak observed in ^1H NMR, whose singularity is an evidence of complete hexa-substitution, is shifted downfield upon coordination of both organometallic pyridines to the metals. On the other hand, it is remarkable that the change of location of signals of the pyridinyl protons α to the nitrogen atom is very minute, whereas the shift of that of the meta protons is more important, as in Lindner's pyridine-silver complexes [28]. The substituted Cp ring protons are also slightly more deshielded in the β positions than in the α one.

The CV of the three cluster-cored poly-organometallic compounds could be recorded in the ferrocenyl and ruthenium regions, but rather little information could be obtained else than a single partially reversible wave for the hexa-ruthenium system as for the monomer. The hexa-ferrocenyl compound **7** shows a major reversible wave and a weak shoulder. This behavior could tentatively be attributable either to small amounts of decoordinated monomeric ferrocene derivative **5** whose potential is the same as that of the shoulder or to the distinction between the two sets of positions (apical and equatorial). Finally, the cluster-cored 18-silylferrocenyl dendrimer appears to share most of the properties of previously reported covalent [25], hydrogen-bonded [29] and gold-nanoparticle cored [24] polyferrocenyl dendrimers except that it is air sensitive due to the nature of the core. As in other polyferrocenyl dendrimers, the apparent equivalence of all the ferrocenyl groups in term of the seemingly unique redox potential allows to use this nanocluster as exo-receptor for the recognition and titration of oxo-anions whose prototype is ATP^{2-}. The sensing property by the 18-silylferrocenyl dendrimer is about the same as with the amidoferrocenyl dendrimers [25], but it is of easier access and presents the advantage that the oxidized ferrocenium form is fully stable, contrary to that of amidoferrocenyl moieties [24,25]. The CVs show a rather nice recognition of ATP^{2-} in spite of the relatively modest wave shift of 90 mV. The advantages of the golden-nanoparticle-cored polyferrocenyl dendrimers, however, are the air stability and their larger size (up to about 360 ferrocenyl groups) allowing a very easy electrode derivatization [24] that does not work at this time precisely because of the reduced size of this cluster-cored dendritic assembly.

4. Concluding Remarks

Three new hexasubstituted octahedral Mo_6 clusters with organometallic groups have been synthesized from the precursor $[n\text{-}Bu_4N]_2[Mo_6Br_8(CF_3SO_3)_6]$ upon prolonged heating. The substitution reactions of the triflate by the functional pyridine- or phenolate ligands were monitored by ^1H NMR that showed clean hexasubstitution. The two cluster-cored hexa-pyridine organometallics obtained are light and air sensitive and the 18-Fc dendrimer is air sensitive, which makes their purification, isolation and analysis tedious. Nevertheless, ^1H NMR is a convenient method to investigate both their synthesis and the electronic changes occurring upon coordination along the organometallic pyridine rods. The Mo_6-cluster-cored 18-silylferrocenyl dendrimers resembles, through its periphery, other polyferrocenyl dendrimers assembled by covalent bonds, coordination to gold nanoparticles and hydrogen bonds and, in particular, it behaves as an exo-receptor allowing to recognize and titrate the biologically important anion ATP^{2-}.

5. Experimental Section

5.1. General data

Reagent-grade tetrahydrofuran (THF) and pentane were predried over Na foil and distilled from sodium-benzophenone anion under argon immediately prior to use. MeOH was distilled from magnesium just before use. All other chemicals were used as received. All manipulations were carried out using Schlenk techniques or in a nitrogen-filled Vacuum Atmosphere dry lab. ^1H NMR spectra were recorded at 25 °C with a Bruker AC 300 (300 MHz) spectrometer. ^{13}C NMR spectra were obtained in the pulsed FT mode at 75 MHz with a Brucker AC 300 spectrometer. All chemical shifts are reported in parts per million (δ, ppm) with reference to Me_4Si (TMS). The product **1** [21] was synthesized from commercial 4-ethynylpyridine and $[RuCp(PPh_3)_2Cl]$ according to Bruce's general method

of synthesis of the complexes $[RuCp(PPh_3)_2(\eta^1$-alcynyl)] [22]. The precursor cluster **3** was synthesized according to reference [12d]. The reaction conditions used for the syntheses of substituted hexa-pyridine complexes were analogous to those reported in Fréchet's article [1].

Cyclic-voltammetric data were recorded with a PAR 273 potentiostat galvanostat. The reference electrode was an Ag quasi-reference electrode (QRE). The QRE potential was calibrated by adding the reference couple $[FeCp_2^*]/[FeCp_2^*]^+$ (Cp* = pentamethylcyclopentadienyl). The working electrode (platinum) was treated by immersion in 0.1 M HNO_3, and then polished before use and between each recording when necessary.

5.2. Synthesis of $[RuCp(PPh_3)_2(CC\text{-}C_5H_4N)]$, *1*

A methanol solution of 4-ethynylpyridine (0.296 g, 2.07 mmol) and 5 ml of triethylamine was added to a suspension of $[RuCp(PPh_3)_2Cl]$ (1.00 g, 1.38 mmol) and NH_4PF_6 (0.449 g, 2.76 mmol) in methanol. The solution was stirred at room temperature for 3 days. The solvent was removed under vacuum and the product was extracted with toluene. The product was precipitated with toluene/pentane. The yellow powder was dried under vacuum. Yield 0.350 g (0.440 mmol) of yellow powder of **1** (32%).

^{1}H NMR (MeOD, 300 MHz), δ_{ppm}: 8.06 (d, NC***H***), 7.30 – 7.04 (m, PPh_3), 6.80 (d, NCC***H***), 4.29 (s, Cp). ^{31}P NMR (MeOD, 100 MHz), δ_{ppm}: 49.60 (PPh_3). Infrared: ν_{CC}= 2 070 cm^{-1}. MS (MALDI-TOF; m/z), calcd. for $C_{48}H_{39}NP_2Ru$: 792.85, found: 794.24. CV in CH_2Cl_2: $E_{1/2}$ = 0.700 V vs. Fc* at 20 °C (partially chemically reversible: i_c/i_a = 0.5).

5.3. Synthesis of the trinuclear $AgRu_2$ complex, *2*

A methanol solution of **1** (0.0530 g, 0.0667 mmol) and $AgBF_4$ (0.007 g, 0.0333 mmol) was stirred at room temperature for 12 h. The solvent was removed under vacuum and the product was precipitated with MeOH/pentane. The orange powder was dried under vacuum. Yield: 0.040 g of **2** as an orange powder (67%). Analysis calcd. for $C_{96}H_{78}AgBF_4N_2P_4Ru_2$: C: 64.76%, H: 4.42%, found: 64.45%, H: 4.13.

^{1}H NMR (MeOD, 300 MHz), δ_{ppm}: 8.08 (d, NC***H***), 7.28 – 7.05 (m, PPh_3), 6.87 (d, NCC***H***), 4.33 (s, Cp). Infrared: ν_{CC} = 2 016 cm^{-1}. CV in CH_2Cl_2: $E_{1/2}$ = 0.940 V vs. Fc* at 20 °C (partially chemically reversible i_c/i_a = 0.5).

5.4. Synthesis of the hexa-substituted cluster Mo_6-Ru_6, *4*

A THF solution of **1** (0.131 g, 0.165 mmol) and **3** (0.069 g, 0.0265 mmol) was stirred at 60 °C for 7 days. The solvent was removed under vacuum and the product was precipitated with THF/pentane. The red powder was dried under vacuum. Yield 0.115 g of red powder of **4** (65%). Analysis calcd. for $Mo_6Br_8C_{292}H_{234}F_{12}S_4O_{12}N_6P_{12}Ru_6$ (%): C 53.39, H 3.39, found: C 52.59, H: 2.97.

^{1}H NMR (MeOD, 300 MHz), δ_{ppm}: 8.12 (d, NC***H***), 7.23 – 7.08 (m, PPh_3), 7.04 (d, NCC***H***), 4.42 (s, Cp). ^{31}P NMR (MeOD, 100 MHz), δ_{ppm}: 49.51(PPh_3). Infrared: ν_{CC} = 2 018 cm^{-1}. CV in CH_2Cl_2: $E_{1/2}$ = 0.650 V vs. Fc* at 20 °C in CH_2Cl_2 (partially chemically reversible i_c/i_a = 0.1).

5.5. Synthesis of the hexa-ferrocenyl Mo_6Fc_6 cluster, *7*

A THF solution of **5** (0.054 g, 0.187 mmol) and **3** (0.063 g, 0.029 mmol) was stirred at 60 °C for 7 days. The solvent was removed in vacuum and the product was precipitated with THF/pentane. The red powder was dried under vacuum. Yield 0.073 g of red powder of **7** (63%). ^{1}H NMR ($CDCl_3$, 300 MHz), δ_{ppm}: 8.64 (d, NC***H***), 7.51 (d, NCC***H***), 4.62 and 4.41 (t, FeC***H***), 4.32 (s, Cp). ^{13}C NMR ($CDCl_3$, 63 MHz), δ_{ppm}: 69.9 (Fe***C***), 70.2 (***Cp***), 72.0 (Fe***C***), 76.95 (C***C***), 125.9 (NC***C***), 147.5 (N***C***). Infrared: ν_{CC} = 2 181 cm^{-1}. Elemental analysis calcd (%): C 36.03, H 2.22; found (%): C 35.29, H 1.59. CV in CH_2Cl_2 at 20 °C: $E_{1/2}$ = 0.800 V vs. $[FeCp^*_2]$ in CH_2Cl_2.

5.6. Synthesis of the trinuclear $AgFc_2$ complex, *6*

A chloroform-*d* solution of **5** (0.044 g, 0.0156 mmol) and $AgSO_3CF_3$ (0.020 g, 0.0078 mmol) was stirred at room temperature for 24 h. The solvent was removed under vacuum, and the product was washed with ether and dried under vacuum. Yield: 0.061 g of red powder of **6** (95%).

^{1}H NMR ($CDCl_3$, 300 MHz), δ_{ppm}: 8.54 (d, NC***H***), 7.41 (d, NCC***H***), 4.61 and 4.40 (t, FeC***H***), 4.30 (s, Cp).

^{13}C NMR ($CDCl_3$, 63 MHz), δ_{ppm}: 71.3 (Fe***C***), 72.2 (***Cp***), 73.5 (Fe***C***), 77.6 (C***C***), 126.7 (NC***C***), 137.2 (NCC***C***), 148.4 (N***C***). Infrared: ν_{CC} = 2 176 cm^{-1}.

Analysis calcd (%): C 50.57, H 3.15; found (%): C 50.28, H 2.91

*5.7. Synthesis of the cluster-cored hexa-tri-silylferrocenylphenolate dendrimer $(Bu_4N)_2[MoBr_8(OC_6H_4C\{C_3H_6SiC_2H_6Fc\}_3)_6]$, **9***

A 20-ml THF solution of (n-$Bu_4N)_2[MoBr_8(CF_3SO_3)_6]$, (0.019 mmol, 0.050 g) and $Na[OC_6H_4C(C_3H_6SiC_2H_6Fc)_3]$ (0.23 mmol, 0.222 g) was magnetically stirred at 60 °C overnight. The solvent was removed under vacuum, and 20 ml of toluene were added. The solution was then stirred at 80 °C for two days, then filtered at room temperature over celite. The volume of the filtrate was reduced to 3-5 ml, and 30 ml of anhydrous pentane was added dropwise. An orange powder precipitated and was re-dissolved with 2-3 ml toluene and re-precipitated with pentane. The compound $(Bu_4N)_2[MoBr_8(OC_6H_4C(C_3H_6SiC_2H_6Fc)_3)_6]$, **9**, is an orange powder. Yield: 57% 0.080 g). ^{1}H NMR (300 MHz, $CDCl_3$): δ 6.85 (m. 12H), 6.45 (m. 12H), 4.12 (s, 12H), 3.91 (s, 30H), 3.86 (s, 12H), 2.72 (m, 16H), 1.40 (m, 36H), 1.07–0.97 (m, 42H), 0.70 (m, 36H), 0.43 (m, 36H), 0.002 (s, 108H). ^{13}C NMR (62.9 MHz, $CDCl_3$) : δ 724.65 (C_5H_4), 72.28 (C_5H_4), 69.81 (C_5H_4), 31.34 (CH_2N), 19.73 (CH_2), 19.20 (CH_2). 15.66 (CH_3), -0.08 (CH_3). CV of the ferrocenyl system: $E_{1/2}$ = 0.40 V vs. [FeCp*$_2$] in CH_2Cl_2 at 20 °C.

Acknowledgment

We are grateful to Dr Jean-Claude Blais (University Paris-6) for recording the MALDI TOF mass spectrum of complex **1**. Financial support from the French 'Ministère de la Recherche' (ACI Nanostructures 2001 No. N18-01), the 'Institut universitaire de France' (IUF), the 'Centre national de la recherche scientifique' (CNRS), the Universities Bordeaux-1, Rennes-1 and Funchal (Portugal) and the Fondation Langlois are gratefully acknowledged.

References

[1] J.H. Golden, H. Deng, F.J. DiSalvo, J.M.J. Fréchet, P.M. Thompson, Science 268 (1995) 1463.
[2] M.T. Reetz, Science 267 (1995) 367.
[3] (a) J.A. Real, E. Andrér, M.C. Munoz, M. Julve, T. Granier, A. Bousseksou, F. Varret, Science 268 (1995) 265; (b) R.F. Ziolo, Science 257 (1992) 219.
[4] V. Balzani, S. Campagna, G. Denti, A. Juris, S. Serrini, M. Venturi, Acc. Chem. Res. 31 (1998) 26.
[5] M.-C. Daniel, D. Astruc, Chem. Rev. 104 (2004) 293.
[6] K.R. Dunbar, Comment Inorg. Chem. 13 (1992) 313.
[7] S.D. Hudson, H.-T. Jung, V. Percec, W.-D. Cho, G. Johansson, G. Ungar, V.S.K. Balagurusamy, Science 278 (1997) 449.
[8] (a) C.B. Gorman, Adv. Mater 10 (1998) 295; (b) C.B. Gorman, W.Y. Su, H. Jiang, C.M. Watson, P. Boyle, Chem. Commun. (1999) 877.
[9] E. Alonso, D. Astruc, J. Am. Chem. Soc. 122 (2000) 3222.
[10] (a) G.R. Newkome, C.N. Moorefield, Dendrimers and Dendrons: Concepts, Syntheses, Applications, Wiley-VCH, Weinheim, 2001; (b) Dendrimers and other Dendritic Polymers, Wiley-VCH, New York, 2002; (c) D. Astruc (Ed.), Dendrimers and Nanosciences, C. R. Chimie 6 (8–10) (2003).
[11] C. Brosset, Ark. Kemi, Mineral. Geol. 20A (7) (1945) 1; 22A (11) (1946) 1.
[12] (a) For reviews, see: C. Perrin, J. Alloys Compds 10 (1997) 262; P. Batail et al., Chem. Rev. 101 (2001) 2037; for recent inorganic substitution chemistry, see: (b) S. Cordier, N. Naumov, D. Salloum, F. Paul, C. Perrin, Inorg. Chem. 43 (2004) 219; (c) G. Pilet, S. Cordier, S. Gohlen, C. Perrin, L. Ouahab, A. Perrin, Solid-State Sci. 5 (2003) 1359; (d) K. Kirakci, S. Cordier, C. Perrin, Z. Anorg. Allg. Chem. 631 (2005) 411.
[13] R. Chevrel, R. Sergent, M. Prigent, J. Solid-State Chem. 3 (1971) 515; R. Chevrel, M. Hirrien, M, Sergent, Polyhedron 5 (1986) 87.
[14] (a) A.W. Maverick, H.B. Gray, J. Am. Chem. Soc. 103 (1981) 1298; (b) J.A. Jackson, C. Turro, M.D. Newsham, D.G. Nocera, J. Phys. Chem. 94 (1990) 4500.
[15] J.C. Sheldon, Nature 184 (1959) 1210; P. Nannelli, B.P. Block, Inorg. Chem. 7 (1968) 2423; 8 (1969) 1767; M.H. Chisholm, J.A. Heppert, J.C., Huffman, Polyhedron 3 (1984) 475.
[16] N. Perchenek, A. Simon, Z. Anorg, Allg. Chem. 619 (1993) (98 and 103).
[17] P. Nannelli, B.P. Block, Inorg. Synth. 13 (1971) 99.
[18] D.H. Johnston, D.C. Gaswick, M.C. Lonergan, C.L. Stern, D.F. Shriver, Inorg. Chem. 31 (1992) 1869.
[19] D. Astruc, Electron Transfer and Radical Processes in Transition Metal Chemistry, Wiley-VCH, New-York, 1995.
[20] (a) I. Cuadrado, M. Morán, C.M. Casado, B. Alonso, J. Losada, Coord. Chem. Rev. 193–195 (1999) 395; C.M. Casado, I. Cuadrado, M. Morán, B. Alonso, B. Garcia, B. Gonzales, J. Losada, Coord. Chem. Rev. 185–186 (1999) 53; (b) Z. Zheng, R. Long, R.H. Holm, J. Am. Chem. Soc. 119 (1997) 2171; R. Wang, Z. Zheng, J. Am. Chem. Soc. 121 (1999) 3549; H.D. Selby, B.K. Roland, Z. Zheng, Acc. Chem. Res. 36 (2003) 933; D. Astruc, Pure Appl. Chem. 75 (4) (2003) 461.

[21] I.-Y. Wu, J.-L. Lin, Organometallics 16 (1997) 2038.
[22] (a) For [RuCp(PPh_3)$_2$ (η^1-alcynyl) complexes, see: M.I. Bruce, B.C. Hall, B.D. Kelly, P.J. Low, B.K. Skelton, A.H. White, J. Chem. Soc., Dalton Trans. (1999) 3719; M. Bruce, Chem. Rev. 98 (1998) 2797; (b) for 4-ethynylpyridine hydrochloride used in the present work, see: T. Yamamoto, A.M. Arif, P.J. Stang, J. Am. Chem. Soc. 125 (2003) 12309.
[23] J.C. Torres, R.A. Pilli, M.D. Vargas, F.A. Violante, S.J. Garden, A.C. Pinto, Tetrahedron 58 (2002) 4487.
[24] (a) M.-C. Daniel, J. Ruiz, S. Nlate, J. Palumbo, J.-C. Blais, D. Astruc, Chem. Commun. 7 (19) (2001) 2000–2001; (b) M.-C. Daniel, J. Ruiz, S. Nlate, J.-C. Blais, D. Astruc, J. Am. Chem. Soc. 125 (2003) 2617.
[25] (a) C. Valério, J.-L. Fillaut, J. Ruiz, J. Guittard, J.-C. Blais, D. Astruc, J. Am. Chem. Soc. 119 (1997) 2588; (b) M.-C. Daniel, J. Ruiz, J.-C. Blais, N. Daro, D. Astruc, Chem. Eur. J. 9 (2003) 4371.
[26] (a) S.R. Miller, D.A. Gustowski, Z.-H. Chen, G.-W. Gokel, L. Echegoyen, A.E. Kaifer, Anal. Chem. 60 (1988) 2021; (b) review: P. D. Beer, P. A Gale, Angew. Chem. Int. Ed. Engl. 40 (2001) 486.
[27] N. Prokopuk, D.F. Schriver, Inorg. Chem. 36 (1997) 5609.
[28] E. Lindner, R. Zong, K. Eichele, U. Weisser, M. Ströbele, Eur. J. Inorg. Chem. (2003) 705.
[29] M.-C. Daniel, J. Ruiz, D. Astruc, J. Am. Chem. Soc. 125 (2003) 1150.

The Simple Hexapyridine Cluster $[Mo_6Br_8Py_6][OSO_2CF_3]_4$ and Substituted Hexapyridine Clusters Including a Cluster-cored Polyolefin Dendrimer

Denise Méry[a], Lauriane Plault[a], Sylvain Nlate[a], Didier Astruc[a,*], Stéphane Cordier[b], Kaplan Kirakci[b], and Christiane Perrin[b,*]

[a] Talence / France, Université Bordeaux I, Nanosciences and Catalysis Group, LCOO, UMR CNRS N° 5802
[b] Rennes / France, Université de Rennes 1, Institut de Chimie de Rennes, LCSIM, UMR CNRS N° 6511

Received March 8th, 2005.

Dedicated to Professor Herbert W. Roesky at the Occasion of his 70th Birthday

Abstract. The yellow octahedral molybdenum cluster $[n\text{-}Bu_4N]_2[Mo_6Br_8(CF_3SO_3)_6]$, (**1**); undergoes substitution of all six terminal triflate ligands by pyridine ligands in pyridine/THF at 60 °C to yield the orange hexapyridine cluster $[Mo_6Br_8(Py)_6][CF_3SO_3]_4$, (**2**). The cluster **1** also reacts in THF at 60 °C with excessof the *para*-substitued pyridines 4-*tert*-Bupy and 4-vinylpy to give the orange *para*-substituted hexapyridine clusters $[Mo_6Br_8(p\text{-}Py\text{-}R)_6][CF_3SO_3]_4$ (**3**: R = *tert*-Bu; **4**: R = vinyl) and with the new dendronic pyridine derivative 3,3′-$\{CH_2Op\text{-}C_6H_4C(CH_2CH{=}CH_2)_3\}_2Py$, (**5**) (7 d), to give the orange relatively air stable Mo_6-cluster-cored 36-allyl dendrimer $[Mo_6Br_8(3,5\text{-}\{CH_2OC_6H_4C(CH_2CH{=}CH_2)_3\}_2Py)_6][CF_3SO_3]_4$, (**6**). All these substitution reactions were easily monitored by ^1H NMR in $CDCl_3$ using the comparison between the intensities of the tetrabutylammonium cation and deshielded coordinated pyridine signals.

Keywords: Cluster compounds; Dendrimer; Molybdenum; Pyridine; Olefin

Introduction

The octahedral hexametallic clusters are excellent starting points for the synthesis of molecular assemblies and nanosized materials with catalytic and physical properties [1]. Among these clusters, the hexamolybdenum series is easily available from the starting materials $[Mo_6X_{14}]^{2-}$ (X = halide) that have been characterized 60 years ago [2]. The octahedral molybdenum clusters became most popular when the superconducting properties of the related chalcogenides $M_xMo_6Y_8$ (Y = chalcogen), known as Chevrel phases, were discovered [3]. Photophysical and redox properties of $[Mo_6X_{14}]^{2-}$ added further interest [4]. Among the 14 halogen ligands, the 8 face-capping ones are relatively unreactive, which makes resistant cluster cores $[Mo_6X_8]^{4+}$. In the case of $[Mo_6Cl_{14}]^{2-}$ units, the inner chlorine ligands can be replaced by chalcogen ligands, a soft route to Chevrel phases. Further apical ligand substitutions in this family of complexes lead to various $[Mo_6Y_8L_6]$ clusters [5]. On the other hand, substitution of the 6 semi-labile apical ligands in $[Mo_6X_{14}]^{2-}$ is rather facile and has been examined for a long time [6]. In particular, the hexa-methoxyclusters $[Mo_6Br_8(OMe)_6]^{2-}$, reported by *Nanelli* and *Block* [7] and the hexatriflate clusters $[Mo_6Br_8(OSO_2CF_3)_6]^{2-}$, reported by *Shriver* et al. [8] are the most useful starting materials for further substitution.

We have investigated hexapyridine complexes of the $[Mo_6Br_8]^{4+}$ core by simple substitution of the six triflate ligands in *Shriver's* complex $[Mo_6Br_8(OSO_2CF_3)_6]^{2-}$, in order to further assemble functional hexapyridine Mo_6 complexes into dendritic and nanoscopic structures. The preliminary synthetic findings are reported here. Although hexapyridine hexametallic clusters are known with Re_6 [9], W_6 [10] and Mo_6S_8 [5b] cluster series, there is no report with the $[Mo_6X_8]^{4+}$ core. Some 4,4′-bipyridine complexes have been reported by *Shriver's* group, however [11]. Our investigation is extended to substituted and dendronic pyridines. Metal-cluster-cored dendrimers have already been reported by *Gorman* [1b, 12a] with the biomimetic Fe_4S_4 core and by *Zheng* [1c, 9] with the $[Re_6Se_8]^{2+}$ cores.

*,[a] Prof. Dr. Didier Astruc
Nanosciences and Catalysis Group, LCOO, UMR CNRS N° 5802
Université Bordeaux I
F-33405 Talence Cedex/France
Fax (33) 540 00 66 46
E-mail: d.astruc@lcoo.u-bordeaux1.fr
*,[b] Dr. Christiane Perrin
Institut de Chimie de Rennes, LCSIM, UMR CNRS N° 6511
Université de Rennes 1
Avenue du Général Leclerc
F-35042 Rennes Cedex/France
Fax (33) 223 23 67 99
E-mail: christiane.perrin@univ-rennes1.fr

Results and Discussion

Ligand substitution with pyridine

After synthesis of the known hexatriflate cluster $[n\text{-}Bu_4N]_2[Mo_6Br_8(CF_3SO_3)_6]$, (**1**), according to *Schriver's* work [8], we examined its substitution properties with pyridine and substituted pyridines. The substitution reaction of the six triflate ligands with six pyridine ligands is completed in two days at 60 °C in pyridine/THF (equation (1)). The reaction is followed by ^1H NMR by comparison of the intensities of the pyridine protons that are all deshielded compared to

  DOI: 10.1002/zaac.200500121 *Z. Anorg. Allg. Chem.* **2005**, *631*, 2746–2750

free pyridine with those of the tetrabutylammonium counter cation. This deshielding effect is most marked for the ortho pyridine protons moving from 7.41 ppm *vs.* TMS in $CDCl_3$ in free pyridine to 7.81 ppm in **2**. From the yellow starting cluster **1**, the new orange complex **2** precipitates from the reaction medium, as it is insoluble in pyridine. The triflate salt [*n*-Bu_4N][CF_3SO_3] is thus readily separated as it is soluble in pyridine and THF. The orange solid product **2** is washed with THF. It is sparingly soluble in dichloromethane and chloroform. In addition to pyridine, it is insoluble in ether, THF and alkanes, and it decomposes in methanol, presumably ligand substitution between pyridine and methanol providing methoxy ligands. It is also unstable in water. The cluster **2** is stable in air even in acetone and in the presence of light.

Ligand substitution with para-tertbutylpyridine and para-vinylpyridine

Ligand substitution reactions of **1** with *para*-substituted pyridines were carried out in THF at 60 °C using approx. hundred fold excess of *para*-substituted pyridine, i.e. in pyridine/THF solvents, and the reactions lasted two days (equation (1)). Reactions were monitored analogously by comparing the intensity of the tetrabutylammonium ^{1}H NMR peaks with those of the *ortho* protons of the pyridine ligands. No precipitate formed, the orange solution remaining homogeneous at the end of the reaction. The separation of [*n*-Bu_4N][CF_3SO_3] from the new clusters **3** and **4** is now tedious, because these clusters are now much more soluble in a variety of solvents such as pyridine and THF. It proceeds by successive precipitation from acetone by controlled addition of pentane, and is checked by ^{1}H NMR. Several such reprecipitations are required in order to remove the salt. Thus, finally, removal of this salt is only complete with the approximation of the ^{1}H NMR accuracy that does not overtake 98 %. Elemental analyses show carbon contents that are often low, presumably due to the presence of this and/or other extra salts in analyzed samples. Again, the orange compounds obtained are air and light stable even in solution for at least several hours. They are unstable in water and methanol.

Ligand substitution by the dendronic pyridine 3,3′-py{CH_2O*p*-$C_6H_4C[(CH_2CH{=}CH_2)_3]_3\}_2$, (5)

The dendronic [12] pyridine 3,3′-py{CH_2O*p*-C_6H_4C-$(CH_2CH{=}CH_2)_3\}_2$, (**5**), is synthesized by reaction of the

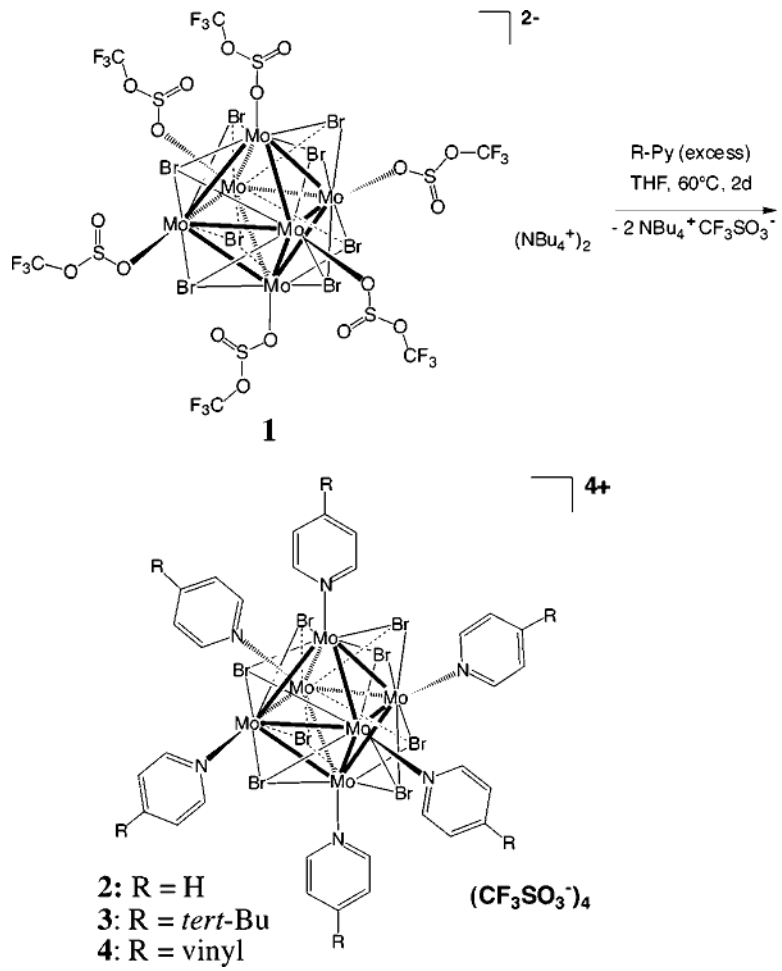

phenol dendron HO*p*-$C_6H_4C(CH_2CH{=}CH_2)_3$ with 3,3′-$py(CH_2Br)_2$. Reaction of **5** with **1** was carried out for six days in refluxing THF using 6.2 equiv. **5**. ^{1}H NMR shows that the reaction is completed from the relative intensity ratio between the ammonium protons and the coordinated pyridine protons. Indeed, the *para*-pyridine proton is deshielded from 7.95 ppm in free pyridine to 8.66 ppm in the coordinated pyridine dendron. The final solution was orange, and the reaction time is seemingly not longer than with the other pyridines, as monitored by ^{1}H NMR. After numerous reprecipitations in order to remove the salts, ^{1}H NMR shows that the ammonium salt is no longer present and the carbon content in the elemental analysis of the cluster-cored dendrimer **6** is acceptable.The orange compound **6** is soluble in dichloromethane, and air- and light stable in this solvent; it is insoluble in pentane, however. After one day in chloroform solution, the solution is still orange, but some decomposition to an insoluble film is observed. Although the conversion is complete as monitored by ^{1}H NMR, the yield is eventually mediocre due to the repeated precipitations.

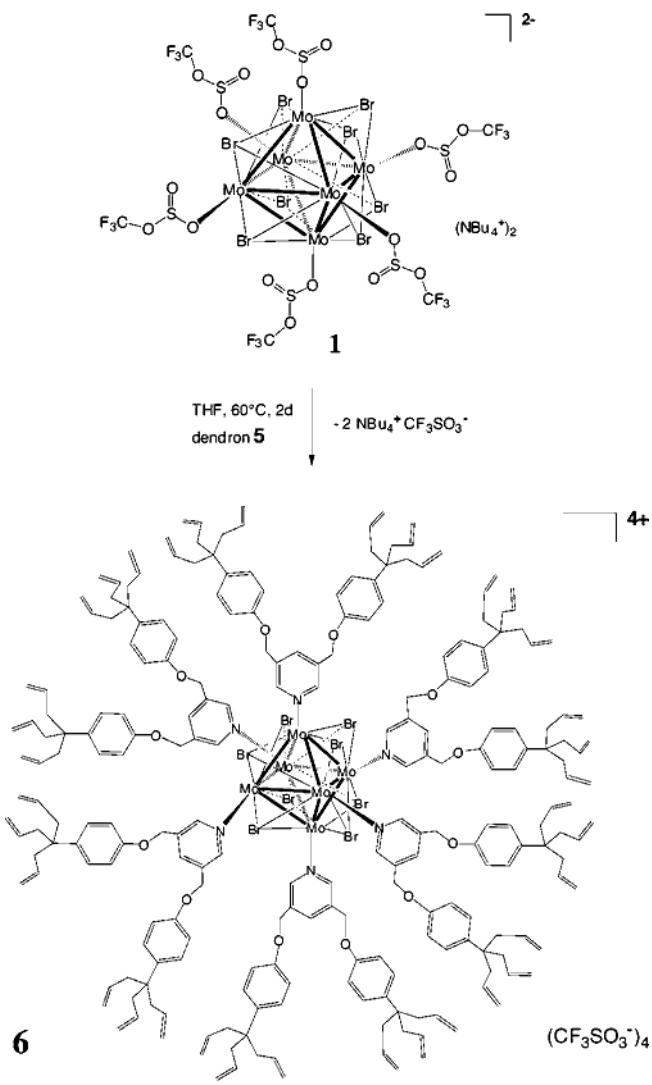

Reaction of **6** with Grubb' second generation metathesis catalyst [$RuCl_2\{(CHMes_2N)_2C\}{=}CHPh$] in dichloromethane at room temperature shows the characteristic signals corresponding to ring-closing metathesis within the six tripods due to the very favorable formation of the cyclopentenyl rings within 0.5 h. Continuation of this reaction and ^{1}H NMR monitoring, however, showed extensive decomposition to pentane soluble dendron fragments whereas the pyridine ligands are no longer coordinated to the cluster core. The pyridine loss from the cluster presumably coordinates to the ruthenium center of the metathesis catalyst (present in only 5 % molar amount *vs.* double bonds) which suppresses its catalytic activity.

Concluding Remarks and Prospects

An easy route to a family of new relatively air stable octahedral hexamolybdenum hexapyridine clusters $[Mo_6Br_8(4\text{-}Py\text{-}R)_6][CF_3SO_3]_4$ has been disclosed starting from the precursor complex $[n\text{-}Bu_4N]_2[Mo_6Br_{14}]$ [2e, 2g] by substitution of the six triflate ligands by pyridine or various pyridine derivatives in $[n\text{-}Bu_4N]_2[Mo_6Br_8(CF_3SO_3)_6]$ (**1**), a starting material that is readily available from $[n\text{-}Bu_4N]_2[Mo_6Br_{14}]$ and $AgOSO_2CF_3$ in THF [8]. The new Mo_6 clusters are quite stable to air and light in the solid state or in acetone, dichloromethane or chloroform solution. The solubility in these solvents allows monitoring their formation by ^{1}H NMR by comparison of the relative intensities of the tetrabutylammonium signals and those of the pyridine protons that become deshielded upon pyridine coordination. The use of substituted pyridine largely increases the solubility of the new clusters, which renders the separation of the Mo_6 cluster from the salt $[n\text{-}Bu_4N][OSO_2CF_3]$ difficult with the tetrabutylammonium salt used at the beginning of the synthesis. This separation can be achieved by successive reprecipitations, however. An X-ray crystal structure could not yet be obtained at this preliminary stage, however, possibly for this reason, and efforts are continuing. Finally, this procedure works well with pyridines bearing *meta* or *para* alkyl substituents. Attempts to extend it to pyridine rods bearing alkynyl substituents in *para* position led to air- and light sensitive materials [13]. Thus, dendronic pyridines in which side pyridine substituents are attached to the pyridine ring *via* methylene groups does not lead to destabilization of the cluster complex, which allows to synthesize the Mo_6-cluster-cored 36-allyl dendrimer $[Mo_6Br_8(3,5\text{-}\{CH_2OC_6H_4C(CH_2CH{=}CH_2)_3\}_2Py)_6][CF_3SO_3]_4$, (**6**). The present strategy is therefore timely to investigate more sophisticated hybrid organic-inorganic materials, and future work will tend towards such directions.

Experimental Section

Reagent-grade tetrahydrofuran (THF) and chloroform-d were predried over Na foil and distilled from sodium benzophenone anion under argon immediately prior to use. Other commercial chemicals were purchased from Aldrich and used as received. All manipu-

lations were carried out using Schlenk flasks, and samples were transferred in a nitrogen-filled vacuum atmosphere drylab. ^{1}H NMR spectra were recorded at 25 °C with a Bruker AC 300 (300 MHz) spectrometer. ^{13}C NMR spectra were obtained in the pulsed FT mode at 75 MHz with a Brucker AC 300 spectrometer. All chemical shifts are reported in parts per million (δ, ppm) with reference to Me_4Si (TMS). Elemental analyses were carried out at the Vernaison CNRS center.

Cluster $Mo_6Br_8py_6Tf_4$ (2)

A yellow THF solution of **1** [8] (0.585 g, 0.231 mmol) and pyridine (1.8 mL, 0.023 mol) was stirred at 60 °C for 2 days. The reaction product progressively precipitated from the reaction mixture as a very fine powder. The solvent was removed under vacuum to give an orange solid that was washed with pentane and THF and dried under vacuum to yield complex **2** as an orange solid. Yield 0.416 g of **2** (79 %). Elemental analysis calcd for $C_{34}H_{30}Br_8F_{12}Mo_6N_6O_{12}S_4$ (%): C 17.87, H 1.32; found (%): C 17.21, H 1.09. M = 2285.76 g.mol^{-1}.

^{1}H NMR ($CDCl_3$, 300 MHz), δ: 8.71 (d, 12H), 8.13 (m, 6H), 7.68 (m, 12H). **^{13}C NMR** ($CDCl_3$, 75.47 MHz), δ: 147.78 (C_o), 141.51 (C_p), 126.38 (C_m).

Cluster Mo_6Br_8(4-*tert*-butylpyridine)$_6Tf_4$ (3)

A THF solution of **1** (1 g, 0.394 mmol) and 4-*tert*-butylpyridine (2 mL) was stirred at 60 °C for 2 days. The solvent was removed under vacuum to give a solid that was washed with pentane and THF and dried under vacuum to yield complex **3** as an orange solid. Yield 0.826 g (80 %). Elemental analysis calcd for $C_{58}H_{78}Br_8F_{12}Mo_6N_6O_{12}S_4$ (%): C 26.56, H 3.00; found (%): C 26.15, H 2.69. M = 2622.40 g.mol^{-1}.

^{1}H NMR ($CDCl_3$, 300 MHz), δ: 8.59 (d, 12H), 7.49 (d, 12H), 1.35 (s, 54H). **^{13}C NMR** ($CDCl_3$, 75.47 MHz), δ: 147.48 (C_o), 122.19 (C_m), 34.50 (CMe_3), 30.76 (CH_3).

Cluster Mo_6Br_8(4-vinylpyridine)$_6Tf_4$ (4)

A THF solution of **1** (0.300 g, 0.141 mmol) and 4-vinylpyridine (1 mL) was stirred at 60 °C for 2 days. The solvent was removed under vacuum to give a solid residue that was washed with pentane and THF and dried under vacuum to yield complex **4** as an orange solid. Yield 0.293 g (85 %). Elemental analysis calcd. for $C_{46}H_{48}Br_8F_{12}Mo_6N_6O_{12}S_4$ (%): C 22.57, H 1.98; found (%): C 22.09; H 1.61. M = 2448.04 g.mol^{-1}.

^{1}H NMR ($CDCl_3$, 300 MHz), δ_{ppm}: 8.57 (d, 12H), 7.27 (d, 12H), 6.65 (q, 6H), 6.00 (d, 6H), 5.51 (d, 6H). **^{13}C NMR** ($CDCl_3$, 75.47 MHz), δ_{ppm}: 150.56 (C_o), 135.15 (CH=CH_2) 121.13 (C_m), 119.03 (CH=**C**H_2).

Dendronic pyridine derivative 5

In a Schlenk tube, 3-5 bis(bromomethyl) pyridine [14] (0,17 mmol), *p.* triallylmethylphenol [15] (1.13 mmol) and K_2CO_3 (2.26 mmol) were stirred for two days in acetonitrile. Then, the solvent was removed under vacuum, and the reaction product was extracted using diethyl ether and filtered on celite. The solvent was evaporated to dryness and the product **5** was chromatographed on silica gel (eluent: diethyl ether/petrolum ether 1/1). Yield: 70 %. Elemental analysis calcd. for $C_{39}H_{45}NO_2$: C 83.68, H 8.10; found C 83.23, H 8.12 %. M = 559.79 g.mol^{-1}.

^{1}H NMR (250 MHz, $CDCl_3$): δ = 8.71 (s, 2H, *o*-H pyridine), 7.95 (s, 1H, *p*-H pyridine), 7.33 and 6.97 (d, 4H, H aromatic), 5.61 (m, 6H, CH allyl), 5.11 (m, 12H, CH_2 allyl), 5,03 (s, 4H, CH_2O), 2.48 (d,12H, Cq-CH_2-CH). **^{13}C NMR** (63 MHz, $CDCl_3$): δ = 156.2 (C_q Ar-O), 148.5-138.5 (CH pyridine), 134.53 (CH allyl), 132.6 (C_q pyridine), 128.6-114.1 (CH Ar), 117.5 (CH_2 allyl), 67.3 (CH_2O), 44.7 (C_q Ar-C_q-CH_2), 41.8 (C_q-CH_2-CH).

Mo_6 Cluster-cored 36-allyl dendrimer $[Mo_6Br_8(3,5\{CH_2OC_6H_4C(CH_2CH=CH_2)_3\}_2Py)_6][CF_3SO_3]_4$ (6)

A yellow THF solution of **1** (0.100 g, 0.038 mmol) and the pyridine dendron **5** (0.143 g, 0.255 mmol) was stirred at 60 °C for 7 days. The solvent was removed under vacuum and the product was precipitated with THF/pentane. The orange powder was dried under vacuum. Yield: 0.097 g of orange powder of **6** (49 %). Elemental analysis calcd. for $C_{238}H_{270}Br_8F_{12}Mo_6N_6O_{24}S_4$ (%): C 55.29, H 5.26; found (%): C 54.85, H 4.98. M = 5169.83 g.mol^{-1}.

^{1}H NMR ($CDCl_3$, 300 MHz), δ: 8.90 (s, 12H, H_o), 8.66 (s, 6H, H_p), 7.27 (d, 24H), 6.96 (d, 24H), 5.53 (m, 36H, $=CH_a$), 5.02 (m, 96H, $=CH_{2\,a}$ + OCH_2), 2.45 (d, 72H, CH_2). **^{13}C NMR** ($CDCl_3$, 75.47 MHz), δ: 155.46 (C_o), 139.19 (C_m), 136.91 (C_p), 134.26 (**C**H=CH_2), 127.96 (C_{ar}), 117.41 (CH=**C**H_2), 114.20 (C_{ar}), 65.95 (O**C**H_2), 42.84 (C_q), 41.85 (C_q-CH_2).

Acknowledgment. Financial support from the Ministère de la Recherche (ACI Nanostructures 2001 N° N18-01 and grants to *DM*, *KK* and *LP*), the Institut Universitaire de France (DA, IUF), the Centre National de la Recherche Scientifique (CNRS), the Universities Bordeaux I and Rennes 1 and the Fondation Langlois is gratefully acknowledged.

References

[1] (a) J. H. Golden, H. Deng, F. J. DiSalvo, J. M. J. Fréchet, P. M. Thompson, *Science* **1995**, *268*, 265; R. F. Ziolo, *Science* **1992**, *257*, 219; J. A. Real, E. Andrér, M. C. Muñoz, M. Julve, T. Granier, A. Bousseksou, F. Varret, *Science* **1995**, *268*, 265; K. R. Dunbar, *Comment Inorg. Chem*. **1992**, *13*, 313; J.-C. P. Gabriel, K. Boubekeur, S. Uriel, P. Batail, *Chem. Rev.* **2001**, *101*, 2037; (b) C. Gorman, J. C. Smith, *Acc. Chem. Res.* **2001**, *34*, 60; (c) H. D. Selby, B. K. Roland, Z. Zheng, *Acc. Chem. Res.* **2003**, *36*, 933.

[2] (a) C. Brosset, *Ark. Kemi, Mineral. Geol*. **1945**, *20A*, *7*, 1 and **1946**, *22A*, *11*, 1; (b) for a review, see: C. Perrin, *J. Alloys Compds.* **1997**, *10*, 262; for recent inorganic substitution chemistry, see: (c) S. Cordier, N. Naumov, D. Salloum, F. Paul, C. Perrin, *Inorg. Chem*. **2004**, *43*, 219; (d) G. Pilet, S. Cordier, S. Gohlen, C. Perrin, L. Ouahab, A. Perrin, *Sol. State Sci*. **2003**, *5*, 1359; (e) K. Kirakci, S. Cordier, C. Perrin, *Z. Anorg. Allg. Chem*. **2005**, *631*, 411; for X-ray crystal structures of Mo_6 halide clusters, see: (f) G. Pilet, K. Kirakci, F. de Montigny, S. Cordier, C. Lapinte, C. Perrin, A. Perrin, *Eur. J. Inorg. Chem*. **2005**, *5*, 919; (g) K. Kirakci, S. Cordier, T. Roisnel, S. Golhen, C. Perrin, *Z. Kristallogr*. NCS, **2005**, *220*, 116.

[3] R. Chevrel, R. Sergent, M. Prigent, *J. Solid State Chem*. **1971**, *3*, 515; R. Chevrel, M. Hirrien, M. Sergent, *Polyhedron* **1986**, *5*, 87.

[4] A. W. Maverick, H. B. Gray, *J. Am. Chem. Soc*. **1981**, *103*, 1298; J. A. Jackson, C. Turro, M. D. Newsham, D. G. Nocera, *J. Phys. Chem*. **1990**, *94*, 4500.

[5] a) R. E. McCarley, S. J. Hilsenbeck, X. Xie, *J. Solid State Chem*. **1995**, *117*, 269; T. Saito, A. Yoshikawa, T. Yamagata, *Inorg. Chem*. **1989**, *28*, 3588; b) for a recent report, see S. J. F.

Popp, S. W. Boettcher, M. Yuan, C. Oertel, F. J. DiSalvo, *J. Chem. Soc. Dalton Trans.* **2002**, 3096.

[6] J. C. Sheldon, *Nature* **1959**, *184*, 1210; P. Nannelli, B. P. Block, *Inorg. Chem*. **1968**, *7*, 2423; **1969**, *8*, 1767; M. H. Chisholm, J. A. Heppert, J. C. Huffman, *Polyhedron* **1984**, *3*, 475; N. Perchenek, A. Simon, *Z. Anorg. Allg. Chem*. **1993**, *619*, 98 and 103.

[7] P. Nannelli, B. P. Block, *Inorg. Syn*. **1971**, *13*, 99.

[8] D. H. Johnston, D. C. Gaswick, M. C. Lonergan, C. L. Stern, D. F. Shriver, *Inorg. Chem.* **1992**, *31*, 1869.

[9] R. Wang, Z. Zheng, *J. Am. Chem. Soc*. **1999**, *121*, 3549.

[10] S. Jin, J. Adamchuk, B. Xiang, F. J. DiSalvo, *J. Am. Chem. Soc*. **2002**, *124*, 9229.

[11] (a) L. M. Robinson, R. L. Brain, D. F. Shriver, D. E. Ellis, *Inorg. Chem*. **1995**, *34*, 5588; (b) R. L. Bain, D. F. Shriver, D. E. Ellis, *Inorg. Chim. Acta* **2001**, *325*, 171.

[12] (a) For previous metal-cluster-cored dendrimers, see refs. [1b, c, 9] and C. B. Gorman, B. L. Parkhurst, W. Y. Su, K.-Y. Chen, *J. Am. Chem. Soc*. **1997**, *119*, 1141; (b) for books on dendrimers, see: G. R. Newkome, C. N. Moorefield, *Dendrimers and Dendrons: Concepts, Syntheses, Applications*, Wiley-VCH, Weinheim, 2001; *Dendrimers and other Dendritic Polymers*, D. Tomalia, J. M. J. Fréchet, Eds.; Wiley-VCH, New York, 2002; *Dendrimers and Nanosciences*, D. Astruc (ed.), *C. R. Chimie* **2003**, *6*, *Vol 8-10*, Elsevier, Paris.

[13] D. Méry, C. Ornelas, M.-C. Daniel, J. Ruiz, J. Rodriguez, D. Astruc, S. Cordier, K. Kirakci, C. Perrin, *C. R. Chimie*, **2005**, ASAP.

[14] M. Momenteau, J. Mispelter, B. Loock, J. M. Lhoste, *J. Chem. Soc., Perkin Trans.* **1985**, 61.

[15] V. Sartor, L. Djakovitch, J.-L. Fillaut, F. Moulines, F. Neveu, V. Marvaud, J. Guittard, J.-C. Blais, D. Astruc, *J. Am. Chem. Soc*. **1999**, *121*, 2929.

From Simple Monopyridine Clusters $[Mo_6Br_{13}(Py\text{-}R)_6][n\text{-}Bu_4N]$ and Hexapyridine Clusters $[Mo_6X_8(Py\text{-}R)_6][OSO_2CF_3]_4$ (X = Br or I) to Cluster-cored Organometallic Stars, Dendrons and Dendrimers.

Abstract

Hexasubstitution of apical triflate ligands in the octahedral clusters $[M]_2[Mo_6X_8(CF_3SO_3)_6]$, (M = *n*-$Bu_4N$ or Cs, X = Br or I) and monosubstitution in $[n\text{-}Bu_4N]_2[Mo_6Br_{13}(CF_3SO_3)]$ was carried in THF at 60°C out with simple pyridines, then extended to organometallic pyridines yielding cluster-cored stars and to dendronic polyallyl and polyferrocenyl pyridines yielding cluster-cores polyallyl- and polyferrocenyl dendrimers and dendrons. The orange pyridine-substituted clusters, whose pyridine protons are deshielded in ^1H NMR (a practical tool for characterization), are air and thermally stable with simple pyridines, light and air sensitive with organometallic pyridines, air and thermally fragile with large dendronized pyridines.

Keywords: cluster, dendrimer, star, iron, ruthenium, molybdenum, pyridine, olefin, redox, assembly

Introduction

Octahedral clusters have been shown by Zheng' s group[1] with hexarhenium selenides to serve as versatile building blocks for the synthesis of various architectures including dendrimers,[1b,2] and coordination networks with structures constructed from hexatungsten sulfides have been disclosed by the DiSalvo group.[3] Other groups have utilized metal clusters for the design of extended molecular arrays,[4] but the two above successful examples illustrate the potential of octahedral hexametallic clusters to be used as starting points for the synthesis of molecular assemblies and nano-sized materials with catalytic and unusual physical properties.[5] Among these clusters based on early transition elements, the hexamolybdenum series built up from $[Mo_6X_{14}]^{2-}$ units (X = Cl, Br, I) constitute relevant starting materials easily available from inorganic solids that have been characterized 60 years ago.[6] The octahedral molybdenum clusters became most popular when the superconducting properties of the related chalcogenides $M_xMo_6Y_8$ (Y = chalcogen), known as Chevrel phases, were discovered.[7] Photophysical and redox properties of $[Mo_6X_{14}]^{2-}$ added further interest.[8] Among the 14 halide ligands, the 8 face-capping ones are relatively unreactive, which makes resistant cluster cores $[Mo_6X_8]^{4+}$. In the case of $[Mo_6Cl_{14}]^{2-}$ units, the inner chloride ligands can be replaced by chalcogen ligands, a soft route to Chevrel phases. The substitution of the 6 semi-labile apical ligands in $[Mo_6X_{14}]^{2-}$ can be achieved easily and leads to various $[Mo_6Y_8L_6]$ clusters,[9] which has been examined for a long time.[10] In particular, the hexa-methoxyclusters $[Mo_6Br_8(OMe)_6]^{2-}$, reported by Nanelli and Block[11] and the hexatriflate clusters $[Mo_6Br_8(OSO_2CF_3)_6]^{2-}$, reported by Shriver and *al.*[4c,12] are the most useful starting materials for further substitution.

We have investigated mono- and hexapyridine complexes of the $[Mo_6Br_8]^{4+}$ and $[Mo_6I_8]^{4+}$ cores by simple substitution of the triflate ligands in Shriver's complex $[Mo_6Br_8(OSO_2CF_3)_6]^{2-}$ and its homologue $[Mo_6I_8(OSO_2CF_3)_6]^{2-}$, in order to further assemble functional mono- and hexapyridine Mo_6 complexes into dendritic and nanoscopic structures. The synthetic findings are reported here. Although hexapyridine hexametallic clusters are known with $[Re_6Se_8]^{2+}$,[1,13] W_6S_8[14] and Mo_6S_8[9b] cluster series, there is no report with the $[Mo_6X_8]^{4+}$ core. Some 4, 4'-bipyridine complexes have been reported by Shriver's group in the chloro series, however.[15a] Our investigation is extended to pyridines substituted by transition metal groups and to dendronic pyridines including ferrocenyl dendronic pyridines. Metal-cluster-cored dendrimers have already been reported by Gorman[5f,16a] with the biomimetic Fe_4S_4 core and by Zheng[1,13] with the $Re_6L_8^{2+}$ cores (L = S, Se).

Results and Discussion

A. Cluster Hexasubstitution

The hexatriflate clusters. Shriver-type hexatriflate clusters $[M]_2[Mo_6X_8(CF_3SO_3)_6]$ **1-4** serve as starting points. They are prepared by reactions of the clusters $Mo_6X_{14}M_2$ and silver triflate, a reaction that is carried out in THF at 45°C for 24 hours in the case of $[M]_2[Mo_6Br_8(CF_3SO_3)_6]$ (M = *n*-Bu_4N or Cs). Starting from the clusters $[M]_2Mo_6I_{14}$ (M = *n*-Bu_4N or Cs) that are insoluble in THF, the clusters $[M]_2[Mo_6I_8(CF_3SO_3)_6]$, **2** (M = *n*-$Bu_4N$) and **4** (M = Cs) are synthesized according to the substitution reaction that is carried out in acetone at 45°C for 24 hours (and the resulting clusters **2** and **4** are THF soluble). The clusters **1-4** are purified by simple filtration of the reaction mixture on celite under an inert atmosphere in order to remove AgX, and the yields are virtually quantitative (equation 1)

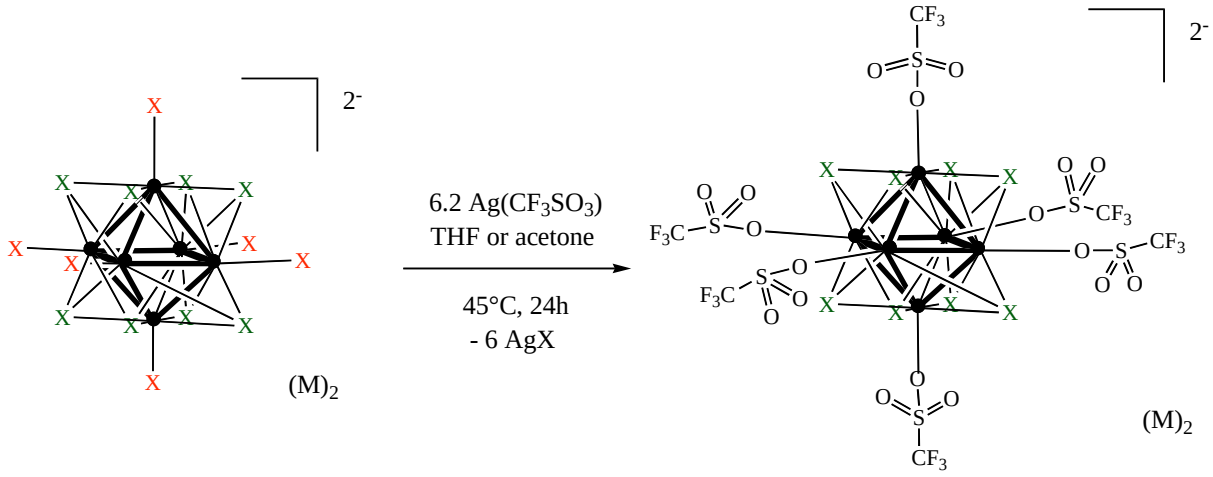

1: M = *n*-Bu_4N^+ and X = Br
2: M = *n*-Bu_4N^+ and X = I
3: M = Cs^+ and X = Br
4: M = Cs^+ and X = I

Equation 1

Clusters 5-10 hexasubstituted with simple pyridines. The substitution reaction of the six triflate ligands with six pyridine ligands in the complexes **1-4** is completed in two days at 60°C in pyridine/THF (equation 2). The reaction is followed by ^1H NMR by comparison of the intensities of the pyridine protons with those of the tetrabutylammonium counter cation. In the pyridine-substituted clusters, the pyridine protons are all deshielded compared to free pyridine. For example, this deshielding effect is most marked for the *ortho* pyridine protons moving from 8.41 ppm *vs.* TMS in $CDCl_3$ in free pyridine to 8.71 ppm in **5**. From the yellow starting cluster **1**, the new orange complex **5** precipitates from the reaction medium. The triflate salt [*n*-Bu_4N][CF_3SO_3] is thus readily separated

as it is soluble in THF, and the orange solid product **5** is washed with THF. It is sparingly soluble in dichloromethane and chloroform. It is insoluble in pyridine, ether, THF and alkanes, and it decomposes in methanol, and water. The cluster **5** is air-stable even in acetone and in the presence of light. The same remarks apply to the synthesis of the cluster **6**. The *ortho* pyridine protons are shifted in ^{1}H NMR from 8.41 ppm *vs.* TMS in $CDCl_3$ for free pyridine to 8.70 ppm for **6**, and the solubility properties are the same for **5** and **6**. The isolated reactions yields are 79 % for **5** and 76 % for **6** (equation 2). The reactivity and yields are seemingly not influenced by the nature of the counter cation, Cs^+ or *n*-Bu_4N^+, but the reaction cannot be followed by ^{1}H NMR with the cesium salt (the relative intensities of the coordinated and free pyridine signals can be compared, however).

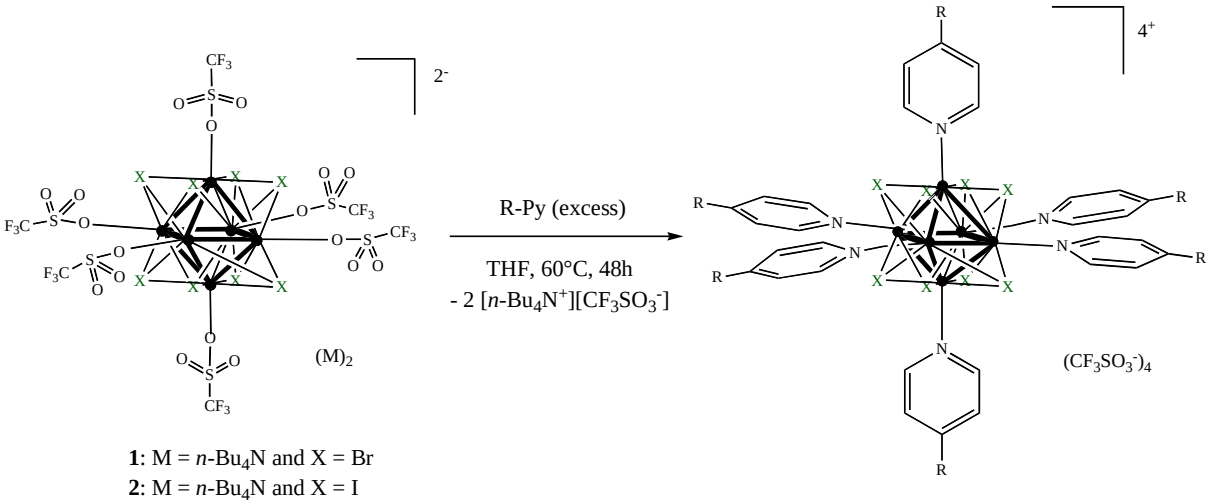

1: M = *n*-Bu_4N and X = Br
2: M = *n*-Bu_4N and X = I
3: M = Cs and X = Br
4: M = Cs and X = I

5: X = Br and R = H
6: X = I and R = H
7: X = Br and R = 4-*tert*-Bu
8: X = Br and R = 4-vinyl
9: X = I and R = 4-*tert*-Bu
10: X = I and R = 4-vinyl

Equation 2

Ligand substitution reactions of **1-4** with *para*-substituted pyridines were carried out in THF at 60°C using about hundred fold excess of *para*-substituted pyridine, i.e. in pyridine/THF solvents, and the reactions lasted two days (equation 2). Reactions were monitored analogously by comparing the intensity of the tetrabutylammonium ^{1}H NMR peaks with those of the *ortho* protons of the pyridine ligands. No precipitate formed, the orange solution remaining homogeneous at the end of the reaction with the 4-*tert*butylpyridine. The separation of [*n*-Bu_4N][CF_3SO_3] from the new clusters **7** and **9** is tedious, because these clusters are now much more soluble in a variety of solvents such as pyridine and THF. It proceeds by successive precipitation from acetone by controlled addition of pentane, and is checked by ^{1}H NMR. Several such re-precipitations are required in order to remove the salt. Thus finally, removal of this salt is only complete with the approximation of the ^{1}H NMR accuracy that does not overtake 98%. Elemental analyses show carbon contents that are often low, presumably due

to the presence of this and/or other extra salts in analyzed samples. Again, the orange cluster compounds obtained are air and light stable even in solution for at least several hours. They are unstable in water. For **8** and **10**, a precipitate forms in the course of the reaction. Simple washing with pentane and THF then purifies the clusters. The yields are analogous whatever the halide ligands in the cluster, the nature of the counter cation seemingly does not influence the reactions, and the color slightly varies from orange for the bromo clusters to dark orange for the iodo clusters.

Clusters 13 and 14 hexasubstituted by organometallic pyridines. We synthesized the known rigid organo-ruthenium pyridine ligand **11**[17] by a new route involving the reaction of commercial 4-ethynylpyridine hydrochloride with $[RuCp(PPh_3)_2Cl]$ in the presence of triethylamine and $[NH_4][PF_6]$ in methanol. This general procedure was reported for the synthesis of the complexes $[RuCp(PPh_3)_2(\eta^1\text{-alcynyl})]$ with (Cp = η^5-C_5H_5).[18,19] The yellow complex **11** was characterized by standard spectroscopic techniques including ^{31}P NMR, infrared spectroscopy (ν_{CC} = 2070 cm^{-1}) and the MALDI TOF mass spectrum with the dominant molecular peak at 794 Dalton. The reaction of **11** with the cluster $[Mo_6Br_8(CF_3SO_3)_6][n\text{-}Bu_4N]_2$, **1**, was carried out in refluxing THF for a week (Equation 3).

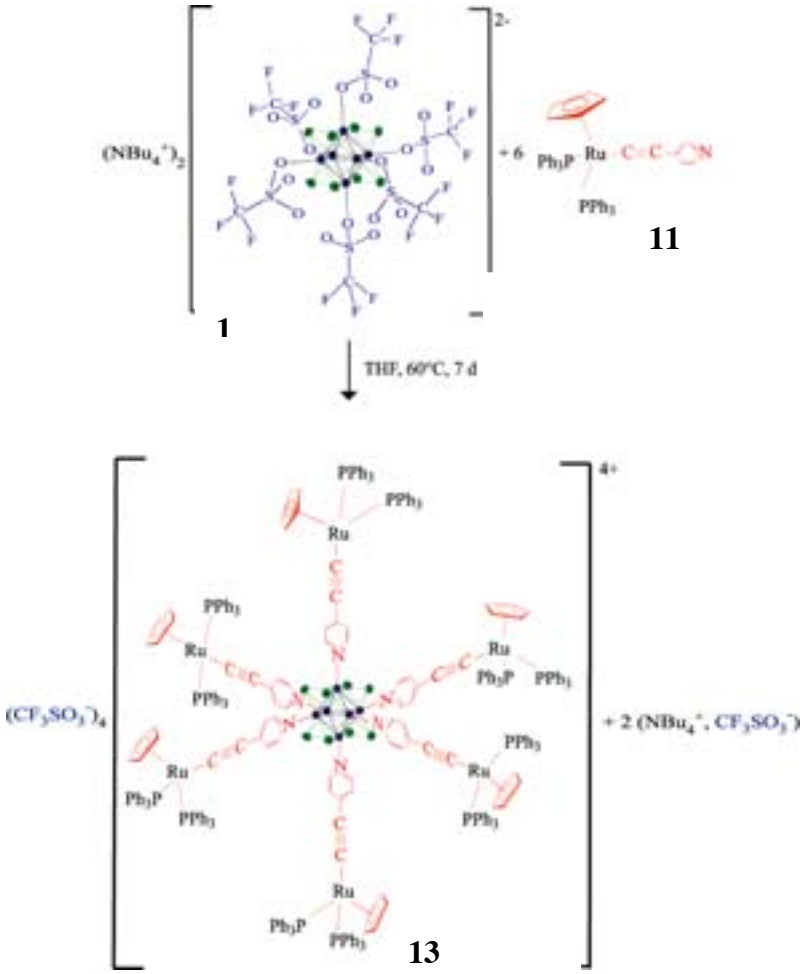

Equation 3

The new hexa-ruthenium hexa-molybdenum cluster **13** was recovered by slow precipitation using pentane. A single peak was found in the ^{31}P NMR spectrum, a single Cp peak was observed in the ^{1}H NMR spectrum at δ = 4.42 ppm, and a single infrared absorption was obtained at ν_{CC} = 2018 cm^{-1}. This behavior is in accord with the coordination of the cluster by the six organo-ruthenium pyridine ligands and the absence of free pyridine ligand in the sample.

In a similar approach, the red complex 1-ferrocenyl-2-(4-pyridinyl)acetylene **12**, was synthesized using the reaction of the Vargas'group.[20] The reaction of the ferrocenyl-containing pyridinyl ligand **12** with the cluster **1** was carried out in refluxing THF for a week to give the new hexasubstituted hexaferrocenyl Mo_6 cluster **14** (Equation 4). The red compound **14** was isolated by precipitation from a THF solution by slow addition of pentane and characterized *inter alia* by an infrared alcynyl absorption at 2181 cm^{-1}, ferrocene signals including a single Cp signal for the free Cp rings in the ^{1}H and ^{13}C NMR spectra. This complex **14** is very light and air sensitive. Its cyclic voltammogram (CV) in CH_2Cl_2 shows two close reversible ferrocenyl waves at $E_{1/2}$ = 0.800 V vs. [$FeCp^*_2$] with a less intense shoulder at $E_{1/2}$ = 0.710 V vs. [$FeCp^*_2$]; these values compare with the value obtained for the starting monomeric complex **12**, $E_{1/2}$ = 0.720 V vs. [$FeCp^*_2$].

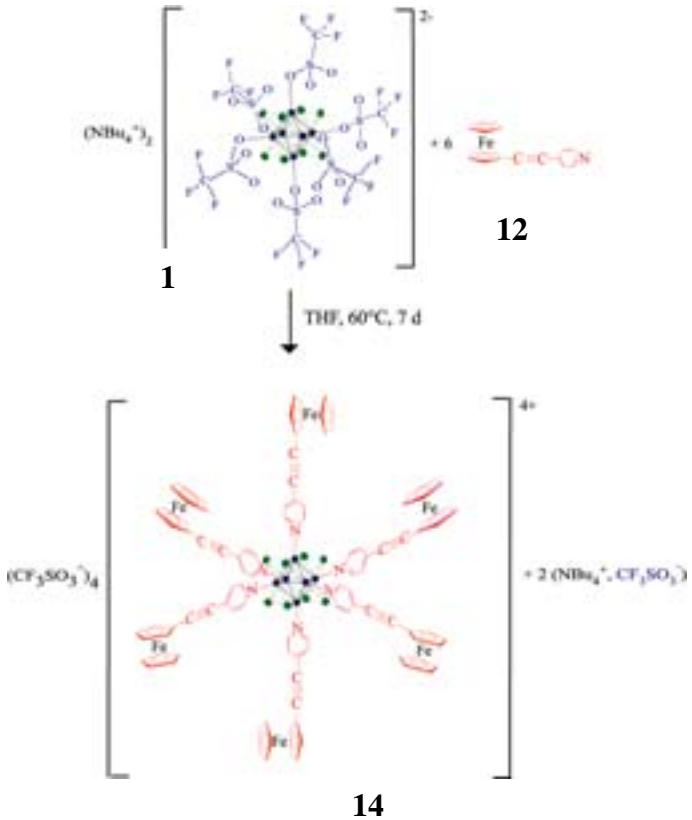

Equation 4

Cluster-cored dendrimers 17 and 18: hexasubstitution by dendronic pyridines. The dendronic pyridine 3,3'-py{CH_2O*p*-$C_6H_4C(CH_2CH{=}CH_2)_3$}$_2$, **15**, is synthesized by reaction of 3,3'-py$(CH_2Br)_2$[22] with the phenol dendron HO*p*-$C_6H_4C(CH_2CH{=}CH_2)_3$.[23] Reaction of **15** with **1** was

carried out for six days in refluxing THF using 6.2 equiv. dendron **15** to give the orange cluster **17** (equation 5). The ^{1}H NMR spectra show that the reaction is completed from the relative intensity ratio between the ammonium protons and the coordinated pyridine protons. Indeed, the *para*-pyridine proton is deshielded from 7.95 ppm in free pyridine to 8.66 ppm in the coordinated pyridine dendron. The solution is orange at the end of the reaction, and the reaction time is seemingly not longer than with the other pyridines, as monitored by ^{1}H NMR. After numerous reprecipitations in order to remove the salts, ^{1}H NMR spectrum shows that the ammonium salt is no longer present, and the carbon content in the elemental analysis of the cluster-cored dendrimer **17** is acceptable. The orange compound **17** is soluble in dichloromethane, and air- and light stable in this solvent; however, it is insoluble in pentane. After one day in chloroform solution under an inert atmosphere, the solution is still orange, but some decomposition to an insoluble film is observed. Although the conversion is complete as monitored by ^{1}H NMR, the yield is eventually mediocre due to the repeated precipitations (equation 5). Olefin metathesis reactions were attempted at 45°C in dichloromethane with Grubbs' second generation commercial catalyst [$RuCl_2$(=CHPh)(NHC)] (N = bis-mesityl N-heterocyclic carbene) with **17**, but all attempts failed presumably because of partial pyridine decoordination and subsequent coordination to the ruthenium of the catalyst, which inhibits metathesis activity.

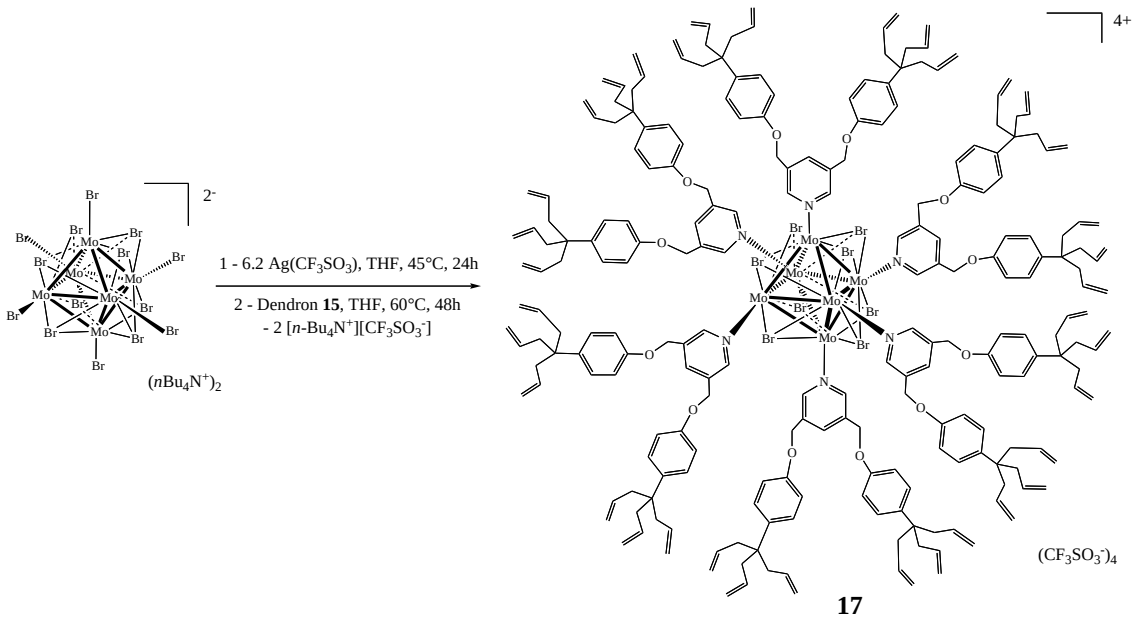

17

Equation 5

The dendronic pyridine 3,3'-{CH_2O*p*-$C_6H_4C(CH_2CH_2CH_2SiMe_2C_5H_5FeCp)_3\}_2$Py **16** is synthesized by reaction of the phenol dendron HO*p*-$C_6H_4C(CH_2CH_2CH_2SiMe_2C_5H_5FeCp)_3$ with 3,3'-py$(CH_2Br)_2$ (equation 6).

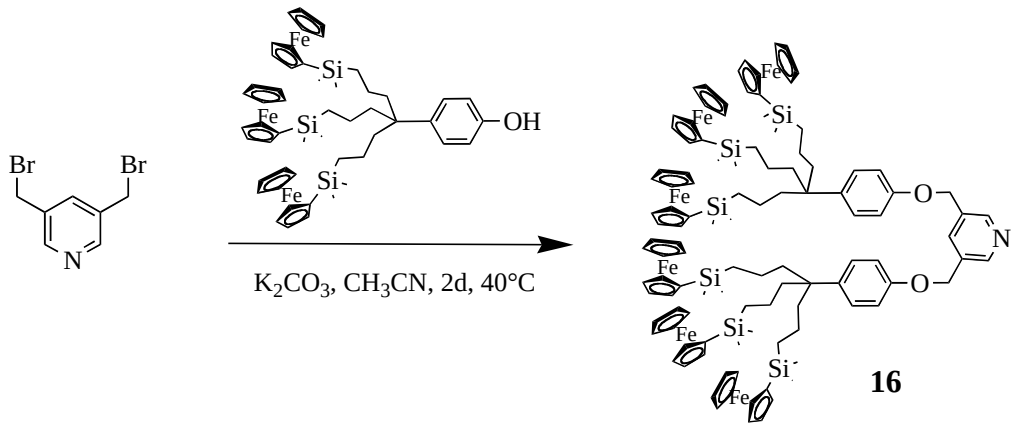

Equation 6

Reaction of **16** with **1** was carried out for six days in refluxing THF using 6.2 equiv. of dendron **16** to give the orange cluster **18** (equation 7). ^{1}H NMR shows that the reaction is completed from the relative intensity ratio between the ammonium protons and the coordinated pyridine protons. Indeed, the *para*-pyridine proton is deshielded from 7.91 ppm in free pyridine to 8.50 ppm in the coordinated pyridine dendron. The final solution is orange. After numerous reprecipitations in order to remove the salts, ^{1}H NMR shows that the ammonium salt is no longer present and the carbon content in the elemental analysis of the cluster-cored dendrimer **18** is acceptable. The orange cluster compound **18**, insoluble in pentane, is soluble in dichloromethane, but it is neither air- nor light stable. Although the conversion is complete as monitored by ^{1}H NMR, the yield is eventually mediocre due to the repeated precipitations required to purify this cluster-cored dendrimer **18**. The thermal stability of **18** is weak as it decomposes over periods of several days at room temperature under an inert atmosphere.

The CV of a freshly prepared sample of **18** in dichloromethane shows a single reversible wave indicating that the 36 ferrocenyl centers are seemingly identical and sufficiently remote from one another to render the electrostatic factor negligible. No adsorption was noted under these conditions, allowing the determination of the number of redox active units by comparison of the current intensity of the cluster wave with that of an internal reference such as decamethylferrocene. The Bard-Anson equation, involving these intensities and the respective molecular weights of the compound and reference,[24] provides a number of ferrocenyl redox centers equal to 37 ± 3 showing a good agreement with the theoretical number of 36.[25]

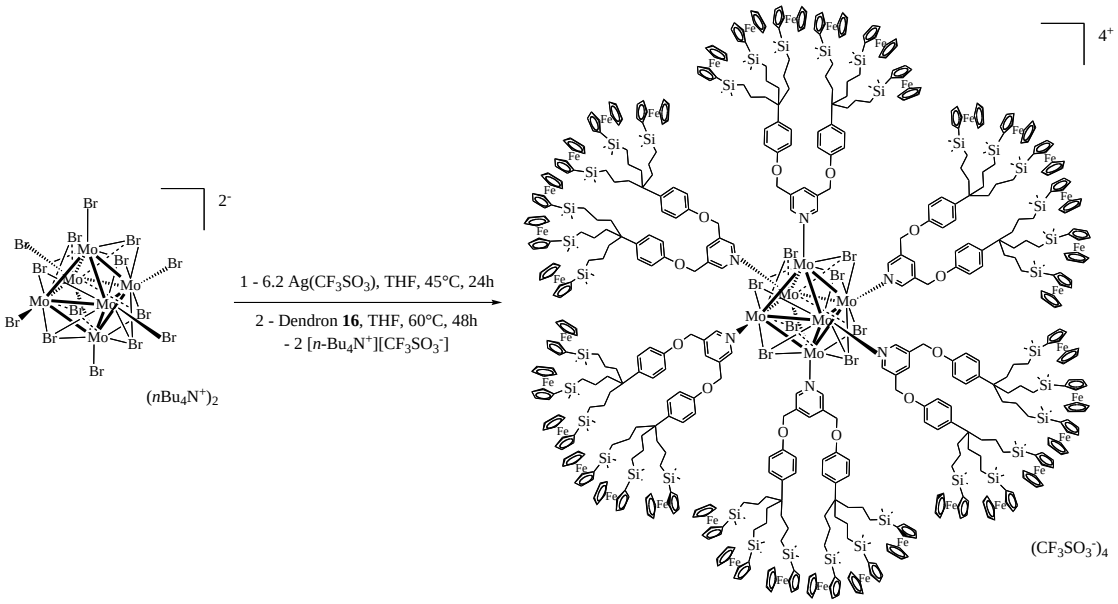

18

Equation 7

B. Cluster Monosubstitution

Clusters monosubstituted by simple pyridines. Given the progressive substitution of the apical halide ligands in the hexamolybdenum clusters, we investigated the possibility of also synthesizing monosubstituted pyridine clusters in order to eventually introduce a single functional group to derivatize the cluster. In a systematic study of the hexarhenium sulfide clusters, Holmes' group could optimize the synthesis of all the possible substituted clusters.[21] The present hexamolydenum clusters are far from being as air stable as hexarhenium clusters, therefore this strategy is much more limited here. In particular, for this reason, chromatographic separation cannot be envisaged. The monosubstitution reaction of a bromide by a triflate is best performed for 24 hours at 45°C (equation 8). Silver triflate is slowly introduced into the reaction medium in order to favor monosubstitution whose yield is virtually quantitative. The monosubstituted triflate cluster **19** is a THF soluble yellow solid serving as an intermediate for further introduction of a pyridine-type ligand. We have not investigated the compared rate of mono- and second substitution, although the yields of monopyridine substituted products indicates that the second substitution does not occur more rapidly than the first one.

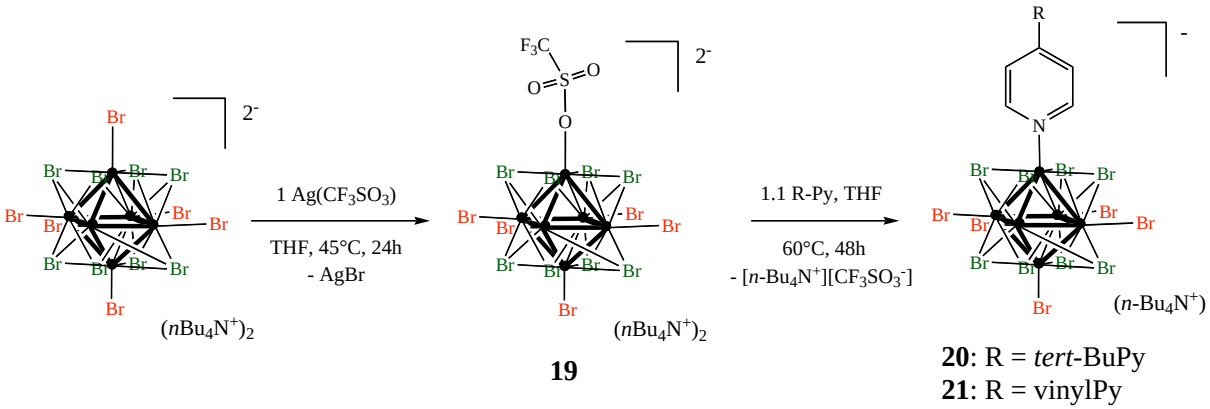

Equation 8

The substitution of the triflate ligand by a pyridine derivative is complete in two days at 60°C in THF (equations 8 and 10). This type of reaction is monitored by ^{1}H NMR by comparing the intensities of the signals of the coordinated pyridine with those of the counter cation *n*-Bu_4N^+. Here again, the signals of the pyridine protons are shifted upon coordination to the cluster. The monosubstituted clusters **20** and **21** are orange, and they are much less soluble in common solvents than the hexasubstituted analogues. They precipitate during the reaction, thus purification is simple by washing the precipitate with pentane, then with THF, followed by filtration on celite, and ^{1}H NMR analysis is carried out in acetone d^6. The yields are modest (48 % for **20** and 37 % for **21**), which indicates that disubstitution also simultaneously occurs because of near-statistical substitution. The disubstituted products are neutral, thus probably well THF soluble, but were not investigated. The unsubstituted triflate–cluster complex being also THF soluble, the monopyridine clusters are the only THF-insoluble products among these three compounds (non-, mono- and disubstituted). Olefin metathesis experiments were carried out with **21** as with **17**, but they were not successful, presumably for the same reason involving some partial decoordination of the substituted pyridine from the cluster and inhibition of the ruthenium catalyst.

Ferrocenyl dendronized cluster 26 monosubstituted by a 12-ferrocenyl pyridine dendron 25. The reaction of one equiv. of **19** with one equiv. of monopyridine dendron **25** bearing 12 ferrocenyl groups at the periphery (scheme 1) is also carried out in THF at 60°C for two days and yields the thermally sensitive pentane soluble orange compound **26** (equation 9).

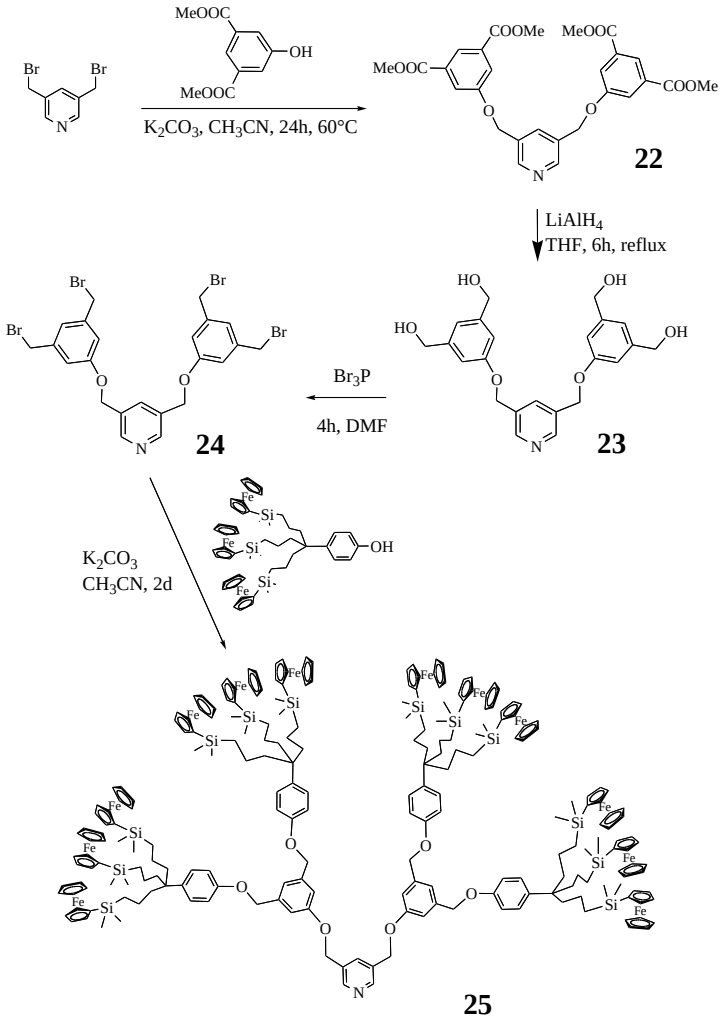

Scheme 1

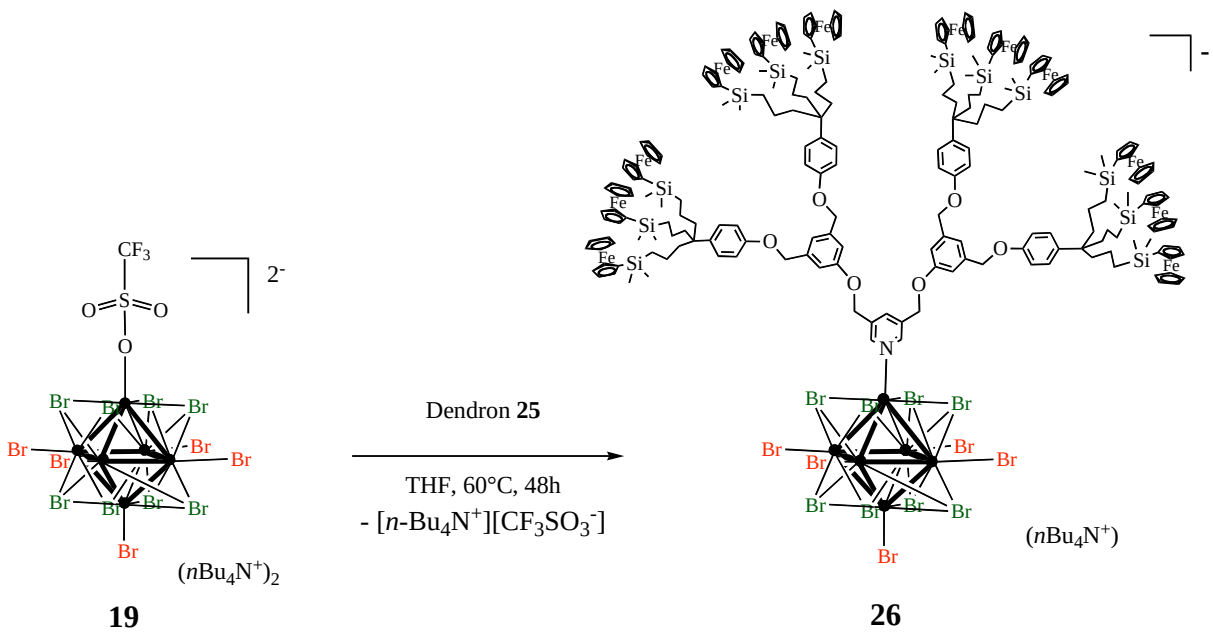

Equation 9

The *para*-pyridine protons of **26** are found at 8.22 ppm vs. TMS in $CDCl_3$ (compare free pyridine are at 7.90 ppm). The solubility of **26** in pentane precludes purification from other pentane soluble impurities such as the free ligand and, in addition, **26** is not thermally stable at room temperature over a few hours. Thus, its synthesis must be carried out in the presence of only one equiv. of dendronic pyridine ligand whose coordination can be monitored by ^1H NMR using the signals of the pyridine protons, and indeed coordination is completed. It is possible, however, that some disubstituted compound is present in the reaction mixture.

The cyclic voltammogram of a freshly prepared sample of **26** shows a single ferrocenyl wave for the 12 ferrocenyl groups, and application of the Bard-Anson equation[21] leads to a number of redox center equal to 14±2. The error on this measurement is somewhat larger than in the case of the cluster-cored ferrocenyl dendrimer **18** presumably because of the purity of the sample that is lower for **26** than for **18**. A modified Pt electrode is prepared with **18** by scanning about 100 times around the ferrocenyl redox potential region, which produced an electrode giving the CV shown in figure 1 in which the 0V difference between E_{pa} and E_{pc} values confirms correct electrode modification. The modified electrode can also recognize the n-Bu_4N^+ salt of ATP^{2-}, and when this salt is added to the electrochemical cell containing the modified electrode, a new reversible wave appear at 90 mV less positive potential.[22]

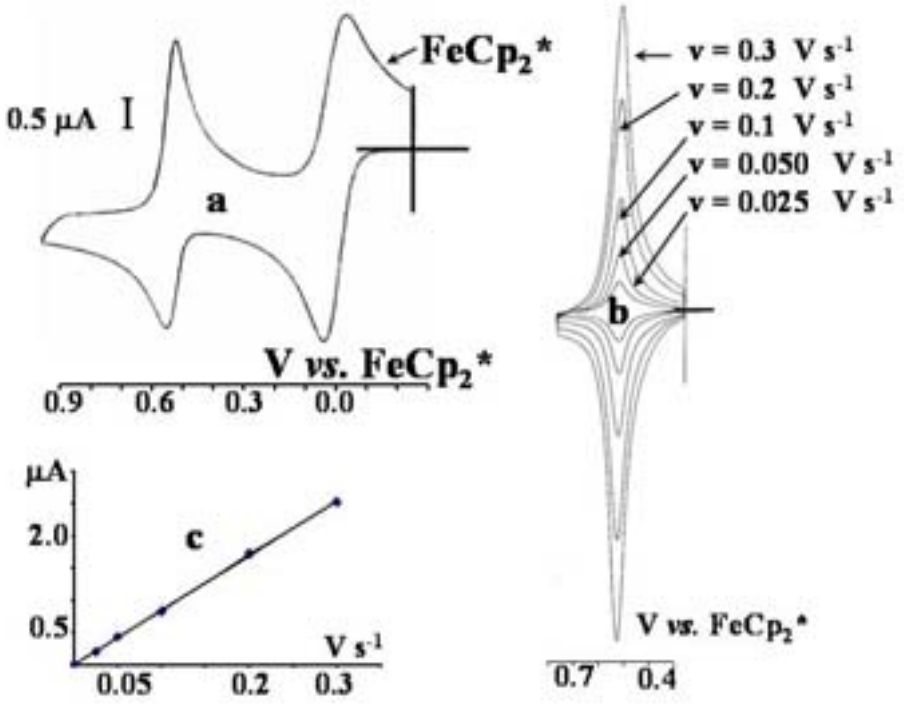

Figure 1. Cyclic voltammograms of the cluster-cored dendron **26**. Solvent, CH_2Cl_2; reference electrode, Ag/Ag^+; working electrode; counter electrode Pt; supporting electrolyte, 0.1 M nBu_4NPF_6; internal reference $FeCp_2$*. **a**) **26** in solution; **b**) **26** coated over a Pt electrode at various scan rates. $E_{1/2}$ = 0.53 V *vs*. $FeCp_2$*. **c**) Inset by **26**, intensity as a function of scan rate; the linearity shows the expected behavior of the modified electrode with full adsorbsion of **26.** The surface coverage by **26** was determined from the integrated charge of the CV wave. Thus, the surface coverage for the electrode modified with **26** was $\Gamma = 1.3 \times 10^{-10}$ mol cm^{-2} (iron sites), corresponding to 1.8×10^{-11} mol cm^{-2} of **26**. The difference between the anodic and cathodic potentials is $\Delta E = E_c - E_a = 0.0$ V, and full width at half-maximum (ΔE_{FWHM}) is 0.90 V.

Concluding Remarks

- An easy route to a family of new mono- and hexa-pyridine octahedral hexamolybdenum hexapyridine clusters $[Mo_6X_8(4\text{-Py-R})_6][CF_3SO_3]_4$ has been disclosed starting from the precursor complex $[M]_2[Mo_6X_{14}]$ via the triflate intermediates. The homogeneity of the reaction mixture allows monitoring their formation by ^1H NMR by comparison of the relative intensities of the tetrabutylammonium signals and those of the pyridine protons that become deshielded upon pyridine coordination. The use of substituted pyridine largely increases the solubility of the new clusters, which renders the separation of the Mo_6 cluster from the salt $[n\text{-}Bu_4N][OSO_2CF_3]$ difficult with the tetrabutylammonium salt used at the beginning of the synthesis. This separation can be achieved by successive reprecipitations, however.
- Organometallic pyridines could be grafted onto the six apical positions of the cluster, yielding light and air sensitive clusters surrounded by organometallics fragments.
- Cluster-cored dendrimers could be prepared including ferrocenyl dendrimers, and the number of redox-active units has been successfully determined therein using the Bard-Anson equation in cyclic voltammetry. The pyridine-substituted clusters with small pyridine substituents are thermally stable, but the cluster-cored polyferrocenyl dendrimers have a limited thermal stability, probably because the large sizes of the dendrons destabilize the cluster-pyridine bond.

Experimental Section

General data

Reagent-grade tetrahydrofuran (THF) and pentane were predried over Na foil and distilled from sodium benzophenone anion under argon immediately prior to use. Other commercial chemicals were purchased from Aldrich and used as received. All manipulations were carried out using Schlenk flasks, and samples were transferred in a nitrogen-filled Vacuum atmosphere drylab. ^1H NMR spectra were recorded at 25°C with a Bruker AC 300 (300 MHz) spectrometer. ^{13}C NMR spectra were obtained in the pulsed FT mode at 75 MHz with a Bruker AC 300 spectrometer. All chemical shifts are reported in parts per million (δ, ppm) with reference to Me_4Si (TMS). Elemental analyses were carried out at the Vernaison CNRS center. The infrared spectra were recorded in KBr pellets on a FT-IR Paragon 1000 Perkin Elmer spectrometer.

MALDI-TOF Mass Spectrometry: The MALDI mass spectra were recorded with a PerSeptive Biosystems Voyager Elite (Framingham, MA) time-of-flight mass spectrometer. This instrument is equipped with a nitrogen laser (337 nm), a delayed extraction, and a reflector. It was operated at an

accelerating potential of 20 kV in both linear and reflection modes. The mass spectra shown represent an average over 256 consecutive laser shots (3 Hz repetition rate). Peptides were used to calibrate the mass scale using the two points calibration software 3.07.1 from PerSeptive Biosystems. Mentioned *m*/*z* values correspond to monoisotopic masses. The solutions (10^{-3} M) were prepared in tetrahydrofuran (THF). Matrix compounds were from Sigma (France) and used without further purification. The matrices, 2,5-dihydroxybenzoic acid (2.5-DHB), 1,8-dihydroxy-9[10*H*]-anthracenone (dithranol), 6-azathiothymine, 2,4,6-trihydroxyacetophenon, 7-hydroxycoumarin, or 2-anthramine, were also dissolved in THF (10 g L^{-1}). One micro liter of solution was mixed with 50 μL of matrix solution. Ten micro liters of alkali iodide (LiI, NaI) solution (5 g L^{-1} in THF) were added in some experiments to induce cationization. One micro liter of the final solution was deposited onto the sample stage and allowed to dry in air.

Cyclic-voltammetry data were recorded with a PAR 273 potentiostat galvanostat. The reference electrode was an Ag quasi-reference electrode (QRE). The QRE potential was calibrated by adding the reference couple $[FeCp_2^*]^+/[FeCp_2^*]$ (Cp* = pentamethylcyclopentadienyl). The working electrode (platinum) was treated by immersion in 0.1 M HNO_3, and then polished before use and between each recording when necessary. The cluster $[n\text{-}Bu_4N]_2[Mo_6Br_8(CF_3SO_3)_6]$ is irreversibly oxidized at +1.5 V vs. $Cp^*_2Fe^{+/0}$ in CH_3CN whereas the hexa-*t*-butylpyridine cluster **7** is irreversibly reduced at -0.7 V vs. $Cp^*_2Fe^{+/0}$ in DMF (both measurements were carried out at 25°C, 0.2 V. s^{-1} with 0.1 M $n\text{-}Bu_4NPF_6$).

The syntheses and characterizations of the starting halogen cluster compounds $M_2Mo_6X_{14}$ have been performed according to the procedure described in reference 6e, and the synthesis of the triflate cluster compounds is reported in Shriver's publication.[12]

Cluster $Mo_6Br_8Py_6Tf_4$, 5

A yellow THF solution of **1** (0.585 g, 0.231 mmol) and pyridine (1.8 mL, 0.023 mol) was stirred at 60ºC for 2 days. The reaction product progressively precipitated from the reaction mixture as a very fine powder. The solvent was removed under vacuum to give an orange solid that was washed with pentane and THF and dried under vacuum to yield complex **5** as an orange solid. Yield: 0.416 g of **5** (79 %). ^{1}H NMR ($CDCl_3$, 300 MHz), δ_{ppm}: 8.71 (d, 12H), 8.13 (m, 6H), 7.68 (m, 12H). ^{13}C NMR ($CDCl_3$, 75.47 MHz), δ_{ppm}: 147.7 (C_o), 141.5 (C_p), 126.3 (C_m). Elemental analysis calcd for $C_{34}H_{30}Br_8F_{12}Mo_6N_6O_{12}S_4$ (%): C 17.87, H 1.32; found (%): C 17.21, H 1.09. M = 2285.76 g.mol^{-1}.

Cluster $Mo_6I_8Py_6Tf_4$, 6

A yellow THF solution of **2** (0.686 g, 0.231 mmol) and pyridine (1.8 mL, 0.023 mol) was stirred at 60ºC for 2 days. The reaction product progressively precipitated from the reaction mixture as a very fine powder. The solvent was removed under vacuum to give an orange solid that was washed with pentane and THF and dried under vacuum to yield complex **6** as an orange solid. Yield: 0.467 g of **6** (76 %). ^{1}H NMR ($CDCl_3$, 300 MHz), δ_{ppm}: 8.70 (d, 12H), 7.81 (m, 6H), 7.42 (m, 12H). ^{13}C

NMR (CD_3COCD_3, 75.47 MHz), δ_{ppm}: 147.9 (C_o), 143.2 (C_p), 128.6 (C_m). Elemental analysis calcd for $C_{34}H_{30}F_{12}I_8Mo_6N_6O_{12}S_4$ (%): C 15.34, H 1.14; found (%): C 14.69, H 0.86. M = 2661.77 g.mol^{-1}.

Cluster Mo_6Br_8(4-*tert*butylpyridine)$_6Tf_4$, 7

A THF solution of **1** (1 g, 0.394 mmol) and 4-*tert*butylpyridine (2 mL) was stirred at 60ºC for 2 days. The solvent was removed under vacuum, the product was precipitated with THF/pentane and dried under vacuum to yield complex **7** as an orange solid. Yield: 0.826 g (80 %). ^{1}H NMR ($CDCl_3$, 300 MHz), δ_{ppm}: 8.59 (d, 12H), 7.49 (d, 12H), 1.35 (s, 54H). ^{13}C NMR ($CDCl_3$, 75.47 MHz), δ_{ppm}: 147.4 (C_o), 122.1 (C_m), 34.5 ($\underline{C}Me_3$), 30.7 (CH_3). Elemental analysis calcd for $C_{58}H_{78}Br_8F_{12}Mo_6N_6O_{12}S_4$ (%): C 26.56, H 3.00; found (%): C 26.15, H 2.69. M = 2622.40 g.mol^{-1}.

Cluster Mo_6Br_8(4-vinylpyridine)$_6Tf_4$, 8

A THF solution of **1** (0.300 g, 0.141 mmol) and 4-vinylpyridine (1 mL) was stirred at 60ºC for 2 days. The solvent was removed under vacuum to give a solid residue that was washed with pentane and THF and dried under vacuum to yield complex **8** as an orange solid. Yield : 0.293 g (85 %). ^{1}H NMR ($CDCl_3$, 300 MHz), δ_{ppm}: 8.57 (d, 12H), 7.27 (d, 12H), 6.65 (q, 6H), 6.00 (d, 6H), 5.51 (d, 6H). ^{13}C NMR ($CDCl_3$, 75.47 MHz), δ_{ppm}: 150.5 (C_o), 135.1 ($\underline{C}H=CH_2$) 121.1 (C_m), 119.0 ($CH=\underline{C}H_2$). Elemental analysis calcd. for $C_{46}H_{48}Br_8F_{12}Mo_6N_6O_{12}S_4$ (%): C 22.57, H 1.98; found (%): C 22.09; H 1.61. M = 2448.04 g.mol^{-1}.

Cluster Mo_6I_8(4-*tert*butylpyridine)$_6Tf_4$, 9

A yellow THF solution of **2** (0.686 g, 0.231 mmol) and 4-*tert*butylpyridine (1.8 mL) was stirred at 60ºC for 2 days. The solvent was removed under vacuum, the product was precipitated with THF/pentane and dried under vacuum to yield complex **9** as an orange solid. Yield: 0.512 g of **9** (74 %). ^{1}H NMR ($CDCl_3$, 300 MHz), δ_{ppm}: 8.52 (d, 12H), 7.33 (m, 12H), 1.32 (m, 54H). ^{13}C NMR ($CDCl_3$, 75.47 MHz), δ_{ppm}: 147.4 (C_o), 122.1 (C_m), 34.5 ($\underline{C}Me_3$), 30.7 (CH_3). Elemental analysis calcd for $C_{58}H_{78}F_{12}I_8Mo_6N_6O_{12}S_4$ (%): C 23.23, H 2.62; found (%): C 22.52, H 2.01. M = 2998.41 g.mol^{-1}.

Cluster Mo_6I_8(4-vinylpyridine)$_6Tf_4$, 10

A yellow THF solution of **2** (0.686 g, 0.231 mmol) and 4-vinylpyridine (1.8 mL) was stirred at 60ºC for 2 days. The reaction product progressively precipitated from the reaction mixture as a very fine powder. The solvent was removed under vacuum to give an orange solid that was washed with pentane and THF and dried under vacuum to yield complex **10** as an orange solid. Yield: 0.528 g of **10** (81 %). ^{1}H NMR ($CDCl_3$, 300 MHz), δ_{ppm}: 8.41 (d, 12H), 7.28 (m, 12H), 6.42 (q, 6H), 5.83 (d, 6H), 5.52 (d, 6H). ^{13}C NMR ($CDCl_3$, 75.47 MHz), δ_{ppm}: 151.6 (C_o), 134.9 ($\underline{C}HCH_2$), 122.3 (C_m), 120.0 (CH_2). Elemental analysis calcd for $C_{46}H_{48}F_{12}I_8Mo_6N_6O_{12}S_4$ (%): C 19.56, H 1.71; found (%): C 19.37, H 1.52. M = 2824.04 g.mol^{-1}.

[RuCp(PPh$_3$)$_2$(CC-C$_5$H$_4$N)], 11

A methanol solution of 4-ethynylpyridine (0.296 g, 2.07 mmol) and triethylamine (5 mL) was added to a suspension of [RuCp(PPh$_3$)$_2$Cl] (1 g, 1.38 mmol) and NH_4PF_6 (0.449 g, 2.76 mmol) in methanol. The solution was stirred at room temperature for 3 days. The solvent was removed under vacuum, and the product was extracted with toluene. The product was precipitated with toluene/pentane. The yellow powder was dried under vacuum. Yield: 0.350 g of **11** (32%). ^{1}H NMR (MeOD, 300MHz), δ_{ppm}: 8.06 (d, NCH), 7.30 – 7.04 (m, PPh$_3$), 6.80 (d, NCCH), 4.29 (s, Cp). ^{31}P NMR (MeOD, 100 MHz), δ_{ppm}: 49.60 (PPh$_3$). Infrared: ν_{CC}= 2 070 cm^{-1}. MS (MALDI-TOF; m/z), calcd. for $C_{48}H_{39}NP_2Ru$: 792.85, found: 794.24. CV in CH_2Cl_2: $E_{1/2}$ = 0.700 V vs. Fc* at 20° C (partially chemically reversible: i_c/i_a = 0.5).

Hexa-substituted Mo$_6$Ru$_6$ cluster, 13

A THF solution of **11** (0.131 g, 0.165 mmol) and **1** (0.069 g, 0.0265 mmol) was stirred at 60ºC for 7 days. The solvent was removed under vacuum, and the product was precipitated with THF/pentane. The red powder was dried under vacuum. Yield : 0.115 g of **13** (65%). Analysis calcd. for $Mo_6Br_8C_{292}H_{234}F_{12}S_4O_{12}N_6P_{12}Ru_6$ (%): C 53.39, H 3.39, found: C 52.59, H: 2.97.

^{1}H NMR (MeOD, 300MHz), δ_{ppm}: 8.12 (d, NCH), 7.23 – 7.08 (m, PPh$_3$), 7.04 (d, NCCH), 4.42 (s, Cp). ^{31}P NMR (MeOD, 100 MHz), δ_{ppm}: 49.51(PPh$_3$). Infrared: ν_{CC} = 2 018 cm^{-1}. CV in CH_2Cl_2: $E_{1/2}$ = 0.650 V vs. Fc* at 20° C in CH_2Cl_2 (partially chemically reversible i_c/i_a = 0.1).

Hexa-ferrocenyl Mo$_6$Fc$_6$ cluster, 14

A THF solution of 1-ferrocenyl-2-(4-pyridinyl) acetylene **12** (0.054 g, 0.187 mmol) and **1** (0.063 g, 0.029 mmol) was stirred at 60ºC for 7 days. The solvent was removed under vacuum and the product was precipitated with THF/pentane. The red powder was dried under vacuum. Yield: 0.073 g of **14** (63%). ^{1}H NMR ($CDCl_3$, 300MHz), δ_{ppm}: 8.64 (d, NCH), 7.51 (d, NCCH), 4.62 and 4.41 (t, FeCH), 4.32 (s, Cp). ^{13}C NMR ($CDCl_3$, 63 MHz), δ_{ppm}: 69.9 (FeC), 70.2 (Cp), 72.0 (FeC), 76.95 (C), 125.9 (NC<u>C</u>), 147.5 (NC). Infrared: ν_{CC} = 2 181 cm^{-1}. Elemental analysis calcd (%): C 36.03, H 2.22; found (%): C 35.29, H 1.59. CV in CH_2Cl_2 at 20°C: $E_{1/2}$ = 0.800 V vs. [FeCp*$_2$] in CH_2Cl_2.

Dendronic pyridine derivative, 15

In a Schlenk tube, 3,5-bis(bromomethyl)pyridine (0,17 mmol),[23] *p*.triallylmethylphenol (1.13 mmol) and K_2CO_3 (2.26 mmol) were stirred for two days in acetonitrile. Then, the solvent was removed under vacuum, and the reaction product was extracted using diethyl ether and filtered on celite. The solvent was evaporated to dryness and the product **15** was chromatographed on silica gel (eluent: diethyl ether/petroleum ether 1/1). Yield: 70 %. ^{1}H NMR (250 MHz, $CDCl_3$): δ_{ppm} = 8.71 (s, 2H, *o*-H pyridine), 7.95 (s, 1H, *p*-H pyridine), 7.33 and 6.97 (d, 4H, H aromatic), 5.61 (m, 6H, CH allyl), 5.11 (m, 12H, CH_2 allyl), 5,03 (s, 4H, CH_2O), 2.48 (d,12H, Cq-*C*H_2-CH). ^{13}C NMR (63 MHz, $CDCl_3$): δ_{ppm} = 156.2

(C_q Ar-O), 148.5-138.5 (CH pyridine), 134.53 (CH allyl), 132.6 (C_q pyridine), 128.6-114.1 (CH Ar), 117.5 (CH_2 allyl), 67.3 (CH_2O), 44.7 (C_q Ar-C_q-CH_2), 41.8 (C_q-CH_2-CH). Elemental analysis calcd. for $C_{39}H_{45}NO_2$: C 83.68, H 8.10; found C 83.23, H 8.12. M = 559.79 g.mol^{-1}.

Dendronic pyridine derivative, 16

In a Schlenk tube, 3,5-bis(bromomethyl)pyridine (0.138 mmol), *p*.triferrocenylphenol[20] (0.415 mmol) and K_2CO_3 (0.83 mmol) were stirred for two days in acetonitrile at 40°C. Then, the solvent was removed under vacuum, and the reaction product was extracted using diethyl ether and filtered on celite. The solvent was evaporated to dryness, and the product was chromatographed on silica gel (eluent: diethyl ether/petroleum ether 1/1). Yield: 44 %. ^{1}H NMR (250 MHz, $CDCl_3$): δ ppm = 8.67 (s, 2H, o-H pyridine), 7.91 (s, 1H, p-H pyridine), 7.22 and 6.93 (d, 4H, H aromatic), 5,06 (s, 4H, CH_2O),4.30-4.08-4.01 (CH ferrocenyl), 1.59-1.17 (m, 12H, Cq-$\underline{CH_2}$-$\underline{CH_2}$-CH), 0.64(m, 6H, CH_2-Si), 0.16 (CH_3). ^{13}C NMR (63 MHz, $CDCl_3$): δ_{ppm} = 155.8 (Cq ar-O), 148.5-132.7 (CH pyridine), 140.8 (Cqar-Cq), 134.6 (Cq pyridine), 127.6-114.0 (CHar),72.9-70.5-68.0 (CH ferrocenyl), 71.3 (Cq ferrocenyl), 67.3 (CH_2O), 43.2(Cqar-$\underline{Cq}$-CH_2), 42.0 (Cq-$\underline{CH_2}$-CH_2), 18.0 (CH_2-$\underline{CH_2}$-CH_2), 17.5 (Si-$\underline{CH_2}$), -1.9 (CH_3). Elemental analysis calcd. (%): C 65.84, H 7.02; found (%): C 66.71, H 6.80.

Hexasubstituted cluster $[Mo_6Br_8(dendron)_6][CF_3SO_3]_4$, 17

A yellow THF solution of **1** (0.100 g, 0.038 mmol) and the pyridine dendron **15** (0.143 g, 0.255 mmol) was stirred at 60ºC for 7 days. The solvent was removed under vacuum, and the product was precipitated with THF/pentane. The orange powder was dried under vacuum. Yield: 0.097 g of **17** (49%). ^{1}H NMR ($CDCl_3$, 300 MHz), δ_{ppm}: 8.90 (s, 12H, H_o), 8.66 (s, 6H, H_p), 7.27 (d, 24H), 6.96 (d, 24H), 5.53 (m, 36H, $=CH_a$), 5.02 (m, 96H, $=CH_{2\ a}$ + OCH_2), 2.45 (d, 72H, CH_2). ^{13}C NMR ($CDCl_3$, 75.47 MHz), δ_{ppm}: 155.46 (C_o), 139.19 (C_m), 136.91 (C_p), 134.26 ($\underline{C}H=CH_2$), 127.96 (C_{ar}), 117.41 (CH=$\underline{C}H_2$), 114.20 (C_{ar}), 65.95 (O$\underline{C}H_2$), 42.84 (C_q), 41.85 (C_q-CH_2). Elemental analysis calcd. for $C_{238}H_{270}Br_8F_{12}Mo_6N_6O_{24}S_4$ (%): C 55.29, H 5.26; found (%): C 54.85, H 4.98. M = 5169.83 g.mol^{-1}.

Hexasubstituted cluster $[Mo_6Br_8(dendron)_6][CF_3SO_3]_4$, 18

A yellow THF solution of **1** (0.012 g, 0.0046 mmol) and 3,3'-{CH_2O*p*-$C_6H_4C(CH_2CH_2CH_2SiMe_2C_5H_5FeCp)_3\}_2$Py **12** (0.058 g, 0.0285 mmol) was stirred at 60ºC for 6 days. The solvent was removed under vacuum, and the product was precipitated with CH_2Cl_2/pentane to give an orange solid **18**. Yield 0.039 g of **18** (59 %).

^{1}H NMR ($CDCl_3$, 300 MHz), δ_{ppm}: 8.82 (m, 12H), 8.50 (m, 6H), 7.22 (d, 24H), 6.92 (d, 24H), 5.20 (s, 24H), 4.31 (s, 72H), 4.08 (s, 180H), 4.02 (s, 72H), 1.63 (m, 72H), 1.12 (m, 72H), 0.64 (m, 72H), 0.16 (s, 216H).

^{13}C NMR ($CDCl_3$, 75.47 MHz), δ_{ppm}: 141.7 (C_{ar}), 127.7 (C_{ar}), 113.9 (C_{ar}), 72.9 (C_{ar}), 71.0 (O$\underline{C}H_2$), 70.6 (C_{ar}), 68.1 (Cp), 43.3 (C_q-$\underline{C}H_2$), 18.0 (CH_2), 17.4 (Si$\underline{C}H_2$), -2.0 (Si$\underline{C}H_3$). Elemental analysis calcd for $C_{670}H_{846}Br_8F_{12}Fe_{36}Mo_6N_6O_{24}S_4Si_{36}$ (%): C 57.64, H 6.11; found (%): C 55.97, H 5.22. M =

13960.80 g.mol^{-1}.

Cluster [Mo_6Br_{13}(4-*tert*-butylpyridine)][*n*-Bu_4N], 20

A THF solution of [*n*-$Bu_4N]_2[Mo_6Br_{13}(CF_3SO_3)]$ **19** (0.426 g, 0.19 mmol) and 4-*tert*-butylpyridine (0.028 mL, 0.19 mmol) was stirred at 60ºC for 2 days. The solvent was removed under vacuum to give a orange solid that was washed with pentane and THF and dried under vacuum to yield complex **20** as an orange solid. Yield: 0.181 g (48 %). ^{1}H NMR ($CDCl_3$, 300 MHz), δ_{ppm}: 8.57 (d, 2H), 7.36 (d, 2H), 1.34 (s, 9H). ^{13}C NMR ($CDCl_3$, 75.47 MHz), δ_{ppm}: 146.8 (C_o), 122.2 (C_m), 33.9 ($\underline{C}Me_3$), 30.1 (CH_3). Elemental analysis calcd for $C_{25}H_{49}Br_{13}Mo_6N_2$ (%): C 15.07, H 2.48; found (%): C 14.68, H 2.27. M = 1992.07 g.mol^{-1}.

Cluster [Mo_6Br_{13}(4-vinylpyridine)][*n*-Bu_4N], 21

A THF solution of [*n*-$Bu_4N]_2[Mo_6Br_{13}(CF_3SO_3)]$ **19** (0.426 g, 0.19 mmol) and 4-vinylpyridine (0.021 mL, 0.19 mmol) was stirred at 60ºC for 2 days. The solvent was removed under vacuum to give a orange solid that was washed with pentane and THF and dried under vacuum to yield complex **20** as an orange solid. Yield: 0.138 g (37 %). ^{1}H NMR ($CDCl_3$, 300 MHz), δ_{ppm}: 8.54 (d, 2H), 7.26 (d, 2H), 6.61 (q, 1H), 5.93 (d, 1H), 5.46 (d, 1H). ^{13}C NMR ($CDCl_3$, 75.47 MHz), δ_{ppm}: 150.5 (C_o), 135.1 ($\underline{C}HCH_2$), 121.1 (C_m), 119.0 (CH_2). Elemental analysis calcd for $C_{23}H_{43}Br_{13}Mo_6N_2$ (%): C 14.08, H 2.21; found (%): C 13.73, H 2.02. M = 1962.00 g.mol^{-1}.

Pyridine dendron 22

In a Schlenk tube, 3,5-bromomethylpyridine (1.5 mmol), dimethyl-5-hydroxy-isophtalate (6 mmol) and K_2CO_3 (12 mmol) were stirred for one day in acetonitrile at 60°C. Then, the solvent was removed under vacuum, and the reaction product was extracted using diethyl ether and filtered on celite. The solvent was evaporated to dryness, and the product was chromatographed on silica gel (eluent: diethyl ether/petroleum ether: 1/1). Yield: 60%. ^{1}H NMR (250 MHz, CDCl3): δ = 8.70 (s, 2H), 7.94 (s, 1H), 8.34 (s, 2H), 7.85 (s, 4H), 5.21 (s, 4H), 3.95 (s, 12H). ^{13}C NMR (63 MHz, CDCl3): δ ppm =165.8 (Cq), 158.3 (CqO), 148.6-134.5 (CH), 132.7 ($\underline{C}$q-CqOO), 123.7 (p-CHar), 120.0 (o-CHar), 67.7 (CH_2-O), 52.4 (CH_3). Elemental analysis: calcd. (%): C 61.95, H 4.81. Found (%): C 61.75, H 4.96.

Pyridine dendron 23

To a suspension of $LiAlH_4$ (19.8 mmol) in dry THF, the pyridine dendron **22** (1.98 mmol) was dissolved to in the same solvent and added to the suspension. After 6 hours of reflux, 4 mL of water was slowly added in an ice bath. Then, the product was filtered and extracted with hot methanol. A yellow solid was obtained after precipitation with diethyl ether (yield 71%). ^{1}H NMR (250 MHz, d^4-methanol): δ = 8.59 (s, 2H), 8.03 (s, 1H),6.95 (s, 6H), 5.19 (s, 4H), 4.57 (s, 8H). ^{13}C NMR (63 MHz, CD_3OD): δ ppm = 158.7 (Cq-O), 147.2-135.1 (CH), 133.8 (Cq), 143.2 (Cq_{ar}), 117.7 (*p*-CH_{ar}), 111.6

(*o*-CH_{ar}), 66.7 (CH_2-O), 63.5 (CH_2OH).

Pyridine dendron 24

In a Schlenk tube, the pyridine dendron **23** (0.79 mmol), is stirred at 0°C during addition of tribromophosphine (1.05 mmol). After 4h in DMF at room temperature, the product was extracted with dichloromethane, this solution was washed several times with water, dried over Na_2SO_4 and the solent was removed under vacuum yielding a white solid (yield : 44%). ^{1}H NMR (250 MHz, CDCl3): δ = 8.67 (s, 2H), 7.90 (s, 1H), 7.05 (s, 2H), 6.95 (s, 4H), 5.13 (s, 4H), 4.44 (s, 8H). ^{13}C NMR (63 MHz, $CDCl_3$): δ ppm = 158.6 (Cq-O), 148.0-134.9 (CH), 132.3 (Cq), 139.8 (Cqar-CH_2Br), 122.5 (p-CH_{ar}), 115.4 (o-CH_{ar}), 67.3 (CH_2-O), 32.6 (CH_2Br). Elemental analysis: Calcd. (%): C 41.66, H 3.19; found (%): C 41.57, H 3.34.

12-ferrocenyl pyridine dendron, 25

In a Schlenk tube, pyridine **24** (0,0052 mmol), *p*.triferrocenylphenol[20] (0.029 mmol) and K_2CO_3 (0.063 mmol) were stirred for two days in acetonitrile at room temperature. Then, the solvent was removed under vacuum, and the reaction product was extracted using diethyl ether and filtered on celite. The solvent was evaporated to dryness and the product was chromatographed on silica gel (eluent: diethyl ether/petroleum ether 7/3). Yield: 22 %. ^{1}H NMR (250 MHz, $CDCl_3$): δ ppm = 8.68 (s, 2H, o-H pyridine), 7.90 (s, 1H, p-H pyridine), 7.26 and 6.90 (d, 16H, H aromatic), 6.97 (s, 4H, *o*-CH ar), 6.93 (s 2H, p-CHar), 5,12 (s, 4H, CH_2O), 5,02 (s, 8H, CH_2O),4.30-4.08-4.01 (CH ferrocene), 1.59-1.17 (m, 12H, Cq-CH2-CH2-CH), 0.64 (m, 6H, CH2-Si), 0.16 (CH3). ^{13}C NMR (63 MHz, $CDCl_3$): δ ppm = 127.6-114.0 (CHar),72.9-70.5-68.0 (CH ferrocenyl), 71.3 (Cq ferrocenyl), 67.3 (CH_2O), 43.6 (Cqar-Cq-CH_2), 42.4 (Cq-CH_2-CH_2), 18.4 (CH_2-CH_2-CH_2), 17.9 (Si-CH_2), -1.53 (CH_3). Elemental analysis calc.: C 66.13, H 7.23; found: C 65.80, H 6.66.

Ferrocenyl dendronized cluster, 26

A yellow THF solution of [*n*-Bu_4N]$_2$[$Mo_6Br_{13}(CF_3SO_3)$] **19** (0.016 g, 0.007 mmol) and 3,3'-{CH_2O*p*-$C_6H_4C(CH_2CH_2CH_2SiMe_2C_5H_5FeCp)_3\}_2$Py **25** (0.032 g, 0.007 mol) was stirred at 60ºC for 2 days. The solvent was removed under vacuum to give an orange solid. Yield: 0.042 g of **26** (35%).

^{1}H NMR ($CDCl_3$, 300 MHz), δ_{ppm}: 8.79 (m, 2H), 8.22 (m, 1H), 7.21 (d, 12H), 7.19 (m, 2H), 6.95 (d, 8H), 5.19 (s, 4H), 5.04 (s, 8H), 4.32 (s, 24H), 4.10 (s, 60H), 4.04 (s, 24H), 3.75 (t, 8H), 1.87 (m, 8H), 1.62 (m, 32H), 1.11 (m, 24H), 0.6 (m, 24H), 0.15 (s, 72H).

^{13}C NMR ($CDCl_3$, 75.47 MHz), δ_{ppm}: 129.5-116.0 (CHar), 74.9-73.3-70.0 (CH ferrocenyl), 72.6 (Cq ferrocenyl), 45.2 (Cqar-Cq-CH_2), 44.0 (Cq-CH_2-CH_2), 20.0 (CH_2), 19.46 (Si-CH_2), 2.9 (CH_3).

Acknowledgment

Financial support from the Ministère de la Recherche (ACI Nanostructures 2001 N° N18-01 and grants to DM, LP and KK), the Fundação para a Ciência e a Tecnologia (FCT), Portugal (Ph. D. grant to CO), the Institut Universitaire de France (DA, IUF), the Centre National de la Recherche Scientifique (CNRS), the Universities Bordeaux I, Rennes 1, Paris VI and Madeira, the GRICES-EGIDE PESSOA exchange program (CO, JR, JRA, DA) and the Fondation Langlois is gratefully acknowledged.

References

1. (a) Selby, H. D.; Roland, B. K.; Zheng, Z. *Acc. Chem. Res*. **2003**, *36*, 933; (b) Wang, R.; Zheng, Z. *J. Am. Chem. Soc*. **1999**, *121*, 3549; (c) Roland, B. K.; Carter, C.; Zheng, Z. *J. Am. Chem. Soc*. **2002**, *124*, 6234.
2. (a) Newkome, G. R.; Moorefield, C. N.; Vögtle, F. *Dendrimers and Dendrons: Concepts, Syntheses and Applications*, Wiley-VCH, 2001; (b) *Dendrimers and Other Dendritic Polymers*, Tomalia, D.; Fréchet, J. M. J. Eds., Wiley-VCH, New York, 2002; (c) *Dendrimers and Nanoscience*, Astruc, D. Ed. *C. R. Chimie*, Elsevier, Paris, 2003, 6 (Vols 8-10).
3. Jin, S.; DiSalvo, F. J. *Chem. Mater*. **2002**, *7*, 109.
4. (a) Rosi, N.; Eckert, J.; Eddaoudi, M.; Vodak, D. T.; Kim, J.; O'Keefe, M.; Yaghi, O. M. *Science* **2003**, *300*, 1127; (b) Seo, J. S.; Whang, D.; Lee, H.; Jun, S. I.; Oh, J.; Jeon, Y. J.; Kim, K. A. *Nature* **2000**, *404*, 982; (c) Bain, R. L.; Shriver, D. F.; Ellis, D. E. *Inorg. Chim. Acta* **2001**, *325*, 171.
5. (a) Golden, J. H.; Deng, H.; DiSalvo, F. J.; Fréchet, J. M. J.; Thompson, P. M. *Science* **1995**, *268*, 1463; (b) Ziolo, R. F. *Science* **1992**, *257*, 219; (c) Real, J. A.; Andrér, E.; Muñoz, M. C.; Julve, M.; Granier, T.; Bousseksou, A.; Varret, F. *Science* **1995**, *268*, 265; (d) Dunbar, K. R. *Inorg. Chem*., **1992**, *13*, 313; (e) Gabriel, J.-C. P.; Boubekeur, K.; Uriel, S.; Batail, P. *Chem. Rev*. **2001**, *101*, 2037; (f) Gorman, C.; Smith, J. C. *Acc. Chem. Res*. **2001**, *34*, 60.
6. (a) Brosset, C.; Kemi, Ark. *Mineral. Geol*. **1945**, *20A*, *7*, 1 and **1946**, *22A*, *11*, 1; (b) for a review, see: Perrin, C. *J. Alloys and Compounds* **1997**, *10*, 262; (c) for recent inorganic substitution chemistry, see: Cordier, S.; Naumov, N.; Salloum, D.; Paul, F.; Perrin, C. *Inorg. Chem*. **2004**, *43*, 219; (d) Pilet, G.; Cordier, S.; Gohlen, S.; Perrin, C.; Ouahab, L.; Perrin, A. *Sol. State Sci*. **2003**, *5*, 1359; for X-ray crystal structures of Mo_6 halide clusters, see: (e) Kirakci, K.; Cordier, S.; Perrin, C. *Z. Anorg. Allgem. Chem*. **2005**, *631*, 411; (f) Pilet, G.; Kirakci, K.; de Montigny, F.; Cordier, S.; Lapinte, C.; Perrin, C.; Perrin, A. *Eur. J. Inorg. Chem*. **2005**, *5*, 919; (g) Kirakci, K.; Cordier, S.; Roisnel, T.; Golhen, S.; Perrin, C. *Z. Kristallogr*. NCS, **2005**, *220*, 116.
7. (a) Chevrel, R.; Sergent, R.; Prigent, M. *J. Solid State Chem*. **1971**, *3*, 515; (b) Chevrel, R.;

Hirrien, M.; Sergent, M. *Polyhedron* **1986**, *5*, 87.

8. (a) Maverick, A. W.; Gray, H. B. *J. Am. Chem. Soc*. **1981**, *103*, 1298; (b) Jackson, J. A.; Turro, C.; Newsham, M. D.; Nocera, D. G. *J. Phys. Chem*. **1990**, 94, 4500.
9. (a) McCarley, R. E.; Hilsenbeck, S. J.; Xie, X. *J. Solid State Chem*. **1995**, *117*, 269; (b) Saito, T.; Yoshikawa, A.; Yamagata, T. *Inorg. Chem*. **1989**, *28*, 3588; (c) for a recent report, see: Popp, Boettcher, S. J. F.; Yuan, S. W.; Oertel, M.; DiSalvo, C.; *J. Chem. Soc. Dalton Trans.* **2002**, 3096.
10. (a) Sheldon, J. C. *Nature* **1959**, *184*, 1210; (b) Nannelli, P.; Block, B. P. *Inorg. Chem*. **1968**, *7*, 2423; **1969**, *8*, 1767; (c) Chisholm, M. H.; Heppert, J. A.; Huffman, J. C. *Polyhedron* **1984**, *3*, 475; (d) Perchenek, N.; Simon, A. *Z. Anorg. Allg. Chem*. **1993**, *619*, 98 and 103.
11. Nannelli, P.; Block, B. P. *Inorg. Syn*. **1971**, *13*, 99.
12. Johnston, D. H.; Gaswick, D. C.; Lonergan, M. C.; Stern, C. L.; Shriver, D. F. *Inorg. Chem.* **1992**, 31, 1869.
13. Roland, B.; Shelby, H. D.; Carducci, M. D.; Zheng, Z. *J. Am. Chem. Soc*. **2002**, *124*, 3222.
14. Jin, S.; Adamchuk, J.; Xiang, B.; DiSalvo, F. J. *J. Am. Chem. Soc*. **2002**, *124*, 9229.
15. Robinson, L. M.; Brain, R. L.; Shriver, D. F.; Ellis, D. E *Inorg. Chem*. **1995**, *34*, 5588.
16. For previous metal-cluster-cored dendrimers, see refs. 1, 9 and Gorman, C. B.; Parkhurst, B. L.; Su, W. Y.; Chen, K.-Y. *J. Am. Chem. Soc*. **1997**, *119*, 1141.
17. Wu, I.-Y; Lin, J. T.; Luo, J.; Sun, S.-S.; Li, C.-S.; Lin, K. J.; Tsai, C.; Hsu, C.-C.; Lin, J.-L. *Organometallics* **1997**, *16*, 2038-2048.
18. Bruce, M. I.; Ke, M.; Kelly, B. D.; Low, P. J.; Smith, M. E.; Skelton, B. W.; White, A. H. *J. Organometal. Chem*. **1999**, *590*, 184-201.
19. Méry, D.; Ornelas, C.; Daniel, M.-C.; Ruiz, J.; Rodrigues, J.; Astruc, D.; Cordier, S.; Kirakci, K.; Perrin, to be published.
20. Torres, J. C.; Pilli, R. A.; Vargas, M. D.; Violante, F. A.; Garden, S. J.; Pinto, A. C. *Tetrahedron*, **2002**, *58*, 4487.
21. Holm, R. H. Zheng, Z. *Inorg. Chem*. **1997**, *36*, 5173 ; Willer, M. W. ; Long, J. R. ; McLauchlan, C. C. ; Hom, R. H. *Inorg. Chem*. **1988**, *37*, 328.
22. Momenteau, M.; Mispelter, J.; Loock, B.; Lhoste, J.M. *J. Chem. Soc. Perkin Trans.* **1985**, 61.
23. Sartor, V.; Djakovitch, L.; Fillaut, J.-L.; Moulines, F.; Neveu, F.; Marvaud, V.; Guittard, J.; Blais, J.-C.; Astruc, D. *J. Am. Chem. Soc*. **1999**, *121*, 2929.
24. Nlate, S.; Ruiz, J.; Sartor, V.; Navarro, R.; Blais, J.-C.; Astruc, D. *Chem. J. Eur*. **2000**, *6*, 2544.
25. Flanagan J. B.; Margel S.; Bard A. J.; Anson F. C. *J. Am. Chem. Soc.* **1978**, *100*, 4248.
26. For earlier detailed related work, see: Daniel, M.-C.; Ruiz, J.; Blais, J.-C.; Daro, N.; Astruc, D. *Chem. Eur. J.* **2003**, *9*, 4371.

Résumé – Conclusion Perspectives

Résumé - Conclusion

Les objectifs de cette thèse se sont inscrits dans l'élaboration de nouveaux métallodendrimères pour différentes applications dans un premier temps. Tout d'abord, nos recherches se sont tournées vers la synthèse de métallodendrimères de palladium pour la catalyse de la réaction de Sonogashira. Dans la continuation de la thèse de S. Gatard, nous avons aussi synthétisé de nouveaux métallodendrimères de ruthénium pour la catalyse de métathèse polymérisante par ouverture de cycle du norbornène, conduisant à des polymères en étoile. Puis, nous avons étudié des aspects plus fondamentaux des dendrimères telle que la fonctionnalisation de grands dendrimères par la métathèse croisée. Pour finir, nous avons construit, en collaboration avec le groupe de C. Perrin et S. Cordier à Rennes, des dendrimères et métallodendrimères à cœur inorganique avec des liaisons de coordination qui se sont avérés être des capteurs électrochimiques d'ATP.

Partie I

Dans cette première partie, nous avons étudié les complexes modèles et dendritiques de palladium (II) pour la réaction de Sonogashira (Schéma 1).

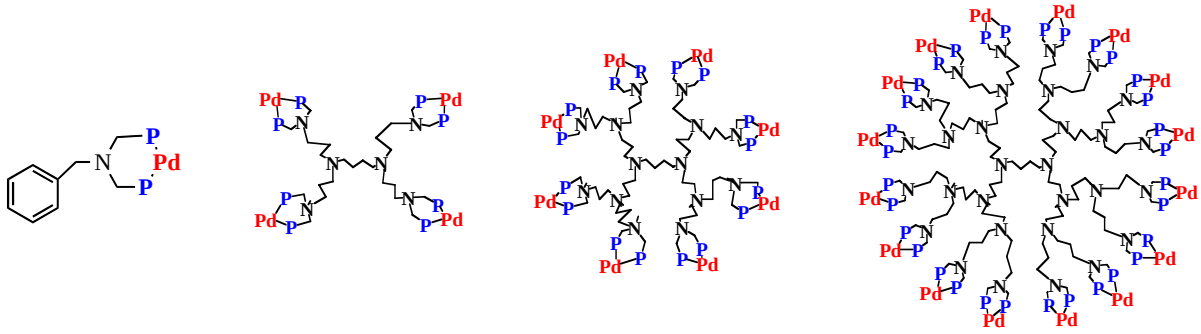

1 **2** **3** **4**

Schéma 1 : Complexes modèle et dendritiques de Palladium (P = Pt-Bu$_2$ et Pd = Pd(OAc)$_2$)

Dans une étude préliminaire, nous avons synthétisé un nouveau complexe de palladium (II), **1**, et étudié ses propriétés catalytiques pour la réaction de couplage de type Sonogashira à température ambiante et sans co-catalyseur (Équation 1).[1] Très peu d'exemples de couplage de Sonogashira n'utilisant pas de co-catalyseur de cuivre I ont été reportés dans la littérature.

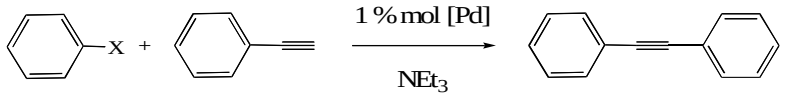

X = I, Br, Cl

Équation 1 : Réaction de Sonogashira

Le complexe modèle de palladium porte des ligands di*tert*butylphosphines P*t*-Bu_2, très encombrants et riches en électrons, qui lui confèrent une remarquable activité. Les résultats obtenus avec ce complexe montrent des réactions de couplages quantitatives et très rapides à température ambiante pour les dérivés iodés et bromés. Une réactivité substantielle en présence de dérivés chlorés activés, même à température ambiante, est observée. Le complexe modèle ayant démontré son activité catalytique, nous avons synthétisé trois générations de métallodendrimères de palladium (II), eux aussi efficaces en l'absence de co-catalyseur.[2]

La réactivité catalytique de ces métallodendrimères a été évaluée avec un apport en catalyseur de 1 mol % par site catalytique. D'une manière générale, une bonne activité a été obtenue avec les dendrimères de petites générations dans le cas du couplage des dérivés iodés. Cependant, un effet dendritique négatif est clairement observé dans le cas du métallodendrimère de 3^{ième} génération, **4**. Cet effet est dû à une augmentation de la gêne stérique entre les sites catalytiques à la périphérie du dendrimère. Les catalyseurs dans la série P*t*-Bu_2 sont très solubles dans les solvants organiques, ils n'ont donc pas pu être recyclés par simple précipitation dans le pentane.

Nous pouvons comparer l'effet de la phosphine grâce à d'autres travaux, menés au laboratoire par K. Heuzé et D. Gauss, avec des dendrimères analogues en série dicyclohexylphosphine, PCy_2. La réactivité des complexes de la série P*t*-Bu_2 est plus importante que celle obtenue avec les complexes de la série PCy_2.[3,4] Cependant, les catalyseurs de cette dernière série sont moins solubles dans les solvants organiques, ce qui a permis de les recycler plusieurs fois par simple précipitation dans le pentane.

Partie II

Nos investigations se sont aussi tournées vers la réaction de métathèse.

Dans un premier temps, nous avons étudié les complexes modèle et dendritiques de ruthénium pour la réaction de métathèse polymérisante par ouverture de cycle (ROMP) (Schéma 2 et Équation 2) dans la continuation des travaux de thèse de S. Gatard au laboratoire.[5,6]

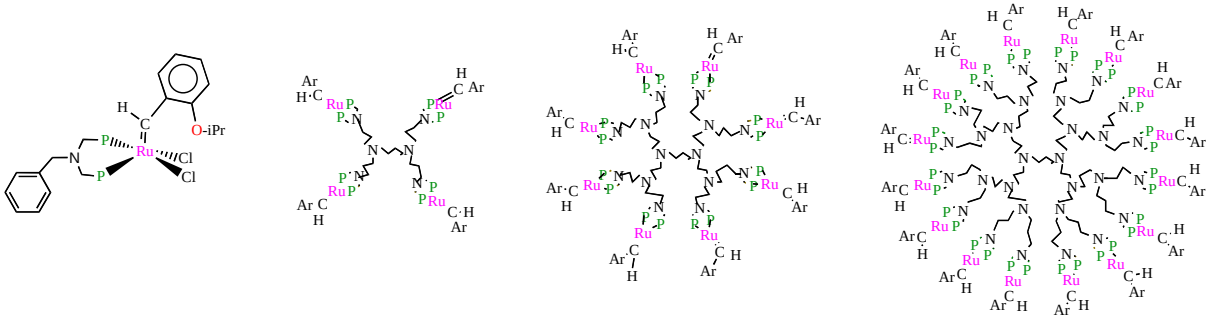

5 **6** **7** **8**

Schéma 2 : Amorceurs modèle et dendritiques de Ruthénium (P = Pt-Bu$_2$ et Ru = RuCl$_2$)

Dans cette partie, nous avons synthétisé des complexes dérivés du catalyseur d'Hoveyda car ce dernier est très actif en catalyse et stable à l'air. Les catalyseurs dendritiques, **6**-**8**, se sont montrés plus actifs que le complexe modèle correspondant, **5**.

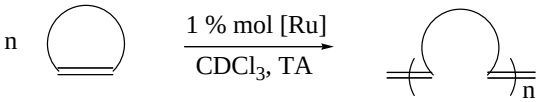

Équation 2 : Métathèse polymérisante par ouverture de cycle (ROMP)

En augmentant la génération de 1 à 3, nous avons une baisse de réactivité, ce qui confirme l'effet dendritique déjà rencontré avec les métallodendrimères de palladium. Dans cette étude, aucune stratégie de recyclabilité de l'initiateur dendritique n'est possible. Cependant, nous formons de nouveaux matériaux : les polymères en étoile (Équation 3). Nous pouvons comparer l'effet de la phosphine grâce à de précédents travaux effectués au laboratoire sur des analogues en série dicyclohexylphosphine, PCy$_2$. Les complexes dendritiques de la série P*t*-Bu$_2$ sont plus réactifs que ceux de la série PCy$_2$. Ces résultats sont semblables à ceux observés dans le cas des métallodendrimères de palladium.[7]

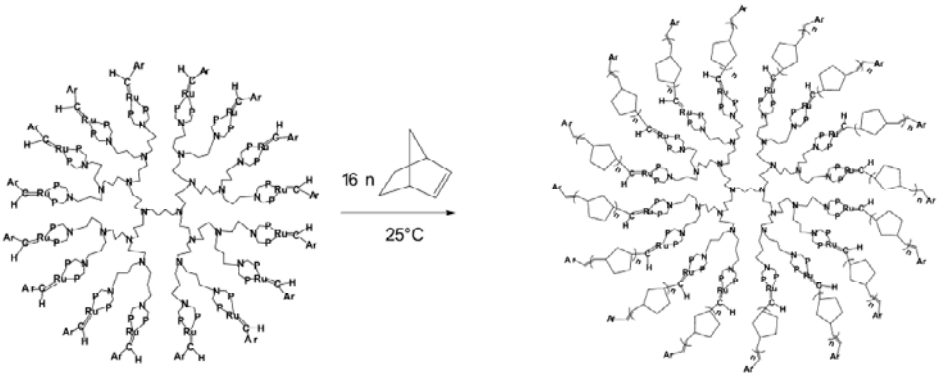

Équation 3 : Synthèse d'un polymère en étoile

Dans un second temps, nous avons fonctionnalisé des dendrimères à longues branches en une seule étape grâce à la réaction de métathèse croisée (CM). En effet, nous avons effectué la métathèse croisée des dendrimères oléfiniques à longues branches et, grâce au catalyseur de Grubbs seconde génération, nous avons pu les fonctionnaliser avec des groupements acides ou esters à 40°C en une nuit (Équation 4).[8]

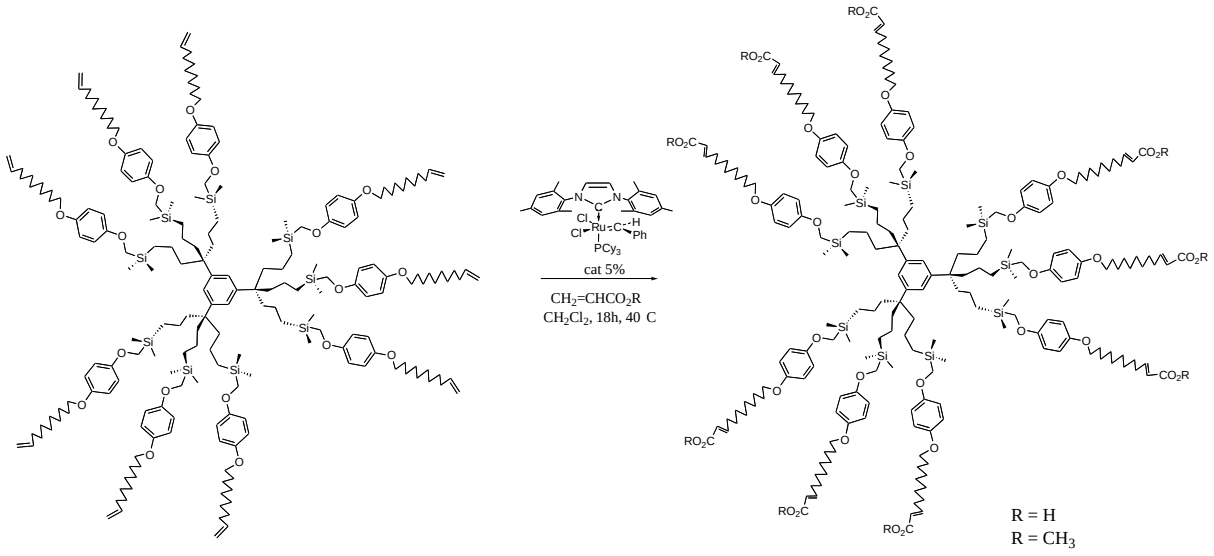

Équation 4 : Synthèse de dendrimères fonctionnalisés par la CM

Sans le rallongement des branches des dendrimères, nous avons pu bifonctionnaliser ces derniers en une seule étape par les réactions de métathèse de fermeture de cycle (RCM) et de métathèse croisée (CM) grâce au même catalyseur (Équation 5). Ainsi, nous avons pu étudier les compétitions possibles entre la métathèse de fermeture de cycle et la métathèse croisée.

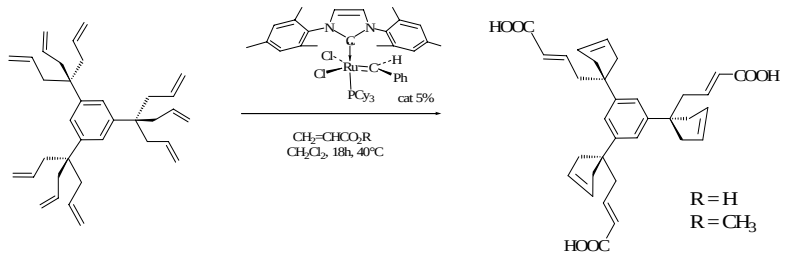

Équation 5 : Synthèses de dendrimères bifonctionnalisés par RCM et CM

Partie III

Dans cette dernière partie, nous avons élaboré de nouveaux dendrimères à cœur inorganique à l'aide de clusters de molybdène synthétisés au LCSIM par le groupe de C. Perrin et S. Cordier. En effet, des dendrimères et métallodendrimères fonctionnalisés à cœur inorganique avec des liaisons de coordination entre le cluster de molybdène et les dendrons pyridines, synthétisés au laboratoire par L. Plault et S. Nlate, ont été élaboré (Équation 6).[9-11] Nous avons ainsi pu noter l'importance des liaisons qui lient le cœur du dendrimère aux dendrons, ainsi que la faible influence de l'halogénure interne (Br ou I) du cluster. De même, la nature des contre-anions des clusters de départ est importante pour suivre la réaction de substitution.

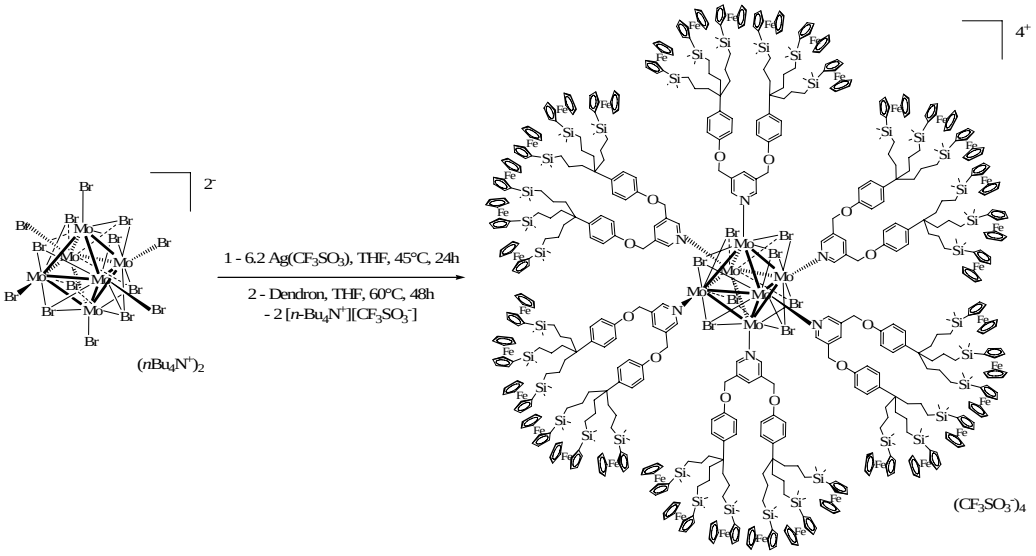

Équation 6 : Synthèse d'un métallodendrimère à cœur inorganique

Pour finir, nous avons réussi à effectuer la monosubstitution de l'un des ligands apicaux du cluster afin de synthétiser un dendron à cœur cluster (Équation 7).

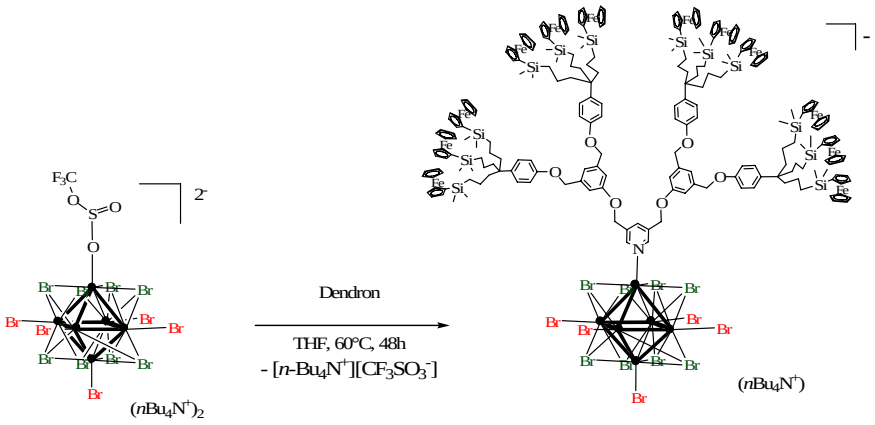

Équation 7 : Synthèse d'un dendron à cœur inorganique

En conclusion, les multiples synthèses dendritiques depuis l'avènement du domaine ont fait place à une recherche des fonctions potentielles des dendrimères dans le champ des Nanosciences. L'ingénierie moléculaire bénéficie de nombreux outils intégrant les dendrons greffés sur des cœurs dendritiques, des nanoparticules, des surfaces, des clusters etc... C'est dans cette optique, pour étudier tant l'aspect fondamental que les applications potentielles, que nous avons synthétisé quatre types de dendrimères différents:

- Des métallodendrimères de palladium pour la catalyse de la réaction de Sonogashira
- Des métallodendrimères de ruthénium pour la métathèse polymérisante par ouverture de cycle afin de synthétiser de nouveaux polymères en étoile
- Des dendrimères fonctionnalisés à la périphérie par la réaction de métathèse croisée
- Des dendrimères et métallodendrimères à cœur inorganique de molybdène

A ces différents types de dendrimères correspondent différentes applications (catalyse, reconnaissance, transport) qui motivent leur synthèse.

Liste des articles issus de cette thèse

1- D. Méry, K. Heuzé, D. Astruc "A very efficient, copper-free palladium catalyst for the Sonogashira reaction with aryl halides" *Chem. Commun.*, **2003**, *15*, 1934-1935.

2- K. Heuzé, D. Méry, D. Gauss, D. Astruc "Copper-free, recoverable dendritic Pd catalysts for the Sonogashira reaction" *Chem. Commun.*, **2003**, *18*, 2274-2275.

3- K. Heuzé, D. Méry, D. Gauss, J.-C. Blais, D. Astruc "Copper-Free Monomeric and Dendritic Palladium Catalysts for the Sonogashira Reaction: Substituent Effects, Synthetic Applications, and the Recovery and Re-Use of the Catalysts" *Chem. A Eur. J.*, **2004**, *10*, 3936-3944.

4- D. Méry, D. Astruc "Nouveau Catalyseur hétérogène au palladium, son procédé de synthèse, et son utilisation dans les réactions de Couplage C-C" *French patent*, **2004**, n° FR 04 08673.

5- S. Gatard, S. Kahlal, D. Méry, S. Nlate, E. Cloutet, J.-Y. Saillard, D. Astruc "Synthesis, Chemistry, DFT Calculations, and ROMP Activity of Monomeric Benzylidene Complexes Containing a Chelating Diphosphine and of Four Generations of Metallodendritic Analogues. Positive and Negative Dendritic Effects and Formation of Dendritic Ruthenium-Polynorbornene Stars" *Organometallics*, **2004**, *23*, 1313-1324.

6- D. Méry, D. Astruc "Synthesis of Monomeric and Dendritic Ruthenium Benzylidene cis-bis-*tertio*butyl phosphine Complexes that Catalyze the ROMP of Norbornene under Ambient Conditions" *J. Mol. Cat. A: Chem*., **2005**, 227 (1-2), 1.

7- D. Astruc, K. Heuzé, S. Gatard, D. Méry, S. Nlate, L. Plault "Metallodendritic Catalysis for Redox and Carbon-Carbon Bond Formation Reactions : A step towards Green Chemistry" *Adv. Synth. Catal.*, **2005**, *347*, 329-338.

8- C. Ornelas, D. Méry, J.-C. Blais, J. Ruiz, D. Astruc “Efficient Mono- and Bifunctionnalization of Poly-olefin Dendrimers by Olefin Metathesis” *Angew. Chem. Int. Ed.,***2005**, accepté.

9- D. Méry, C. Ornelas, M.-C. Daniel, J. Ruiz, J. Rodrigues, D. Astruc, S. Cordier, K. Kiraki, C. Perrin “Mo_6Br_8-Cluster-cored Organometallic Stars and Dendrimers” Comptes Rendus Chimiques, numéro spécial, **2005**, sous presse.

10- D. Méry, L. Plault, S. Nlate, D. Astruc, S. Cordier, K. Kirakci, C. Perrin “The Simple Hexapyridine Cluster $[Mo_6Br_8Py_6][OSO_2CF_3]_4$ and Substituted Hexapyridine Clusters Including a Cluster-cored Polyolefin Dendrimer” *Z. Anorg. Allg. Chem.,* **2005**, accepté.

11- S. Cordier, K. Kirakci, D. Méry, C. Perrin, D. Astruc “$Mo_6X^i_8$ Nanocluster Cores (X= Br, I): from Inorganic Solid State Compounds to Hybrids” *Inorg. Chimi. Acta,* **2005**, accepté.

Perspectives

Les travaux réalisés durant cette thèse permettent d'ouvrir plusieurs voies afin d'étendre le domaine d'applications des dendrimères. Les réactions de métathèse de fermeture de cycle, d'hydrogénation et d'hydrosilylation sont primordiales pour la synthèse organique et industrielle. Afin de compléter nos travaux, nous envisageons donc de synthétiser de nouveaux métallodendrimères de ruthénium et de rhodium pour la catalyse de ces réactions (Schéma 1). Les métaux seront greffés sur le dendrimère par le biais de ligands imidazoles. Ces derniers ont déjà montrés une amélioration non négligeable de l'activité des catalyseurs en comparaison avec les ligands phosphines.

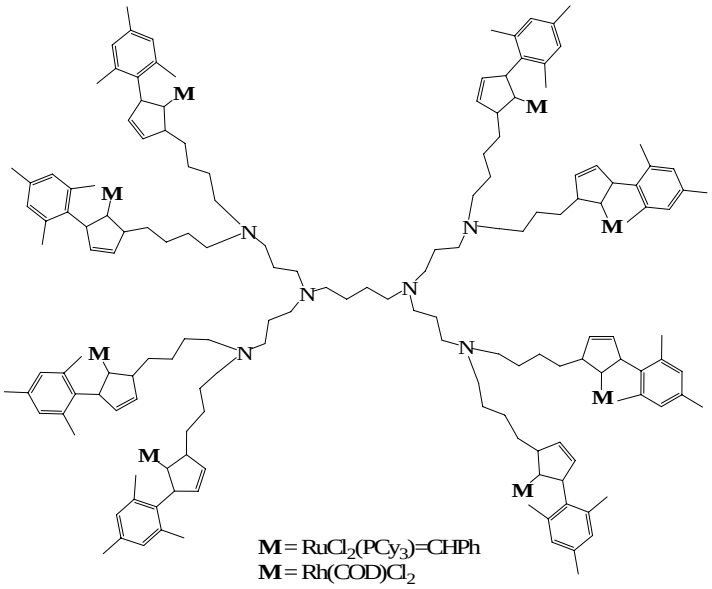

Schéma 1 : Métallodendrimères de ruthénium et de rhodium

De plus, les polymères en étoile ouvrent la voie vers l'élaboration de nouveaux matériaux. En effet, on peut envisager de nouvelles propriétés de ce type de polymères liées à leurs topologies tels que le transport de médicaments vers des cibles biologiques ou encore l'encapsulation de catalyseurs et de capteurs.

Annexes

Annexe 1

Synthesis, Chemistry, DFT Calculations, and ROMP Activity of Monomeric Benzylidene Complexes Containing a Chelating Diphosphine and of Four Generations of Metallodendritic Analogues. Positive and Negative Dendritic Effects and Formation of Dendritic Ruthenium−Polynorbornene Stars

Sylvain Gatard,[†] Samia Kahlal,[‡] Denise Méry,[†] Sylvain Nlate,*[,†] Eric Cloutet,*[,§] Jean-Yves Saillard,*[,‡] and Didier Astruc*[,†]

Nanoscience and Catalysis Group, LCOO, UMR CNRS No. 5802, Université Bordeaux I, 33405 Talence Cedex, France, LCSIM, UMR CNRS No. 6511, Institut de Chimie de Rennes, Université de Rennes 1, 35042 Rennes Cedex, France, and LCPO, UMR CNRS No. 5629, ENSCPB, Université Bordeaux I, 33405 Talence Cedex, France

Received September 23, 2003

The reaction of Hoveyda's catalyst [Ru{η^2-(=CHAr)}(PCy_3)Cl_2] (**1**; Ar = *o*-O-*i*-Pr-C_6H_4) with the diphosphine $PhCH_2N(CH_2PCy_2)_2$ (**2**) gives the new air-stable green ruthenium carbene complex [Ru{η^1-(=CHAr)}{η^2-$(Cy_2PCH_2)_2N(CH_2Ph)$}Cl_2] (**3A**), in which **2** models a dendritic branch of poly(diphosphine) dendrimers DAB-*dendr*-$[N(CH_2PCy_2)_2]_n$ (G_1, $n = 4$; G_2, $n = 8$; G_3, $n = 16$; G_4, $n = 32$). The complex **3A** reversibly dimerizes in concentrated solution, a trend favored at low temperature. The structure of **3A** was also confirmed by DFT calculations, which also establish the dimeric structure of **3B** and the fact that the dimerization energy of **3A** is small. Facile halide abstraction is shown by MALDI-TOF mass spectroscopy, and reaction with $AgPF_6$ gives the air-stable green dicationic dimer **5**, whose structure has been confirmed by DFT calculations and whose reactions with ligands (I^- and DMSO) gives monomeric alkylidene complexes. The diiodo analogue of **3A**, **7A**, is also synthesized by addition of NaI to either **3A** or **5** and dimerizes more readily than the dichloro analogue **3A**. On the basis of this chemistry, metallodendrimers DAB-*dendr*-$[PCy_2CH_2NCH_2$-$PCy_2Ru(=CHAr)(PPh_3)(Cl)_2]_n$ (**8**−**11**) derived from the four first generations of DAB polyamines containing, respectively, 4, 8, 16, and 32 ruthenium branches have been synthesized and characterized by elemental and standard spectroscopic analysis. Dimerization of the ruthenium alkylidene species of these dendrimers is found to increase upon dilution, which is taken into account by intradendritic dimerization and larger extension of the branches, providing more freedom for dimerization in dilute solution. These dendritic ruthenium−carbene complexes are shown to initiate the ROMP of norbornene at room temperature to form star-shaped metallodendritic polymers. Interestingly, the metallodendrimer G_1 initiates the ROMP of norbornene much faster than the model ruthenium complex **3**, the overall rate order being $G_1 > G_2 > G_3 >$ model. The dramatic positive dendritic effect is rationalized in terms of the labilization of a ruthenium−phosphorus bond at each Ru within the dendrimers. Such a speculative dissociative metathesis mechanism (**3A**, 16e → 14e) would be in accord with the limited ROMP activity, the lack of RCM activity, the instability in air, and the DFT calculations showing that the interaction of **3A** with ethylene is repulsive. The second dendritic effect, negative among the generations, is taken into account by the increasing bulk as the generation number increases, slowing down the approach of Ru by norbornene. Cleavage of the polynorbornene branches of these metallodendritic polymer stars using ethyl vinyl ether followed by SEC analysis shows that the observed masses are close to the theoretical ones, indicating that dendritic-star polymers have formed in the ROMP process.

Introduction

The design of nanoscale architectures combining dendrimers and polymers[1] is challenging and should provide useful devices for future materials chemistry. Along this line, we have been interested in polymerization using dendritic initiators by extension of the branches to polymers. This type of strategy has already been approached inter alia by atom transfer radical

* To whom correspondence should be addressed. E-mail: S.N., s.nlate@lcoo.u-bordeaux1.fr; D.A., d.astruc@lcoo.u-bordeaux1.fr; J.-Y.S., Saillard@univ-rennes1.fr; E.C., cloutet@enscpb.fr.

[†] LCOO, Université Bordeaux I.
[‡] LCSIM, Université de Rennes 1.
[§] LCPO, Université Bordeaux I.

10.1021/om030608r CCC: $27.50
Publication on Web 02/13/2004

polymerization (ATRP), anionic polymerization,[2] and cationic polymerization of styrene using star-shaped initiators.[3] Given the success of the metathesis reaction[4] and the rich chemistry of metallodendrimers[5] and metallodendritic catalysts,[6] we wished to start from transition metal−carbene dendrimers[7] that might be able to serve as metallodendritic metathesis catalysts for RCM as well as initiators for ROMP.

To first form stable metallodendritic carbene complexes, we chose chelating phosphines, although in Grubbs' catalyst $[Ru(=CHPh)Cl_2(PR_3)_2]$,[8] the dissociation of a phosphine is the rate-limiting step of the catalysis.[9] There are known metathesis catalysts, however, that contain a chelating diphosphine.[10−12] In particular, Hofmann et al. have reported ruthenium benzylidene complexes containing the diphosphines $t\text{-}Bu_2P(CH_2)_nPtBu_2$ (n = 1, 2) that are very active catalysts for RCM and ROMP after addition of a Lewis acid.[10] The groups of Fogg[11] and Leitner[12] demonstrated that some neutral *cis*-bis(phosphine)ruthenium complexes could also be very active ROMP catalysts without addition of a Lewis acid.

In our ligands *dendr*-$N(CH_2PCy_2)_2$, derived from Reetz's ligands *dendr*-$N(CH_2Ph_2)_2$,[13] the two phosphorus atoms are separated by the $CH_2N(R)CH_2$ link. In the model monomeric compound R = Ph, this phenyl group can be replaced by a dendritic branch (*dendr*) of commercial DAB dendrimers of various generations. As a precursor complex, we are using Hoveyda's catalyst $[Ru\{\eta^2\text{-}(=CH\text{-}o\text{-}PhO\text{-}i\text{-}Pr)\}Cl_2(PPh_3)]$.[14]

Reetz's group has reported catalytic properties of metallodendrimers based on his ligands,[13] and we have already used these ligands for the introduction of ruthenium clusters at the dendrimer periphery.[15] In a preliminary communication, we have reported the synthesis of new monomeric and dendrimeric ruthenium−benzylidene complexes containing the chelating ligands and their ROMP activity.[16] In this article, we detail the syntheses and propertries of this new family of complexes, including the synthesis of the fourth-generation metallodendric carbene complex, their electrochemistry, theoretical DFT calculations showing the structures of monomeric and dimeric complexes of close energy and the energy of approach of the olefin, and their ROMP activity.

Results and Discussion

The Model Ruthenium−Benzylidene Complex 3 and Its Chemistry. The reaction between 1 equiv of Hoveyda's catalyst $[Ru\{\eta^2\text{-}(=CH\text{-}o\text{-}PhO\text{-}i\text{-}Pr)\}Cl_2(PPh_3)]$[14] (**1**) and 1 equiv of the diphosphine $PhCH_2N(CH_2PCy_2)_2$ (**2**), reported by Russel et al.,[17] in CH_2Cl_2 under ambient conditions gives the new air-stable green ruthenium−benzylidene complex **3A** in 76% yield, together with free triphenylphosphine (eq 1).

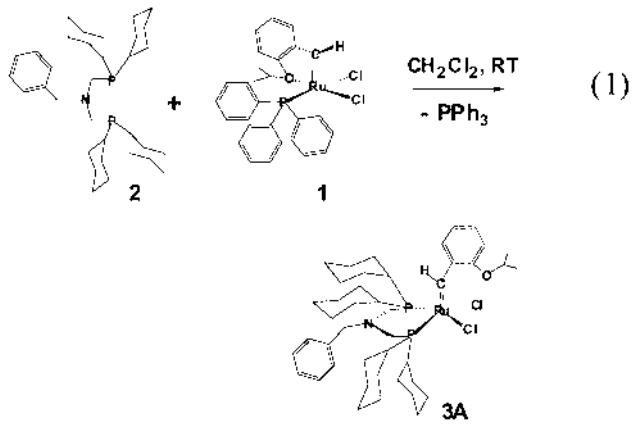

(1)

The ^1H NMR spectrum of **3A** diluted in $CDCl_3$ shows a triplet at δ 15.66 ppm vs $SiMe_4$ characteristic of a meta carbene proton coupled with two equivalent phosphorus atoms bound to the metal. The coupling constant $^3J_{P-H}$ is 15.7 Hz, this value being comparable to that obtained by Werner et al. for $[RuCl_2(=CHPh)(PCy_2(CH_2)_3\text{-}PCy_2)]$ (16.1 Hz).[18] The ortho proton of the phenyl ring of the benzylidene ligand is deshielded at δ 9.33 ppm, unlike the case for Hoveyda's complex **1**, indicating that it is now in the ruthenium−benzylidene plane in **3A**, whereas this conjugation is inhibited by the coordination of the ether oxygen atom in **1**. This is a very good characteristic of the decoordination of the oxygen atom

(1) Newkome, G. R.; Moorefield, C. N.; Vögtle, F. *Dendrimers and Dendrons, Concepts, Synthesis and Applications*; VCH-Wiley: Weinheim, Germany, 2001. *Dendrimers and Other Dendritic Polymers*; Tomalia, D., Fréchet, J. M. J., Eds.; Wiley-VCH: New York, 2002. *Dendrimers and Nanosciences*; Astruc, D., Ed.; Comptes Rendus Chimie 6; Elsevier: Amsterdam, 2003.

(2) (a) Leduc, M. R.; Hawker, C. J.; Dao, J.; Fréchet, J. M. J. *J. Am. Chem. Soc.* **1996**, *118*, 11111. (b) Gitsov, I.; Ivanova, P. T.; Fréchet, J. M. J. *Macromol. Rapid Commun.* **1994**, *15*, 387.

(3) Cloutet, E.; Fillaut, J.-L.; Gnanou, Y.; Astruc, D. *J. Chem. Soc., Chem. Commun.* **1994**, 2433. Cloutet, E.; Fillaut, J. L.; Astruc, D.; Gnanou, Y. *Macromolecules* **1998**, *31*, 6748.

(4) Trnka, T.; Grubbs, R. H. *Acc. Chem. Res.* **2001**, *34*, 18. Schrock, R. R. *Tetrahedron* **1999**, *55*, 8141. Fürstner, A. *Angew. Chem., Int. Ed.* **2000**, *39*, 3012. Buchmeiser, M. R. *Chem. Rev.* **2000**, *100*, 1565. Rouhi, A. M. *Chem. Eng. News* **2002**, Dec 23, 29.

(5) (a) Newkome, G. R.; He, E.; Moorefield, C. N.; *Chem. Rev.* **1999**, *99*, 1689. (b) Janssen, H. M.; Meijer, E. W. *Chem. Rev.* **1999**, *99*, 1665. (c) Cuadrado, I.; Morán, M.; Casado, C. M.; Alonso, B.; Losada, J. *Coord. Chem. Rev.* **1999**, *189*, 123. (d) Hearshaw, M. A.; Moss, J. R. *Chem. Commun.* **1999**, 1. See also ref 6.

(6) (a) Astruc, D.; Chardac, F. *Chem. Rev.* **2001**, *101*, 2991. (b) Oosterom, G. E.; Reek, J. N. H.; Kamer, P. C. J.; van Leeuwen, P. W. N. M. *Angew. Chem., Int. Ed.* **2001**, *40*, 1828. (c) Kreiter, R.; Kleij, A. W.; Klein Gebbink, R. J. M.; van Koten, G. In *Dendrimers IV: Metal Coordination, Self-Assembly, Catalysis*; Topics in Current Chemistry 217; Vögtle, F., Schalley, C. A., Eds.; Springer: Berlin, 2001; p 163. (d) van Heerbeek, R.; Kamer, P. C. J.; van Leuwen, P. W. N. M.; Reek, J. N. H. *Chem. Rev.* **2002**, *102*, 3717.

(7) (a) Garber, S. B.; Kingsbury, J. S.; Gray, B. L.; Hoveyda, A. H. *J. Am. Chem. Soc.* **2000**, *122*, 8168. (b) Wijkens, P.; Jastrzebski, J. T. B. H.; van der Schaaf, P. A.; Kolly, R.; Hafner, A.; van Koten, G. *Org. Lett.* **2000**, *2*, 1621. (c) Beerens, H.; Verpoort, F.; Verdonck, L. *J. Mol. Catal.* **2000**, *151*, 279; **2000**, *159*, 197.

(8) Schwab, P.; France, M. B.; Ziller, J. W.; Grubbs, R. H. *Angew. Chem., Int. Ed. Engl.* **1995**, *34*, 2039.

(9) Sanford, M. S.; Ulman, M.; Grubbs, R. H. *J. Am. Chem. Soc.* **2001**, *123*, 749.

(10) Hansen, S. M.; Volland, M. A. O.; Rominger, F.; Eisenträger, F.; Hofmann, P. *Angew. Chem., Int. Ed.* **1999**, *38*, 1273. Hansen, S.; Rominger, F.; Metz, M.; Hofmann, P. *Chem. Eur. J.* **1999**, *5*, 557. Adlhart, C.; Volland, M. A. O.; Hofmann, P.; Chen, P. *Helv. Chim. Acta* **2000**, *83*, 3306.

(11) (a) Amoroso, D.; Fogg, D. E. *Macromolecules* **2000**, *33*, 2815. (b) Amoroso, D.; Yap, G. P. A.; Fogg, D. E. *Can. J. Chem.* **2001**, *79*, 958.

(12) Six, C.; Beck, K.; Wegner, A.; Leitner, W. *Organometallics* **2000**, *19*, 4639.

(13) Reetz, M. T.; Lohmer, G.; Schwickardi, R. *Angew. Chem., Int. Ed.* **1997**, *36*, 1526.

(14) Kingsbury, J.; Harrity, J. P. A.; Bonitatebus, P. J.; Hoveyda, A. H. *J. Am. Chem. Soc.* **1999**, *121*, 791.

(15) Alonso, E.; Astruc, D. *J. Am. Chem. Soc.* **2000**, *122*, 3222.

(16) Gatard, S.; Nlate, S.; Cloutet, E.; Bravic, G.; Blais, J.-C.; Astruc, D. *Angew. Chem., Int. Ed.* **2003**, *42*, 452.

(17) Fawcet, J.; Hoye, P. A. T.; Kemmitt, R. D. W.; Law, D. J.; Russell, D. R. *J. Chem. Soc., Dalton Trans.* **1993**, 2563.

(18) Werner, H.; Jung, S.; Gonzales-Herrero, P.; Ilg, K.; Wolf, J. *Eur. J. Inorg. Chem.* **2001**, 1957.

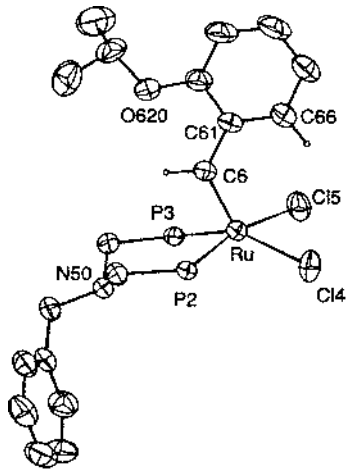

Figure 1. ORTEP diagram (50% probability ellipsoids) of the X-ray crystal structure of **3A** reported in ref 16. Reproduced with permission. Selected bond distances (Å) and angles (deg): Ru−O620 = 4.565(2), Ru−P2 = 2.3211(6), Ru−P3 = 2.2798(6), Ru−Cl4 = 2.3889(8), Ru−Cl5 = 2.3975(8), C6−C61 = 1.464(4), Ru−C6 = 1.860(3); Ru−C6−C61 = 127. The Cy groups are omitted throughout for clarity.

Table 1. Cyclic Voltammetry Data[a]

	oxidn		redn	
	CH_2Cl_2	THF	CH_2Cl_2	THF
3A	1.23	1.08	−1.42	−1.42
7A	0.61; 0.86	0.54; 1.12	−1.33; −1.00	−1.36; −1.20
12	0.70	0.73	/	−0.98

[a] Cyclic voltammetry (CV) data of **3A** (10^{-4} M in CH_2Cl_2 or THF) and **7A** (10^{-4} M in CH_2Cl_2 or THF): supporting electolyte, [*n*-Bu_4N][PF_6] 0.1 M; temperature, −30 °C; internal reference, decamethylferrocene; reference electrode, Ag; auxiliary and working electrodes, Pt. The CV data recorded for Grubbs' catalyst [Ru(=CHPh)Cl_2(PCy_3)$_2$] (**12**) have also been recorded and included in the table for comparison (the two phosphine ligands are trans).

from ruthenium that is useful all along the study of the chemistry of **3A**. In addition, the tertiary proton of the isopropyl group is considerably shielded at δ 4.79 ppm compared to δ 5.43 ppm for **1**. In the ^{13}C NMR spectrum of **3A**, the carbene signal is found at δ 291.5 ppm as a triplet, showing again the coupling with the two equivalent phosphorus atoms of the diphosphine ligand. This equivalence of the two phosphorus atoms is confirmed by the singlet found at δ 40.9 ppm in the ^{31}P NMR spectrum of **3A**.

Thus, the molecular structure of **3A** is clearly that of a ruthenium benzylidene complex in which the oxygen atom of the styryl isopropyl ether is no longer coordinated and the diphosphine **2** is coordinated with two equivalent phosphorus atoms. This structure represented in eq 1 is confirmed by the elemental analysis and by the X-ray crystal structure (Figure 1).

The geometry is that of a distorted square pyramid with a Ru=C distance of 1.860(3) Å, a C−C distance between the carbenic carbon and the phenyl ring of 1.464(4) Å, and a nonbonding Ru−O distance of 4.565(2) Å, the Ru=C−C angle being 127°.

The MALDI-TOF mass spectrum of **3A** shows a peak at *m*/*z* 812.45 as the major peak of the spectrum, corresponding to $[M - Cl]^+$: i.e., complex **3A** that has lost a chloride ligand to give the unsaturated 14-electron species **4** (no molecular peak was observed). This facile loss is suggestive of further chemistry in this direction (eq 2).

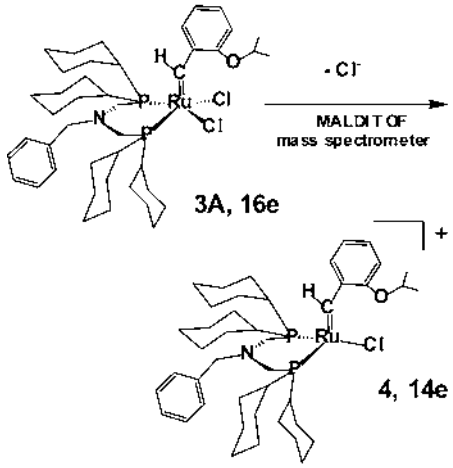

(2)

The electrochemical oxidation and reduction of **3A** on a Pt electrode are both chemically irreversible in CH_2Cl_2 or THF even at −30 °C (E_p = 1.23 and −1.42 V, respectively, vs decamethylferrocene in CH_2Cl_2; Table 1 including the data for Grubbs' catalyst).

Spontaneous, Reversible Dimerization of 3A to 3B in Concentrated Solution. Whereas the NMR spectra of **3A** in dilute solution only show the signals corresponding to this compound, concentrated solutions show additional signals. The ^1H NMR spectrum shows, in addition to the triplet of **3A** at δ 15.66 ppm, another triplet at δ 16.96 ppm ($^3J_{P-H}$ = 13.3 Hz) attributable to another carbenic proton. The ^{31}P NMR spectrum of the concentrated solution shows, in addition to the singlet of **3A** at δ 40.9 ppm, two doublets at δ 36.8 and δ 41.3 ppm ($^2J_{P-P}$ = 45.9 Hz) attributable to two nonequivalent phosphorus atoms that are coupled with each other, which means that they must be both coordinated to the ruthenium atom. Other new signals are detected in the NMR spectra, indicating the presence of another carbenic complex in concentrated solution: a new signal is observed at δ 9.55 ppm in addition to the signal of **3A** at δ 9.33 ppm. This new signal signifies that the oxygen atom is also decoordinated in this other carbene complex **3B**. The isopropyl signal at δ 4.79 ppm is unchanged. In the ^{13}C NMR spectrum of the concentrated solution, a new carbenic carbon is seen at δ 308.8 ppm in addition to the signal of **3A** at δ 291.5 ppm. The proportion of the two carbenic complexes **3A** and **3B** in the concentrated mixture is unchanged by switching from $CDCl_3$ to CD_3COCD_3 solution or upon addition of [*n*-Bu_4N]Cl; thus, it appears that only **3A** is involved in the reaction leading to the new ruthenium−carbene complex **3B** present in concentrated solution. All these features converge toward a monomer−dimer equilibrium (eq 3).

Thus, as expected, the monomer−dimer ratio reversibly varies upon dilution and the equilibrium constant *K* was found not to vary significantly upon variation of the concentration (Table 2). A value of $K = 5.3 \pm 0.5$ L mol^{-1} was found at 25 °C. The DFT calculations (vide infra) confirm that the energy of the 18e dimer **3B** is close to that of two molecules of the 16e monomer **3A**. In the solid state, however, the monomer **3A** is favored, as shown by the X-ray crystal structure data. The

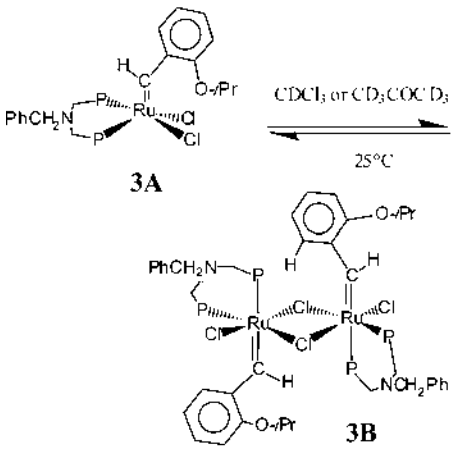

(3)

dimerization equilibrium is strongly temperature dependent, as expected for entropic reasons. Thus, at −40 °C, ^{1}H NMR measurements led to the value $K = 117 \pm 10$ L mol^{-1}, the equilibrium being shifted toward the dimer **3B**.

Chloride Abstraction from 3A, Formation of the Dicationic Dimer 5, and Introduction of Other Ligands. After the facile formation of **4** from **3A** observed by mass spectroscopy, we investigated the removal of the chloride ion using chemical reagents. We found that the cleanest Lewis acid in our hands was $AgPF_6$. Thus, addition of 1 equiv of $AgPF_6$ to 1 equiv of of **3A** at room temperature in CH_2Cl_2 leads to another air-stable green complex, **5**, in 52% yield. The ^{1}H NMR spectrum of **5** shows a new triplet signal at δ 17.24 ppm ($^3J_{P-H} = 12.7$ Hz). The deshielded ortho aromatic proton at 9.64 ppm and the location at δ 4.76 ppm of the tertiary proton of the isopropyl group indicate that the oxygen atom is again decoordinated. The carbenic carbon is characterized by its signal at δ 311.9 ppm in the ^{13}C NMR spectrum. The ^{31}P NMR spectrum shows only one peak at δ 45.2 ppm, indicating the equivalence of the two phosphorus atoms. These data are in accord with the 16e dicationic dimeric structure (eq 4) obtained by Hofmann for a similar system lacking the O-*i*-Pr fragment, and with other alkylidene ligands.

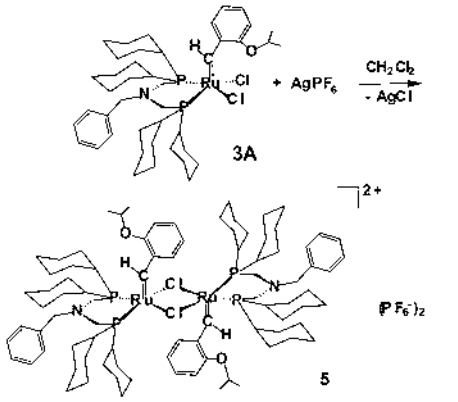

(4)

Addition of 2 equiv of [*n*-Bu$_4$N]Cl to **5** in $CDCl_3$ or CH_2Cl_2 gives back complex **3 (**eq 5), which supports the proposed structure of **5**.

In d_6-DMSO, the dimeric complex **5** gives a new species **6**, for which a new carbene triplet is observed in the ^{1}H NMR spectrum at δ 15.56 ppm (Table 2).

Table 2. ^{1}H NMR Chemical Shifts (δ in ppm vs $SiMe_4$) and Relative Intensities (%) for the Carbenic Proton of the Monomeric and Dimeric Forms of the Model and Dendritic Ruthenium Complexes 2−5[a]

Ru complex	monomeric form			dimeric form		
	δ (ppm)	amt, %[c]	amt, %[b]	δ (ppm)	amt, %[b]	amt, %[c]
2	15.65	98	47	16.85	2	53
3A	15.63	58	87	16.87	42	13
4	15.63	55	81	16.90	45	19
5	15.63	48	77	16.95	52	23

[a] The percentages are given at two concentrations to show the dilution effect. [b] Diluted solution (5 mg of Ru complex in 0.3 mL of $CDCl_3$). [c] Concentrated solution (20 mg of Ru complex in 0.3 mL of $CDCl_3$).

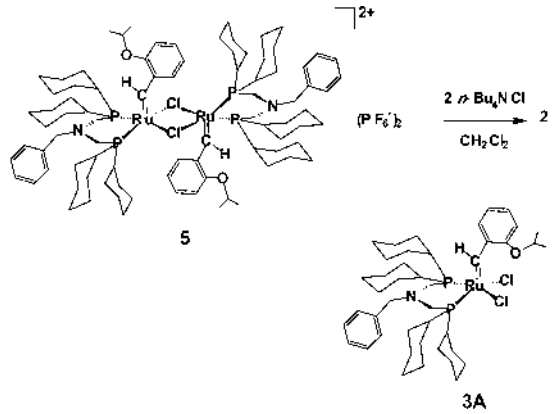

(5)

The shielding of the ortho phenyl proton at δ 8.36 ppm indicates that the oxygen atom is not coordinated to ruthenium in **6**. In the ^{31}P NMR spectrum, only a new singlet is observed at δ 34.5 ppm. The fact that these two phosphorus atoms are equivalent indicates that two DMSO ligands have replaced the two chloride ligands of **3A** (eq 6). The species **6** has only been observed in

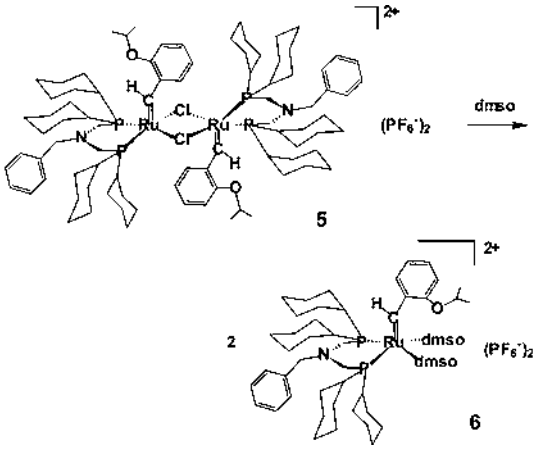

(6)

solution. It is clear that many other ligands could be added to the dicationic dimer **5**.

Syntheses and Properties of the Diiodo Analogue of 3, 7. The reaction of **5** with ligands has been used to synthesize the diiodo analogue of **3A**, **7A**. Thus, addition of 4 equiv of NaI to 1 equiv of **5** in CH_2Cl_2 under ambient conditions gives a 81% yield of **7A** (eq 7).

The ^{1}H NMR spectrum of **7A** contains the signal of a carbene triplet at δ 15.50 ppm and a deshielded ortho phenyl proton at δ 9.69 ppm characteristic of oxygen decoordination, whereas the signal of the tertiary iso-

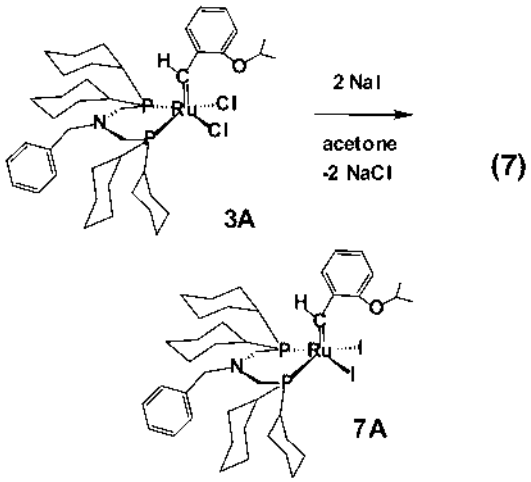

(7)

propyl proton is located at δ 4.80 ppm. As for **3A**, the ^{31}P NMR spectrum only contains a singlet at δ 40.9 ppm and the carbene signal is found at δ 289.6 ppm in the ^{13}C NMR spectrum. Likewise, the MALDI-TOF mass spectrum shows a dominant peak at *m*/*z* 904.21 corresponding to $[M - I]^+$.

A simpler way to synthesize **7A** is to add 2 equiv of NaI to the parent complex **3A** in acetone, which avoids using the Lewis acid. The diiodo complex **7A** is then obtained as a yellow microcrystalline powder in 55% yield (eq 7). The reaction is driven by the formation of NaCl, whose lattice energy is superior to that of NaI, whereas this difference is not compensated by the difference in bond energies between Ru−Cl and Ru−I, since they are both weak, due to the repulsion between the filled d_{Ru} and p_π orbitals.

The diiodo complex **7A** behaves in the same way as the dichloro complex **3A** in solution. The ^{1}H NMR spectrum of **7A** in concentrated solution shows a new triplet for the carbene proton at δ 17.04 ppm, corresponding to the dimer **7B**. Likewise, the ^{31}P NMR spectrum also contains two new doublets at δ 31.7 and 33.5 ppm ($^2J_{P-P}$ = 36.8 Hz). The equilibrium constant *K* found at 25 °C is now $K = 18.5 \pm 0.5$ L mol^{-1}. This value is larger than that obtained for **3A**, which means that **7A** has more tendency than **3A** to dimerize. This is presumably due to the more diffuse orbitals of the iodo ligands, which bridge the two ruthenium fragments more easily than those of the chloro ligands (eq 8).

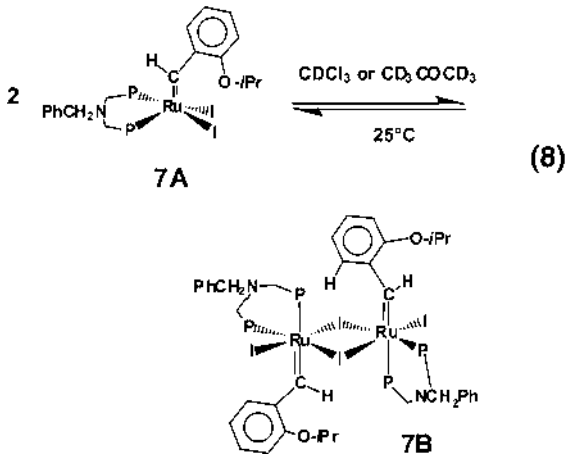

(8)

The electrochemical oxidation and reduction of **7A** on a Pt electrode are, as for **3A**, chemically irreversible even at −30 °C (oxidation, 0.61 and 0.86 V; reduction, −1.00 and −1.33 V vs decamethylferrocene; compare with **3A** in Table 1).

DFT Calculations. Full geometry optimization assuming C_1 symmetry has been carried out on complex **3A**. The major computed data are given in Table 3. Taking into account that such calculations are known to overestimate by ∼3% the metal−ligand bond distances,[19] the optimized geometry is in very good agreement with the X-ray structure (compare Table 3 and Figure 1). The computed HOMO/LUMO gap is significant (1.47 eV), and the LUMO is π^* Ru−C_6 in character. In fact, no strong σ-accepting ability can be attributed to the 16-electron complex **3A** from the analysis of its MO diagram.

To facilitate DFT calculations on its dimer with a reasonable computing time, we have simplified **3A** by replacing its peripheral phenyl, isopropyl, and cyclohexyl substituents by hydrogen atoms: i.e., by the model $Cl_2Ru(=CH\text{-}o\text{-}OHC_6H_4)(HN(CH_2PH_2)_2)$ (**3A°**). The optimized geometry of **3A°**, assuming C_s symmetry, is shown in Figure 2. Its major computed data are given in Table 3. The DFT structures of **3A** and **3A°** are quite similar. The major differences lie in the Ru−P distance and in the Cl−Ru−Cl angle, which are somewhat shorter and larger in **3A°**, respectively. Obviously, these differences originate from the presence of the bulky cyclohexyl groups in **3A**. The frontier orbital diagram of **3A°** is similar to that of **3A**. Thus, **3A°** is not a strong σ-acceptor. Consistently, the optimization of the (**3A°** + ethylene) system led to dissociation.

Apart from the moderate structural differences between **3A** and **3A°,** the charge distributions and electronic structures are quite similar. This gives confidence for using **3A°** as a model of **3A** in the study of its dimerization. Geometry optimization of the dimer model $[Cl_2Ru(=CH\text{-}o\text{-}OHC_6H_4)(HN(CH_2PH_2)_2)]_2$ (**3B°**) led to the molecular structure of C_i symmetry shown in Figure 2, which confirms the spectroscopic evidence of the existence of **3B** in solution (see above). The major computed data of **3B°** are given in Table 3. The large Ru···Ru separation (3.38 Å) indicates clearly that **3B°** is made of two independent distorted-octahedral 18e centers. Consistently, the HOMO−LUMO gap of **3B°** is large and the Ru atom is significantly less positively charged in **3B°** than in **3A°** or **3A**, indicating a significantly lower electrophilic character for the dinuclear species. The total energy of **3B°** is computed to be 0.28 eV higher than twice that of **3A°**. This rather small energy difference is in good agreement with the experimental observation of a monomer−dimer equilibrium in solution at room temperature (see above).

We have also investigated the stability and structure of the dinuclear cationic complex $[Cl_2\{Ru(=CH\text{-}o\text{-}O\text{-}i\text{-}PrC_6H_4)(PhCH_2N(CH_2PCy_2)_2)\}_2]^{2+}$ (**5**) by carrying out calculations on **5** and its simplified model $[Cl_2\{Ru(=CH\text{-}o\text{-}OHC_6H_4)(HCH_2N(CH_2PH_2)_2)\}_2]^{2+}$ (**5°**), assuming C_i and C_{2h} symmetries, respectively. Their major computed data are given in Table 3, and the optimized structure of **5°** is shown in Figure 2. As in the case of **3A** and **3A°**, the geometries and electronic structures of **5** and **5°** are quite similar. Their Ru···Ru distances are 3.917

(19) Garland, M. T., Halet, J.-F., Saillard, J.-Y., *Inorg. Chem.* **2001**, *40*, 3342.

Table 3. Major DFT Computed Data for 3A, 3A°, 3B°, 7B°, 5, 5°, 5I, and 5I°

	C_1	C_s		C_i			C_{2h}	
	3A	**3A°**	**7A°**	**3B°**	**7B°**	**5**	**5°**	**5I°**
				HOMO−LUMO Gap (eV)				
	1.47	1.50	1.50	1.16	1.79	1.40	1.78	1.27
				Distances (Å)				
Ru−C6	1.907	1.916	1.909	1.956	1.956	1.917	1.934	1.919
Ru−P2	2.372	2.292	2.282	2.269	2.264	2.338	2.299	2.297
Ru−P3	2.331			2.558	2.493	2.358		
Ru−X14	2.469	2.440	2.769	2.514	2.811	2.544	2.548	2.832
Ru−X15	2.465			2.618	2.900	2.564		
Ru−Xt				2.469	2.812			
				Angles around C6 (deg)				
Ru−C6−C61	127	126	128	137	138	128	128	130
Ru−C6−H	121	122	121	110	111	120	119	118
C61−C6−H	112	113	112	112	110	112	113	112
				Angles around Ru (deg)				
C6−Ru−P2	88	90	90	96	96	86	88	90
C6−Ru−P3	88			177	176	88		
C6−Ru−X14	104	108	109	90	90	107	112	109
C6−Ru−X15	120			88	87	124		
C6−Ru−Xt				97	97			
P2−Ru−P3	93	92	92	87	88	94	90	91
P2−Ru−X14	90	85	85	97	94	92	90	88
P2−Ru−Xt				87	90			
P3−Ru−X14				90	90			
P3−Ru−X15	86			90	89	87		
P3−Ru−Xt				82	82			
X14−Ru−X15	86	93	92	83	85	80	84	87
Xt−Ru−X15				93	90			
				Mulliken Net Charges				
Ru	1.01	0.90	0.29	0.62	−0.17	0.82	0.73	0.14
C6	−0.38	−0.28	−0.25	−0.22	−0.21	−0.39	−0.25	−0.22
P	0.65; 0.69	0.20	0.20	0.42; 0.25	0.38; 0.31	0.72; 0.74	0.26	0.27
X	−0.45; −0.47	−0.43	−0.13	−0.43	−0.15; 0.23	−0.40; −0.40	−0.30	0.28

and 3.792 Å, respectively, indicating no metal−metal bonding between the two 16e centers. **5** and **5°** can be described as resulting from the fusion of two molecules of **3A** and **3A°** through their chlorine atoms, respectively. Consistently, as for **3A** and **3A°**, their frontier orbitals do not show strong σ-accepting properties.

We have also carried out DFT calculations on the iodine analogues of **3A°**, **3B°**, and **5°**: namely, **7A°**, 7**B°,** and **5°-I**. Their optimized geometries, not shown here, are similar to those of their chlorine relatives, as can be seen from the major computed data shown in Table 3. The major difference between both series concerns the metal net charge, which is significantly lower in the iodine compounds, because of the larger donor ability of I as compared to Cl. This suggests a lower catalytic activity for **7A**. The total energy of **7B°** is computed to be 0.10 eV higher than twice that of **7A°**. This energy difference is significantly lower than that corresponding to the chlorine system, in full agreement with our experimental equilibrium constants (see above).

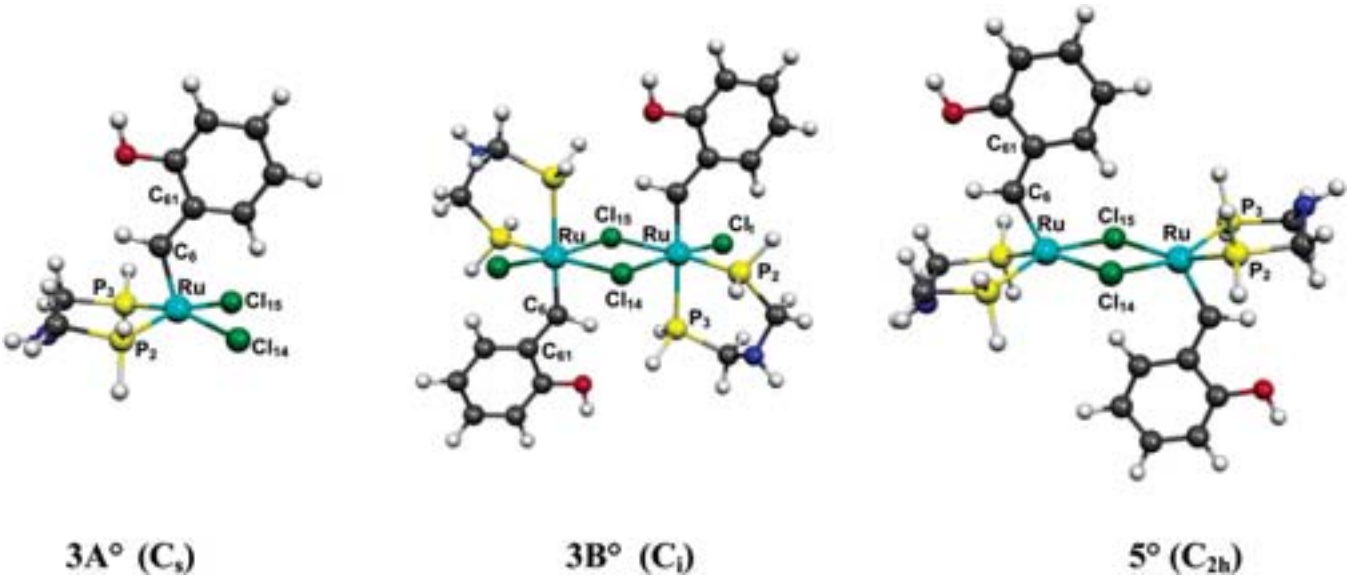

Figure 2. DFT optimized structures of **3A°**, **3B°**, and **5°**.

Syntheses of Four Generations of Dendritic Ruthenium−Benzylidene Complexes. The synthesis of the dendritic ruthenium−benzylidene complexes follows the same procedure as that of the model compound in CH_2Cl_2 under an inert atmosphere. Thus, reaction of the dendritic diphosphine DAB-*dendr*-$[N(CH_2PCy_2)_2]_n$ (G_1, $n = 4$; G_2, $n = 8$; G_3, $n = 16$; G_4, $n = 32$) with 1 equiv of complex **1** per dendritic diphosphine branch gives the dendritic chelating diphosphine ruthenium−benzylidene complexes DAB-*dendr*-$[N(CH_2PCy_2)_2Ru(=CHAr)(Cl)_2]_n$ with Ar = *o*-*i*-Pr-C_6H_4 (G_1, $n = 4$, **8**; G_2, $n = 8$, **9**; G_3, $n = 16$, **10**; G_4, $n = 32$, **11**) (eq 9).

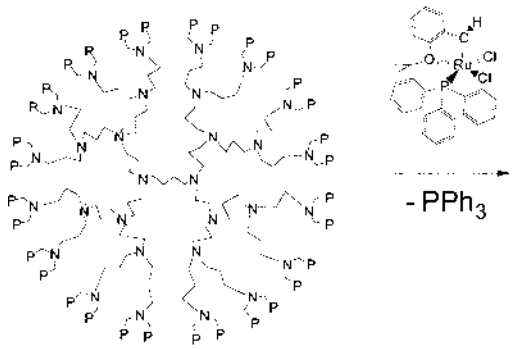

(9)

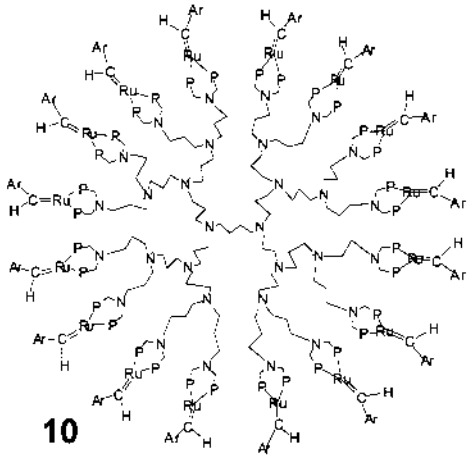

We have also carried out the reaction of the first-generation dendritic diphosphine DAB-*dendr*-$[N(CH_2PCy_2)_2]_4$ with a ratio of 1 equiv of complex **1** per phosphine group, and the ^{31}P NMR spectrum shows, in this case, the formation of a mixture of the same chelating phosphine−ruthenium species DAB-*dendr*-$[N(CH_2PCy_2)_2Ru(=CHAr)(Cl)_2]_4$ (δ 40.9 ppm) and monodentate phosphine−ruthenium complex DAB-*dendr*-$[PCy_2\ CH_2NCH_2PCy_2Ru(=CHAr)(PPh_3)(Cl)_2]_n$ (δ 50.9 ppm). Even with variation of the stoichiometry, this species cannot be obtained alone, and the chelated ruthenium species was always found. Thus, in further experiments, we have always adopted the straighforward stoichiometry of one chelating phosphine per 1 equiv of complex **1**, which avoids the formation of this monodentate diphosphine species.

The metallodendrimers **8** (G_1), **9** (G_2), **10** (G_3), and **11** (G_4) obtained are air-sensitive, in contrast to the monomeric model **3A**, which is air stable. These ruthenium−benzylidene dendrimers are obtained as green microcrystalline powders, the yields of the reactions being between 49 and 65%. They have been characterized by ^1H and ^{31}P NMR and by elemental analysis.

Scheme 1. Intra- vs Interdendritic Dimerization of the Ruthenium Centers in the Metallodendrimers 8−10 (Compare 3A → 3B)

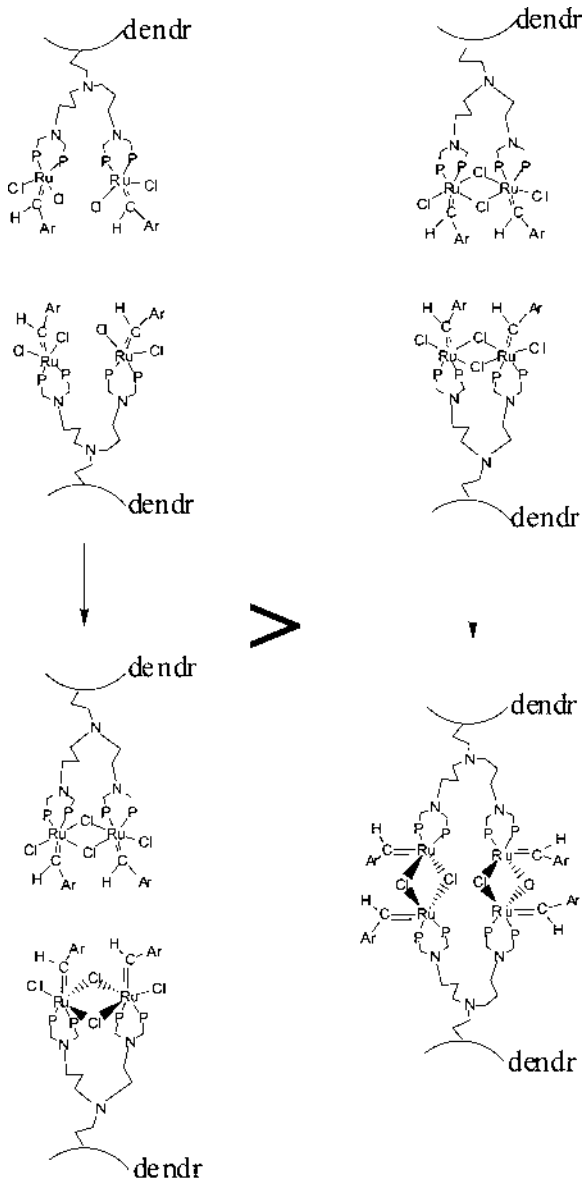

The same kind of dimerization phenomenon occurs as for **3A**. Carbenic protons appear as triplets at both δ 15.66 and 16.96 ppm, which are exactly the same position as for the monomeric model compound **3A**. An importance difference (a dendritic effect) with the model, however, is that, for the dendrimers, the two signals are observed even in very dilute solutions, whereas only the signal at 15.66 ppm was observed in dilute monomer solution. Moreover, the intensity of the other signal at 16.96 ppm increases upon dilution for all the dendrimers, whereas it had disappeared upon dilution in the case of **3A**. Another dendritic effect is also noted among the dendrimer generations: the proportion of the signal at 16.96 ppm increases as the generation number increases at a given concentration of ruthenium−benzylidene species (Table 2). This means that, logically, the dendritic effect increases as the dendrimer generation increases. That the tendency of the ruthenium

species to dimerize is opposite in monomers and dendrimers can be rationalized as follows. It is well-known that the tendency to dimerize monomeric species is decreased with dilution, as noted from the value of the dimerization equilibrium constant. The fact that an opposite trend is observed with the dendrimers means that interdendrimer dimerization must be of minor importance compared to intradendrimer dimerization (dimerization of two ruthenium species located on two different branches of the same dendrimer) because of the entropy effect. Intradendrimer dimerization is not inhibited by dilution. Not only is this the case but also, in contrast, dimerization is favored as dilution increases. We believe that the conformation of the dendrimers is deeply influenced by the dilution to such an extent that it has a consequence on the ability of intradendrimer dimerization. When the dilution increases, the branches of the dendrimers can better expand and rotate in order to find the best possible conformation to dimerize according to specific geometric constraints (Scheme 1).

Ring-Opening-Metathesis Polymerization (ROMP) of Norbornene Using the Monomeric Model Complex 3A, the Dicationic Dimer 5, and the Diiodo Complex 7A. The complex **3** slowly initiates the ROMP of norbornene at 25 °C in $CDCl_3$. This solvent was chosen because all the reactants are soluble in order to follow the reaction by ^1H NMR using the olefinic protons of polynorbornene at 5.19 and 5.32 ppm (respectively cis and trans isomers) and of norbornene at 6 ppm (eq 10).

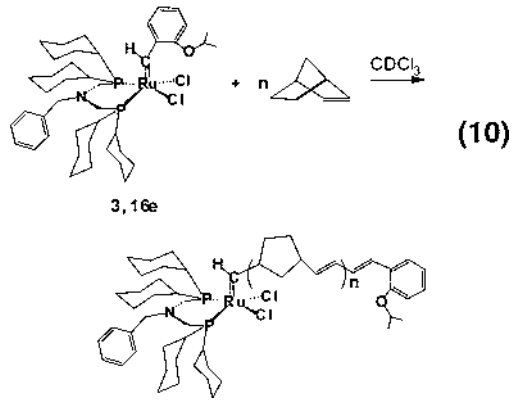

(10)

Using 1% of complex **3A**, the conversion was traces after 3 h, and 24, 38, and 63% after, respectively, 1, 4, and 6 days (trans/cis ratio 80/20). This activity turns out to be much lower that that of Grubbs' catalyst $[Ru(=CHPh)Cl_2(PCy_3)_2]$[20] and Fogg's system, $[RuCl_2(dcypb)(PPh_3)] + 5$ equiv of diazomethane,[11a] which both convert 99% of norbornene to polynorbornene in less than 1 h with the same trans/cis ratio as above. The polynorbornenes have been analyzed by size exclusion chromatography (SEC) after treatment of the Ru polymer with ethyl vinyl ether in order to stop the chain growth and cleave the polynorbornene chain (eq 11).

Table 4. SEC Data for the Norbornene Polymers Obtained by Cleavage of the Metallodendritic Stars Using Ethyl Vinyl Ether after Polymerization in $CDCl_3$ (4 mL) at Room Temperature with Various Norbornene (nb)/Ru Ratios

cat.	nb/Ru	$\overline{M}_n$(obsd)[a]	$\overline{M}_w/\overline{M}_n$	$\overline{DP}_n$[b]	conv[c]	trans[d]
3A	100	5300	2.7	53.2	63	82
8	400	8000	3.4	85.1	100	77
9	800	9500	3.2	101.1	98	86
10	1600	9541	2.2	101.5	98	80

[a] $\overline{M}_n$(obsd) = observed number-averaged molecular weight; $\overline{M}_w$ = weight-average molecular weight. [b] $\overline{DP}_n$ = average number of norbornene units in the polymer in THF based on polystyrene standard (detector: refraction indices). [c] Conversion (%) determined by ^1H NMR; [d] Trans/cis proportions: trans (%) determined by ^1H NMR.

After conversion of 60% norbornene, the observed number-average molecular weight (abbreviated $\overline{M}_n$(exptl)), corresponding to 100 norbornene units/equiv of **3A**, is 5300 (and $\overline{DP}_n = \overline{M}_n(exp)/M$(norbornene) = 53.2), close to the theoretical value ($\overline{M}_n$(theor)), 6000, but the polydispersity index (PDi = 2.7) is relatively high. These data are consistent with initiation activity of almost all the molecules of **3A** with a rather slow initiation compared to propagation. The catalytic system is a living one, since addition of more norbornene (NB) after a polymerization reaction leads to progression of the reaction, as shown by Grubbs.[19] The linearity of $\ln([NB]_0/[NB])$ shows the absence of termination reactions, confirming that the polymerization is living (also checked by the linearity of $\overline{M}_n$(exptl) as a function of the conversion).

At 60 °C, the conversion reaches 80%, but with $\overline{M}_n$(exptl) = 64 300 higher than $\overline{M}_n$(theor) (10 200) with PDi = 2 and $\overline{DP}_n$ = 684. At that temperature, transfer side reactions occur, and only 13% of the ruthenium species are active, which shows that these conditions should not be extended to dendrimers (Table 4).

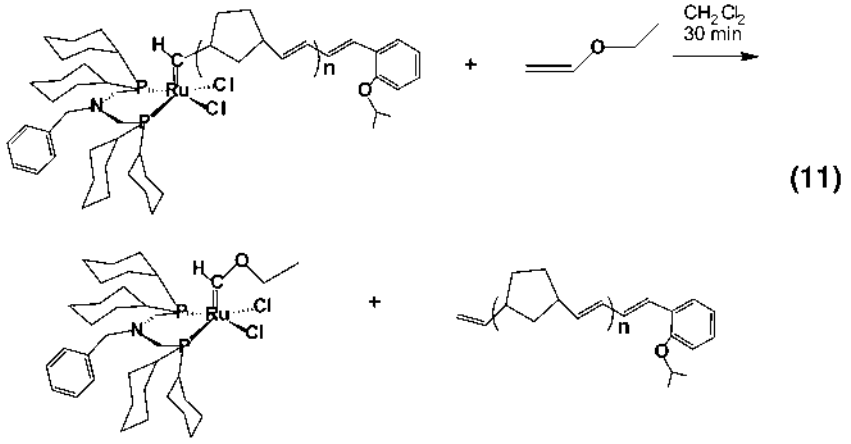

(11)

Scheme 2. Speculated ROMP Mechanism from 3A Involving the Decoordination of One Phosphorus Atom from the Ruthenium Center

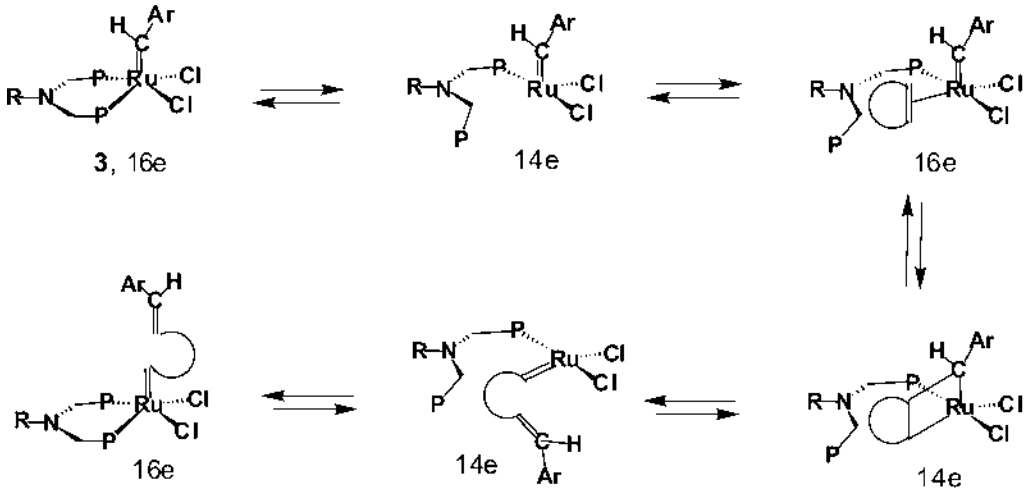

The dicationic dimer **5** also initiates the polymerization of norbornene at 25 °C in $CDCl_3$, but more slowly than **3A**. The conversion using 1% of **5** is only 28% after 2 days and 40% after 6 days (trans/cis ratio 72/28). This result is at first surprising, in view of Hofmann's finding that similar dications are very efficient metathesis catalysts,[10] but the presence of the dangling styryl isopropyl ether group that is present in **5** and not in Hofmann's dicationic dimers may considerably slow the coordination of the olefin by reversibly binding the metal at high rates, preventing NMR observation (for instance, note that the ortho phenyl proton is much less deshielded than in the other compounds **3A**, **7A**, and **8**−**11**). The diiodo complex **7A** gives only traces of polynorbornene under the same conditions, as expected from the results reported by Grubbs[21] and Hofmann,[22] who showed that the iodo analogues were less efficient than the chloro derivatives.

ROMP of Norbornene Initiated by the Three Generations of Dendritic Complexes 8−10. Synthesis of Dendritic-Star Polymers. The ROMP of norbornene has been carried out at 25 °C in $CDCl_3$ with the three dendritic ruthenium−carbene dendrimers DAB-*dendr*-$[N(CH_2PCy_2)_2Ru(=CHAr)(Cl)_2]_n$, ($n$ = 4, 8, and 16; **8**−**10**), in a way similar to that carried out with the monomeric model **3**. The solubilility of the fourth-generation dendrimer DAB-*dendr*-$[N(CH_2PCy_2)_2Ru(=CHAr)(Cl)_2]_{32}$ (**11**) was too weak to undertake norbornene polymerization study with this metallodendrimer. The kinetics of the ROMP reactions were followed by ^{1}H NMR, and the compared data (including those obtained with the model **3**) are represented in Figure 3.

Figure 3 very clearly shows that ROMP of norbornene proceeds more rapidly with the metallodendritic Ru−carbene complexes **8**−**10** than with the monomeric model **3A**. This is the first dramatic dendritic effect. For instance, after 3.5 h at 25 °C in $CDCl_3$, the conversions are as follows: **8** (G_1; 94%) > **9** (G_2; 65%) > **10** (G_3; 59%) > **3** (model; traces) (see Table 4). Thus, the second dendritic effect is that, among the metallodendrimers, the most active initiator is **8**, the first-generation complex, and the activity slowly but regularly decreases upon increasing the dendrimer generations. A possible reason for the dramatically increased rate of polymerization with the dendrimers compared to the model (first dendritic effect, positive) is the labilization of metal−ligand bonds in the dendrimers by interbranch collisions of the metal groups. For instance, it is known that phosphine dissociation plays an important role in the Grubbs catalyst.[8,9] Also, note that the monomeric model **3** is air stable, in contrast to all the corresponding metallodendrimers, although the structure in the coordination sphere is the same for all these complexes. The instability in air could be due to the oxidation of the decoordinated phosphorus atom, since noncoordinated trialkylphosphines are air sensitive. Thus, the destabilization as well as the instability in air provoked in the metallodendrimers might concern the decoordination from the metal of one phosphorus atom of the diphosphine. This path is obviously not favorable, but it could explain why the various other ruthenium−carbene systems in the literature mentioned in the Introduction are more reactive than the present one (for ROMP, and even more so for RCM, for which the present complexes are inactive). Also, the DFT data show that the interaction of ethylene with **3A** is repulsive, which rules out the associative metathesis mechanism. More mechanistic studies are called for in the present system in order

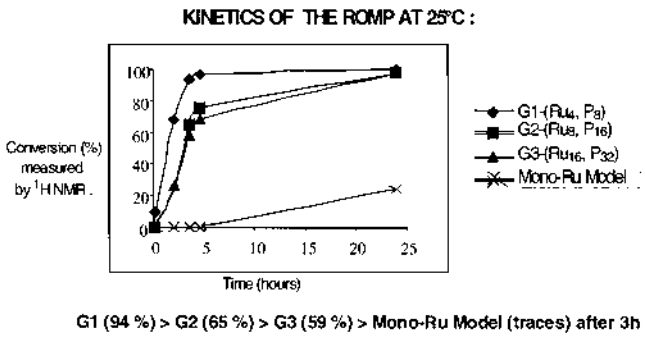

Figure 3. Comparison of norbornene ROMP rates for **3A** and the dendrimers **8**−**10**.

(20) Schwab, P.; Grubbs, R. H.; Ziller, J. W. *J. Am. Chem. Soc.* **1996**, *118*, 100.
(21) Dias, E. L.; Nguyen, S. T.; Grubbs, R. H. *J. Am. Chem. Soc.* **1997**, *119*, 3887.
(22) Volland, M. A. O.; Adhart, C.; Kiener, C. A.; Chen, P.; Hofmann, P. *Chem. Eur. J.* **2001**, *79*, 958.

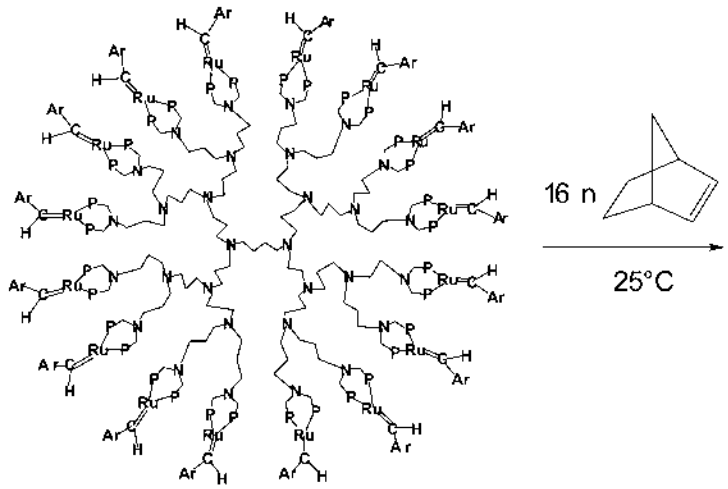

(12)

10

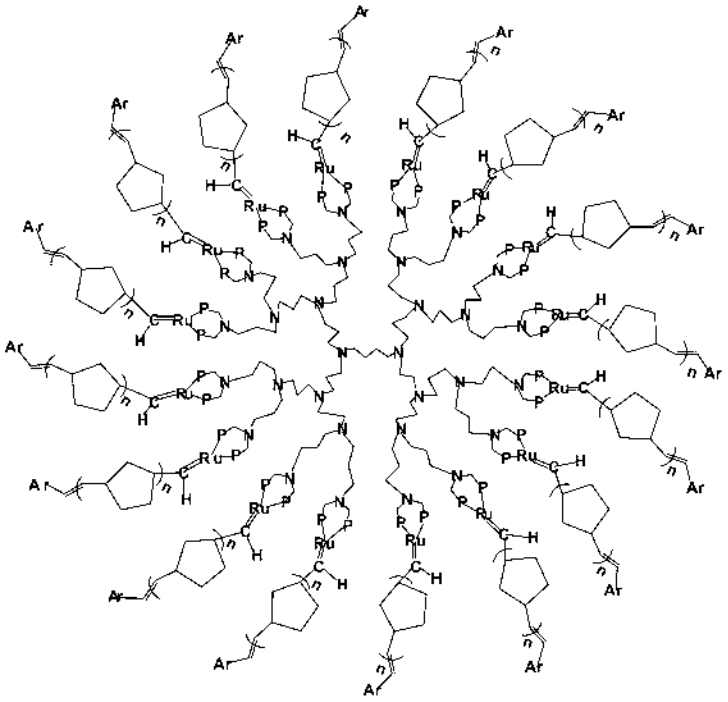

to obtain a better insight into this phenomenon, but the speculated mechanism is represented in Scheme 2.

Indeed, such a situation should be found in other metallodendrimer-catalyzed reactions, but mentions are scarce. Mizigaki et al. have shown that the selective hydrogenation of conjugated dienes catalyzed by the metallodendrimer DAB-*dendr*-$[NCH_2PPh_2)_2PdCl_2]_{16}$ proceeds faster than that catalyzed by $[PdCl_2\{PhN(CH_2PPh_2)_2\}]$.[23]

Among the dendrimers, it is also interesting that the rate decreases when the generation number is increased. We believe that this negative dendritic effect is due to increased bulk around the ruthenium centers when the generation number increases, a classic phenomenon in metallodendrimers. This bulk slows down the approach of the incoming norbornene monomer onto the ruthenium center which is required in the ROMP mechanism.[24] Indeed, the solubility of the metallodendritic carbene complex **11** of this series drops at the 4th generation, which is also a sign of steric congestion. For instance, such a negative dendritic effect was reported by the group of van Koten for the catalysis of the Kharash reaction. Formation of mixed-valent species and chlorine-bridged dimers upon increasing the dendrimer generation was invoked.[25] This explanation is relevant to the dimerization encountered here for the ruthenium−benzylidene complexes. In our case, however, it is difficult to extract the role of the dimerization in the rationalization of the dendritic effects. It is indeed all the more so that the two dendritic effects are operating in opposite directions, whereas dimerization of the ruthenium species is found for all the compounds studied. Thus, we must conclude that the negative role of the dimerization on the ROMP of norbornene is of

(23) Mitzugaki, T.; Oe, M.; Ebitani, K.; Kaneda, K. J. *Mol. Catal. A: Chem.* **1999**, *145*, 329.

(24) Hérisson, J.-L.; Chauvin, Y. *Makromol. Chem.* **1971**, *141*, 161.

(25) Kleij, A. W.; Gossage, R. A.; Jastrzebski, J. T. B. H.; Boersma, J.; van Koten, G. *Angew. Chem., Int. Ed.* **2000**, *39*, 176.

minor importance compared to the other factors mentioned above.

The dendritic-star norbornene polymers have been cleaved using ethyl vinyl ether, as indicated above in the case of the polymerization of norbornene initiated by the monomer **3A**, and submitted to SEC analysis. Gratifyingly, the molar masses of each branch could be determined after cleavage of the metallodendritic cores. Thus, we checked the number of arms in all cases in this way. The data are summarized in Table 4, which contains the experimental and theoretical molar masses as well as the $\overline{DP_n}$ and PDi values; it also includes the data obtained with the polymerization initiated by the monomeric model **3A** for comparison. The observed number-average molecular weight (abbreviated $\bar{M}_n$(obsd)) are similar to the theoretical values, which is an excellent indication that all the Ru−carbene species of the dendrimers are efficient initiators: i.e, converted into propagating species, yielding *metallodendritic stars* (eq 12).

To check if the dendritic system provides living systems, we have added new portions of norbornene at the end of reactions and observed new progresses of the reactions. Also, the plots of $\ln([NB_0]/[NB]) = f(t)$ give straight lines, which shows the absence of termination reactions and indicates that the polymerization reactions follow a unitary internal partial kinetic order in norbornene.

Conclusion and Outlook

We have synthesized a new air-stable ruthenium benzylidene complex that bears a chelating diphosphine and characterized it thoroughly, including by X-ray crystal structure, and have shown that this complex reversibly dimerizes in concentrated solution. The DFT calculations show the structure of this dimer and indicates that the dimerization energy is small. The removal of halide is so facile that it could not be prevented in the low-energy MALDI-TOF mass spectrometry technique. Halide abstraction forms a stable dicationic dimer, whose structure has been determined by DFT calculations, which reacts with ligands to form new benzylidene complexes.

Metallodendritic analogues have been synthesized for four generations. The influence of the concentration on the dimerization of their ruthenium centers was shown to be opposite to that observed for the model, consistent with an essentially intradendritic dimerization that is favored by expansion of the wedges allowed by dilution.

ROMP of norbornene was observed at room temperature and is much faster with the metallodendrimers than with the monomeric model, probably because interbranch collisions labilize metal−ligand bonds, but the polymerization rates decrease as the generation number increases due to the inhibiting steric effects.

These dendritic effects are of great interest, because they play a key role in understanding the chemistry, catalytic properties, and physicochemistry of branched macromolecules. We believe that the large positive dendritic effect is in favor of a decoordination of one phosphorus atom from the metal leading to a 14-electron intermediate to let the olefin coordinate onto the ruthenium center of **3** en route for the Chauvin mechanism.[24] Indeed, these complexes are inactive in RCM and the DFT calculations are in accord with this argument by showing that the interaction between **3A** and ethylene is repulsive, which eliminates the associative mechanism via an 18-electron intermediate before metallacyclobutane formation.

Experimental Section

General Data. The reactions were carried out under an inert atmosphere using Schlenk techniques. Solvents were freshly distilled under argon. Dichloromethane and acetonitrile were dried over calcium hydride, tetrahydrofuran, diethyl ether, and dimethoxymethane were dried over sodium wire using ketyl radical as an indicator, pentane was dried over a Na/K alloy, and methanol was dried over magnesium. Chromatography and filtration were performed using alumina (Prolabo 50−160 μm, II-III). Infrared spectra were carried out using a Paragon 1000 Fourier transform Perkin-Elmer apparatus, calibrated with polystyrene. Samples were analyzed between two NaCl plates, in KBr pellets, or in solution in 0.1 mm thick cells. The 250 MHz ^{1}H and 62.9 MHz ^{13}C NMR spectra were recorded using a Bruker 250 FT spectrometer, and chemical shifts are given in parts per million (δ, ppm) vs tetramethylsilane (TMS). The polynorbornenes have been analyzed by SEC using a Varian 5500 chromatograph equipped with a JASCO HPLC pump of 880-PU type and with three styrene−divinylbenzene copolymer gel (TSK) columns of variable porosity (G 2000 HXL, pore diameter 250 Å; G 3000 HXL, pore diameter 1500 Å; G 4000 HXL, pore diameter 10 000 Å) and double detection (UV spectrophotometer and differential refractometer). Analytical conditions were as follows: flow rate of 0.8 mL/min, pressure of 53 atm, and analysis time of 45 min. The electrochemical studies were carried out under argon using a PAR 273 EG & G galvanostat potentiostat for cyclic voltammetry with the three-electrode format: the working electrode was a METROHM AG CH 9100 HERISSAU hanging mercury drop, the reference electrode was a saturated calomel electrode, and the counter electrode was a platinum wire. Elemental analyses were carried out at the Vernaison CNRS center.

Ruthenium−Benzylidene Complexes. The mixture of the diphosphine or dendritic phosphine DAB-*dendr*-[N(CH$_2$-PCy$_2$)$_2$]$_n$ and [RuCl$_2$(=CH-*o*-O-^{i}PrC$_6$H$_4$)PPh$_3$] was stirred at room temperature in CH_2Cl_2 under nitrogen for 72 h (24 h for the diphosphine). The reaction mixture was concentrated under reduced pressure to about 2 mL, and pentane (20 mL) was added. The product precipitated in the form of green microcrystals and dried under high vacuum.

Monomer 3A. Yield: 86%. ^{1}H NMR ($CDCl_3$, 400 MHz): δ 0.91−2.60 (m, Cy), 1.32 (d, $^3J_{H,H}$ = 6.5 Hz, OCH(C*H*$_3$)$_2$), 2.94 (m, NC*H*$_2$P), 3.69 (s, NC*H*$_2$Ph), 4.79 (m, OC*H*(CH$_3$)$_2$), 6.70−7.63 (m, H arom), 9.33 (d, $^1J_{H,H}$ = 7.2 Hz, 1H, H arom), 9.55 (d, $^1J_{H,H}$ = 7.2 Hz, 2H, H arom), 15.66 (t, $^3J_{H,P}$ = 15.7 Hz, 1H, Ru=CH), 16.96 (t, $^3J_{H,P}$ = 13.3 Hz, 2H, Ru=CH). ^{13}C NMR ($CDCl_3$, 100 MHz): δ 22.8 (s, OCH(*C*H$_3$)$_2$), 26.3−30.2 (m, Cy), 34.6 (d, $^2J_{C,P}$ = 23.2 Hz, Cy), 35.4 (t, $^3J_{C,P}$ = 11.6 Hz, N*C*H$_2$Ph), 36.6 (d, $^2J_{C,P}$ = 23.2 Hz, Cy), 37.7 (t, $^3J_{C,P}$ = 11.6 Hz, N*C*H$_2$Ph), 38.9 (dd, $^1J_{C,P}$ = 52.6 Hz, $^3J_{C,P}$ = 23.2 Hz, Cy), 41.6 (dd, $^1J_{C,P}$ = 154.8 Hz, $^3J_{C,P}$ = 38.7 Hz, Cy), 45.5 (N*C*H$_2$P), 69.3 (N*C*H$_2$P), 70.0 (s, OCH(*C*H$_3$)$_2$), 70.5 (s, OCH(*C*H$_3$)$_2$), 112.0, 112.7, 120.7, 122.1, 128.6, 130.5, 131.1, 132.4, 134.0, 134.2, 135.0, 135.4, 135.7, 136.9, 137.2, 140.5, 143.7, 148.1, 150.4 (C arom), 291.5 (t, $^2J_{C,P}$ = 80.1 Hz, Ru=*C*H), 308.8 (t, $^2J_{C,P}$ = 80.1 Hz, Ru=*C*H). ^{31}P{^{1}H,^{13}C} NMR ($CDCl_3$, 81.03 MHz): δ 40.9 (s, CH_2PCy_2), 36.8 and 41.2 (d, $^2J_{P,P}$ = 45.9 Hz, CH_2PCy_2). MALDI-TOF mass spectrum (*m*/*z*): calcd for $C_{43}H_{67}P_2OCl_2RuN$, 847.92; found, 812.45 [M − Cl]$^+$. Anal. Calcd for $C_{43}H_{67}P_2OCl_2RuN$: C, 60.91; H, 7.96. Found: C, 60.42; H, 7.91.

G$_1$-Ru$_4$P$_8$ (8). Yield: 65%. ^{1}H NMR ($CDCl_3$, 200 MHz): δ 0.52−4.14 (m, OCH(CH$_3$)$_2$, Cy, NCH$_2$CH$_2$CH$_2$N, NCH$_2$CH$_2$CH$_2$-CH$_2$N, NCH$_2$P), 4.70 (m, OCH(CH$_3$)$_2$), 6.45−7.88 (m, H arom), 9.40 (d, $^1J_{H,H}$ = 9,1 Hz, 4H, H arom), 9.67 (m, 8H, H arom), 15.63 (t, $^3J_{H,P}$ = 15,6 Hz, 4H, Ru=CH), 16.87 (m, 8H, Ru=CH).

$^{31}P\{^{1}H,^{13}C\}$ NMR ($CDCl_3$, 81.03 MHz): δ 40.9 (s, CH_2PCy_2). Anal. Calcd for $C_{160}H_{272}Cl_8N_6O_4P_8Ru_4$: C, 58.59; H, 8.36. Found: C, 57.64; H, 8.35.

G_2-Ru_8P_{16} (9). Yield: 63%. ^1H NMR ($CDCl_3$, 200 MHz): δ 0.52−4.15 (m, $OCH(CH_3)_2$, Cy, $NCH_2CH_2CH_2N$, $NCH_2CH_2CH_2$-CH_2N, NCH_2P), 4.71 (m, $OCH(CH_3)_2$), 6.45−8.07 (m, H arom), 9.40 (m, 8H, H arom), 9.63 (m, 16H, H arom), 15.63 (br., 8H, Ru=CH), 16.90 (broad, 16H, Ru=CH). $^{31}P\{^{1}H,^{13}C\}$ NMR ($CDCl_3$, 81.03 MHz): δ 40.89 (s, CH_2PCy_2). Anal. Calcd for $C_{328}H_{560}Cl_{16}Ru_8O_8P_{16}N_{14}$: C, 58.80; H, 8.42. Found: C, 58.64; H, 8.25.

G_3-$Ru_{16}P_{32}$ (10). Yield: 60%. ^1H NMR ($CDCl_3$, 200 MHz): δ 0.24−4.25 (m, $OCH(CH_3)_2$, Cy, $NCH_2CH_2CH_2N$, $NCH_2CH_2CH_2$-CH_2N, NCH_2P), 4.71 (m, $OCH(CH_3)_2$), 6.45−8.07 (m, H arom), 9.40 (m, 16H, H arom), 9.63 (m, 32H, H arom), 15.63 (broad, 16H, Ru=CH), 16.90 (broad, 16H, Ru=CH). $^{31}P\{^{1}H,^{13}C\}$ NMR ($CDCl_3$, 81.0 MHz): δ 40.9 (s, CH_2PCy_2). Anal. Calcd for $C_{664}H_{1136}Cl_{32}Ru_{16}O_{16}P_{32}N_{30}$: C, 58.90; H, 8.46. Found: C, 58.73; H, 8.61.

G_4-$Ru_{32}P_{64}$ (11). Yield: 49%. ^1H NMR ($CDCl_3$, 200 MHz): δ 0.79−3.95 (m, $OCH(CH_3)_2$, Cy, $NCH_2CH_2CH_2N$, $NCH_2CH_2CH_2$-CH_2N, NCH_2P), 4.69 (m, $OCH(CH_3)_2$), 6.45−8.07 (m, H arom), 9.42 (m, 32H, H arom), 9.61 (m, 64H, H arom), 15.62 (broad, 32H, Ru=CH), 16.89 (broad, 32H, Ru=CH). $^{31}P\{^{1}H,^{13}C\}$ NMR ($CDCl_3$, 81.0 MHz): δ 40.9 (s, CH_2PCy_2). Anal. Calcd for $C_{664}H_{1136}Cl_{32}Ru_{16}O_{16}P_{32}N_{30}$: C, 60.83; H, 8.74. Found: C, 55.16; H, 8.10. The analysis was repeatedly low in C, due to large amounts of entrapped inorganic impurities inside the dendrimer.

Dicationic Dimer 5. $AgPF_6$ (0.060 g, 0.353 mmol) and complex **3** (0.200 g, 0.235 mmol) were stirred in 5 mL of CH_2Cl_2 under a nitrogen atmosphere for 1 day at room temperature, and then the solvent was partly removed under vacuum until a volume of 2 mL was reached. Complex **5** was then precipitated by adding 30 mL of pentane. The obtained green powder was washed with 3 × 10 mL of pentane and dried overnight under vacuum. Complex **5** was obtained in 52% (200 mg) yield as a green powder. ^1H NMR ($CDCl_3$, 200 MHz): δ 0.65−2.57 (m, 88H, Cy), 1.32 (d, $^3J_{H-H}$ = 6.5 Hz, 12 H, $OCH(CH_3)_2$), 3.12 (m, 8H, NCH_2P), 3.70 (s, 4H, NCH_2Ph), 4.76 (m, 2H, $OCH(CH_3)_2$), 6.85−7.95 (m, 16H, H arom), 9.64 (d, $^1J_{H-H}$ = 7.6 Hz, 2H, H arom), 17.24 (t, $^3J_{H-P}$ = 12.7 Hz, 2H, Ru=CH). ^{13}C NMR ($CDCl_3$, 100 MHz): δ 21.9 (s, $OCH(CH_3)_2$), 25.7−29.8 (m, Cy), 32.9 (m, Cy), 35.7 (m, NCH_2Ph), 40.9 (m, NCH_2P), 69.9 (s, $OCH(CH_3)_2$), 112.7−148.7 (s, C arom), 311.9 (m, Ru=CH). $^{31}P\{^{1}H,^{13}C\}$ NMR ($CDCl_3$, 81.0 MHz): δ 45.2 (s, CH_2PCy_2), 117.6−170.4 (sept., $^1J_{P-F}$ = 81.2 Hz, PF_6^-).

Diodo Complex 7. From 3. NaI (0.017 g, 0.116 mmol) and complex **3** (0.049 g, 0.058 mmol) were stirred for 1 day in 5 mL of acetone under a nitrogen atmosphere, the reaction medium was filtered, the solvent was removed under vacuum, and the solid residue was extracted with 3 × 10 mL of CH_2Cl_2. The solution was concentrated to 2 mL, and 30 mL pentane was added. The precipitate was washed with 3 × 10 mL of pentane and dried overnight under vacuum. Compound **7** was then obtained as a yellow powder in 55% (33 mg) yield.

From 5. NaI (0.040 g) and complex **5** (0.110 mg, 0.067 mmol) were stirred for 1 day in 5 mL of acetone at room temperature, the reaction mixture was filtered, the solvent was removed under vacuum, and the solid residue was extracted with 3 × 10 mL of CH_2Cl_2. The solution was concentrated to 2 mL, and 30 mL of pentane was added. The precipitate was washed with 3 × 10 mL of pentane and dried overnight under vacuum, Compound **7** was obtained as a yellow powder in 81% (113 mg) yield.

^1H NMR ($CDCl_3$, 250 MHz): δ 0.37−2.97 (m, Cy), 1.32 (d, $^3J_{H-H}$ = 6.6 Hz, $OCH(CH_3)_2$), 3.34 (m, NCH_2P), 3.75 (NCH_2Ph), 4.80 (m, $OCH(CH_3)_2$), 6.70−7.63 (m, H arom), 9.69 (d, $^1J_{H-H}$ = 7.5 Hz, 1H, H arom), 10.49 ($^1J_{H-H}$ = 7.5 Hz, 2H, H arom), 15.50 (t, $^1J_{P-H}$ = 13.4 Hz, 1H, Ru=CH). ^{13}C NMR ($CDCl_3$, 100 MHz): δ 22.5 (s, $OCH(CH_3)_2$), 25.2−30.2 (m, Cy), 35.1 (m, Cy), 36.2 (m, NCH_2Ph), 36.9 (m, Cy), 40.5 (m, NCH_2P), 42.3 (m, Cy), 44.2 (NCH_2P), 68.8 (s, $OCH(CH_3)_2$), 69.3 (s, $OCH(CH_3)_2$), 69.8 (s, $OCH(CH_3)_2$), 111.3−149.2 (C arom), 289.6 (m, Ru=CH), 308.8 (m, Ru=CH). $^{31}P\{^{1}H,^{13}C\}$ NMR ($CDCl_3$, 81.0 MHz): δ 40.9 (s, CH_2PCy_2); 31.7 and 33.5 (d, $^2J_{P-P}$ = 36.8 Hz, CH_2PCy_2). MALDI-TOF mass spectrum (*m*/*z*): calcd for $C_{43}H_{67}NRuOI_2P_2$, 1030.82; found, 904.21 $[M - I]^+$.

Polymerization of Norbornene by Monomeric and Dendrimeric Ruthenium Complexes. Norbornene and the ruthenium−benzylidene catalyst (0.003 mmol) were introduced in a dry Schlenk tube under an inert atmosphere in 5 mL of $CDCl_3$, and the reaction was followed at 25 °C by ^1H NMR (see text). At the end of this polymerization reaction, the solvent was removed under vacuum, and traces of ethyl vinyl ether were added in 5 mL of CH_2Cl_2 solution in order to remove the polymer chain from the ruthenium center. After 30 min, the mixture was filtered over silica gel and the filtered solution was added to 30 mL of methanol, which resulted in the precipitation of polynorbornene. These samples were analyzed by SEC using THF as the eluent at 25 °C.

Computational Details. Density functional calculations were carried out using the Amsterdam density functional (ADF) program[26] developed by Baerends and co-workers.[27] The Vosko−Wilk−Nusair parametrization[28] was used for the local density approximation (LDA) with gradient correction for exchange (Becke88)[29] and correlation (Perdew86).[30] Relativistic corrections were added using the ZORA (Zeroth Order Regular Approximation) scalar Hamiltonian for all the computed iodine compounds.[31] The atom electronic configurations were described by a triple-ξ Slater-type orbital (STO) basis set for H 1s, C, O, and N 2s and 2p, P and Cl 3s and 3p, and I 5s, 5p, and 4d augmented with a 3d single-ξ polarization function for C, O, P, and Cl with a 2p single-ξ polarization function for H. A triple-ξ STO basis set was used for Ru 4d and 5s and a single-ξ for Ru 5p. The frozen-core approximation was used to treat the core electrons.

Acknowledgment. We are grateful to Dr. George Bravic (ICMCB, University Bordeaux I) for recording and discussing the X-ray crystal structure of **3** reported in ref 16, to Dr. Jean-Claude Blais (University Paris 6) for recording and discussing the MALDI-TOF mass spectra of **3** and **7**, to Dr. Jaime Ruiz for assistance in the electrochemical experiments, to the Ministère de la Recherche et de la Technologie for a thesis grant to S.G., and to the Institut Universitaire de France (D.A.), the CNRS and the Universities of Bordeaux I (including the Centre de Recherche de Chimie Moléculaire) and of Rennes I for financial support. Computing facilities were provided by the Centre de Ressources Informatiques (CRI) of Rennes and the Institut de Développement et de Ressources en Informatique Scientifique du Centre National de la Recherche Scientifique (IDRIS-CNRS).

OM030608R

(26) Amsterdam Density Functional program (ADF 2000.02); Division of Theoretical Chemistry, Vrije Universiteit, De Boelelaan 1083, 1081 HV Amsterdam, The Netherlands; http://www.scm.com.

(27) (a) Baerends, E. J.; Ellis, D. E.; Ros, P. *Chem. Phys.* **1973**, *2*, 41. (b) Baerends, E. J.; Ros, P. *Int. J. Quantum Chem.* **1978**, *S12*, 169. (c) Boerringter, P. M.; te Velde, G.; Baerends, E. J. *Int. J. Quantum Chem.* **1988**, *33*, 87. (d) te Velde, G.; Baerends, E. J. *Int. J. Quantum Chem.* **1992**, *99*, 84.

(28) Vosko, S. H.; Wilk, L.; Nusair, M. *Can. J. Phys.* **1980**, *58*, 1200.

(29) (a) Becke, A. D. *J. Chem. Phys.* **1986**, *84*, 4524. (b) Becke, A. D. *Phys. Rev. A* **1988**, *38*, 3098.

(30) Perdew, J. P. *Phys. Rev. B* **1986**, *33*, 8822.

(31) (a) van Lenthe, E.; Baerends, E. J.; Snijders, J. G. *J. Chem. Phys.* **1993**, *99*, 4597. (b) van Lenthe, E.; Baerends, E. J.; Snijders, J. G. *J. Chem. Phys.* **1994**, *101*, 9783. (c) van Lenthe, E.; van Leeuwen, R.; Baerends, E. J. *Int. J. Quantum Chem.* **1996**, *57*, 281. (d) van Lenthe, E.; Baerends, E. J.; Snijders, *J. Chem. Phys.* **1996**, *105*, 6505. (e) van Lenthe, E.; Ehlers, A.; Baerends, E. *J. Chem. Phys.* **1999**, *110*, 8943.

Annexe 2

$Mo_6X^i_8$ NANOCLUSTER CORES (X= Br, I): FROM INORGANIC SOLID STATE COMPOUNDS TO HYBRIDS.

Stéphane Cordier*[a], Kaplan Kirakci[a], Denise Méry[b], Christiane Perrin[a], Didier Astruc[b]

[a]Institut de Chimie de Rennes, LCSIM, UMR 6511 CNRS-Université de Rennes 1, Avenue du Général Leclerc, 35042 Rennes cedex, France.
[b]Nanosciences and Catalysis Group, LCOO, UMR CNRS N° 5802, Université Bordeaux I, 351 Cours de la Libération, 33405 Talence Cedex, France.

Corresponding author: Stéphane Cordier, stephane.cordier@univ-rennes1.fr, FAX: (+33) 2 23 23 67 99. Institut de Chimie de Rennes, LCSIM UMR 6511 CNRS, Université de Rennes 1, Campus de Beaulieu, Avenue du Général Leclerc, 35042 Rennes Cedex, France.

This micro-review article is dedicated to our distinguished colleague and friend Professor Gerard van Koten

Abstract:

The $[(M_6L^i_8)L^a_6]$ units (^{a} = apical, ^{i} = inner) are the basic building blocks in the molybdenum, tungsten and rhenium octahedral cluster chemistry. Nano-sized metallic clusters are easily obtained by solid-state synthesis with transition elements associated with halogens or chalcogens (L). The intrinsic properties of M_6 cluster units -one electron reversible redox process, magnetism and luminescence- depend on the nature of the metal and ligands. The solubilization of M_6 solid state compounds provides $[(M_6L^i_8)L^a_6]^{n-}$ building blocks with individual properties that can be further used for the design of hybrid organic/inorganic materials. In this microreview, we will focus on our recent results concerning the synthesis and the use of solid state Mo_6 cluster bromides and iodides for the design of hybrid organic/inorganic Mo_6 cluster compounds.

Keywords: metallic cluster, hybrid compounds, molybdenum, molecular assembly, functionalization, dendrimer.

I. Introduction.

Numerous hybrid materials based on metal-oxo and metal-oxo-alkoxo clusters in which the metal exhibits a high oxidation state have been reported in the literature [1]. Such clusters must be differentiated from metallic clusters in which the metal exhibits a low oxidation state. The term *metal atom cluster* was introduced by F.A. Cotton to define a finite group of metal atoms held together via metal-metal bonds [2]. In a *metal-atom cluster,* the metallic electrons are delocalized on all the metal centers leading to particular intrinsic properties (magnetic, optical, redox processes [3]). Nano-sized metallic clusters are routinely obtained by solid state synthesis with transition elements associated with halogen or chalcogen ligands (L). The $[(M_6L^i_8)L^a_6]^{n-}$ unit (^{a} = apical, ^{i} = inner according to the Schäfer and Schnering notation [4] (figure 1)) constitutes the basic building blocks in the rhenium and molybdenum octahedral cluster chemistry [3, 5]. The octahedral cluster is bonded to eight face capping ligands to form a rigid $Mo_6X^i_8$ cluster core that is stalibilized by six additional semi-labile apical ligands (L^a) located in terminal position. The condensation within the solid of $M_6L^i_8L^a_6$ units *via* shared L^{i-a} and L^{a-i} ligands engenders significant electronic interactions between neighboring units resulting in transport properties, as illustrated by the well known Chevrel phases [6]. On the other hand, cluster compounds based on discrete $M_6L^i_8L^a_6$ and/or L^{a-a} interconnected units exhibit a strong molecular character characterized by insulating properties.

The solubilization of M_6 solid state compounds provides $[(M_6L^i_8)L^a_6]^{n-}$ building blocks with individual properties that can be used in the design of hybrid organic/inorganic compounds. Many hybrid compounds based on $Re_6Se^i_8$ [7] and, to a less extend, on $Mo_6Cl^i_8$ cluster [8] cores have been reported in the literature. In this microreview, we will focus on our recent results concerning the synthesis and the use of solid state Mo_6 cluster bromides and

iodides as precursors for the design of hybrid organic/inorganic cluster compounds by solution reactions.

II. Experimental: synthesis of solid state precursors and their solubilization.

$MoBr_2$ and MoI_2 cluster precursors are prepared at high temperature by solid/gas and solid/solid reactions respectively [9]. The structures of these two halides are based on $Mo_6X^i_8X^a_6$ units that share four apical ligands with four adjacent units in the equatorial plane. These interconnections lead to $Mo_6X^i_8X^{a\text{-}a}{}_{4/2}X^a_2$ layers that are interpenetrated and held together *via* van der Walls contacts between halogen ligands of adjacent layers. Owing to this bi-dimensional interconnection of units, these binary compounds are poorly soluble in common organic solvents and are insoluble in water. However, $Mo_6Br^i_8Br^{a\text{-}a}{}_{4/2}Br^a_2$ can be hardly solubilized in a H_2O/ethanol mixture (50/50) in an erlenmeyer flask equipped with a soxhlet device (3 days). The addition of a NaN_3 saturated solution to the previous one leads to a direct apical ligand exchange to form $[Mo_6Br_8(N_3)_6]^{2-}$ units that can be crystallized as $Na_2Mo_6Br^i_8(N_3)^a_6.2H_2O$ salt after evaporation of the solvents [10]. The substitution of N_3^- groups for Br^- anions provide original $[Mo_6Br_8(N_3)_6]^{2-}$ units soluble in organic solvents. On the other hand, the reactions between binary halides and cesium salts (excision reaction) yield to the formation of $Cs_2Mo_6X^i_8X^a_6$ ternary compounds [11], characterized by isolated $(Mo_6X^i_8X^a_6)^{2-}$ units, that are soluble in common organic solvents. However, exchange in solution of Cs^+ by $(Bu_4N)^+$ cations enables to obtain $(Bu_4N)_2Mo_6X^i_8X^a_6$, more soluble in common organic solvents [11]. The use of the inorganic ternary compounds, $Cs_2Mo_6X^i_8X^a_6$, in the preparation of $(Bu_4N)_2Mo_6X^i_8X^a_6$ avoids acido-basic reactions contrary to usual methods reported in the literature in particular for $(Bu_4N)_2Mo_6Br^i_8Br^a_6$ [11]. Indeed, the $(Bu_4N)_2Mo_6X^i_8X^a_6$ (X = Cl, Br) series makes relevant precursors for axially substituted

clusters containing $M_6L^i_8$ cluster cores [8a]. The $M_6L^i_8$ core is very stable owing to the covalent M-X^i bonds, but the weaker M-X^a bonds favour apical ligand exchanges.

III. Crystallization of Mo_6 anionic units with organometallic cations.

Novel hybrid inorganic/organometallic compounds have been obtained from the crystallization of inorganic $[M_6L_{14}]^{2-}$ anionic cluster units with $[Cp^*(dppe)Fe\text{-}NCMe]^+$ organometallic entities as the cationic counter cation (Cp* = pentamethylcyclopentadienyl, dppe = 1,2-bis(diphenylphosphino)ethane). After dissolution at room temperature of $Cs_2M_6L_{14}$ precursors in acetonitrile (M_6L_{14} = $[Mo_6Br_{14}]^{2-}$ and $[Mo_6I_{14}]^{2-}$ and even $[Re_6S_6Br_8]^{2-}$) and [Cp*(dppe)Fe-NCMe]Cl, the reaction consists in a metathesis of Cl^- anion by $[M_6L_{14}]^{2-}$ di-anions by precipitation of the CsCl salt. The crystal structures of the $[Cp^*(dppe)Fe\text{-}NCMe]_2.M_6L_{14}$ [12] series reveal that inorganic and organic entities can be assembled without any structural modification of each partner whatever the M_6L_{14} unit. Indeed these M_6L_{14} units could be further used for the crystallization of other novel cationic organometallic entities when usual anionic counter parts (BF_4^- or PF_6^-) give unfruitful results. In particular, the $Cs_2M_6L_{14}$ series could be avantageously used instead of M'ReX_6 (M'= manovalent cation) salts for the crystallization of organic or organometallic cations from chloride precursors by precipitation of CsCl.

Another interesting recent result has been the synthesis of the $(BEDO\text{-}TTF)_2Mo_6Br_{14}(PhCN)_2$ hybrid [13a] by electro-oxydation of [BEDO-TTF] (BEDO-TTF = bis(ethylenedioxy)tetrathiafulvalene) in the presence of $[Mo_6Br_{14}]^{2-}$ anionic units and Ph-CN. In this compound, the $[Mo_6Br_{14}]^{2-}$ anionic units act as spacers in the $[BEDO\text{-}TTF]^+$ network that prevent the formation of cationic dimers. Contrary to other $[TTF\text{-}BEDO]^{n+}$ based compounds, as for instance (BEDO-TTF)-I_3 [13b], no overlapping occurs between the oxygen

and sulfur atomic orbitals of adjacent $[TTF\text{-}BEDO]^{n+}$ organic cations. Consequently, instead of a metallic character in (BEDO-TTF)-I_3, a paramagnetic behavior from to the $[BEDO\text{-}TTF]^{+}$ entity is observed in $(BEDO\text{-}TTF)_2Mo_6Br_{14}(PhCN)_2$.

IV. Functionalization of Mo_6 clusters.

The functionalization of Mo_6 clusters consists in the substitution of apical halogen ligands by functional coordinating ligands. Contrary to the direct exchange of apical bromine by azide groups in hydro-alcoholic mixture, the substitution of apical bromine or iodine cannot be reached by the direct reaction of $Mo_6X^i_8X^a_6$ anionic units and coordinating ligands in organic solvents. Indeed, a previous reaction with silver salts is necessary to replace apical ligands by more labile groups such as triflates $(CF_3SO_3)^-$ [8a, 14] or solvent molecules. $(Bu_4N)_2Mo_6X^i_8(CF_3SO_3)^a_6$ (figure 2) and $(SbF_6)_4Mo_6X^i_8(CH_3CN)^a_6$ precursors are easily obtained from $(Bu_4N)_2Mo_6X^i_8X^a_6$ by reaction with $AgCF_3SO_3$ and $AgSbF_6$ in organic solvents. In a second step, solvent or triflate molecules are easily replaced by functionalized phenolate or pyridine ligands.

For instance, the octahedral molybdenum cluster compound $[n\text{-}Bu_4N]_2[Mo_6Br_8(CF_3SO_3)_6]$ undergoes substitution of all six terminal triflate ligands with the dendronic phenolate ligand *p*-NaO-$C_6H_4C\{CH_2CH_2CH_2Si(Me)_2Fc\}_3$ to give the Mo_6-cluster-cored octadecylferrocenyl dendrimer [14] (figure 3). The CV of these nanomolecules showed a single oxidation wave for the 18 ferrocenyl redox centers indicating that these 18 ferrocenyl centers are seemingly equivalent as in other polyferrocenyl dendrimers [15]. Addition of $[n\text{-}Bu_4N]_2[ATP]$ (ATP = adenosyl triphosphate) to the electrochemical cell leads to the appearance of a new ferrocenyl wave at less positive potential (ΔE = 90 mV) whose intensity is proportional to the proportion of $[n\text{-}Bu_4N]_2[ATP]$ salt added. This is the indication of an

interaction of strong type according to the Kaifer-Echegoyen model [16] as already observed previously with other polyamidoferrocenyl and polysilylferrocenyl dendrimers. It is noteworthy that the shift of potential is much smaller than in gold-nanocluster-cored dendrimers.

The substitution of the six triflate ligands by pyridine or various pyridine derivatives has also been achieved [17]. Indeed, $[n\text{-}Bu_4N]_2[Mo_6Br_8(CF_3SO_3)_6]$ undergoes substitution of all six terminal triflate ligands by pyridine ligands in pyridine at 60°C (2 d) to yield the hexapyridine clusters. It also reacts in refluxing THF with the *para*-substitued pyridines 4-*tert*-Bupy and 4-vinylpy to give the *para*-substituted hexapyridine clusters $[Mo_6Br_8(p.Py\text{-}R_x)_6]$ $[CF_3SO_3]_4$ (R_x = *tert*-Bu, $CH{=}CH_2$) and with the new dendronic pyridine derivative 3,3'-$\{CH_2Op\text{-}C_6H_4C(CH_2CH{=}CH_2)_3\}_2Py$, (7 d), to give the relatively air stable Mo_6-cluster-cored 36-allyl dendrimer $[Mo_6Br_8(3,5\text{-}\{CH_2OC_6H_4C(CH_2CH{=}CH_2)_3\}_2Py)_6]$ $[CF_3SO_3]_4$ (figure 4). Other, original hexa-functionalized Mo_6 have been successfully obtained [14] using organometallic pyridine ligands such as $[RuCp(PPh_3)_2(\eta^1\text{-}C_2\text{-}4\text{-pyridinyl})]$, and 1-ferrocenyl-2-(4-pyridinyl) acetylene.

V. Concluding remark.

In the present microreview, we have presented an overview of our recent research concerning the elaboration of hybrid organic/inorganic Mo_6 nanocluster materials starting from solid state precursors. It clearly illustrates the strong complementarity between the solid state and solution synthetic routes. Hybrid materials can be prepared according to two approaches : (i) cristallization of cluster anionic units with organic or hybrid organic/inorganic counter cations, (ii) functionnalization of Mo_6 cluster by organic or hybrid organic/inorganic ligands in apical position. The introduction of functionalized ligands around

$Mo_6Br^i_8$ and $Mo_6I^i_8$ cluster cores has open a new field of research in material chemistry. Indeed, new hybrid materials could be obtained *via* polymerization reactions or sol-gel processes by the introduction of vinylpyridin or *N*-vinyl-imidazol (as previously obtained with $Re_6Se^i_8$ [18a] and $Mo_6Cl^i_8$ cluster cores [18b]) but also organosilanol ligands around the clusters. In particular, $[Mo_6X_8(3,5\text{-}\{CH_2OC_6H_4C(CH_2CH{=}CH_2)_3\}_2Py)_6]^{4-}$ functionnalized units could be used as a building block for the elaboration of original nanocomposite. We will focus on the design of materials in which the individual properties (luminescence, magnetism) of metallic clusters will interact with those of ligands, transition elements or rare earths in an organic matrix.

Acknowledgments: We are indebted to the Universities of Rennes 1 and Bordeaux I, the Institut Universitaire de France (IUF, DA), the CNRS, the French Research Ministry for thesis grants to D. M. and to K. K., "ACI Nanosciences 2001 - *N° 18-01*" contract and to the "Fondation Langlois" for financial support.

REFERENCES

[1] C. Sanchez, G. J. de A. A. Soler-Illia, F. Ribot, T. Lalot, C. R. Mayer, V. Cabuil, Chem. Mater., 13 (2001) 3061.

[2] F. A. Cotton, *Inorg. Chem*., 3 (1964) 1217.

[3] J.-C. P. Gabriel, K. Boubekeur, S. Uriel, and P. Batail, Chem. Rev., 101 (2001) 2037.

[4] H. Schäfer, H.-G. v. Schnering, Angew. Chem., 76 (1964) 833.

[5] S. Cordier, N. Naumov, D. Salloum, F. Paul, C. Perrin, Inorg. Chem., 43 (2004) 219.

[6] R. Chevrel, M. Sergent dans Topics in Current Physics *"Superconductivity in Ternary Compounds"*, éds Ø Fischer et M. P. Maple, Springer Verlag, Berlin, Heidelberg et New York, *Vol. 32* (1982) 25.

[7] (a) H. D. Selby, B. K. Roland, Z. Zheng, Acc. Chem. Res., 36 (2003) 933. (b) Y. Kim, S. K. Choi, S. M. Park, W. Nam, S. J. Kim, Inorg. Chem. Comm., 5 (2002) 612. (c) N. G. Naumov, A. V. Virovets, V. E. Fedorov, J. Struc. Chem., 41 (2000) 499.

[8] (a) D. H. Johnston, D. C. Gaswick, M. C. Lonergan, C. L. Stern, D. F. Shriver, Inorg. Chem., 31 (1992) 1869. (b) N. Prokopuk, D. Shriver, Inorg. Chem., 36 (1997) 5609. (c) C. B. Gorman, W. Y. Su, C. M. Watson, P. Boyle, Chem. Comm., (1999) 877.

[9] H. Schäfer, H. G. von Schnering, J. Tillack, F. Kuhnen, H. Wöhrle, H. Baumann, Z. Anorg. Allg. Chem., 353 (1967) 281.

[10] G. Pilet, S. Cordier, S. Golhen, C. Perrin, L. Ouahab, A. Perrin, Solid State Sciences, 5 (2003) 1263.

[11] K. Kirakci, S. Cordier, C. Perrin, Z. Anorg. Allg. Chem., 631 (2005) 411.

[12] G. Pilet, F. de Montigny, K. Kirakci, S. Cordier, C. Lapinte, C. Perrin, A. Perrin, Eur. J. Inorg. Chem., 5 (2005) 919.

[13] (a) K. Kirakci *et al.*, to be published. (b) S. Horiuchi, H. Yamochi, G. Saito, K. Matsumoto, Mol. Cryst. Liq. Cryst., 284 (1996) 357.

[14] D. Méry, C. Ornelas, M.-C. Daniel, J. Ruiz, J. Rodrigues, D. Astruc, S. Cordier, K. Kirakci, C. Perrin, Comptes Rendus Chimie, (**2005**) ASAP.

[15] (a) C. Valério, J.-L. Fillaut, J. Ruiz, J. Guittard, J.-C. Blais, D. Astruc, J. Am. Chem. Soc., 119 (1997) 2588. (b) M.-C. Daniel, J. Ruiz, J.-C. Blais, N. Daro, D. Astruc, Chem. Eur. J., 9 (2003) 4371.

[16] (a) S. R. Miller, D. A. Gustowski, Z.-H. Chen, G.-W. Gokel, L. Echegoyen, A. E. Kaifer, Anal. Chem. 60 (1988) 2021. (b) P. D. Beer, P. A Gale, Angew. Chem. Int. Ed. 40 (2001) 486.

[17] D. Méry, L., S. Nlate, D. Astruc, S. Cordier, K. Kirakci, C. Perrin, Z. Anorg. Allg. Chem., (2005) ASAP.

[18] (a) B. K. Roland, W. H. Flora, J. Clust. Sci., 14 (2003) 449. (b) J. H. Golden, H. Deng, F. Di Salvo, J . M. Fréchet, P. M. Thompson, 268 (1995) 1463.

Dendrimères Inorganiques et Organométalliques
Design et Catalyse

Résumé :

Les dendrimères constituent une thématique primordiale de la recherche dans le domaine des Nanosciences. Les objectifs de cette thèse se sont inscrits autant dans un aspect fondamental des dendrimères que dans les applications potentielles. Dans un premier temps, nous avons élaboré de nouveaux métallodendrimères pour la catalyse, dans l'esprit de la *Chimie Verte*, et pour la synthèse de nouveaux matériaux : les polymères en étoile. Puis, nous avons étudié des aspects plus fondamentaux des dendrimères tels que la fonctionnalisation de grands dendrimères ainsi que la synthèse des premiers dendrimères à cœur cluster de molybdène avec des liaisons de coordination.

Mots-clés :

Dendrimère, Catalyse, Sonogashira, Métathèse, Polymère en étoile, Cluster, Assemblage.

Organometallic and Inorganic Dendrimers
Design and Catalysis

Abstract :

Dendrimers constitute a major research field for Nanosciences. The studies presented herein focuse on fundamental and applied dendrimer chemistry. Firstly, new metallodendrimers were synthesised for catalysis application in *Green Chemistry* and for the development of new materials such as Star Polymers. Other fundamental points studied include giant dendrimer functionalisation as well as synthesis of the first dendrimers comprising a Molybdenum-cluster cored *via* coordination bonds.

Keywords :

Dendrimer, Catalysis, Sonogashira, Metathesis, Star Polymer, Cluster, Assembly.